

University of Cambridge

Bromotyrosine-Derived Natural Products: Synthetic and Biological Studies

A dissertation presented by

James Shearman

This dissertation is submitted for the degree of

Doctor of Philosophy

of the

University of Cambridge



Sidney Sussex College
Cambridge
CB2 3HU

April 2011

Declaration

This dissertation is submitted in partial fulfillment of the requirements for the degree of Doctor of Philosophy. It describes work carried out from August 2007 to March 2011. Unless otherwise indicated, the research described is my own and not the product of collaboration.

James W. Shearman

Statement of Length

This dissertation, in partial fulfillment of the requirements for the award of the degree of Doctor of Philosophy, does not exceed the word limit of 60,000 as set by the Degree Committee for the Faculty of Physics and Chemistry.

James W. Shearman

To Dad
In loving memory

Abstract

Bromotyrosine-derived natural products are a fascinating class of compounds that are produced by marine sponges of the order Verongida. Furthermore, they exhibit a rich variety of chemical structures and display a diverse range of bioactivities which makes them of great interest to both the chemical and biological research communities.

This thesis is divided into four Chapters and describes the total syntheses of five bromotyrosine-derived natural products and analogues thereof. The anticancer activity of these compounds was also investigated. In addition, studies towards the total syntheses of the ceratamines are reported.

The first Chapter gives a general introduction into the history, biosynthesis, structures and biological activities of bromotyrosine-derived natural products. A background into the anticancer properties of ceratamines A and B is also provided.

The research in Chapter two is concerned with bromotyrosine-derived oximes and is divided into two parts. The syntheses of the natural products (5)-bromoverongamine, ianthelline and JBIR-44 are described in Part one and the structure-activity relationship studies into these products is described in Part two.

The total syntheses of subereamollines A and B are discussed in Chapter three. Furthermore, both enantiomers of the natural products were accessed and their absolute stereochemistry was unambiguously assigned.

The first section of Chapter four provides an in-depth review of the research carried out by the Andersen and Coleman groups into the ceratamines. This is followed by an account of the Ley group approach towards the syntheses of these natural products.

Contents

| | |
|---|-----------|
| Abstract..... | iv |
| Contents | v |
| Acknowledgements..... | vii |
| Symbols and Abbreviations..... | viii |
| CHAPTER 1..... | 1 |
| 1.1 PERSPECTIVE..... | 2 |
| 1.2 MARINE NATURAL PRODUCTS | 3 |
| 1.3 BROMOTYROSINE-DERIVED NATURAL PRODUCTS | 3 |
| 1.3.1 Biosynthesis: Vanadium Bromoperoxidases | 5 |
| 1.3.2 Structures of Bromotyrosine-Derived Natural Products..... | 7 |
| 1.3.3 Biological Activities..... | 9 |
| 1.3.4 The Ceratamines | 12 |
| 1.3.4.1 Microtubules as an Anticancer Target | 13 |
| 1.3.4.2 Ceratamines: Biological Activity | 16 |
| 1.4 REFERENCES | 18 |
| CHAPTER 2 PART I..... | 22 |
| 2.1.1 OXIME BROMOTYROSINE DERIVATIVES..... | 24 |
| 2.1.2 BIOLOGICAL ACTIVITY OF BROMOTYROSINE-DERIVED OXIMES..... | 26 |
| 2.1.2.1 Antifouling Activity | 26 |
| 2.1.2.2 Anticancer Activity..... | 28 |
| 2.1.3 (5)-BROMOVERONGAMINE, IANTHELLINE AND JBIR-44..... | 29 |
| 2.1.3.1 Isolation and Biological Activity | 29 |
| 2.1.3.2 Synthetic Strategy | 31 |
| 2.1.4 RESULTS AND DISCUSSION..... | 33 |
| 2.1.4.1 Synthesis of α -Oximino Acid 17..... | 33 |
| 2.1.4.2 Synthesis of (5)-Bromoverongamine | 35 |
| 2.1.4.3 Synthesis of Ianthelline..... | 36 |
| 2.1.4.4 Synthesis of JBIR-44..... | 37 |
| 2.1.4.5 Improving the Synthesis of α -Oximino Acid 17 | 39 |
| 2.1.4.6 Biological Screening..... | 41 |
| 2.1.5 CONCLUSION | 43 |
| 2.1.6 CHEMISTRY: EXPERIMENTAL..... | 44 |
| 2.1.7 BIOLOGY: EXPERIMENTAL | 63 |
| 2.1.8 APPENDIX..... | 65 |
| 2.1.8.1 NMR Data of Natural Products | 65 |
| 2.1.8.2 NMR Spectra of Natural Products..... | 66 |
| 2.1.8.3 Crystal Structure Data | 74 |
| 2.1.9 REFERENCES | 77 |
| CHAPTER 2 PART II..... | 80 |
| 2.2.1 INTRODUCTION | 81 |
| 2.2.2 RESULTS AND DISCUSSION..... | 85 |
| 2.2.2.1 Synthesis of 3,5-Dichloro-4-methoxy Benzaldehyde (51) | 86 |
| 2.2.2.2 Synthesis of 3,5-Diiodo-4-methoxy Benzaldehyde (52)..... | 89 |
| 2.2.2.3 Synthesis of α -Oximino Acid Derivatives..... | 90 |
| 2.2.2.4 Synthesis of (5)-Bromoverongamine Analogues..... | 92 |
| 2.2.2.5 Synthesis of JBIR-44 Analogues | 94 |
| 2.2.2.6 Biological Activity..... | 95 |
| 2.2.2.6.1 (5)-Bromoverongamine Series | 96 |
| 2.2.2.6.1 JBIR-44 Series..... | 97 |
| 2.2.3 CONCLUSION AND FUTURE WORK..... | 100 |
| 2.2.4 CHEMISTRY: EXPERIMENTAL..... | 101 |
| 2.2.5 BIOLOGY: EXPERIMENTAL | 139 |
| 2.2.6 APPENDIX..... | 140 |
| 2.2.6.1 NMR Spectra | 140 |
| 2.2.6.2 Crystal Structure Data | 143 |

| | |
|--|------------|
| 2.2.7 REFERENCES | 145 |
| CHAPTER 3..... | 147 |
| 3.1 SPIROCYCLOHEXADIENYLISOXAZOLINE BROMOTYROSINE DERIVATIVES | 149 |
| 3.1.1 Structure | 149 |
| 3.1.2 Biological Activity..... | 151 |
| 3.2 SUBEREAMOLLINES A AND B..... | 152 |
| 3.2.1 Isolation and Biological Activity..... | 152 |
| 3.2.2 Synthetic Strategy..... | 153 |
| 3.3 RESULTS AND DISCUSSION..... | 156 |
| 3.3.1 Synthesis of Spiroisoxazoline Acid 18 | 156 |
| 3.3.2 Synthesis of Amines 19 and 20..... | 160 |
| 3.3.3 Synthesis of Subereamollines A and B..... | 161 |
| 3.3.4 Side Chain Variations..... | 162 |
| 3.3.5 Separation of Racemic Subereamollines A and B..... | 163 |
| 3.3.6 Confirmation of the Absolute Stereochemistries at C-1 and C-6..... | 164 |
| 3.3.7 Biological Screening..... | 166 |
| 3.4 CONCLUSION AND FUTURE WORK..... | 167 |
| 3.5 CHEMISTRY: EXPERIMENTAL | 169 |
| 3.6 BIOLOGY: EXPERIMENTAL | 192 |
| 3.7 APPENDIX..... | 192 |
| 3.7.1 NMR Data of Natural Products | 192 |
| 3.7.2 NMR Spectra of Natural Products..... | 193 |
| 3.7.3 Analytical Chiral HPLC Traces..... | 201 |
| 3.7.4 Crystal Structure Data..... | 203 |
| 3.8 REFERENCES | 206 |
| CHAPTER 4..... | 209 |
| 4.1 INTRODUCTION | 211 |
| 4.1.2 Andersen Group Approaches to the Ceratamines | 212 |
| 4.1.2.1 First-Generation Approach | 212 |
| 4.1.2.2 Second-Generation Approach..... | 213 |
| 4.1.3 Coleman Group Total Synthesis | 216 |
| 4.1.4 Ceratamine A Structure-Activity Relationship..... | 219 |
| 4.1.5 Ley Group Strategy..... | 221 |
| 4.2 RESULTS AND DISCUSSION..... | 223 |
| 4.3 CONCLUSION AND FUTURE WORK..... | 234 |
| 4.4 CHEMISTRY: EXPERIMENTAL..... | 236 |
| 4.5 APPENDIX..... | 252 |
| 4.5.1 Crystal Structure Data..... | 252 |
| 4.6 REFERENCES | 255 |
| 5 PUBLICATIONS | 257 |

Acknowledgements

If you've picked up this thesis and are reading these acknowledgements it's common knowledge that you are probably going to put it right back on the shelf once you get to the end of this page. Therefore, you could say that all I have done over past four (and a bit!) years in Cambridge will be judged by what I write on this page. I genuinely hope that this isn't the case because not only will I have wasted three months of my life writing this beast, but it would also do a major disservice to all of my family, friends, and acquaintances who have guided, influenced, and supported me through this enjoyable (but sometimes stressful) journey.

I have been very fortunate to be a part of such a fantastic research group. Steve has been a first-class supervisor and his never-ending enthusiasm and positivity were great motivators through the tough times! I am also grateful for his generosity in funding the naughtiness at Christmas parties and summer BBQs. Thanks to all the Whiffenites, especially E-bay (past and present plus the honorary Dr Pearson!), Team CRUK (Tom, Danny, Crusty, Lily Chan and Rebecca), the Riga crew and the Predator for making those long hours all the more bearable!

I would like to thank James Brenton for his invaluable input on this project and the rest of the Brenton group (especially Xian and Jill) for making me feel welcome.

The work carried out by all of the technical officers and support staff is usually taken for granted, but without them everything would grind to a halt. In particular, I would like to thank Richard Turner, Melvyn and Keith, John Davies, Paul Skelton and Peter Grice for making my life as easy as possible.

As you will find out when you read the rest of this document, my proofreaders (Colin, Tommy, Danny, Reed and Rebecca) have done a stellar job. I trust there are no mistakes but if there are...I forgive you!

Special thanks goes to the Gentlemen of the Porcupines and the lads of CUARLFC for the epic swaps, victorious Varsity matches and the unforgettable memories. You guys kept me sane!

Jen, thanks for putting up with me! Your unwavering love and support over the years has been amazing. I'm very lucky to have you!

Finally, I would like to thank my parents for providing all the love, support, encouragement and opportunities required to get me to where I am today. Dad, I'm sorry you're not around to see this day. This one's for you.

Symbols and Abbreviations

| | |
|------------|---|
| α | optical rotation or alpha-position |
| Å | Ångström(s) |
| δ | chemical shift |
| ν | frequency |
| μ | micro |
| Ac | acetyl |
| aq | aqueous |
| Ar | aryl |
| ATP | adenosine-5'-triphosphate |
| Bn | benzyl |
| Boc | <i>tert</i> -butoxycarbonyl |
| BOM | benzyloxymethyl |
| br | broad |
| Bu | butyl |
| <i>c</i> | concentration |
| °C | degrees centigrade |
| CD | circular dichroism |
| CDI | 1,1'-carbonyldiimidazole |
| <i>cf.</i> | compare with |
| cLogP | computed LogP |
| CNS | central nervous system |
| COLOC | correlation through long-range coupling |
| COSY | correlation spectroscopy |
| CSA | camphorsulfonic acid |
| d | doublet |
| <i>d</i> | deuterium |
| dba | dibenzylideneacetone |
| DCC | <i>N,N'</i> -dicyclohexylcarbodiimide |
| DCU | <i>N,N'</i> -dicyclohexylurea |
| DDQ | 2,3-dichloro-5,6-dicyano-1,4-benzoquinone |
| <i>de</i> | diastereomeric excess |
| decomp | decomposition |

| | |
|------------------|--|
| DEPT 135 | distortionless enhancement by polarisation transfer using a 135 degree decoupler pulse |
| DIC | <i>N,N'</i> -diisopropylcarbodiimide |
| DMAP | 4-dimethylaminopyridine |
| DMEDA | <i>N,N'</i> -dimethylethylenediamine |
| DMF | <i>N,N</i> -dimethylformamide |
| DMP | Dess–Martin periodinane |
| DMSO | dimethyl sulfoxide |
| DNA | deoxyribonucleic acid |
| <i>dr</i> | diastereomeric ratio |
| <i>E</i> | <i>entgegen</i> |
| EC ₅₀ | half maximal effective concentration |
| EDCI | 1-ethyl-3-(3-dimethylaminopropyl)carbodiimide |
| <i>ee</i> | enantiomeric excess |
| EGF | endothelial growth factor |
| eq | equivalent(s) |
| ESI | electrospray ionisation |
| Et | ethyl |
| FKBP12 | FK506 binding protein 12 |
| FT | Fourier transform |
| g | gram |
| GTP | guanosine-5'-triphosphate |
| h | hour |
| HDAC | histone deacetylase |
| HIV | human immunodeficiency virus |
| HMBC | heteronuclear multiple bond coherence |
| HMDS | hexamethyldisilazane |
| HMPA | hexamethylphosphoramide |
| HMQC | heteronuclear multiple quantum coherence |
| HOBt | <i>N</i> -hydroxybenzotriazole |
| HPLC | high performance liquid chromatography |
| HRMS | high resolution mass spectrometry |
| HUVEC | human umbilical vein endothelial cell |

| | |
|------------------|---|
| $h\nu$ | irradiation with light |
| Hz | Hertz |
| <i>i</i> | <i>iso</i> |
| IBX | 2-iodoxybenzoic acid |
| IC ₅₀ | half maximal inhibitory concentration |
| IR | infrared |
| <i>J</i> | coupling constant |
| K | Kelvin |
| L | litre |
| LCMS | liquid chromatography-mass spectrometry |
| LDA | lithium diisopropylamide |
| Lit | literature |
| LogP | logarithm of the partition coefficient |
| LRI | London Research Institute |
| <i>m</i> | <i>meta</i> |
| m | metre or multiplet (NMR) or medium (IR) |
| M | molar or mitotic |
| <i>m/z</i> | mass / charge ratio |
| MCF | Michigan Cancer Foundation |
| <i>m</i> CPBA | <i>meta</i> -chloroperbenzoic acid |
| Me | methyl |
| Mes | mesityl |
| MIC | minimum inhibitory concentration |
| min | minute(s) |
| mol | mole |
| m.p. | melting point |
| MS | mass spectrometry or molecular sieves |
| MTS | 3-(4,5-dimethylthiazol-2-yl)-2,5-diphenyltetrazolium |
| <i>m/z</i> | mass-to-charge ratio |
| n | nano |
| <i>N</i> | normality |
| N/A | not active |
| NBS | <i>N</i> -bromosuccinimide |
| NCI | National Cancer Institute |

| | |
|------------------|-------------------------------------|
| NMR | nuclear magnetic resonance |
| Np | nitrophenol |
| Org | organic |
| p | protein |
| <i>p</i> | <i>para</i> |
| P | partition coefficient |
| PDS | diphenyl disulfide |
| Pg | unspecified protecting group |
| Ph | phenyl |
| PMB | <i>para</i> -methoxybenzyl |
| ppm | parts per million |
| Pr | propyl |
| PS | polymer-supported |
| py | pyridine |
| q | quartet |
| QP | QuadraPure |
| quant | quantitative |
| quint | quintet |
| <i>R</i> | <i>rectus</i> |
| R | generic alkyl substituent |
| Ras | Rat sarcoma |
| RNA | ribonucleic acid |
| rt | room temperature |
| R_f | retention factor |
| R_t | retention time |
| s | singlet (NMR) or strong (IR) |
| <i>S</i> | <i>sinister</i> |
| SA | sulfonic acid |
| SAR | structure-activity relationship |
| SARS | severe acute respiratory syndrome |
| sec | second |
| t | triplet |
| <i>t or tert</i> | tertiary |
| TBP | tributylphosphine |

| | |
|------------------|--|
| TBS | <i>tert</i> -butyldimethylsilyl |
| TBTU | <i>O</i> -(benzotriazol-1-yl)- <i>N,N,N',N'</i> -tetramethyluronium tetrafluoroborate |
| Tf | trifluoromethanesulfonyl |
| TFA | trifluoroacetic acid |
| THF | tetrahydrofuran |
| TIPS | triisopropylsilyl |
| TLC | thin-layer chromatography |
| TMS | trimethylsilyl |
| [®] T3P | propylphosphonic anhydride |
| Ts | <i>para</i> -toluenesulfonyl |
| UV | ultraviolet |
| V | Volt(s) |
| VBPO | vanadium bromoperoxidase |
| VT | variable temperature |
| v/v | volume to volume |
| w | weak |
| w/w | weight to weight |
| Xphos | 2-dicyclohexylphosphino-2',4',6'-triisopropylbiphenyl |
| <i>Z</i> | <i>zusammen</i> |

CHAPTER 1

Introduction

1.1 Perspective

Global research efforts have led to remarkable advances in our understanding of cancer biology in recent years. However, as the incidence of cancer rises, the disease presents major health problems for ever-widening populations, bringing in turn, increasing strain on healthcare systems. Huge investments in research have been made to try and tackle these problems. One aspect of the solution lies in the need for new anticancer drugs and more effective treatment strategies. Cancer therapy has already had some success generated by this momentum, particularly with mechanism-based drugs that interact with protein kinases and their signalling pathways *e.g.* Gleevec. However, the continued search for improved cytotoxic agents that act on ubiquitous targets such as DNA (*e.g.* cisplatin) or tubulin (*e.g.* natural products) continues. As the major types of solid human tumours are multi-causal in nature, there is a movement towards treatments that involve combinations of signal transduction inhibitors (mechanism-based) with improved and more specific cytotoxic drugs.

The search for lead compounds is an essential component of pharmaceutical research, and for many thousands of years natural products have made enormous contributions to human health. However, it was not until the 1950s that, as a result of a concerted effort made by the NCI in the United States supporting screening programmes, the speed of discovery of new naturally occurring anticancer agents began to surge. The range of natural products with striking anticancer profiles is quite remarkable.¹ Indeed, natural product-derived anticancer therapies are now relatively common treatments in the clinic *e.g.* paclitaxel and vinorelbine. Newer anticancer therapies such as the combretastatins² are in late stage clinical trials, and an epothilone analogue (ixabepilone) has recently been approved for clinical use.³

Sadly, in spite of this, the use of natural products and their importance as a source of molecular diversity has been overshadowed by various industry-favoured approaches including high-throughput screening and combinatorial approaches for generating synthetic small molecules. However, drug discovery from natural sources has a robust historical justification and good biochemical and chemical rationales. Natural products will continue to serve as an inspiration for the discovery of new drugs.

1.2 Marine Natural Products

Marine life differs from terrestrial life in many respects and this has implications on the natural product diversity observed in these environments. It has been established that while terrestrial life is far richer in species, marine life is richer in phyla. In examining the higher taxa, there is greater biodiversity exhibited in the sea.⁴ This is paralleled in the increased diversity in the molecular frameworks possessed by marine natural products. The members of this chemically diverse family of natural products also exhibit a broad spectrum of bioactivities. Indeed, some of the most toxic compounds known to man are of marine origin.⁵

The last few years have seen an unprecedented rise in the number of newly discovered marine natural products that have been reported in the literature. To put this in context, over 1000 new compounds were identified in both 2008 and 2009.⁶ In part, this increase is testament to recent scientific advances in the collection, isolation and structural elucidation of these substances; many of the stereochemical and connectivity problems encountered when trying to unravel complex chemical structures have been solved by the emergence of new techniques in nuclear magnetic resonance, mass spectrometry and X-ray crystallography.

This rise in the number of reported compounds can also be attributed to the interest that marine natural products generate within the scientific community. Besides the obvious desire that pharmaceutical companies have in transforming novel bioactive entities into marketable drugs, synthesis chemists revel in the challenge of constructing complex molecular architectures and biochemists need new chemical tools that aid in delineating biological pathways and the identification of new biological targets.

1.3 Bromotyrosine-Derived Natural Products

Seawater is known for its high chloride ion concentration (~ 0.5 M); however, the occurrence of the other halides is often overlooked. Bromide (the fourth most abundant anion in seawater) is the second most abundant halide ($[\text{Br}^-] \sim 0.8$ mM), followed by fluoride ($[\text{F}^-] \sim 70$ μM) and then iodide ($[\text{I}^-] \sim 0.4$ μM).⁷ These halide ions are believed to originate from minerals that have been washed out of the ground and carried into the sea by rivers—a process known as continental weathering.

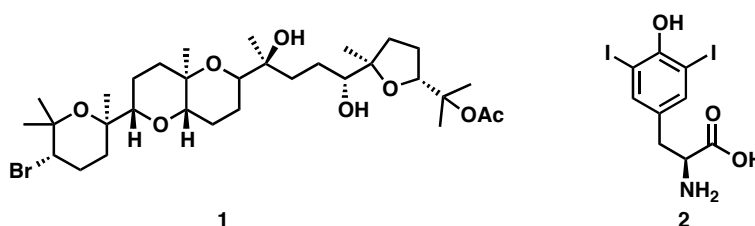


Figure 1 Structures of thysiferyl acetate (**1**) and diiodotyrosine (**2**).

Although the concentration of bromide is much lower than that of chloride, the number of naturally occurring organochlorine compounds (2320^{*}) that have been identified only slightly exceeds the number of natural organobromine compounds (2050^{*}).¹¹ This non-statistical outcome is due to the fact that it is easier for marine organisms to incorporate bromide into organic compounds; the standard oxidation potential of bromide is -1.07 V compared to -1.36 V for chloride.¹² The research described herein focuses on bromotyrosine-derived natural products, a specific class of brominated secondary metabolites.

Bromotyrosine-derived natural products are produced by horny sponges of the order Verongida. These sponges possess an unusual biochemistry and, as a result, have promoted much biological and chemical interest. Characteristics of these sponges include a lack of terpenes, production of large amounts of sterol that contain the aplystane skeleton[†] and an ability to synthesise bromotyrosine derivatives. Further to this, as bromotyrosine metabolites occur in virtually all Verongida sponges they have been used as chemotaxonomic markers to correctly identify different species due to the difficulty of identifying sponges on their morphology alone.¹³

* 2004 estimate (See Ref 10).

[†] There is an extra methyl group at C-26 in steroids containing the aplystane skeleton.

Following the first reported isolation of 3,5-dibromotyrosine (**3**) from two species of coral by Morner in 1913,¹⁴ over half a century passed before the first bromotyrosine derivative, verongiaquinol (**4**), was discovered (Figure 2).¹⁵ Since then, knowledge of these fascinating compounds has grown immensely as a consequence of their diverse bioactivity (Section 1.3.3). To date, over 300 of these secondary metabolites have been reported in the literature.

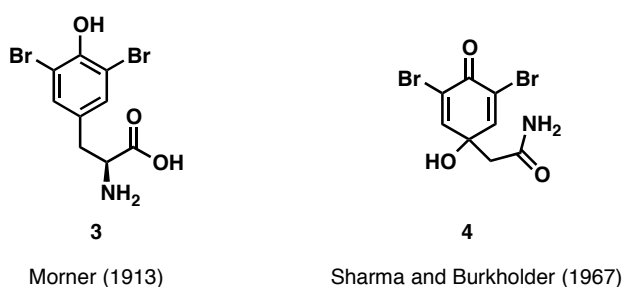


Figure 2 Structures of 3,5-dibromotyrosine (**3**) and verongiaquinol (**4**).

1.3.1 Biosynthesis: Vanadium Bromoperoxidases

Biosynthetically, enzymes collectively known as the vanadium bromoperoxidases (VBPO) are believed to install the bromine functionality within bromotyrosine-derived secondary metabolites.¹⁶ They are able to do this by catalysing the bromide-assisted disproportionation of hydrogen peroxide to an electrophilic brominating species and water (Scheme 1, equation 1). This is followed by concomitant bromination of the organic substrate held in the active site (Scheme 1, equation 2).



Scheme 1 Process catalysed by VBPOs illustrated in the simplest form.

These enzymes have attracted much interest due to their ability to introduce bromine atoms into aromatic compounds and their dependence on the transition metal vanadium.¹⁷ Vanadium bromoperoxidases are dodecameric in structure with each of the 12 protein subunits containing cationic vanadium(V) (Figure 3).¹⁸

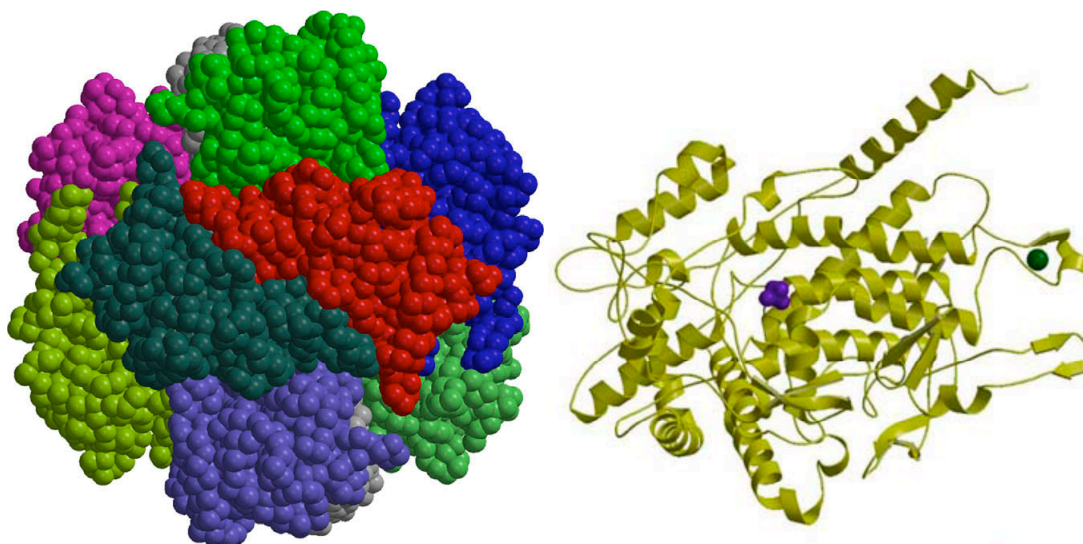


Figure 3 Left: dodecameric structure of *Corallina* VBPO; right: ribbon diagram of a single subunit (vanadate shown in purple). Images taken from *J. Inorg. Biochem.*, **2009**, 103, 617 and *J. Biol. Inorg. Chem.*, **2005**, 10, 275.

As previously mentioned, bromination reactions catalysed by these enzymes proceed *via* an electrophilic mechanism and not a radical process.¹⁹ The actual electrophilic brominating species is thought to be either a free halogenating agent such as Br_2 , Br_3^- , or HOBr , or an enzyme–Br complex *e.g.* $\text{V}_{\text{enz}}\text{-OBr}$.²⁰ A combination of mechanistic and X-ray diffraction studies has helped to elucidate the intricacies of the catalytic bromination process.²¹

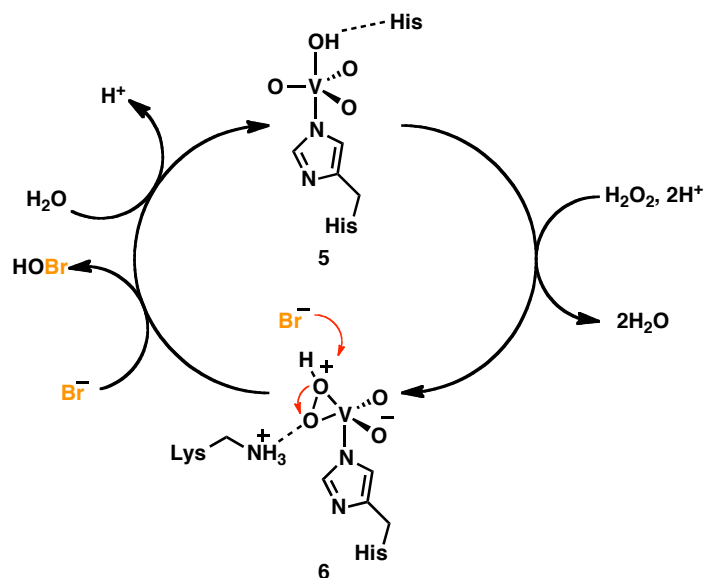


Figure 4 Simplified diagram representative of the VBPO catalytic cycle.

In the resting state of the enzyme, the vanadate(V) ion housed in the active site is bound to the protein by a histidine residue (Figure 4). Hydrogen peroxide can

Tyrosine (7) $\xrightarrow[\text{Vanadium Bromoperoxidase}]{\text{Br}^-, \text{H}_2\text{O}_2}$ 8 and 9

The research described within this thesis relates to compounds derived from a dibromotyrosine subunit.

The 300 or so bromotyrosine-derived natural products that are currently known exhibit a rich variety of chemical structures and this has led to them being classified into six main categories: simple bromotyrosine derivatives, oximes, bastadins, spirocyclohexadienylisoxazolines, spirooxepineisoxazolines, and other structural classes.²³ To review all these classes in detail would be excessive and beyond the scope of this thesis; however, by way of a few examples some of the important structural features are worth mentioning (Figure 5).

7

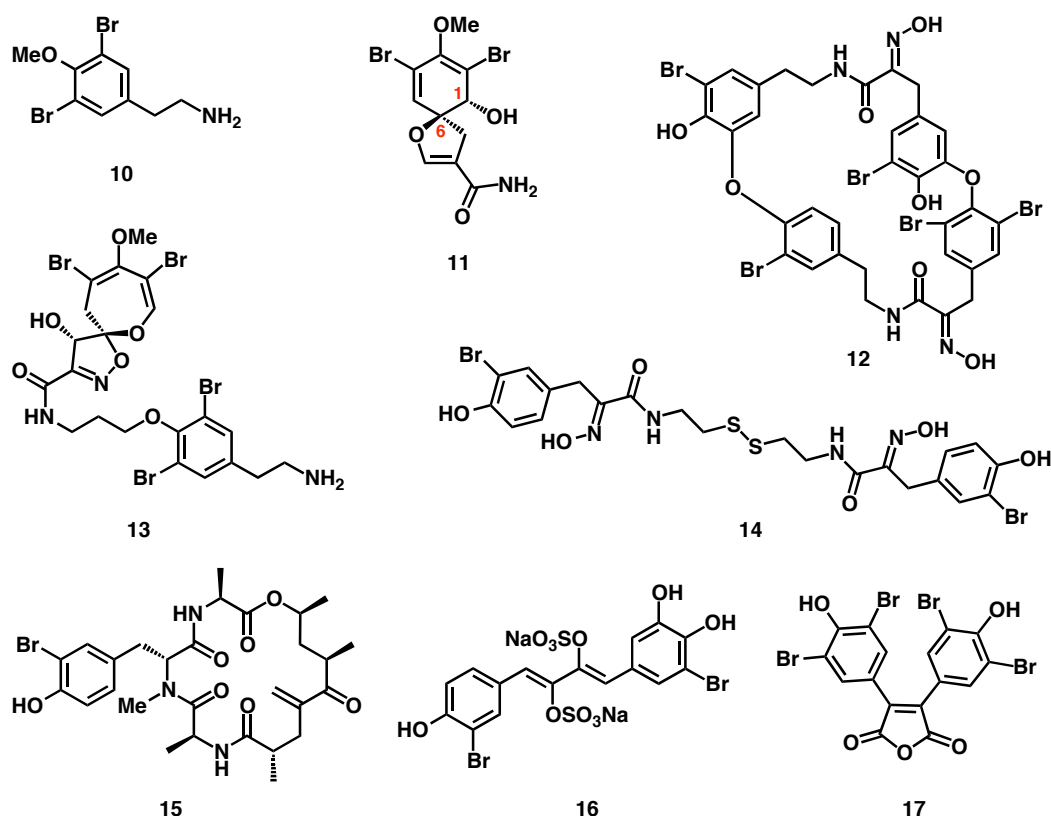


Figure 5 Examples of structures from the six classes of bromotyrosine products.

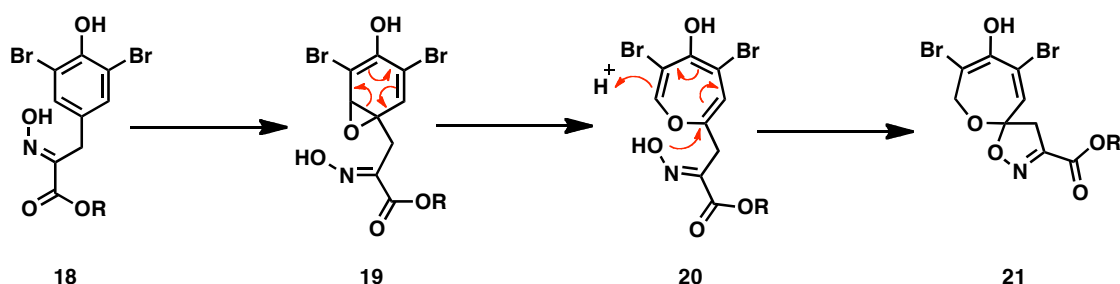
The simple derivatives contain a single bromotyrosine subunit and are products of degradation, reduction, hydroxylation, alkylation or esterification with simple functional groups; 3,5-dibromo-4-methoxyphenethylamine (**10**) is a member of this class.²⁴ Oxidation of the tyrosine amino functionality give rises to the oxime derivatives, *e.g.* psammaphin A (**14**),²⁵ and these will be discussed in greater depth in Chapter 2.

Members of the bastadins are predominantly macrocyclic in structure as exemplified by bastadin-19 (**12**).²⁶ To date, around 30 members of this class have been identified from natural sources and they consist of four bromotyrosine subunits stitched together by amide and biaryl ether linkages. Some bastadins are currently used as biochemical tools to study calcium ion channels as they are novel allosteric modulators of the ryanodine receptor 1/FKBP12 complex, responsible for releasing Ca^{2+} ions from the sarcoplasmic reticulum.²⁷

The spirocylcohexadienylisoxazolines all contain a [6,5]-spirocyclic unit of the type possessed by compound **11**. They are further catagorised as either mono- or *bis*-spirocylcohexadienylisoxazolines depending on whether they contain one or two of these units, respectively. As a consequence of their biosynthesis the relative

stereochemistry between the hydroxyl group at C-1 and oxygen in the oxazoline ring is conserved (Section 3.1.1), however, both absolute configurations at C-1 and C-6 are possible. A more detailed insight into these compounds will be provided in Chapter 3.

Bromotyrosine-derived natural products bearing a spirooxepineisoxazoline core (compound **13**) make up the smallest class with the identification of only 10 members to date: the psammaphysins A-G and ceratinamides A and B.²⁸ Biosynthetically, oxidation of a tyrosine precursor **18** by an epoxidase yields **19**. This then undergoes a rearrangement to give **20** which subsequently reacts with the hydroxyl group of the oxime to give the spirooxepineisoxazoline **21** (Scheme 3).



Scheme 3 Mechanism of the formation of spiroketal **21**.

The final class of natural products is a miscellany of compounds that bear no apparent structural relationship to one another; their common feature being that they are derived from bromotyrosine. When more is known about these compounds in the future, it may be possible to further categorise them. From a synthesis chemist's perspective these molecules are perhaps the most intriguing with regards to their structure, as is illustrated by geodiamolide J²⁹ (**15**), aplysillin A³⁰ (**16**) and prepolyctrin A³¹ (**17**). The ceratamines (Section 1.3.4 and Chapter 4), a family of novel heterocyclic marine alkaloids, also fall into this category.

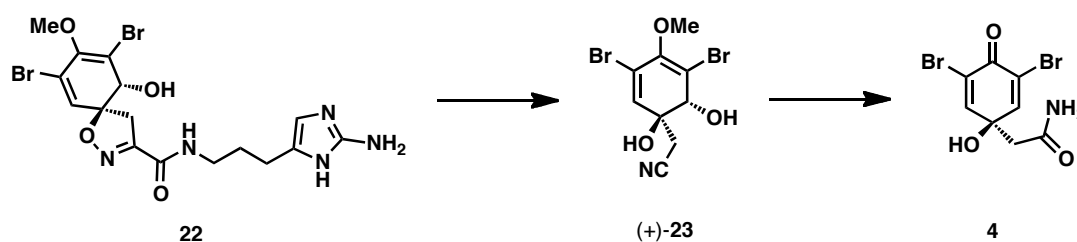
1.3.3 Biological Activities

Like terrestrial plant life, marine sponges have evolved a sophisticated chemical defense system to protect against their perilous environment. In addition to the obvious threat of predation, sponges may also be compromised by biofouling,[§] pathogenic infections and the overgrowth of other marine invertebrates. Up to 40% of the total biomass in Verongida sponges is made up from bacteria, suggesting that

[§] Biofouling is the undesired attachment of microorganisms, plants, algae and animals to a surface. Sponges are filter-feeders and the build-up of organisms on their surface can be particularly damaging because the flow of water through the body of the sponge is reduced.

brominated secondary metabolites may also have a role in controlling bacterial colonisation.^{**32}

A particularly interesting facet of this defense mechanism is the response of these sponges to wounding. Typically, the chemical defense strategies of marine invertebrates are constitutive and rely on the accumulation of preformed toxins in tissues. These are either constantly secreted into the surrounding marine environment or are released upon wounding.³³ In addition to this, Verongida sponges have an activated defense system that is highly dynamic and responds within seconds if said sponge comes under attack. Evidence suggests that if damaged is inflicted on the sponge, enzymes will convert high molecular weight isoxazoline bromotyrosine derivatives (Chapter 3) into lower molecular weight metabolites that exhibit greater bioactivities. Proksch and co-workers demonstrated that extracts of the sponge *Aplysina aerophoba* were able to convert several isoxazoline derivatives, including aerophobin-2 (**22**), into (+)-aerophysinin-1 (**23**) which in turn was converted into verongiaquinol (**4**) (Scheme 4).³⁴ It has since been postulated that the latter transformation is catalysed by a nitrile hydratase.³⁵



Scheme 4 Bioconversion of aerophobin-2 (**22**) to aerophysinin-1 (**23**) and verongiaquinol (**4**).

This process was complete within 40 seconds of mechanical wounding and both **23** and **4** were found to have an increased ability to deter fish relative to **22**. Around the same time Woerdenbag and co-workers discovered that **23** and **4** could form semiquinone radicals which could also contribute to their cytotoxic activity and concluded that, “compound **23** will generate free radicals after metabolic activation by the predator’s cells, which results in an antifeedant effect. Simultaneously, the dienone **4** is liberated, which immediately yields free radicals in the water surrounding the sponge, thereby shielding the sponge from further predation or attack”.³⁶

^{**} Recent work by Becerro and co-workers found a significant positive correlation between bromotyrosine products and certain bacterial strains suggesting that bacteria could either be involved in their production or be directly affected by them (*Appl. Environ. Microbiol.*, **2011**, 77, 862).

Consistent with their role as defensive agents, bromotyrosine-derived products isolated from Verongida sponges exhibit a rich diversity of biological activities that include: antiviral,³⁷ Na⁺/K⁺ ATPase inhibition,³⁸ anti-HIV,³⁹ HDAC inhibition,⁴⁰ antifouling,⁴¹ histamine H₃ antagonism,⁴² antifungal,⁴³ thrombin receptor antagonism,³⁰ mycothiol *S*-conjugate amidase inhibition,⁴⁴ and isoprenylcysteine carboxy methyltransferase (Icmt) inhibition.⁴⁵ In addition, the vast majority of bromotyrosine secondary metabolites also possess significant antimicrobial activities.²³ For example, both enantiomers of **23** show activity against both Gram-positive and Gram-negative bacteria.⁴⁶ Furthermore, **23** has been found to inhibit the growth of *Plasmodium falciparum* (IC₅₀ 17.7 µM) and *Trypanosoma cruzi* (IC₅₀ 37.7 µM).⁴⁷

The anticancer activity of bromotyrosine-derived natural products has also been investigated and a significant number of compounds have been found to elicit cytotoxic responses in cancer cells both *in vitro* and *in vivo*. The anticancer properties of oxime and spirocyclohexadienylisoxazoline-type derivatives will be reviewed in Chapters 2 and 3, respectively, but by way of an example, aeroplysinin (**23**) has been shown to be cytotoxic towards numerous neoplastic cell lines that have a marked dependence on growth factors.⁴⁸

In particular, the growth inhibitory activity of **23** against L5178y cells (IC₅₀ 0.5 µM) is greater than other agents such as bleomycin (IC₅₀ 0.9 µM) and distamycin (IC₅₀ 13.1 µM). Further studies by Kreuter and co-workers found that (+)-**23** could inhibit EGF receptor tyrosine protein kinase and block the EGF-dependent proliferation of both MCF-7 and ZR-75-1 human breast cancer cells.⁴⁹ More recently, it has come to light that (+)-**23** is also a potent antiangiogenic^{††} agent, with the ability to inhibit the growth, migration and invasion of endothelial cells.⁵⁰ Following on from this, Plumet and co-workers synthesised a library of analogues in an attempt to optimise these antiangiogenic properties.⁵¹ Using **23** as a starting point they sought to increase the ratio of sprouting inhibition/cytotoxicity—their lead compound exhibited a ratio of 921:1 (*cf.* 54:1 for **23**).

^{††} Angiogenesis is growth of new blood vessels from pre-existing vessels. As tumour growth is dependent on the formation of new blood vessels, targetting angiogenesis with antiangiogenic agents is a recognised therapeutic strategy.

Historically, bromotyrosine compounds were screened against a variety of cell lines as a means of quantifying their cytotoxic activity; however, the mode of action of many of these products is still unknown. The reasons for this are multifactorial but the availability of natural material and lack of the appropriate biochemical assays were probably the main cause. Nowadays, an understanding of a molecule's cellular target is vital given the highly stringent nature of current drug approval guidelines. Therefore, it is clear that further collaborative research will be required in order for the full potential of these fascinating compounds to be realised in a cancer setting.

1.3.4 The Ceratamines

The inspiration for the research discussed in this thesis stemmed from a family of bromotyrosine-derived products whose members were unique in terms of both structure and biological activity. Extracts of the marine sponge *Pseudoceratina* sp. collected around Papua New Guinea showed promising activity in a cell-based assay^{††} designed to detect new antimitotic natural product chemotypes.⁵² The active components of the sponge were isolated using bioassay guided fractionation, which yielded two heterocyclic alkaloids: ceratamine A (**24**) and B (**25**) (Figure 6).⁵³

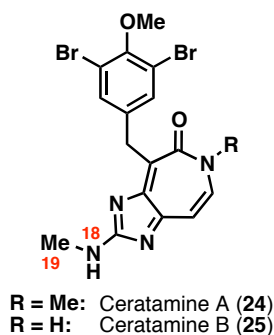
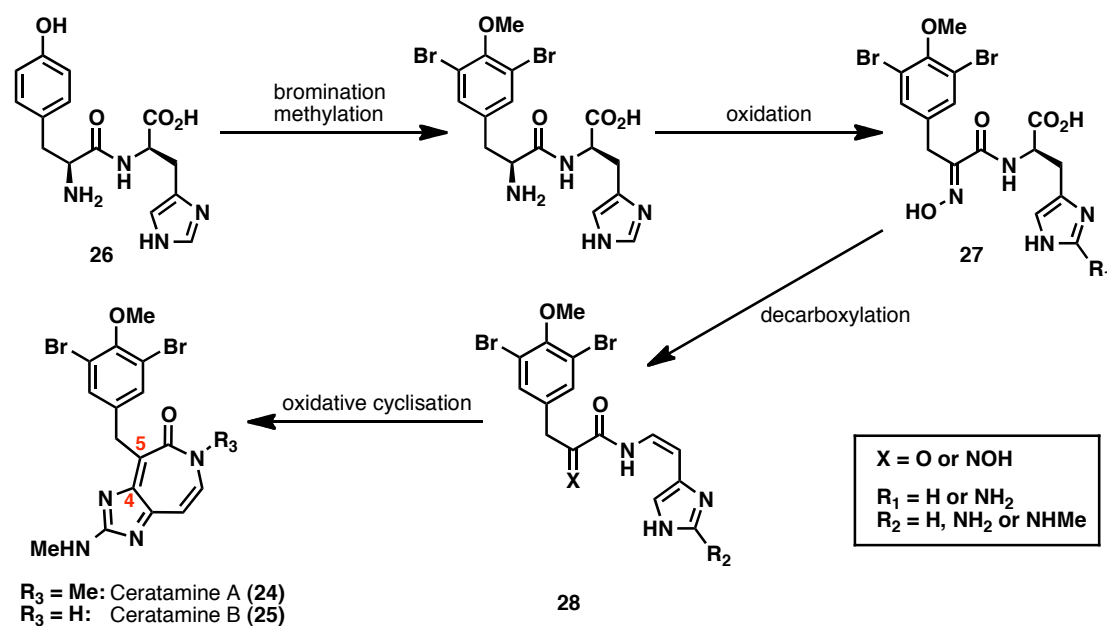


Figure 6 Structures of ceratamine A and B.

The presence of signals for slowly interconverting forms in the ^1H and ^{13}C NMR spectra indicated the ceratamines existed preferentially as one of two tautomeric forms (4:1 ratio). Scalar coupling observed between Me-19 and NH-18 suggested the major tautomer was of that illustrated in Figure 6. Structurally, the ceratamines are unlike any bromotyrosine-derived products previously isolated; the characteristic 3,5-

^{††} This assay quantitatively determined antimitotic activity by detecting MCF-7 cells halted in mitosis by an Enzyme-Linked ImmunoSorbant Assay (ELISA) using the monoclonal antibody TG-3 (See Ref 52).

dibromo-4-methoxybenzyl motif is appended to a novel imidazo[4,5,*d*]azepine core.^{§§} Commencing with a tyrosine–histidine dipeptide (**26**) the proposed biosynthesis is depicted in Scheme 5. Following *bis*-bromination (by a VBPO) and methylation, the amino functionality is oxidised to give oxime **27**. Subsequent decarboxylation forms the *Z*-enamide **28** and it is also possible that the aminomethyl group is installed at this stage. Finally, an oxidative cyclisation between C-4 and C-5 furnishes the natural product.



Scheme 5 Proposed biosynthesis of the ceratamines.

In order to fully appreciate the biological activity of the ceratamines, it is necessary to describe their biological target, microtubules, in more depth.

1.3.4.1 Microtubules as an Anticancer Target

Microtubules are highly dynamic filamentous polymeric proteins that are key components of the eukaryotic cytoskeleton. They are involved in the development and maintenance of cell shape, cell motility, and cell surface specialisation.^{54,55} They also act as intracellular highways, trafficking organelles such as mitochondria and vesicles through the highly congested cytoplasm.⁵⁶ A key cellular function of microtubules is the role they play in the assembly of the mitotic spindle and thus the separation of duplicated chromosomes during mitosis.⁵⁷ Microtubules are composed of tight α - and

^{§§} Interestingly, Andersen and co-workers claimed, “The...core heterocycle in the ceratamines appears to have no precedent at any oxidation level among known natural products or synthetic compounds.” In fact, Waly and co-workers were the first to report the synthesis of a imidazo[4,5,*d*]azepine ring system (*J. Prakt. Chem.*, **1994**, 336, 86).

β -tubulin heterodimeric units that are arranged head to tail in a polar fashion into linear protofilaments (Figure 7).

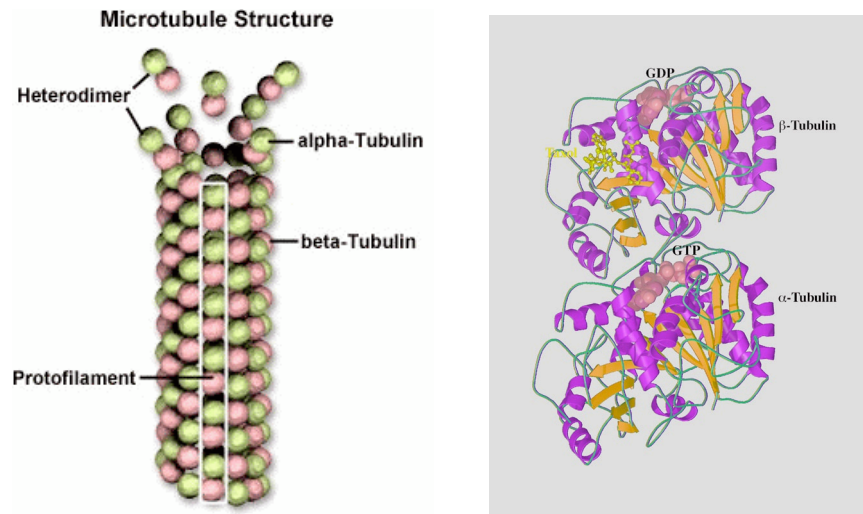


Figure 7 Left: structure of a microtubule; right: the $\alpha\beta$ -tubulin heterodimer. Images taken from http://vbaulin.front.ru/research/a_microtub.html and http://cryoem.berkeley.edu/papers/cyto_review/index.html.

In order for microtubules to perform their many tasks in maintaining a fully functional cell, they exhibit complex non-equilibrium dynamics.⁵⁸ Modulation of the sensitive non-equilibrium dynamics by external stimuli has a profound and detrimental effect on the structure and function of microtubules. Thus, exploiting the dependence of cellular processes such as mitosis on this dynamic behaviour makes microtubules an important target for anticancer agents.

Mitosis is a sequential series of cellular events that leads to the duplication and synchronous separation of sister chromatids to generate two identical daughter nuclei (Figure 8). It is an exquisitely sensitive process that relies on proper spindle function throughout all stages.

Upon the onset of mitosis, the interphase microtubule network disassembles and is replaced by a new microtubule population which is responsible for the formation of the mitotic spindle. This new population exhibits high levels of dynamic instability.⁵⁹ Following breakdown of the nuclear membrane in the prophase, microtubules sprout out from their centrosomal anchor in an attempt to capture kinetochores to form the bipolar metaphase spindle (prometaphase).⁶⁰

As this spindle provides the structural framework for segregation of duplicated chromosomes, failure of even a single chromosome to achieve bipolar attachment to the spindle can lead to cell cycle arrest and the onset of the apoptotic cascade.⁶¹ Thus, disruption of these sensitive dynamics has critical consequences for cell fate and makes microtubules a valuable therapeutic target, especially in oncology.

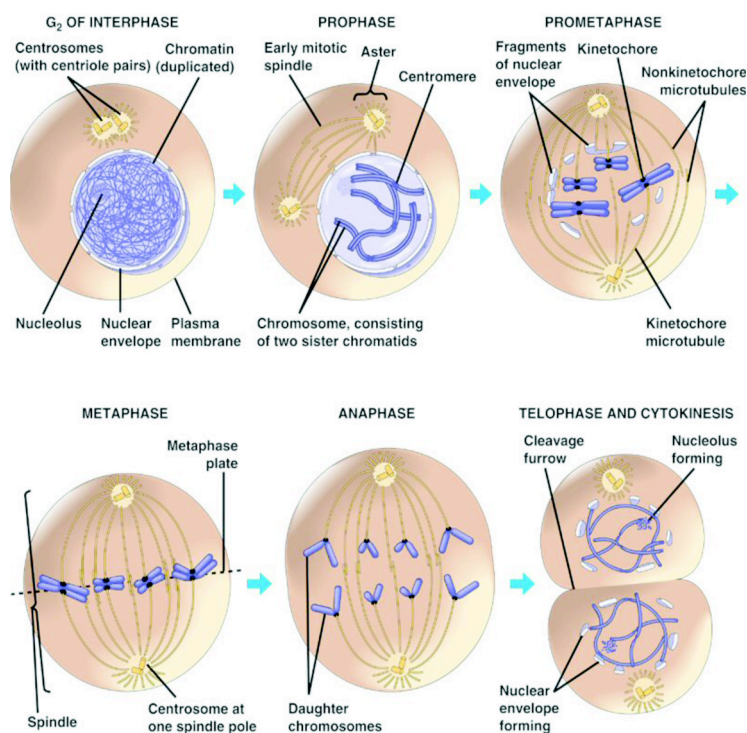


Figure 8 Microtubules are important in all phases of mitosis. Image reproduced from http://kvhs.nbed.nb.ca/gallant/biology/mitosis_phases.html.

Microtubule-targeted antimetabolic drugs can be categorised into two distinct functional classes based on their mechanistic ability to disrupt microtubule polymerisation. Microtubule destabilising agents inhibit microtubule polymerisation and comprise of a large number of structural chemotypes such as the *Vinca* alkaloids (vinblastine), halichondrin B, estramustine, spongistatin 1, colchicine and combretastatin. In 1979, Horwitz and co-workers discovered that the potent biological activity of paclitaxel arose from its ability to stabilise microtubules, a previously uncharacterised mode of action.⁶² To date, there are approximately ten known microtubule-stabilising chemotypes and therefore are far less numerous than their destabilising counterparts. Significantly, all naturally-occurring stabilising agents have complex architectures that contain multiple stereocentres. As a consequence, synthesising the gram/kilogram quantities required for clinical trials and global distribution following approval is technically demanding and therefore costly. This expense is then reflected in the price

of the drug and ultimately prevents some patients gaining access to a potentially life-saving treatment. However, industrial and academic efforts to discover non-natural microtubule-stabilising chemotypes have proved unsuccessful^{***} and currently, microtubule-stabilising agents are either natural products or semi-synthetic derivatives. Arguably the most famous example is the taxanes with others including the epothilones, discodermolides, sarcyodyctins and eleutherosides.¹

The taxanes represent some of the most important drugs in cancer chemotherapy and are testament to the relevance of microtubules as a therapeutic target.⁶³ However, sub-optimal pharmaceutical properties such as poor solubility, undesirable side effects and more crucially the development of resistance, limits their effectiveness and emphasises the need for a new generation of superior microtubule-stabilising agents.

1.3.4.2 Ceratamines: Biological Activity

The ceratamines were found to be capable of directly promoting the polymerisation of microtubules *in vitro*.⁶⁴ These are reportedly the first heterocyclic alkaloids of marine or terrestrial origin known to stabilise microtubules, the inference being that small achiral drug-like molecules may be able to modulate microtubule dynamics through microtubule stabilisation.

Both ceratamine A and B inhibited proliferation of MCF-7 cells (breast cancer) at low micromolar concentrations (IC₅₀ 2 μ M and 3 μ M, respectively). Treatment of cells with ceratamine A and B for 16 hours resulted in a concentration-dependent accumulation of cells with condensed mitotic chromosomes. Flow cytometry showed that these cells were halted in M phase and not G₂ of the cell cycle thus proving the ceratamines are genuine antimitotic agents. Microtubule turbidity assays showed that, **24** and **25** could promote polymerisation at a concentration of 100 μ M. Despite the fact this was to a lesser extent and at a ten-fold higher concentration than paclitaxel it was still a remarkable result. Furthermore there is a possibility that ceratamines bind to a previously unidentified site on tubulin as it was observed that a 25-fold excess of ceratamine A failed to displace [³H]-paclitaxel from its binding site on β -tubulin.

^{***} The exception being the discovery of GS-164, a novel small synthetic molecule, reported to polymerise microtubules *in vitro* and in HeLa cells. (*Cancer Chemother. Pharmacol.*, **1997**, *40*, 513).

Immunofluorescence microscopy revealed that ceratamines produced some interesting effects at the cellular level that have not been observed with other microtubule-stabilising agents. At 20 μ M, ceratamine A disrupted the interphase microtubule network of MCF-7 cells by causing a pronounced accumulation of microtubules that partially or completely encircled the nucleus (Figure 9 b and d).

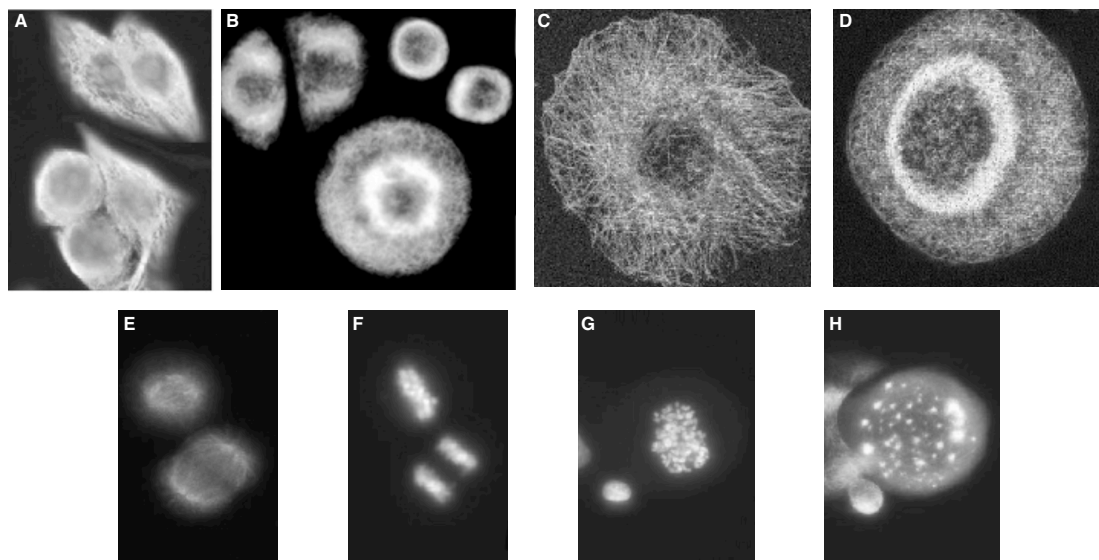


Figure 9 Effect of ceratamine A (20 μ M) on cellular microtubules. (a & c) Untreated interphase cells; (b & d) treated interphase cells; (e) mitotic spindle of untreated cell; (f) alignment of chromatids in untreated mitotic cells; (g) treated mitotic cell showing no alignment of chromatids; (h) treated mitotic cell showing multiple foci of staining. Microtubules stained with β -tubulin E7 monoclonal antibody (a-e and h); DNA stained with Hoechst 33258 (f and g). Images reproduced from *Cancer Res.*, **2005**, 65, 3040.

In mitotic cells, the condensed sister chromatids were not equatorially aligned and there was no evidence of a mitotic spindle (Figure 9 g and h, respectively). Instead, multiple foci of β -tubulin staining were scattered throughout the cell, which on cross sectional analysis revealed them to be pillar like structures that spanned the entire thickness of the cell.

These biological properties made it clear that the ceratamines were worthy of further investigation. However, due to the limited amounts of **24** (8 mg), and **25** (14 mg) obtained from the natural source, total synthesis represented the only viable way of accessing material on which to conduct further testing. During the course of this project, the groups of Andersen and Coleman have disclosed synthesis strategies towards the ceratamines.⁶⁵ These will be reviewed in Chapter 4 prior to a discussion of the Ley group approach.

1.4 References

- ¹ K. H. Altmann and J. Gertsch, *Nat. Prod. Rep.*, **2007**, *24*, 327; Anticancer Agents from Natural Products. Eds. G. M. Cragg, D. G. I. Kingston and D. J. Newman, **2005**, CRC Taylor and Francis, Boca Raton.
- ² G. C. Tron, T. Pirali and G. Sorba, *J. Med. Chem.*, **2006**, *49*, 3033.
- ³ A. Conlin, M. Fornier, C. Hudis, S. Kar and P. Kirkpatrick, *Nature Rev. Drug. Discov.*, **2007**, *6*, 953.
- ⁴ Biodiversity and Natural Product Diversity. Ed. F. Pietra, *Tetrahedron Organic Chemistry Series*, **2002**, *21*, 79.
- ⁵ M. Satake, *Top. Heterocycl. Chem.*, **2006**, *5*, 21.
- ⁶ J. W. Blunt, B. R. Copp, W-P. Hu, M. H. G. Munro, P. T. Northcote and M. R. Prinsep, *Nat. Prod. Rep.*, **2008**, *25*, 35; J. W. Blunt, B. R. Copp, W-P. Hu, M. H. G. Munro, P. T. Northcote and M. R. Prinsep, *Nat. Prod. Rep.*, **2009**, *26*, 170.
- ⁷ G. W. Gribble, *Naturally Occurring Organohalogen Compounds – A Comprehensive Update*, Springer, New York, **2010**, 4.
- ⁸ G. W. Gribble, *J. Chem. Ed.*, **1994**, *71*, 907.
- ⁹ T. Suzuki, M. Suzuki, A. Furusaki, T. Matsumoto, E. Kurosawa, A. Kato and Y. Imanaka, *Tetrahedron Lett.*, **1985**, *26*, 1329.
- ¹⁰ E. Drechsel, *Zeitschrift fur Biologie*, **1896**, *33*, 85.
- ¹¹ G. W. Gribble, *Am. Sci.*, **2004**, *92*, 342.
- ¹² <http://dl.clackamas.cc.or.us/ch105-09/standard.htm>
- ¹³ P. Ciminiello, E. Farrourusso, S. Magno and M. Pansini, *J. Nat. Prod.*, **1995**, *58*, 689.
- ¹⁴ C. T. Morner, *Z. Physiol. Chem.*, **1913**, *88*, 138.
- ¹⁵ G. M. Sharma and P. R. Burkholder, *Tetrahedron Lett.*, **1967**, *8*, 4147; G. M. Sharma and P. R. Burkholder, *J. Antibiot. (Tokyo)*, **1967**, *20*, 200.
- ¹⁶ H. Vilter, *Phytochemistry*, **1984**, *23*, 1387.
- ¹⁷ A. Butler and J. N. Carter-Franklin, *Nat. Prod. Rep.*, **2004**, *21*, 180.
- ¹⁸ M. N. Isupov, A. R. Dalby, A. A. Brindley, Y. Izumi, T. Tanabe, G. N. Murshudov and J. A. Littlechild, *J. Mol. Biol.*, **2000**, *299*, 1035.
- ¹⁹ H. S. Soedjak, J. V. Walker and A. Butler, *Biochemistry*, **1995**, *34*, 12689.
- ²⁰ A. Butler, *Coord. Chem. Rev.*, **1999**, *187*, 88.

- ²¹ M. C. Feiters, C. Leblanc, F. C. Küpper, W. Meyer-Klaucke, G. Michel and P. Potin, *J. Am. Chem. Soc.*, **2005**, *127*, 15340; H. Eshtiagh-Hosseini, M. R. Housaindokht, M. Chahkandi and A. Morsali, *Transit. Metal Chem.*, **2010**, *35*, 939; E. de Boer and R. Wever, *J. Biol. Chem.*, **1988**, *263*, 12326; J. Littlechild, E. G. Rodriguez and M. Isupov, *J. Inorg. Biochem.*, **2009**, *103*, 617; A. Butler and M. Sandy, *Nature*, **2009**, *460*, 848.
- ²² H. Yamada, N. Itoh, S. Murakami and Y. Izumi, *Agric. Biol. Chem.*, **1985**, *49*, 2961.
- ²³ J. Peng, J. Li and M. T. Hamann, *The Alkaloids*, **2007**, *61*, 59.
- ²⁴ R. M. van Wagoner, J. Jompa, A. Tahir, C. M. Ireland, *J. Nat. Prod.*, **1999**, *62*, 794.
- ²⁵ L. Arabshahi and F. J. Schmitz, *J. Org. Chem.*, **1987**, *52*, 3584.
- ²⁶ M. M. Mack, T. F. Molinski, E. D. Buck and I. N. Pessah, *J. Biol. Chem.*, **1994**, *269*, 23236.
- ²⁷ L. Chen, T. F. Molinski and I. N. Pessah, *J. Biol. Chem.*, **1999**, *274*, 32603; I. N. Pessah, T. F. Molinski, T. D. Meloy, P. Wong, E. D. Buck, P. D. Allen, F. C. Mohr and M. M. Mack, *Am. J. Physiol.*, **1997**, *272*, C601.
- ²⁸ D. M. Roll, C. W. J. Chang, P. J. Scheuer, G. A. Gray, J. N. Shoolery, G. K. Matsumoto, G. D. van Duyne and J. Clardy, *J. Am. Chem. Soc.*, **1985**, *107*, 2916; S. Tsukamoto, H. Kato, H. Hirota and N. Fusetani, *Tetrahedron*, **1996**, *52*, 8181.
- ²⁹ J. E. Coleman, R. van Soest and R. J. Andersen, *J. Nat. Prod.*, **1999**, *62*, 1137;
- ³⁰ N. K. Gulavita, S. A. Pomponi and A. E. Wright, *J. Nat. Prod.*, **1995**, *58*, 954.
- ³¹ A. Rudi, T. Evan, M. Aknin and Y. Kashman, *J. Nat. Prod.*, **2000**, *63*, 832.
- ³² A. B. Friedrich, I. Fischer, P. Proksch, J. Hacker and U. Hentschel, *FEMS Microbiol. Ecol.*, **2001**, *38*, 105.
- ³³ R. P. Walker, J. E. Thompson and D. J. Faulkner, *Mar. Biol.*, **1985**, *88*, 27.
- ³⁴ R. Ebel, M. Brenzinger, A. Kunze, H. J. Gross and P. Proksch, *J. Chem. Ecol.*, **1997**, *23*, 1451.
- ³⁵ P. Proksch, A. Putz, S. Ortlepp, J. Kjer and M. Bayer, *Phytochem. Rev.*, **2010**, *9*, 475.

- ³⁶ A. Koulman, P. Proksch, R. Ebel, A. C. Beekman, W. van Uden, A. W. T. Konings, J. A. Pedersen, N. Pras and H. J. Woerdenbag, *J. Nat. Prod.*, **1996**, *59*, 591.
- ³⁷ S. P. Gunasekera and S. S. Cross, *J. Nat. Prod.*, **1992**, *55*, 509.
- ³⁸ H. Nakamura, H. Wu and J. Kobayashi, *Tetrahedron Lett.*, **1985**, *26*, 4517.
- ³⁹ S. A. Ross, J. D. Weete, R. F. Schinazi, S. S. Wirtz, P. Tharnish, P. J. Scheuer and M. T. Hamann, *J. Nat. Prod.*, **2000**, *63*, 501.
- ⁴⁰ M. W. McCulloch, G. S. Coombs, N. Banerjee, T. S. Bugni, K. M. Cannon, M. K. Harper, C. A. Veltri, D. M. Virshup and C. M. Ireland, *Bioorg. Med. Chem.*, **2009**, *17*, 2189.
- ⁴¹ S. Tsukamoto, H. Kato, H. Hirota and N. Fusetani, *J. Org. Chem.*, **1996**, *52*, 8181.
- ⁴² R. A. K. Mierzwa, M. A. Conover, S. Tozzi, M. S. Puar, M. Patel and S. J. Covan, *J. Nat. Prod.*, **1994**, *57*, 175.
- ⁴³ J-H. Jang, R. W. M. van Soest, N. Fusetani and S. Matsunaga, *J. Org. Chem.*, **2007**, *72*, 1211.
- ⁴⁴ G. M. Nicholas, G. L. Newton, R. C. Fahey and C. A. Bewley, *Org. Lett.*, **2001**, *3*, 1543.
- ⁴⁵ M. S. Buchanan, A. R. Carroll, G. A. Fechner, A. Boyle, M. Simpson, R. Addepalli, V. M. Avery, J. N. A. Hooper, T. Cheung, H. Chen and R. J. Quinn, *J. Nat. Prod.*, **2008**, *71*, 1066.
- ⁴⁶ E. Fattorusso, L. Minale and G. Sodano, *J. Chem. Soc., Chem. Commun.*, **1970**, 751; W. Fulmor, G. E. van Lear, G. O. Morton and R. O. Mills, *Tetrahedron Lett.*, **1970**, *11*, 4551.
- ⁴⁷ M. Gutiérrez, T. L. Capson, H. M. Guzmán, J. González, E. Ortego-Barría, E. Quiñoá and R. Riguera, *Pharm. Biol.*, **2005**, *43*, 762.
- ⁴⁸ M. H. Kreuter, A. Bernd, H. Holzmann, W. Müller-Klieser, A. Maidhof, N. Weißmann, Z. Kljajic and R. Patel, *Z. Naturforsch.*, **1989**, *44c*, 680.
- ⁴⁹ M. H. Kreuter, R. E. Leake, F. Rinaldi, W. Müller-Klieser, A. Maidhof, W. E. G. Müller and H. C. Schröder, *Comp. Biochem. Physiol. B Comp. Biochem.*, **1990**, *97*, 151.
- ⁵⁰ S. Rodríguez-Nieto, M. González-Iriarte, R. Carmona, R. Muñoz-Chápuli, M. A. Medina and A. R. Quesada, *FASEB J.*, **2002**, *16*, 261; M. González-Iriarte,

- R. Carmona, J. M. Pérez-Pomares, D. Macís, M. Á. Medina, A. R. Quesada and R. Muñoz-Chapuli, *Angiogenesis*, **2003**, *6*, 251.
- ⁵¹ R. Córdoba, N. S. Tormo, A. F. Medarde and J. Plumet, *Bioorg. Med. Chem.*, **2007**, *15*, 5300.
- ⁵² M. Roberge, B. Cinel, H. J. Anderson, L. Lim, X. Jiang, L. Xu, C. M. Bigg, M. T. Kelly and R. J. Andersen, *Cancer Res.*, **2000**, *60*, 5052.
- ⁵³ E. Manzo, R. van Soest, L. Matainaho, M. Roberge and R. J. Andersen, *Org. Lett.*, **2003**, *5*, 4591.
- ⁵⁴ M. A. Handel and L. E. Roth, *Dev. Biol.*, **1971**, *25*, 78; I. Karl and J. Hahn-Bereiter, *Cell Biochem. Phys.*, **1998**, *29*, 225.
- ⁵⁵ L. V. Domnina, J. A. Rovensky, J. M. Vasiliev and I. M. Gelfand, *J. Cell Sci.*, **1985**, *74*, 267; S. Rhee, H. Jiang, C. H. Ho and F. Grinnell, *Proc. Natl. Acad. Sci. U. S. A.*, **2007**, *104*, 5425.
- ⁵⁶ G. S. Bloom and L. S. Goldstein, *J. Cell Biol.*, **1998**, *141*, 1277.
- ⁵⁷ A. Khodjakov and T. Kapoor, *Curr. Biol.*, **2005**, *15*, R966; J. G. DeLuca, *Curr. Biol.*, **2007**, *17*, R966.
- ⁵⁸ T. Mitchison and M. Kirschner, *Nature*, **1984**, *312*, 237.
- ⁵⁹ N. M. Rusan, C. J. Fagerstrom, A-M. C. Yvon and P. Wadsworth, *Mol. Biol. Cell*, **2001**, *12*, 971.
- ⁶⁰ J. H. Hayden, S. S. Bowser and C. L. Rieder, *J. Cell Biol.*, **1990**, *111*, 1039.
- ⁶¹ K. L. Wendell, L. Wilson and M. A. Jordan, *J. Cell Sci.*, **1993**, *104*, 261.
- ⁶² P. B. Schiff, J. Fant and S. B. Horwitz, *Nature*, **1979**, *277*, 665.
- ⁶³ M. L. Miller and I. Ojima, *Chem. Rev.*, **2001**, *1*, 195.
- ⁶⁴ G. Karjala, Q. Chan, E. Manzo, R.J. Andersen and M. Roberge, *Cancer Res.*, **2005**, *65*, 3040.
- ⁶⁵ R. S. Coleman, E. L. Campbell and D. J. Carper, *Org. Lett.*, **2009**, *11*, 2133; M. Nodwell, J. L. Riffell, M. Roberge and R. J. Andersen, *Org. Lett.*, **2008**, *10*, 1051; M. Nodwell, A. Pereira, J. L. Riffell, C. Zimmerman, B. O. Patrick, M. Roberge and R. J. Andersen, *J. Org. Chem.*, **2009**, *74*, 995; M. Nodwell, C. Zimmerman, M. Roberge and R. J. Andersen, *J. Med. Chem.*, **2010**, *53*, 7843.

CHAPTER 2 *Part I*

Total Syntheses of (5)-Bromoverongamine,
Ianthelline and JBIR-44

Compound Numbering

In this chapter, the numbering of the carbon atoms in (5)-bromoverongamine and ianthelline is according to the convention outlined by Braekman and co-workers (Figure 10).¹

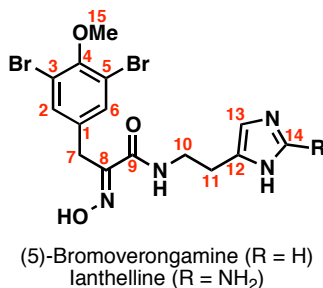


Figure 10 Atom labeling of (5)-bromoverongamine and ianthelline.

When discussing JBIR-44, the numbering system outlined by Fujiwara *et al.* will be adopted (Figure 11).²

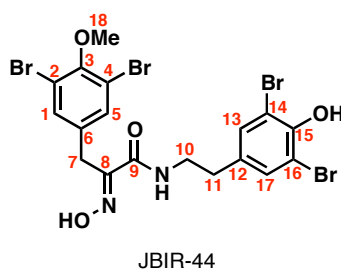


Figure 11 Atom labeling of JBIR-44.

2.1.1 Oxime Bromotyrosine Derivatives

Bromotyrosine compounds that possess oxime functionalities represent a fascinating class of compounds since naturally occurring oxime derivatives are relatively rare. Bromotyrosine-derived oximes are categorised into three subgroups* based on their structure: oxime–histamines, oxime–disulfides, and oxime–tyramines.

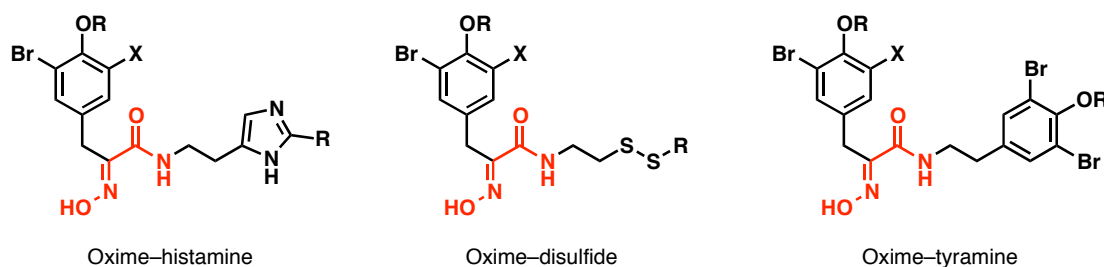


Figure 12 Structural classes of bromotyrosine-derived oximes. The (*E*)-2-(hydroxyimino)-*N*-alkylamide functionality is highlighted in red.

Upon isolation, the majority of these derivatives have been shown to possess a (*E*)-2-(hydroxyimino)-*N*-alkylamide functional motif (Figure 12). However, in 1987, Schmitz and co-workers reported the isolation of (*E,E*)-psammaplin A (1.18 g) along with much smaller quantities of (*E,Z*)-psammaplin A (**1**) (19 mg), the first bromotyrosine derivative known to possess the corresponding *Z*-isomeric motif.³ The geometry of the oxime groups could be assigned on the basis of the ¹H and ¹³C NMR chemical shifts corresponding to the methylene carbons (*C*-7 and *C*-7') α to the oximes (Figure 13).

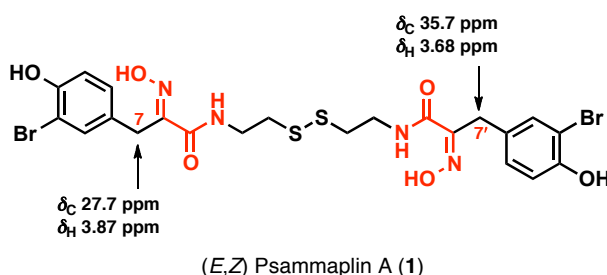


Figure 13 Structure of (*E,Z*)-psammaplin A (**1**) showing the signature chemical shifts.

The shift of *C*-7' (δ_C 35.7 ppm) is significantly downfield with respect to *C*-7 (δ_C 27.7 ppm) because, in the case of the *E*-oxime, the oxime hydroxyl and *C*-7 are in a *cis* relationship and this results in a phenomenon known as steric compression.⁴ The opposite trend is observed for the chemical shifts of the methylene protons (*H*-7', δ_H

* The bastadins also contain oxime functionalities but due to their unique macrocyclic structures, constitute their own group (see Section 1.3.2).

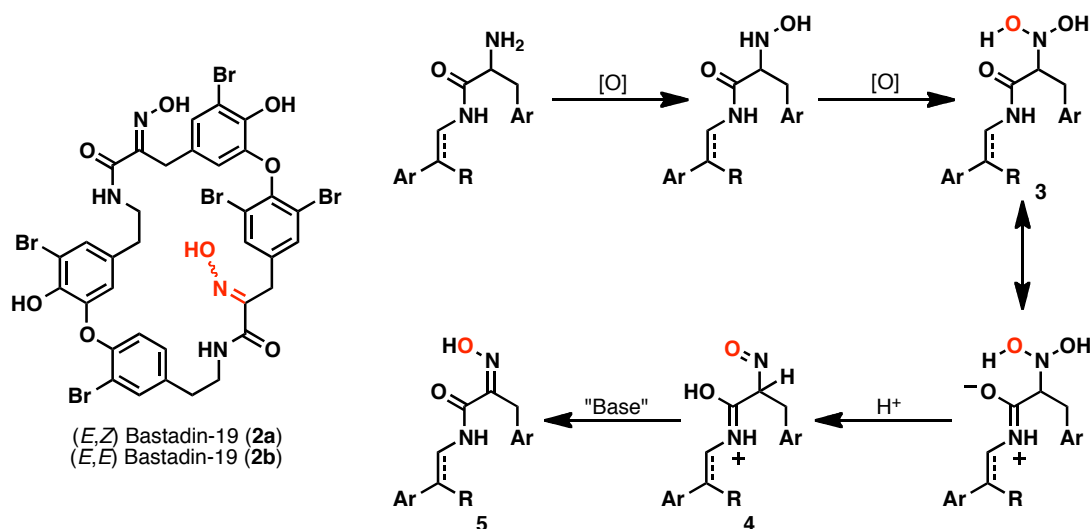
3.68 ppm; *H*-7, δ_{H} 3.87 ppm). ^1H NMR studies conducted by Karbatsos and co-workers showed that the α -methylene protons *cis* to an oxime hydroxyl are deshielded and appear further downfield than α -methylene protons *trans* to an oxime hydroxyl.⁵

Interestingly, it was discovered that a sample of **1** had isomerised to the corresponding (*E,E*)-isomer over the course of a couple of weeks; during this time it had been necessary to heat the sample to facilitate the evaporation of deuterated solvents. This led Schmitz and co-workers to postulate that the natural metabolite was in fact the (*Z,Z*)-isomer and that isomerisation occurred during the isolation procedure. It is therefore possible that all reported structures of bromotyrosine-derived oximes are, in fact, artifacts from isolation procedures. Despite the obvious implications, the scientific community has largely ignored this finding.

However, in 2010, Crews and co-workers isolated (*E,Z*)-bastadin-19 (**2a**) along with the previously reported (*E,E*)-bastadin-19 (**2b**) (Scheme 6) and agreeing with the hypothesis put forward by Schmitz, they sought to carry out further investigations.⁶ They were able to affect the photoisomerisation of **2b** to **2a** (310–330 nm) and showed that upon standing in *d*₆-DMSO (720 hours), **2a** reverted to the more thermodynamically stable **2b**.[†] Molecular mechanics calculations on a simplified structure showed that, where intramolecular H-bonding is minimised due to solvation, the *E*-oxime is lower in energy than the corresponding *Z*-oxime by 4.0 kJ/mol. Furthermore, a plausible biosynthetic pathway was proposed[‡] for the bastadins and psammaplins which accounted for the initial formation of the *Z*-oxime (Scheme 6). Initially, it is thought two successive hydroxylations of the amine give intermediate **3**. Next, elimination of water from the oxyanion amide resonance forms the nitroso species **4** and this can then undergo base-catalysed tautomerisation to furnish *Z*-oxime **5**.

[†] Oximes are known to exhibit configurational stability in the solid state. In solution, there exists an equilibrium between the *E* and *Z* isomers and over time, the thermodynamically favoured isomer predominates.

[‡] It is an extension of the proposed pathway for the biosynthesis of nocardicin A (*J. Bacteriol.* **2005**, *187*, 739).



Scheme 6 Left: structures of **2a** and **2b**; right: biosynthetic pathway of psammaplins and bastadins proposed by Crews and co-workers.⁶

Given that the neighbouring amide facilitates the specific elimination of the *anti* hydroxyl group, it would appear this biosynthetic pathway is applicable to all bromotyrosine derivatives that contain the α -oximino amide motif. This then raises the pertinent issue regarding which oxime geometry is of biological relevance to the parent sponge. Investigations examining the bioactivity of bromotyrosine derivatives as a function of oxime geometry have not been undertaken, however, one would assume that by altering the spatial arrangement (*E* vs. *Z*) of a hydrogen bond donor, the activity of the derivative would be significantly affected.

2.1.2 Biological Activity of Bromotyrosine-Derived Oximes

2.1.2.1 Antifouling Activity

Biofouling is the growth and accumulation of macro and microorganisms on the surface of submerged objects.⁷ This process is largely undesirable and the cost to industry, caused by the build-up of crustaceans (in particular barnacles) and microorganisms on man-made structures, runs in to billions of dollars on an annual basis. For example, it has been estimated that biofouling can reduce the speed of a ship by 10% and that 40% more fuel is needed to overcome the added drag.⁸

Traditionally, surfaces were coated with paint that contained toxic agents such as tributyltin and triphenyltin compounds to prevent the accumulation of marine organisms. However in recent years, the use of these organotin compounds has been

phased out[§] and therefore, there is a need for the development of new non-toxic antifouling agents. Over the last decade, the search for novel compounds that fulfill this criteria has focused on marine sponges since it is well known that their surfaces are devoid of biofouling organisms (Section 1.3.3). Two excellent reviews by Fusetani focus on the ecological roles of antifouling marine natural products together with their industrial applications.⁹

Recent studies by Proksch and co-workers identified the oxime moiety as the common pharmacophore of bromotyrosine compounds that inhibited the settlement of barnacle larvae (*Balanus improvisus*).¹⁰ Hemibastadin-1 (**6**), psammaplin A (**10**) and aplysamine-2 (**9**), along with several bastadin derivatives, were shown to inhibit settlement in a dose-dependent fashion (1–10 μ M). Several analogues of **6** were synthesised to evaluate the basic structure–activity relationship (Figure 14). The dibromo analogue **7** exhibited the same potency (MIC 10 μ M) whereas the desbromo analogue **8** was significantly less active (MIC 100 μ M); the analogue lacking the oxime functionality (**11**) had no effect on larvae settlement.

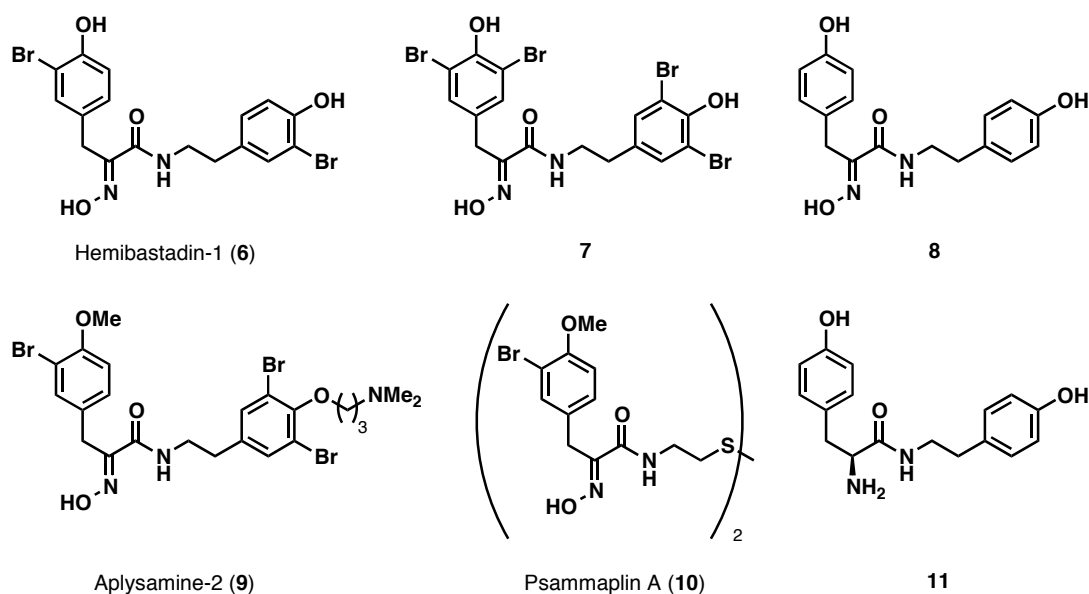


Figure 14 Structures of antifouling natural products and analogues.

Whilst the mode of action of these antifouling agents is still unknown,^{**} the antifouling activities of **6** are currently being tested in a more relevant environment.¹¹

[§] In 2008, the use of organotin compounds for antifouling purposes was prohibited.

^{**} It has been suggested that either the oxime may be converted to nitric oxide, or, these derivatives directly perturb the levels of intracellular Ca^{2+} in barnacle larvae.

2.1.2.2 Anticancer Activity

A number of bromotyrosine oximes including purealidin A¹² and C,¹³ aplysamines 3–5,¹⁴ purpuramines I and J,¹⁵ and bastadin 4, 8, and 9¹⁶ are known to exhibit cytotoxicity in a variety of cancer cell lines. In particular, purealidin N (**12**) (an oxime–histamine) showed significant cytotoxicity against murine lymphoma L1210 cells (EC_{50} 147 nM) and KB human epidermoid carcinoma cells (EC_{50} 155 nM) (Figure 15).¹⁷ In addition to these cytotoxic products, compounds with more specific modes of action, relevant to preventing cancer progression have also been discovered.

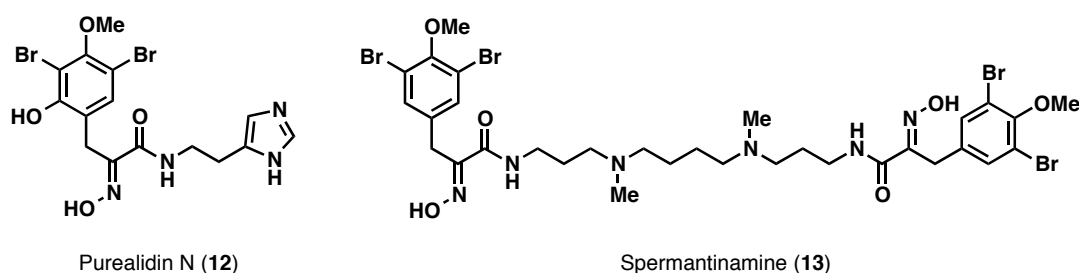


Figure 15 Structures of purealidin N (**12**) and spermatinamine (**13**).

Isoprenylcysteine carboxyl methyl transferase (Icmt) is a relatively new enzyme target in anticancer drug discovery. Icmt catalyses the methylation of the *C*-terminal prenylcysteine found on prenylated proteins; this is required for the correct localisation and functions of these proteins, most notably GTPases in the Ras superfamily. Ras is an oncogene and its hyperactivation is thought to contribute to carcinogenesis, therefore, inhibiting post-translational modification and preventing correct localisation of this family of proteins is attractive. Whilst several small-molecule inhibitors have been reported in the literature, spermatinamine (**13**) was the first natural product inhibitor of Icmt (IC_{50} 1.9 μ M) to be discovered (Figure 15).¹⁸ Since then, aplysamine 6 (another bromotyrosine derivative) has also been found to inhibit Icmt to a similar degree (IC_{50} 14 μ M).¹⁹

Psammaphin A (**10**) (Figure 14) is an oxime disulfide that is cytotoxic (EC_{50} 180–980 nM) towards human lung, ovarian, CNS, skin and colon cancer cell lines. Furthermore it was found to be a potent inhibitor (IC_{50} 4.2 ± 2.4 nM) of histone deacetylase (HDAC), an enzyme that modulates the levels of histone acetylation. In fact, **10** is more potent than the canonical HDAC inhibitor trichostatin A. HDAC inhibition by **10** in human endometrial cancer cells caused increased levels of acetylated histone H3 and H4, cell cycle arrest, and induction of an apoptotic pathway.²⁰ Mechanistically, it is thought the disulfide bond is cleaved in the reducing

environment of the cell and that the resulting sulfhydryl group coordinates a zinc ion in the HDAC active site.²¹

Over recent years, research into this class of compounds has gathered pace given their diverse biological activity profile, and it is clear that they warrant further investigation as potential anticancer lead compounds. The research within this chapter describes the synthesis of three bromotyrosine-derived oximes and analogues thereof. Their cytotoxic activities were then evaluated on human cancer cell lines.

2.1.3 (5)-Bromoverongamine, ianthelline and JBIR-44

2.1.3.1 Isolation and Biological Activity

(5)-Bromoverongamine (**14**) (Figure 16) was isolated in 1998 from a *Pseudoceratina* sp. and was reported to inhibit the settlement of barnacle larvae at 10 mg/mL (IC₅₀ 1.03 mg/mL).¹ More recently, **14** has also been shown to be bactericidal towards methicillin-resistant *Staphylococcus aureus* (MRSA) (MIC 0.0625-0.5 mg/L).²² The isolation of ianthelline (**15**) (Figure 16) from *Ianthella ardis* was reported in 1986 and it exhibited moderate activity as an antibacterial and antifungal agent against *S. aureus* and *Candida albicans*.²³ It has since been isolated from at least two more species of sponge and was also shown to be an antifouling agent by inhibiting bacterial attachment to agar blocks.^{24,25} A virtual screen has also suggested that **15** may be a SARS-coronavirus proteinase inhibitor.²⁶

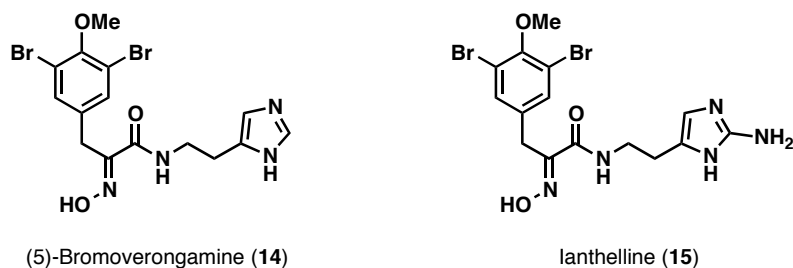
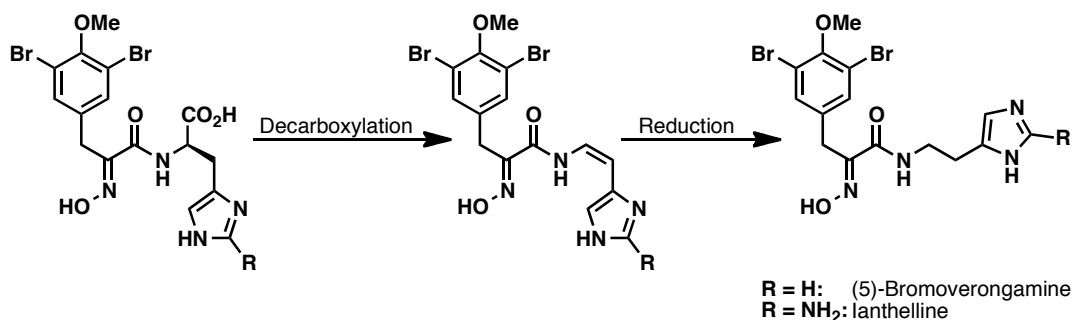


Figure 16 Structures of (5)-bromoverongamine (**14**) and ianthelline (**15**).

Structurally, **14** and **15** are analogous and possess the signature 3,5-dibromo-4-methoxyaryl group and *E*-oxime. They differ only at C-14, with **15** having an exocyclic amino group at this position. Furthermore, they are purported to share a

biogenetic relationship with ceratamines A and B (Section 1.3.4) and could be envisaged as cyclisation precursors (Scheme 7).^{††}



Scheme 7 Part of the proposed biosynthetic pathway of **14** and **15**. The oxime geometry is drawn as *E* to avoid confusion.

These two products were attractive synthetic targets for a number of reasons. Firstly, no total syntheses had been reported therefore, access to synthetic material would allow confirmation of the proposed structures. More importantly, despite their biogenetic relationship to the ceratamines and structural similarity to purealidin N (Figure 15) the anticancer properties of **14** and **15** had not been explored. Taking these considerations into account, both **14** and **15** warranted further investigation.

In 2009, during the course of the research into **14** and **15**, the isolation of JBIR-44 (**16**) from *Psammaphysilla purpurea* was reported. It was shown to exhibit cytotoxic activity in a dose-dependent manner against a human cervical cancer cell line (HeLa, EC₅₀ 3.7 μ M, 48 h) (Figure 17). Therefore, in light of this biological activity, and, as the left-hand portion of **16** is identical to that of both **14** and **15**, the total synthesis of **16** was also undertaken.

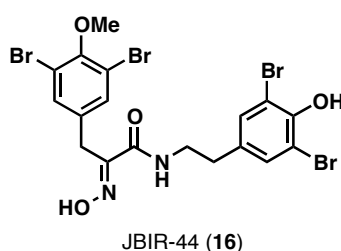
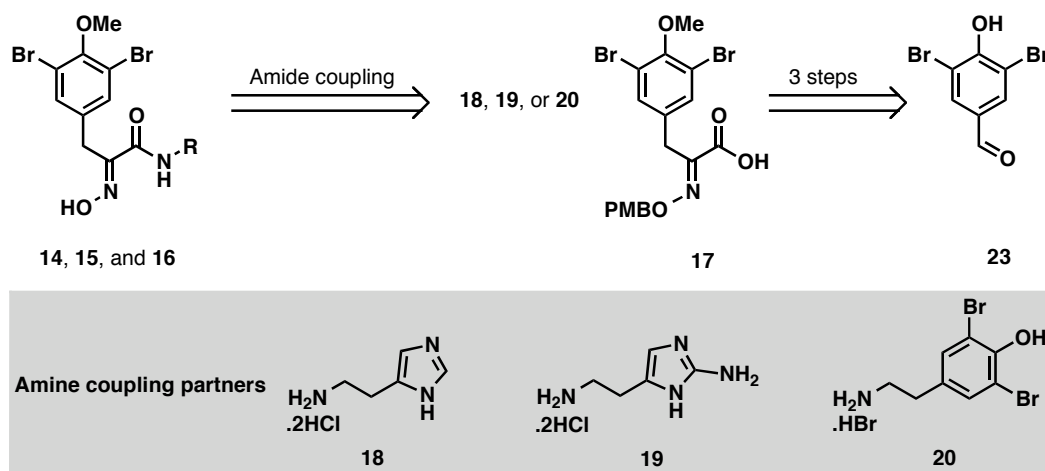


Figure 17 Structure of JBIR-44 (**16**).

^{††} It is not yet known if either **14** or **15** are direct biosynthetic precursors to the ceratamines.

2.1.3.2 Synthetic Strategy

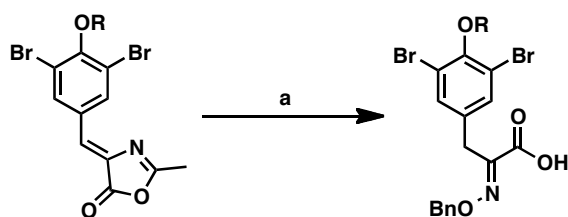
Retrosynthetically, it was envisaged that all three natural products could be accessed by elaboration of a common α -oximino acid (**17**) intermediate which in turn could be obtained in three steps from the commercially available 3,5-dibromo-4-hydroxybenzaldehyde (**23**) (Scheme 8). Amide coupling of **17** with the amine salts **18**, **19** or **20** followed by the removal of the PMB protecting group would furnish the desired bromotyrosine-derivatives **14**, **15**, and **16**, respectively.



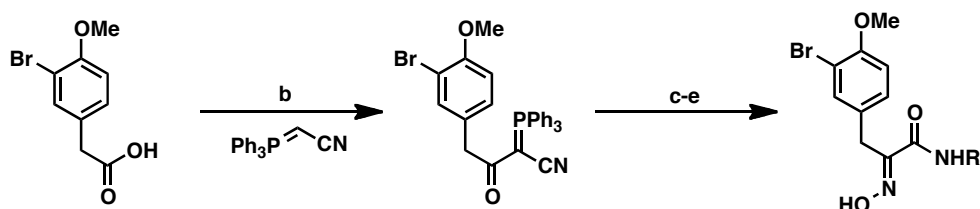
Scheme 8 Retrosynthetic analysis for the proposed synthesis of **14**, **15**, and **16** involving a common α -oximino acid intermediate **17**.

Synthetic routes to α -oximino acids, esters and amides closely related to **17** have been widely discussed in the literature. In addition to the most common approach *via* an azlactone intermediate (Scheme 9a),²⁷ other pathways include cyano ylide couplings (Scheme 9b)²⁸ and conversion of either amines (Scheme 9c),²⁹ or α -keto compounds (Scheme 9d)³⁰ directly to their corresponding oxime derivative. A more elegant approach employed a Horner–Wadsworth–Emmons reaction to couple Nakamura’s α -OTBS-functionalised dimethyl phosphonate (**22**) to an elaborated aldehyde (**21**) (Scheme 9e). This has been used to good effect in the synthesis of purealidin N (**12**)³¹ and bastadin analogues.³²

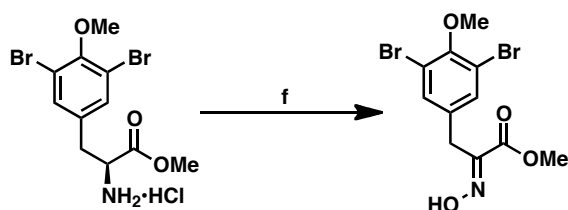
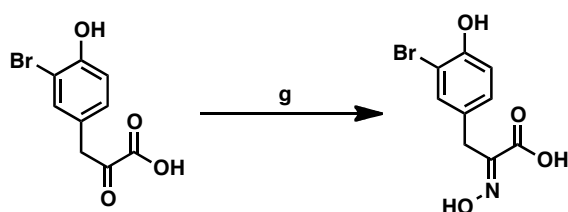
a) Azlactone intermediate



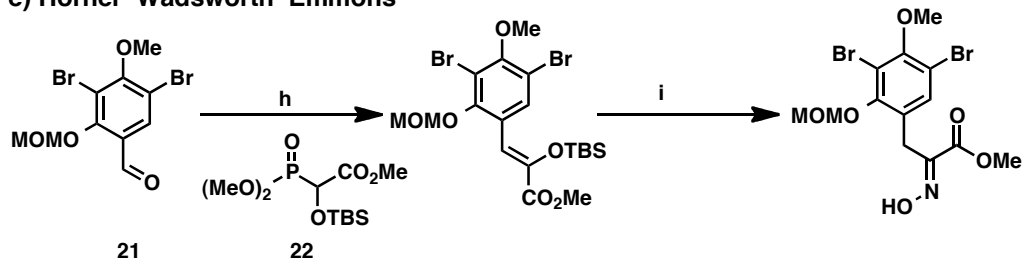
b) Cyano ylide coupling



c) Amine oxidation

d) α -Keto acid approach

e) Horner–Wadsworth–Emmons

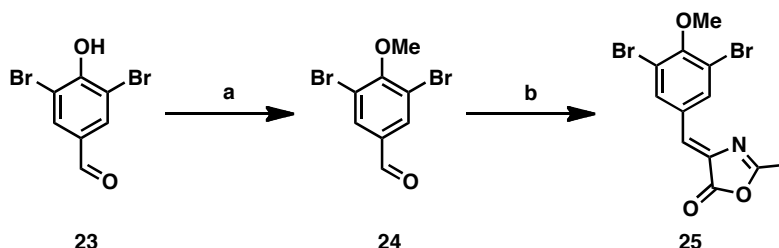
**Scheme 9** Different approaches to α -oximino compounds closely related to 17.

Reagents and conditions: (a) $\text{Ba}(\text{OH})_2 \cdot 8\text{H}_2\text{O}$, $\text{BnONH}_2 \cdot \text{HCl}$, 1,4-dioxane/ H_2O , 60 °C, 34%; (b) EDCI, CH_2Cl_2 , 82%; (c) O_3 , CH_2Cl_2 , -78 °C; (d) RNH_2 , *t*-BuOH; (e) $\text{NH}_2\text{OH} \cdot \text{HCl}$, NaOAc, EtOH, 52% three steps; (f) $\text{Na}_2\text{WO}_4 \cdot 2\text{H}_2\text{O}$, EtOH, H_2O_2 , H_2O , 25 °C, 4 h, 68%; (g) $\text{NH}_2\text{OH} \cdot \text{HCl}$, NaOAc, EtOH, rt, 57%; (h) LDA, THF, -78 °C, 92%; (i) $\text{HF} \cdot \text{Et}_3\text{N}$, MeOH then $\text{NH}_2\text{OH} \cdot \text{HCl}$, rt, 90%.

2.1.4 Results and Discussion

2.1.4.1 Synthesis of α -Oximino Acid **17**

The α -oximino acid intermediate **17** was accessed in three steps from the commercially available 3,5-dibromo-4-hydroxybenzaldehyde (**23**) (Scheme 10). Methylation of the phenol **23** was achieved with methyl iodide in the presence of potassium carbonate.³³ Then, azlactone **25** was subsequently formed by the treatment of **24** with *N*-acetylglycine and sodium acetate in acetic anhydride (Erlenmeyer conditions).³⁴



Scheme 10 Synthesis of azlactone **25**.

Reagents and conditions: (a) MeI, K₂CO₃, acetone, reflux, 6 h; (b) *N*-acetylglycine, NaOAc, Ac₂O, 120 °C, 90 min, 82% over 2 steps.

These two steps proceeded in an overall yield of 82% and the geometry of **25** was confirmed by X-ray crystallographic analysis to be the thermodynamically favoured *Z*-isomer (Figure 18).

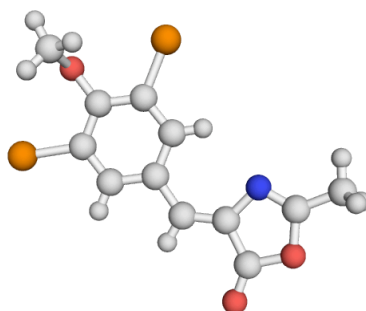
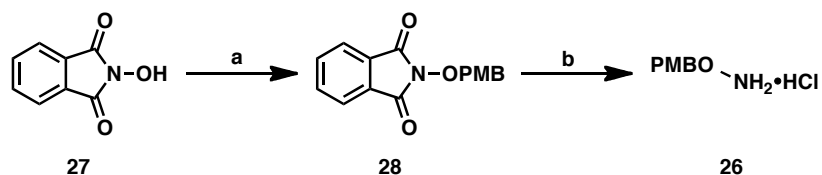


Figure 18 X-ray crystal structure of azlactone **25**.

Prior to formation of **17**, it was necessary to prepare *O*-*para*-methoxybenzyl (PMB) hydroxylamine hydrochloride (**26**) using a modified literature procedure (Scheme 11).³⁵ Protection of the free hydroxyl group of *N*-hydroxyphthalimide (**27**) with PMB chloride gave **28** in 59% yield. Removal of the phthalimide group with hydrazine

hydrate released the free hydroxylamine which, upon treatment with methanolic hydrogen chloride, furnished the desired hydrochloride salt **26**.

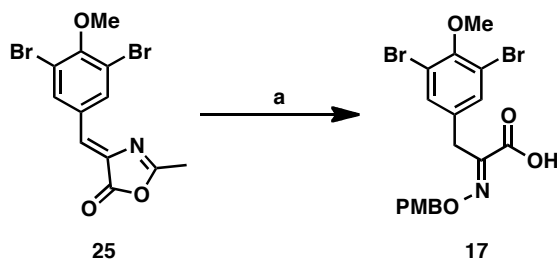


Scheme 11 Synthesis of protected hydroxylamine **26**.

Reagents and conditions: (a) PMB-Cl, Et₃N, DMF, 90 °C, 59%; (b) hydrazine hydrate, DMF/MeOH (1:2), 60 °C, then 1.25 M MeOH in HCl, 77%.

The one-pot saponification of the crude azlactone **25** with barium hydroxide octahydrate and subsequent condensation with **26** afforded the α -oximino acid intermediate (**17**) (Scheme 12). Furthermore, this reaction could be performed on a multi-gram scale with an isolated yield of up to 54%.

Chromatographic purification was problematic and co-elution of the product (**17**) with the unconsumed hydroxylamine **26** could not be prevented. Removal of excess **26** prior to the purification was attempted, however, several acidic/basic work up procedures were unsuccessful, as was the use of scavenger resins (PS-isocyanate or QP-SA). The reaction was also performed on purified **25** but no improvement was observed. Nevertheless, the isolated yield was an improvement on the literature precedent of 35% reported for similar systems.²⁷



Scheme 12 Synthesis of α -oximino acid **17**.

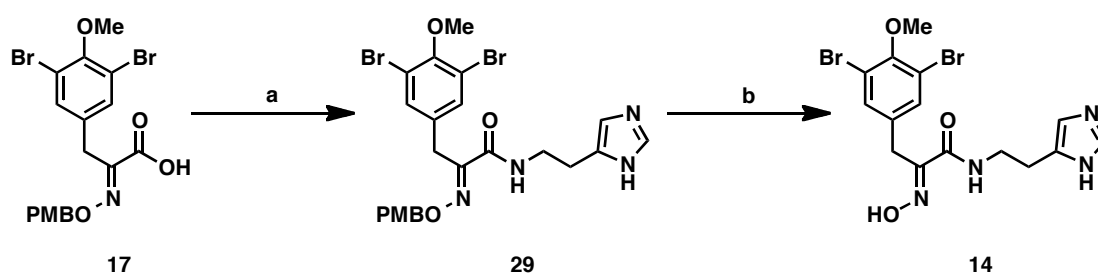
Reagents and conditions: (a) Ba(OH)₂·8H₂O, 1,4-dioxane/H₂O (1:1), 60 °C, 30 min then **26**, 6 h, 54%.

With a view to shortening the synthesis, it was investigated whether the PMB protection of the oxime was required. Following the saponification of **25** as previously described, hydroxylamine hydrochloride was used in place of **26** for the

subsequent condensation. However, efforts to isolate the desired product proved unsuccessful due to the intractability^{††} of the crude reaction mixture.

2.1.4.2 Synthesis of (5)-Bromoverongamine

With **17** in hand, the first task was to undertake the synthesis of (5)-bromoverongamine (**14**) as the required amine coupling partner was commercially available. Amide coupling of **17** and histamine dihydrochloride (**18**) with DCC and HOBT furnished *O*-PMB-(5)-bromoverongamine (**29**) in 81% yield (Scheme 13).



Scheme 13 Synthesis of (5)-bromoverongamine (**14**).

Reagents and conditions: (a) Histamine dihydrochloride, DCC, HOBT, $i\text{Pr}_2\text{EtN}$, CH_2Cl_2 , rt, 18 h, 81%; (b) AlCl_3 , anisole, CH_2Cl_2 , rt, 5 min, 78%.

The final step of the synthesis involved removal of the PMB protecting group. Investigations by Day and co-workers²⁷ on similar substrates found that an aluminium trichloride/anisole mixture cleanly unmasked PMB protected oximes whereas treatment with either DDQ or TMSCl/NaI led to decomposition. However, in our case there was a concern that these Lewis acidic conditions may also lead to demethylation of the activated *para*-methoxy functionality on the dibrominated aryl unit. Pleasingly, treatment of **29** with the aluminium trichloride/anisole mixture led to complete conversion after only 5 minutes^{§§} to furnish the natural product in 78% yield.

Whilst the ^1H NMR spectral data of synthetic **14** matched with that reported for the natural material, the assignment of the C-12 quaternary centre (δ_{C} 134.0 ppm) in the natural material did not correlate with the shift of C-12 (δ_{C} 135.9 ppm) in the synthetic material (see appendix).^{***} However, X-ray crystallographic analysis confirmed that the structure of synthetic **14** matched with that proposed for the natural

^{††} Given the already polar nature of PMB-oxime acid **17**, the additional polarity gained by the introduction of an unprotected oxime meant that purification was not possible by normal-phase chromatography.

^{§§} No demethylation was observed even up to a reaction time of 3 hours.

^{***} The original ^{13}C NMR spectrum for the natural material was kindly provided by Professor Jean Claude Braekman for comparison and is included in the appendix of this chapter.

material (Figure 19). Furthermore, this data also confirmed the *E*-geometry of the oxime and the tautomeric form of the imidazole ring.

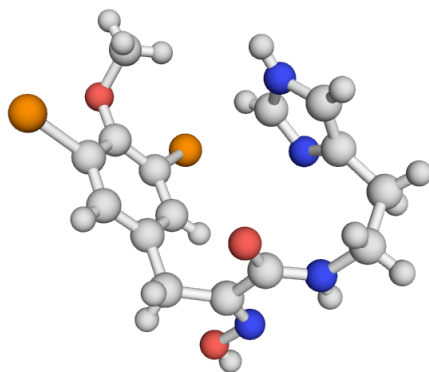
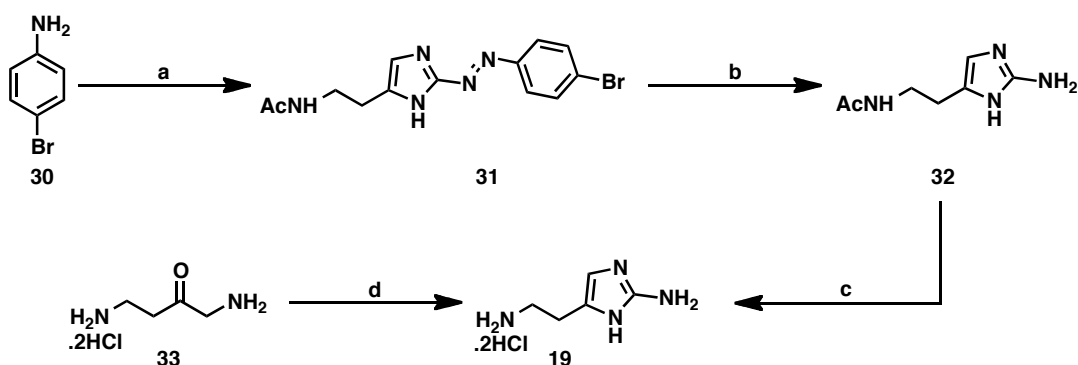


Figure 19 X-ray crystal structure of (5)-bromoverongamine (**14**).

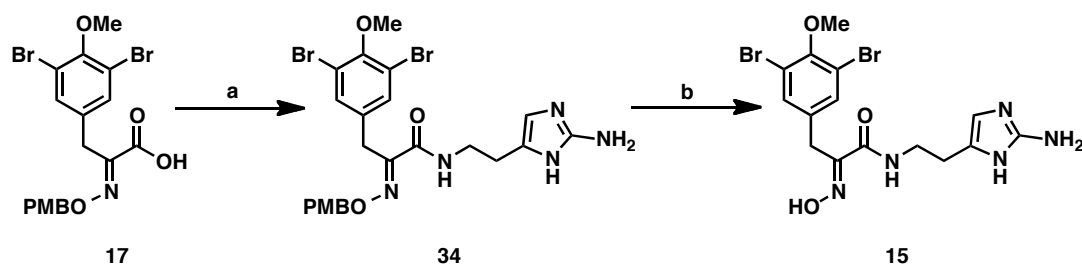
2.1.4.3 Synthesis of Ianthelline

As mentioned previously, Ianthelline is structurally analogous to **14**, differing only by the presence of an exocyclic amino group on the imidazole ring. However, the required 2-aminohistamine (**19**) coupling partner was neither inexpensive nor widely available from commercial sources. Coupling partner **19** could be synthesised by heating 1,4-diamino-2-butanone dihydrochloride (**33**) with excess cyanamide but it was not possible to isolate the product (Scheme 14) and using the crude mixture in the subsequent coupling reaction was unreliable. In an alternative strategy,³⁶ *N*-acetylhistamine was coupled to the diazonium species formed *in-situ* from sodium nitrite and *p*-bromoaniline (**30**) to form the desired 2-arylazo derivative **31**, along with the undesired 4-arylazo regioisomer and *bis*-adduct in a 3.4:2.4:1 ratio. Reductive cleavage of the azo-linkage with hydrogen over a platinum oxide catalyst initially gave the hydrobromide salt of **32** which could be freebased using a Dowex 50W X8 ion exchange resin to yield **32** in 14%. The acetate group was then hydrolysed with 6 *N* HCl to give **19** quantitatively.

Scheme 14 Synthesis of **19**.

Reagents and conditions: (a) NaNO₂, HCl, 0 °C, 30 min then *N*ω-acetylhistamine, NaHCO₃, 52%; (b) PtO₂, H₂, 4 bar, rt, 42 h, 14%; (c) 6 *N* HCl, 100 °C, 14 h, 100%; (d) cyanamide 50% w/w in H₂O, H₂O, pH 6, 60 °C, 2 h.

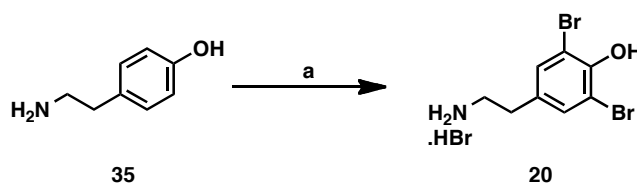
With quantities of **19** in hand, the synthesis of **15** could be realised (Scheme 15). A DCC/HOBt mediated coupling between **17** and **19** gave *O*-PMB-ianthelline (**34**) in 41% yield. PMB removal was achieved using the conditions previously mentioned to furnish ianthelline (**15**) in 44% yield. The ¹H and ¹³C NMR spectral data of synthetic ianthelline (**15**) were identical with those reported for the natural material (see appendix).

Scheme 15 Synthesis of ianthelline (**15**).

Reagents and conditions: (a) Histamine dihydrochloride, DCC, HOBt, *i*Pr₂EtN, CH₂Cl₂, rt, 18 h, 41%; (b) AlCl₃, anisole, CH₂Cl₂, rt, 5 min, 44%.

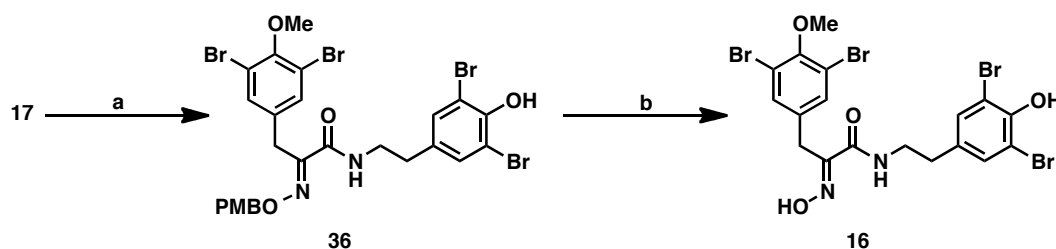
2.1.4.4 Synthesis of JBIR-44

The synthesis of dibromotyrosine side chain **20** had been reported previously in the literature. Following the procedure by Hamann and co-workers,³⁷ treatment of tyramine (**35**) with excess bromine in acetic acid only yielded a mixture of the desired product **20**, mono-brominated product and starting material in a 1:1:1.45 ratio. However, the synthesis of the amine side chain of JBIR-44 could be achieved in one step by heating **35** with bromine in methanol for 14 hours (Scheme 16).³⁸

Scheme 16 Synthesis of **20**.

Reagents and conditions: (a) MeOH, Br₂, 60 °C, 14 h, 68%.

The side chain **20** could then be coupled to acid **17** under the conditions described previously to furnish *O*-PMB-JBIR-44 (**36**) in moderate yield; alternative protocols (EDCI/HOBt, [®]T3P) were unsuccessful in improving this coupling. Removal of the PMB moiety proceeded cleanly to furnish JBIR-44 (**16**) in 85% yield (Scheme 17).

Scheme 17 Synthesis of JBIR-44 (**16**).

Reagents and conditions: (a) **20**, DCC, HOBt, *i*Pr₂EtN, CH₂Cl₂, rt, 18 h, 42%; (b) AlCl₃, anisole, CH₂Cl₂, rt, 5 min, 85%.

The ¹H and ¹³C NMR spectra for synthetic **16** matched those reported for the natural materials. However, the original assignments of C-8 (δ_C 153.8 ppm) and C-3 (δ_C 152.0 ppm) should be reversed on the basis of HMBC spectroscopy (Figure 20). For natural **16**, Fujiwara and co-workers reported a strong *m*-coupling between the aromatic protons *H*-1 and *H*-5 (δ_H 7.52 ppm) and the aromatic carbon (δ_C 152.0 ppm) and also observed the long range coupling of methylene protons *H*-7 (δ_H 3.87 ppm) to C-8 (δ_C 153.8 ppm). In the synthetic sample, we observed a strong *m*-coupling between aromatic protons *H*-1 and *H*-5 (δ_H 7.52 ppm) and the signal at (δ_C 153.8 ppm) which we have assigned to C-3. We also observed a long range coupling of the methylene protons *H*-7 (δ_H 3.87 ppm) to the signal at (δ_C 152.0 ppm) which we have assigned to C-8. Unfortunately, the HMBC spectrum for natural **16** was not available for direct comparison.

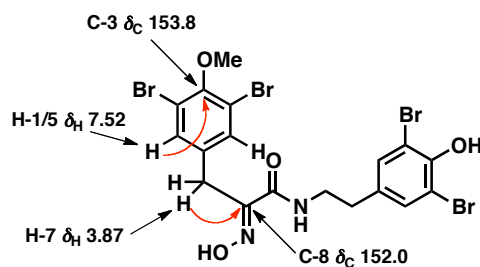


Figure 20 ^1H ^{13}C HMBC correlations for synthetic JBIR-44 (**16**).

2.1.4.5 Improving the Synthesis of α -Oximino Acid **17**

On completing the syntheses of **14**, **15** and **16** we wanted to investigate the possibility of improving the transformation of azlactone **25** to α -oximino acid **17** (due to its moderate yield and troublesome purification) as an efficient procedure would be necessary for analogue development. Instead of a one-pot procedure, a two-step procedure was envisaged as it is known that azlactones hydrolyse efficiently with acid under refluxing conditions to furnish the corresponding phenylpyruvic acid derivative³⁹ and that these can then be converted directly to the corresponding oxime by treatment with an appropriate hydroxylamine (Scheme 9d).

In the literature, the reaction times reported for the hydrolysis of azlactones to their phenylpyruvic acid derivatives vary from 3–48 h depending on the aryl substituents. Mechanistically, the acidic hydrolysis of azlactones proceeds *via* an α -(aroylamino) cinammic acid intermediate that in turn hydrolyses to the phenylpyruvic acid derivative. In our case, hydrolysis of **25** to the α -(aroylamino) cinammic acid **37** occurred within 1 hour. However, the subsequent hydrolysis of **37** to acid **38** was much slower (Table 1). Monitoring the reaction by ^1H NMR^{†††} indicated the reaction had gone to completion after 20 hours and, following a standard work-up, **38** was obtained in excellent yield.

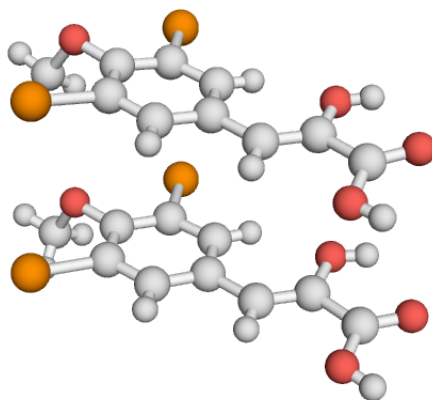
^{†††} In d_4 -MeOH, **38** existed exclusively in the enol tautomeric form. Furthermore, the sample decomposed after standing in d_4 -MeOH at room temperature for 24 h.

Table 1 Reaction progress for the acidic hydrolysis of azlactone **25** to **38**.

| Entry | Time (h) | Ratio of 37:38 ^a | Yield |
|-------|----------|-----------------------------|-------|
| 1 | 1.5 | 6:1 | — |
| 2 | 6 | 1:4.3 | — |
| 3 | 20 | 0:1 | 92% |

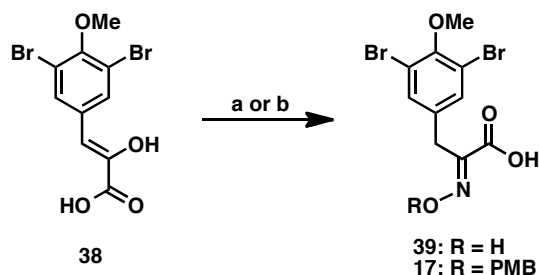
^a Product ratios were calculated by ¹H NMR.

It is important to note that when crude **25** was used in the reaction, the product (**38**) was an orange solid and although no impurities were visible by NMR, it was not pure by microanalysis. Attempts to purify this product by chromatography resulted in decomposition. Hydrolysis of purified **25** (chromatography) furnished **38** as a white solid which required no subsequent purification. Furthermore, it was possible to obtain crystals of **38** from diethyl ether and the structure and the geometry about the enol double bond could be confirmed by X-ray diffraction (Figure 21).

**Figure 21** X-ray crystal structure of **38**. The diethyl ether co-solvent has been hidden.

Next, condensation of **38** with a stoichiometric amount of hydroxylamine **26** in the presence of sodium acetate furnished α -oximino acid **17** without the need for purification (Scheme 18). The overall yield of 93% for this two-step transformation (from **25**) represents a significant improvement on the 54% yield from the one-pot procedure (Scheme 12). Using this improved procedure, it was also possible to access

the free oxime **39** in quantitative yield. Accordingly, it was demonstrated that this unprotected congener of **17** could be coupled to histamine dihydrochloride using DCC/HOBt to furnish **14** albeit in 30% yield (not shown).^{†††}



Scheme 18 Synthesis of α -oximino acids **17** and **39**.

Reagents and conditions: (a) Hydroxylamine hydrochloride, NaOAc, EtOH, rt, 19 h, quant; (b) **26**, NaOAc, EtOH, rt, 19 h, quant.

2.1.4.6 Biological Screening

The three natural products and their PMB-protected congeners were screened against human cancer cell lines in order to evaluate their cytotoxicity (Table 2). In the MTS assays that were conducted, JBIR-44 (**16**) was found to be cytotoxic against cervical (HeLa) and ovarian (SK-OV-3) cancer cell lines (EC_{50} 14 μM ^{§§§} and 22 μM). Ianthelline (**15**) exhibited moderate cytotoxicity against HeLa cells (EC_{50} 35 μM) but had lower activity against SK-OV-3 cells (EC_{50} >50 μM). (5)-Bromoverongamine (**14**) was the least active (EC_{50} >50 μM) although loss of cell viability was observed in all three cell lines between 70 and 100 μM .

In the case of **14** and **15**, PMB-protection of the oxime resulted in a marked increase in potency. Following the trend in activity for the corresponding natural products, **29** (EC_{50} 23 μM) was more cytotoxic than **34** (EC_{50} 30–45 μM) with the inference being that the exocyclic amino functionality at C-14 improves the interaction of the molecule with its cellular target. Interestingly, **36** (the PMB-protected counterpart of JBIR-44) showed no activity against HeLa or SK-OV-3 cell lines. Because the intracellular target for **36** is not known, accounting for the observed trends can only be hypothesised upon. Protecting a free oxime moiety with a PMB group is known to increase the cLogP value by approximately two units, thereby drastically altering the pharmacokinetic and pharmacodynamic properties of the molecule concerned.

^{†††} Unprotected α -oximino acids are known to form nitriles by loss of carbon dioxide and water (*Synthesis*, **2010**, 181).

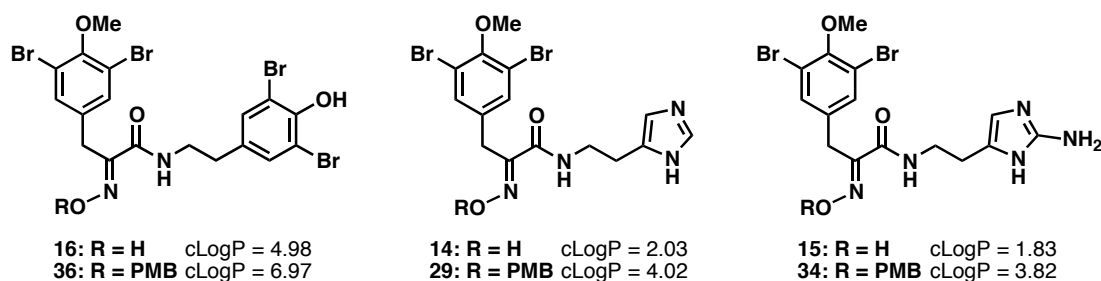
^{§§§} This value agreed with that reported for the natural material against the same cell line (IC_{50} 3.7 μM).

Table 2 MTS assay results for the natural products and their PMB protected derivatives. Screened against SK-OV-3, HeLa, TR-175 and HUVEC cells. Drug incubations were for 48 h

| Compound | Cell Line (EC ₅₀ /μM) | | | |
|----------------------------------|----------------------------------|----------------------|---------------------|--------|
| | HeLa (cervical) | SK-OV-3 (ovarian) | TR-175 (ovarian) | HUVECs |
| 5-Bromoverongamine (14) | >50 | >50 | >50 | 36 |
| Ianthelline (15) | 35 | >50 | – | 74 |
| JBIR-44 (16) | 14 | 22 | – | 24 |
| 29 | 45 | 40 | 30 | – |
| 34 | – | 23 | – | – |
| 36 | N/A | N/A | – | – |

N/A (not active); – (not tested)

In the case of JBIR-44, an already lipophilic molecule (cLogP 4.98), the introduction of a PMB group may either prevent the compound from exiting the cell membrane^{****} or from binding in the active site of its target protein. Alternatively, protection of the free oxime would negate its ability to hydrogen bond donate to a protein target. This latter explanation may be more likely given the importance of the free oxime in eliciting the antifouling properties in similar compounds (Section 2.1.2.1).

**Figure 22** cLogP values of tested compounds.

On the other hand, the natural products **14** and **15** are more polar (cLogP 2.03 and 1.83, respectively) due to the imidazole moiety in their side chain. For these compounds, the introduction of a lipophilic (PMB) group may be favourable as a result of improving their pharmacokinetic and pharmacodynamic properties. In general, increasing a compound's lipophilicity can aid its diffusion across cell membranes and improve binding to an intracellular target by exploiting hydrophobic pockets. Following on from this, lipophilic molecules often lack specificity for a

^{****} Highly lipophilic molecules have a reduced ability to exit the cell membrane as they tend to get retained due to their increased affinity for the phospholipid bilayer (Expert Opin. Drug Discov., **2010**, 235).

particular target. It is this promiscuity that is often linked to an increase in general toxicity due to off-target effects.⁴⁰ Taking this into account it is likely that the cytotoxicity observed for **29** and **34** is directly related to the increase in lipophilicity, gained by the introduction of a PMB group.

Since aeroplysinin-1 (Section 1.3.3) was reported to inhibit the proliferation of bovine arterial endothelial cells ($IC_{50} \sim 2 \mu M$) **14**, **15** and **16** were also screened against human umbilical vein endothelial cells (HUVECs).^{††††} These cells are an established model of tumour vascular endothelium and are used to investigate the antiangiogenic properties of molecules. In these assays, all three compounds were found to be cytotoxic to HUVECs in the micromolar range (EC_{50} 24–74 μM).

2.1.5 Conclusion

In conclusion, the total syntheses of the related bromotyrosine-derived natural products (5)-bromoverongamine, ianthelline, and JBIR-44 have been achieved in yields of 58, 17 and 33%, respectively from the commercially available 3,5-dibromo-4-hydroxybenzaldehyde. In addition, a robust and efficient route to α -oximino acid **17** has been established which can be readily exploited for analogue development. The cytotoxicity of JBIR-44 was confirmed in HeLa and SK-OV-3 cancer cell lines. Ianthelline was also biologically active in HeLa cells. Furthermore, all three natural products were cytotoxic towards HUVECs. These biological results prompted us explore the SAR of these molecules in greater depth, the details of which can be found in part II of this chapter.

^{††††} These assays were performed by Thomas M. Beale Esq.

2.1.6 Chemistry: Experimental

General Experimental Details

All non-aqueous reactions were performed under an atmosphere of argon in oven-dried glassware cooled under vacuum unless otherwise stated. Reagents were used as supplied from commercial sources. All reactions were performed at room temperature unless otherwise stated. Following extraction, the organic phase was dried with anhydrous magnesium sulfate. For mixtures of solvents, the ratios given refer to the volumes used. Analytical TLC was carried out on Merck 60 F254 silica gel plates and visualised by UV irradiation (254 nm) and developed with either acidic aqueous ammonium molybdate(IV) solution or alkaline potassium permanganate solution, and appropriate heating. Flash column chromatography was performed using Merck Kieselgel (230-400 mesh). All chromatography solvents were distilled before use except methanol, ether, water, formic acid and acetic acid which were used as supplied. "Petrol" refers to petroleum ether b.p. 40-60 °C.

NMR spectra were recorded at room temperature on Bruker DPX-400, Bruker DRX-500 or Bruker DRX-600 spectrometers using the deuterated solvent as internal deuterium lock; ^1H spectra at 400, 500 and 600 MHz respectively, and ^{13}C spectra at 100, 120 and 150 MHz. Chemical shifts are reported in parts per million (ppm) and internal references were the residual protic solvent: for d_1 -chloroform, $\delta_{\text{H}} = 7.26$ ppm and $\delta_{\text{C}} = 77.0$ ppm; for d_4 -methanol, $\delta_{\text{H}} = 3.31$ ppm and $\delta_{\text{C}} = 49.0$ ppm; for d_6 -acetone $\delta_{\text{H}} = 2.05$ ppm and $\delta_{\text{C}} = 29.8$ ppm. Coupling constants (J) are reported in Hz and recorded to the nearest 0.1 Hz. In reporting the spectral data, the following abbreviations were used: br = broad, s = singlet, d = doublet, t = triplet, q = quartet, dd = doublet of doublets. Spectra were assigned with information gained from DEPT 135, COSY, HMBC and HMQC experiments.

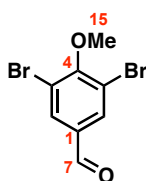
IR spectra were recorded on a Perkin-Elmer Spectrum I FTIR spectrometer. Samples were applied neat. Only selected absorbances (ν_{max}) are reported and relative intensities are indicated as s - strong; m - medium; w - weak and br - broad. Peaks are reported in wavenumbers (cm^{-1}).

HRMS were recorded using a Waters Micromass LCT Premier spectrometer or by Paul Skelton at the Department of Chemistry, University of Cambridge and are reported in units of m/z .

Melting points were measured either on an automated Stanford Research Systems MPA100 (Optimelt) melting point machine or a Reichert hot stage apparatus equipped with a digital thermometer.

Microanalysis was performed in the microanalytical laboratories at the Department of Chemistry, University of Cambridge, using an Exeter analytical elemental analyzer, model CE-440. X-ray structure determination was performed by Dr John E. Davies at the Department of Chemistry, University of Cambridge using a Nonius Kappa CCD detector.

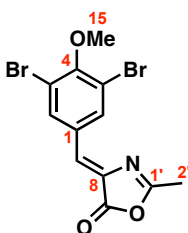
cLogP values were calculated using the OSIRIS Property Explorer,
<http://www.organic-chemistry.org/prog/peo/>.

3,5-Dibromo-4-methoxybenzaldehyde (24)

To a stirred solution of 3,5-dibromo-4-hydroxybenzaldehyde (**23**) (10.1 g, 36.1 mmol) in acetone (200 mL) was added anhydrous K_2CO_3 (6.74 g, 48.8 mmol). The resulting mixture was stirred for 30 min then treated with iodomethane (4.48 mL, 71.9 mmol) and heated under reflux for a further 6 h. After this time, acetone and excess iodomethane were removed *in vacuo* and the resulting residue was partitioned between EtOAc (200 mL) and H_2O (200 mL). The organic layer was separated and the aqueous layer was extracted with EtOAc (3 x 200 mL). The combined organic extracts were washed with brine, dried and concentrated *in vacuo*. The residue was purified by flash column chromatography (20% Et_2O /Petrol) to furnish **24** (9.60 g, 32.7 mmol, 91%) as a white crystalline solid.

R_f 0.50 (20% Et_2O /Petrol); ν_{max} (thin film)/ cm^{-1} 1685s, 1547m, 1469m, 1260s, 980s; δ_H (400 MHz, $CDCl_3$) 9.86 (1H, s, H-7), 8.03 (2H, s, H-2/6), 3.97 (3H, s, H-15); δ_C (100 MHz, $CDCl_3$) 188.3 (C-7), 159.1 (C-4), 134.2 (C-1), 133.9 (C-2/6), 119.3 (C-3/5), 60.9 (C-15); m.p. 83-85 °C (lit.,⁴¹ 87-88 °C); *elem. anal.* $C_8H_6Br_2O_2$ (^{79}Br) requires C 32.69%, H 2.06%, Br 54.37%, found C 32.75%, H 2.03%, Br 53.88%.

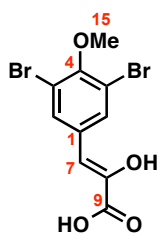
Consistent with literature data.⁴²

(Z)-4-(3,5-Dibromo-4-methoxybenzylidene)-2-methyloxazol-5(4H)-one (25)

A mixture of aldehyde **24** (6.86 g, 23.3 mmol), *N*-acetylglycine (3.55 g, 30.3 mmol), sodium acetate (2.49 g, 30.4 mmol) and acetic anhydride (11 mL, 116 mmol) were heated at reflux for 1.5 h. After cooling to room temperature, H₂O (400 mL) and CH₂Cl₂ (400 mL) were added. The organic layer was separated and washed with H₂O (400 mL), brine (400 mL), dried and concentrated *in vacuo*. The residue was purified by flash column chromatography (40% CH₂Cl₂/Petrol) to furnish **25** (7.86 g, 21.1 mmol, 91%) as a yellow solid.

R_f 0.32 (10% Et₂O/Petrol); ν_{\max} (thin film)/cm⁻¹ 1806s, 1792s, 1765s, 1660s, 1260s; δ_{H} (400 MHz, CDCl₃) 8.24 (2H, s, H-2/6), 6.90 (1H, s, H-7), 3.92 (3H, s, H-15), 2.43 (3H, s, H-2'); δ_{C} (100 MHz, CDCl₃) 167.3 (C-1'), 167.1 (C-9), 155.9 (C-4), 135.8 (C-2/6), 133.7 (C-8), 131.7 (C-1), 127.1 (C-7), 118.5 (C-3/5), 60.8 (C-15), 15.7 (C-2'); *m/z* (ESI+) found 373.9029, [M+H]⁺ C₁₂H₁₀Br₂NO₃ (⁷⁹Br) requires 373.9027; m.p. 167-168 °C (lit.,⁴³ 154-155 °C); *elem. anal.* C₁₂H₉Br₂NO₃ requires C 38.43%, H 2.42%, N 3.73%, found C 38.31%, H 2.30%, N 3.60%.

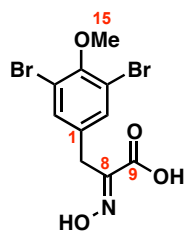
Crystals of **25** were obtained by slow evaporation of CDCl₃. The structure was confirmed by X-ray crystallographic analysis and given the unique identifier sl1031.

(Z)-3-(3,5-Dibromo-4-methoxyphenyl)-2-hydroxyacrylic acid (38)

A suspension of azlactone **25** (2.39 g, 6.37 mmol) and 3 *N* HCl (50 mL) were heated to reflux for 20 h. The mixture was cooled to room temperature and the white precipitate was isolated by filtration, washed with H₂O (20 mL) and evaporated to dryness *in vacuo* to furnish **38** (2.09 g, 5.94 mmol, 93%) as a white solid.

ν_{max} (thin film)/cm⁻¹ 3469s, 2939br, 1674s, 1446s, 1248s; δ_{H} (600 MHz, CD₃OD) 7.96 (2H, s, H-2/6), 6.33 (1H, s, H-7), 3.84 (3H, s, H-15); δ_{C} (150 MHz, CD₃OD) 167.5 (C-9), 153.9 (C-4), 135.6 (C-1), 134.4 (C-2/6), 118.6 (C-3/5), 107.8 (C-7), 61.1 (C-15); m.p. 186-188 °C; *elem. anal.* C₁₀H₈Br₂O₄ requires C 34.12 %, H 2.29 %, found C 34.01 %, H 2.16 %.

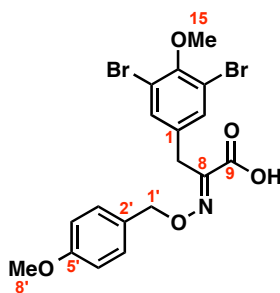
Crystals of **38** were obtained by slow evaporation of Et₂O. The structure was confirmed by X-ray crystallographic analysis and given the unique identifier sl1033.

(E)-3-(3,5-Dibromo-4-methoxyphenyl)-2-(hydroxyimino)propanoic acid (39)

To a stirred solution of **38** (348 mg, 0.989 mmol) and hydroxylamine hydrochloride (68.7 mg, 0.99 mmol) in EtOH (10 mL) was added sodium acetate (243 mg, 2.96 mmol). After 19 h, H₂O (150 mL) was added, the mixture was acidified (pH 0) by the addition of aqueous HCl (3 N) and extracted with EtOAc (3 × 100 mL). The combined organic extracts were dried and evaporated to dryness *in vacuo* to furnish **39** (363 mg, 0.99 mmol, 100%) as a white solid.

R_f 0.10 (10% MeOH/CH₂Cl₂); ν_{\max} (thin film)/cm⁻¹ 3064br, 1694s, 1471s, 1030s, 698s; δ_H (400 MHz, CDCl₃) 7.47 (2H, s, H-2/6), 3.95 (2H, s, H-7), 3.85 (3H, s, H-15); δ_C (100 MHz, CDCl₃) 165.6 (C-9), 153.3 (C-4), 148.9 (C-8), 133.38 (C-2/6), 133.35 (C-1), 118.2, (C-3/5), 60.6 (C-15), 29.3 (C-7); m/z (ESI+) found 387.8799, [M+Na]⁺ C₁₀H₁₀Br₂NO₄Na (⁷⁹Br) requires 387.8796. m.p. 171-173 °C (lit.,²⁹ 142-145 °C).

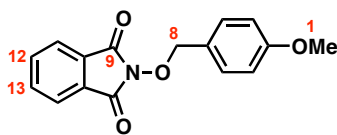
Consistent with literature data.²⁹

(E)-3-(3,5-Dibromo-4-methoxyphenyl)-2-(((4-ethoxybenzyl)oxy)imino)propanoic acid (17)

Procedure 1: A mixture of azlactone **25** (6.83 g, 18.2 mmol) and Ba(OH)₂·8H₂O (17.2 g, 54.5 mmol) in dioxane (100 mL) and H₂O (100 mL) were stirred at 60 °C. After 1 h, *O*-para-methoxybenzyl hydroxylamine hydrochloride (**26**) (3.45 g, 18.2 mmol) was added and the mixture was stirred vigorously. After 6 h, the reaction mixture was cooled to 0 °C and acidified (pH 0) with aqueous 3 N HCl. The mixture was extracted with EtOAc (3 × 400 mL) and the combined organic extracts were dried and concentrated *in vacuo*. The residue was purified by flash column chromatography (0:100:0.1-2:100:0.1 MeOH/CH₂Cl₂/AcOH) to furnish **17** (4.81 g, 9.87 mmol, 54%) as a white solid.

Procedure 2: To a stirred solution of **38** (297 mg, 0.844 mmol) and *O*-para-methoxybenzyl hydroxylamine hydrochloride (**26**) (160 mg, 0.844 mmol) in EtOH (8.40 mL) was added sodium acetate (207 mg, 2.52 mmol). After 19 h, the mixture was acidified (pH 0) with aqueous 3 N HCl. The mixture was extracted with EtOAc (3 × 100 mL) and the combined organic extracts were dried and evaporated to dryness *in vacuo* to furnish **17** (409 mg, 0.84 mmol, quant.) as a white solid.

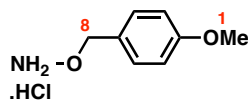
R_f 0.43 (10% MeOH/CH₂Cl₂); *v*_{max} (thin film)/cm⁻¹ 2934br, 1702s, 1513s, 1473s, 1256s; *δ*_H (400 MHz, CDCl₃) 7.38 (2H, s, H-2/6), 7.28 (2H, d, *J* 8.6 Hz, H-3'/7'), 6.93 (2H, d, *J* 8.6 Hz, H-4'/6'), 5.24 (2H, s, H-1'), 3.85 (3H, s, H-15), 3.83 (3H, s, H-8'), 3.80 (2H, s, H-7); *δ*_C (100 MHz, CDCl₃) 164.2 (C-9), 160.0 (C-5'), 152.9 (C-4), 148.6 (C-8), 133.7 (C-1), 133.3 (C-2/6), 130.4 (C-3'/7'), 127.4 (C-2'), 117.9 (C-3/5), 114.1 (C-4'/6'), 78.5 (C-1'), 60.6 (C-15), 55.3 (C-8'), 29.1 (C-7); *m/z* (ESI⁺) found 507.9391, [M+Na]⁺ C₁₈H₁₇Br₂NO₅Na (⁷⁹Br) requires 507.9371; m.p. 101-103 °C.

2-((4-Methoxybenzyl)oxy)isoindoline-1,3-dione (28)

A mixture of *N*-hydroxyphthalimide (**27**) (26.1 g, 160 mmol), 4-methoxybenzyl chloride (21.7 mL, 160 mmol), and Et₃N (53.0 mL, 380 mmol) in DMF (400 mL) was heated at 90 °C. After 40 min, the reaction was quenched by the addition of ice-cold water (500 mL). The orange precipitate was washed with H₂O and the resulting white solid was taken up in CH₂Cl₂ (300 mL), washed with H₂O (300 mL), brine (300 mL), dried and evaporated to dryness *in vacuo* to furnish **28** (26.6 g, 94.0 mmol, 59%) as a beige solid which was used without further purification.

R_f 0.35 (40% Et₂O/Petrol); ν_{max} (thin film)/cm⁻¹ 1785w, 1724s, 1611m, 1515m; δ_{H} (400 MHz, CDCl₃) 7.80 (2H, dd, *J* 5.4, 3.1 Hz, H-12/13), 7.72 (2H, dd, *J* 5.4, 3.1 Hz, C-11/14), 7.45 (2H, d, *J* 8.5 Hz, C-4/6), 6.88 (2H, d, *J* 8.5 Hz, C-3/7), 5.15 (2H, s, C-8), 3.80 (3H, s, C-1); δ_{C} (100 MHz, CDCl₃) 163.5 (C-9/16), 160.3 (C-2), 134.3 (C-12/13), 131.6 (C-4/6), 128.8 (C-10/15), 125.7 (C-5), 123.4 (C-11/14), 113.8 (C-3/7), 79.9 (C-8), 55.2 (C-1); *m/z* (ESI+) found 306.0736, [M+Na]⁺ C₁₆H₁₃NO₄Na requires 306.0737; m.p. 125-127 °C (lit.,⁴⁴ 129-130 °C).

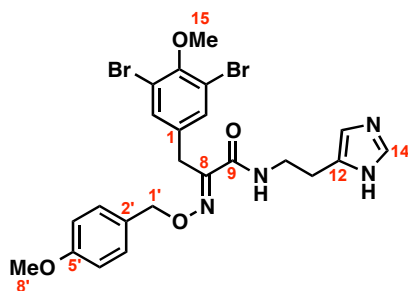
Consistent with literature data.⁴⁵

O-(4-Methoxybenzyl)hydroxylamine hydrochloride (26)

To a stirred solution of **28** (32.5 g, 115 mmol) in DMF/MeOH (460 mL, 1:2) at 60 °C was added hydrazine hydrate (17.4 mL, 358 mmol). After 5 min, the reaction was cooled to room temperature and quenched by the addition of H₂O (150 mL). Excess solvent was removed *in vacuo* and the resulting residue was extracted with EtOAc (3 x 500 mL). The combined organic layers were washed with brine (500 mL), dried and concentrated *in vacuo*. Methanolic hydrogen chloride (1.25 M, 100 mL) was added dropwise to the residue at 0 °C with stirring. The resulting precipitate was isolated *via* filtration and washed with Et₂O to furnish **26** (16.7 g, 88.1 mmol, 77%) as white platelets.

ν_{max} (thin film)/cm⁻¹ 2803w, 2650m, 1611m, 1504m, 1255m; δ_{H} (400 MHz, CD₃OD) 7.37 (2H, d, *J* 8.5 Hz, H-4/6), 6.98 (2H, d, *J* 8.5 Hz, H-3/7), 4.95 (2H, s, H-8), 3.82 (3H, s, H-1); δ_{C} (100 MHz, CD₃OD) 162.7 (C-5), 132.8 (C-4/6), 126.6 (C-2), 115.7 (C-3/7), 78.4 (C-8), 56.2 (C-1); *m/z* (ESI+) found 137.0604, [M+H]⁺ C₈H₉O₂ requires 137.0597; m.p. decomp. 200-202 °C (lit.,⁴⁶ decomp. 196-197 °C); *elem. anal.* C₈H₁₂O₂Cl requires C 50.67% H 6.38%, N 7.39%, Cl 18.69%, found C 50.69%, H 6.34%, N 7.25%, Cl 18.75%.

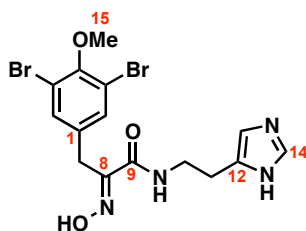
Consistent with literature data.⁴⁷

(E)-N-(2-(1H-Imidazol-4-yl)ethyl)-3-(3,5-dibromo-4-methoxyphenyl)-2-(((4-methoxybenzyl)oxy)imino)propanamide (29)

To a stirred solution of acid **17** (42.0 mg, 86.2 μmol) in CH_2Cl_2 (2 mL) were added *N,N'*-dicyclohexylcarbodiimide (21.0 mg, 0.102 mmol) and *N*-hydroxybenzotriazole (13.8 mg, 0.102 mmol). After stirring for 5 min, histamine dihydrochloride (28.0 mg, 0.152 mmol) and *i*Pr₂EtN (43.0 μL , 0.250 mmol) were added. After 24 h, the solvent was removed *in vacuo* and the residue partitioned between H_2O (20 mL) and EtOAc (20 mL). The organic layer was separated and the aqueous layer was extracted with EtOAc (3 \times 20 mL). The combined organic extracts were washed with brine (20 mL), dried and concentrated *in vacuo*. The residue was purified by flash column chromatography (1-10% MeOH/ CH_2Cl_2) to furnish **29** (40.6 mg, 70.0 μmol , 81%) as a white foam.

R_f 0.43 (10% MeOH/ CH_2Cl_2); ν_{max} (thin film)/ cm^{-1} 3283br, 2929w, 1734w, 1661s, 1611s, 1512s, 1256s, 980s; δ_{H} (600 MHz CDCl_3) 7.56 (1H, s, H-14), 7.38 (2H, s, H-2/6), 7.24 (2H, d, J 8.6 Hz, H-3'/7'), 6.89 (2H, d, J 8.6 Hz, H-4'/6'), 6.78 (1H, s, H-13), 5.10 (2H, s, H-1'), 3.81 (3H, s, H-15), 3.80 (3H, s, H-8'), 3.78 (2H, s, H-7), 3.59 (2H, apparent q, J 6.6 Hz, H-10), 2.84 (2H, t, J 6.6 Hz, H-11); δ_{C} (150 MHz, CDCl_3) 162.3 (C-9), 159.7 (C-5'), 152.5 (C-4), 150.9 (C-8), 135.5 br (C-12), 134.9 (C-1), 134.8 (C-14), 133.4 (C-2/6), 130.1 (C-3' and C-7'), 128.4 (C-2'), 117.6 (C-3/5), 116.0 br (C-13), 114.0 (C-4'/6'), 77.3 (C-1'), 60.5 (C-15), 55.2 (C-8'), 39.2 (C-10), 28.6 (C-7), 27.0 (C-11); m/z (ESI+) found 579.0240, $[\text{M}+\text{H}]^+$ $\text{C}_{23}\text{H}_{25}\text{Br}_2\text{N}_4\text{O}_4$ (^{79}Br) requires 579.0243.

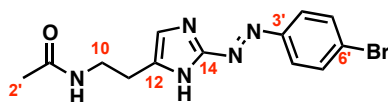
(E)-N-(2-(1H-Imidazol-4-yl)ethyl)-3-(3,5-dibromo-4-methoxyphenyl)-2-(hydroxyimino)propanamide. (5)-Bromoverongamine (14**)**



To a stirred solution of amide **29** (78.0 mg, 0.134 mmol) and anisole (146 μ L, 1.34 mmol) in CH_2Cl_2 (5 mL) was added aluminium trichloride (179 mg, 1.34 mmol). After 5 min, a saturated aqueous solution of NaHCO_3 (15 mL) was added followed by a saturated aqueous solution of Rochelle's salt (25 mL). After stirring for 10 min the aqueous phase was extracted with CH_2Cl_2 (3×25 mL) and the combined organic layers were dried, and concentrated *in vacuo*. The residue was purified by flash column chromatography (2-10% MeOH/ CH_2Cl_2) to furnish **14** (48.1 mg, 0.105 mmol, 78%) as a white foam.

R_f 0.10 (10% MeOH/ CH_2Cl_2); ν_{max} (thin film)/ cm^{-1} 1655s, 1542m, 1471s, 1421s, 1259s; δ_{H} (600 MHz CD_3OD) 7.57 (1H, s, H-14), 7.47 (2H, s, H-2/6), 6.82 (1H, s, H-13), 3.83 (2H, s, H-7), 3.80 (3H, s, H-15), 3.49 (2H, t, J 7.1 Hz, H-10), 2.79 (2H, t, J 7.1 Hz, H-11); δ_{C} (150 MHz, CD_3OD) 165.3 (C-9), 153.8 (C-4), 152.1 (C-8), 137.3 (C-1), 136.1 (C-14), 135.9 br (C-12), 134.5 (C-2/6), 118.5 (C-3/5), 117.9 br (C-13), 61.0 (C-15), 40.3 (C-10), 28.8 (C-7), 27.7 (C-11); m/z (ESI+) found 458.9682, $[\text{M}+\text{H}]^+$ $\text{C}_{15}\text{H}_{17}\text{Br}_2\text{N}_4\text{O}_3$ (^{79}Br) requires 458.9667; m.p. 100-102 $^\circ\text{C}$.

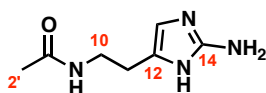
Crystals of **14** were obtained by slow evaporation of a solution of Et_2O /Petrol/ EtOH . The structure was confirmed by X-ray crystallographic analysis and given the unique identifier sl1006.

(E)-N-(2-(2-((4-Bromophenyl)diazenyl)-1H-imidazol-5-yl)ethyl)acetamide (31)

To a stirred solution of bromoaniline (**30**) (3.84 g, 22.3 mmol) in aqueous HCl (2 *N*, 120 mL) was added, *via* cannula, a solution of sodium nitrite (1.54 g, 22.3 mmol) in H₂O (32 mL) over 30 min, ensuring the temperature did not exceed 0 °C. After this time, the mixture was added to a vigorously stirred solution of *N*ω-acetylhistamine (4.00 g, 26.1 mmol) in aqueous NaHCO₃ (10% w/w, 200 mL) at 0 °C. After 24 h at 4 °C the orange solid was isolated *via* filtration and purified by flash column chromatography (1-20% MeOH/CH₂Cl₂) to furnish **31** (3.91 g, 11.6 mmol, 52%) as a yellow solid.

R_f 0.44 (10% MeOH/CH₂Cl₂); *v*_{max} (thin film)/cm⁻¹ 3057w, 2314w, 1618m, 1570m, 1460s; δ_H (400 MHz, CD₃OD) 7.82 (2H, d, *J* 8.7, H-4' and H-8'), 7.71 (2H, d, *J* 8.7, H-5' and H-7'), 7.15 (1H, s, H-13), 3.49 (2H, t, *J* 6.9, H-10), 2.87 (2H, t, *J* 6.9, H-11), 1.93 (3H, s, H-2'); δ_C (125 MHz, CD₃OD) 173.4 (C-1'), 155.4 (C-14, br) 152.7 (C-3'), 133.7 (C-5' and C-7'), 130.1 (C-12, br), 126.8 (C-6'), 125.4 (C-4' and C-8'), 118.0 (C-13, br), 40.1 (C-10), 29.2 (C-11, br), 22.5 (C-2'); *m/z* (ESI+) Found: 336.0456, [M+H]⁺ C₁₃H₁₅BrN₅O (⁷⁹Br) requires 336.0460; m.p. 102-106 °C.

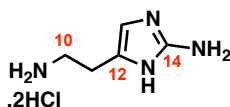
Consistent with literature data.⁴⁸

***N*-(2-(2-Amino-1*H*-imidazol-5-yl)ethyl)acetamide (**32**)**

A solution of diazo compound **31** (4.55 g, 13.5 mmol) in absolute ethanol (100 mL) was hydrogenated over PtO₂ (455 mg, 2.00 mmol) under an H₂ atmosphere (4 bar). After 24 h, a second batch of PtO₂ (455 mg) was added. After 18 h, the PtO₂ was removed *via* filtration through celite and the reaction mixture was concentrated *in vacuo*. The residue was partitioned between H₂O (100 mL) and EtOAc (100 mL). The aqueous layer was extracted with EtOAc (2 x 100 mL) and passed through a Dowex 50W X8 column which was eluted with aqueous ammonium hydroxide (10%, 200 mL). This was evaporated to dryness *in vacuo* to furnish **32** (326 mg, 1.94 mmol, 14%) as a brown oil.

ν_{\max} (thin film)/cm⁻¹ 3299br, 1632s, 1568s; δ_{H} (400 MHz, CD₃OD) 6.29 (1H, s, H-13), 3.34 (2H, t, *J* 7, H-10), 2.58 (2H, t, *J* 7, H-11), 1.92 (3H, s, H-2'); δ_{C} (100 MHz, CD₃OD) 173.2 (C-1'), 150.8 (C-14), 132.0 (C-12), 112.1 (C-13), 40.4 (C-10), 28.0 (C-11), 22.5 (C-2'); *m/z* (ESI+) found 169.1090, [M+H]⁺ C₇H₁₃N₄O requires 169.1084.

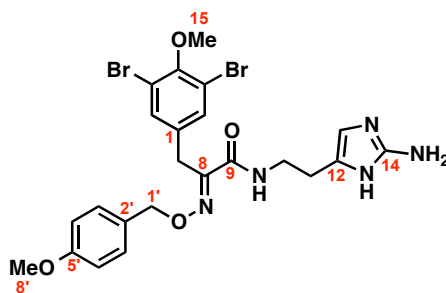
Consistent with literature data.⁴⁸

5-(2-Aminoethyl)-1*H*-imidazol-2-amine dihydrochloride (19)

A stirred solution of amide **32** (39.0 mg, 0.232 mmol) and aqueous HCl (6 *N*, 6 mL) was heated at 100 °C for 14 h. After this the mixture was evaporated to dryness in *vacuo* to furnish **19** (46.2 mg, 0.232 mmol, 100%) as a brown solid which was used without further purification.

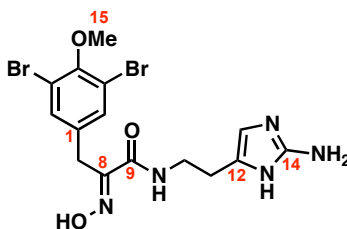
ν_{max} (thin film)/cm⁻¹ 3326s, 3233s, 1565s; δ_{H} (400 MHz CD₃OD) 6.74 (1H, s, H-13), 3.23 (2H, t, *J* 7.0 Hz, H-10), 2.95 (2H, t, *J* 7.0 Hz, H-11); δ_{C} (100 MHz, CD₃OD) 123.3 (C-14), 117.7 (C-12), 112.0 (C-13), 39.0 (C-10), 23.7 (C-11); *m/z* (ESI+) found 127.0982, [M-H-2Cl]⁺ C₅H₁₁N₄ requires 127.0982.

Consistent with literature data.⁴⁸

(E)-N-(2-(2-Amino-1H-imidazol-4-yl)ethyl)-3-(3,5-dibromo-4-methoxyphenyl)-2-(((4-methoxybenzyl)oxy)imino)propanamide (34)

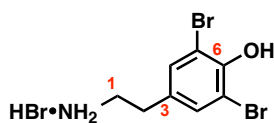
To a stirred solution of acid **17** (380 mg, 0.780 mmol) in CH₂Cl₂/DMF (1:1, 15 mL) were added *N,N'*-dicyclohexylcarbodiimide (218 mg, 1.06 mmol) and *N*-hydroxybenzotriazole (143 mg, 1.06 mmol). After stirring for 5 min, a solution of aminohistamine dihydrochloride (**19**) (168 mg, 0.844 mmol) and *i*Pr₂EtN (290 μL, 1.69 mmol) in CH₂Cl₂/DMF (1:1, 15 mL) were added. After 24 h, the mixture was concentrated *in vacuo* and the residue was purified by flash column chromatography (15:9:0.5:0.5 EtOAc/acetone/H₂O/formic acid) to furnish **34** (190 mg, 0.319 mmol, 41%) as a brown oil.

*R*_f 0.63 (15:9:1:1 EtOAc/acetone/H₂O/formic acid); *v*_{max} (thin film)/cm⁻¹ 2929w, 1666s, 1513s, 1470s, 1247s; δ_H (400 MHz CD₃OD) 7.36 (2H, s, H-2/6), 7.25 (2H, d, *J* 8.6 Hz, H-3'/7'), 6.90 (2H, d, *J* 8.6 Hz, H-4'/6'), 6.50 (1H, s, H-13), 5.17 (2H, s, H-1'), 3.81 (3H, s, H-15), 3.80 (3H, s, H-8'), 3.77 (2H, s, H-7), 3.49 (2H, t, *J* 6.8 Hz, H-10), 2.71 (2H, t, *J* 6.8 Hz, H-11); δ_C (125 MHz, CD₃OD) 164.8 (C-9), 161.3 (C-5'), 154.0 (C-8), 152.5 (C-4), 148.9 (C-14), 136.8 (C-1), 134.5 (C-2/6), 131.2 (C-3'/7'), 129.9 (C-2'), 126.4 (C-12), 118.6 (C-3/5), 115.0 (C-4'/6'), 110.8 (C-13), 78.5 (C-1'), 61.0 (C-15), 55.7 (C-8'), 39.1 (C-10), 29.6 (C-7), 25.9 (C-11); *m/z* (ESI⁺) found 594.0346, [M+H]⁺ C₂₃H₂₆Br₂N₅O₄ (⁷⁹Br) requires 594.0352.

(E)-N-(2-(2-Amino-1H-imidazol-4-yl)ethyl)-3-(3,5-dibromo-4-methoxyphenyl)-2-(hydroxyimino)propanamide (15)

To a stirred solution of amide **34** (140 mg, 0.235 mmol) and anisole (102 μ L, 0.939 mmol) in CH_2Cl_2 (5 mL) was added aluminium trichloride (125 mg, 0.939 mmol). After 5 min, a saturated aqueous solution of NaHCO_3 (10 mL) was added followed by a saturated aqueous solution of Rochelle's salt (20 mL). After stirring for 10 min the aqueous phase was extracted with CH_2Cl_2 (3×20 mL) and the combined organic layers were dried and concentrated *in vacuo*. The residue was purified by flash column chromatography (15:9:1:1, EtOAc/acetone/ H_2O /formic acid) to furnish **15** (48.9 mg, 0.103 mmol, 44%) as a white solid.

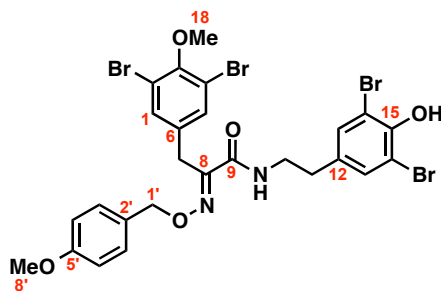
R_f 0.29 (15:9:1:1 EtOAc/acetone/ H_2O /formic acid); ν_{max} (thin film)/ cm^{-1} 3162br, 1678s, 1532s, 1471s, 1420s, 1257s; δ_{H} (400 MHz CD_3OD) 7.47 (2H, s, H-2/6), 6.50 (1H, s, H-13), 3.83 (2H, s, H-7), 3.81 (3H, s, C-15), 3.47 (2H, t, J 7.0 Hz, H-10), 2.70 (2H, t J 7.0 Hz, H-11); δ_{C} (100 MHz, CD_3OD) 165.6 (C-9), 153.8 (C-4), 152.0 (C-8), 148.8 (C-14), 137.4 (C-1), 134.5 (C-2/6), 126.0 (C-12), 118.6 (C-3/5), 110.6 (C-13), 61.0 (C-15), 38.9 (C-10), 28.8 (C-7), 25.8 (C-11); m/z (ESI+) found 473.9761, $[\text{M}+\text{H}]^+$ $\text{C}_{15}\text{H}_{18}\text{Br}_2\text{N}_5\text{O}_3$ (^{79}Br) requires 473.9776.

4-(2-Aminoethyl)-2,6-dibromophenol hydrobromide (20)

To a stirred suspension of tyramine (**35**) (1.00 g, 7.29 mmol) in MeOH (20 mL) was added bromine (750 μ L, 14.6 mmol). The mixture was heated to 60 $^{\circ}$ C for 14 h and then cooled to room temperature after which the precipitate was isolated by filtration, washed with Et₂O (20 mL) and dried *in vacuo* to furnish **20** (1.85 g, 4.92 mmol, 68%) as a brown powder.

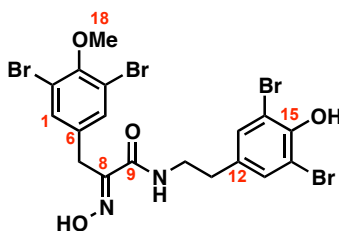
ν_{max} (thin film)/cm⁻¹ 2985w, 2915w, 1601w, 1472s, 1143s, 1133s; δ_{H} (400 MHz, *d*₆-DMSO) 9.77 (1H, br s, OH), 7.84 (3H, br s, NH₃), 7.46 (2H, s, H-4/8), 3.03 (2H, br q, *J* 6.2 Hz, H-1), 2.80 (2H, t, *J* 7.5 Hz, H-2); δ_{C} (100 MHz, *d*₆-DMSO) 149.4 (C-6), 132.5 (C-4/8), 131.7 (C-3), 112.0 (C-5/7), 39.6 (C-1), 31.1 (C-2); m.p. 208-210 $^{\circ}$ C. *elem. anal.* C₈H₁₀Br₃O requires C 25.56% H 2.68%, N 3.73%, found C 25.56%, H 2.57%, N 3.56%.

(E)-N-(3,5-Dibromo-4-hydroxyphenethyl)-3-(3,5-dibromo-4-methoxyphenyl)-2-(((4-methoxybenzyl)oxy)imino)propanamide (36)



To a stirred solution of acid **17** (287 mg, 0.589 mmol) in CH₂Cl₂ (10 mL) were added *N,N'*-dicyclohexylcarbodiimide (132 mg, 0.64 mmol) and *N*-hydroxybenzotriazole (86.5 mg, 0.640 mmol). After stirring for 5 min, a solution of amine **20** (240 mg, 0.64 mmol) and *i*Pr₂EtN (223 μL, 1.28 mmol) were added. After 19 h, H₂O (20 mL) was added, the organic layer separated and the aqueous layer was extracted with CH₂Cl₂ (3 × 20 mL). The combined organic extracts were washed with brine, dried and concentrated *in vacuo*. The residue was purified by flash column chromatography (10-50% Et₂O/Petrol) to yield **36** (189 mg, 0.247 mmol, 42%) as a white foam.

*R*_f 0.38 (50% Et₂O/Petrol); *v*_{max} (thin film)/cm⁻¹ 3391w, 2930w, 1664s, 1513s, 1471s, 1245s; δ_H (400 MHz, CDCl₃) 7.41 (2H, s, H-1/5), 7.28 (2H, s, H-13/17), 7.22 (2H, d, *J* 8.7 Hz, H-3'/7'), 6.90 (2H, d, *J* 8.7 Hz, H-4'/6'), 6.75 (1H, t, *J* 6.0 Hz, NH), 5.96 (1H, s, OH), 5.12 (2H, s, H-1'), 3.83 (3H, s, H-18), 3.82 (3H, s, H-8'), 3.80 (2H, s, H-7), 3.50 (2H, apparent q, *J* 6.8 Hz, H-10), 2.73 (2H, t, *J* 7.0 Hz, H-11); δ_C (100 MHz, CDCl₃) 162.2 (C-9), 159.7 (C-5'), 152.6 (C-3), 150.9 (C-8), 148.2 (C-15), 134.7 (C-6), 133.4 (C-1/5), 133.3 (C-12), 132.2 (C-13/17), 130.0 (C-3'/7'), 128.2 (C-2'), 117.7 (C-2/4), 114.0 (C-4'/6'), 109.9 (C-14/16), 77.4 (C-1'), 60.5 (C-18), 55.3 (C-8'), 40.4 (C-10), 34.2 (C-11), 28.6 (C-7); *m/z* (ESI⁺) found 760.8492, [M+H]⁺ C₂₆H₂₅Br₄N₂O₅ (⁷⁹Br) requires 760.8492.

(E)-N-(3,5-Dibromo-4-hydroxyphenethyl)-3-(3,5-dibromo-4-methoxyphenyl)-2-(hydroxyimino)propanamide. JBIR-44 (16)

To a stirred solution of amide **36** (152 mg, 0.199 mmol) and anisole (108 μ L, 0.995 mmol) in CH_2Cl_2 (5 mL) was added aluminium trichloride (133 mg, 0.995 mmol). After 5 min, a saturated aqueous solution of NaHCO_3 (10 mL) was added followed by a saturated aqueous solution of Rochelle's salt (20 mL). After stirring for 10 min the aqueous phase was extracted with CH_2Cl_2 (3×20 mL) and the combined organic layers were dried, and concentrated *in vacuo*. The residue was purified by flash column chromatography (20-50% Et_2O /hexanes) to furnish **16** (109 mg, 0.169 mmol, 85%) as a white foam.

R_f 0.30 (50% Et_2O /Petrol); ν_{max} (thin film)/ cm^{-1} 3220br, 2928w, 1655s, 1623m, 1533s, 1471s; δ_{H} (400 MHz, CD_3OD calibrated to 7.52) 7.52 (2H, s, H-1/5), 7.36 (2H, s, H-13/17), 3.87 (2H, s, H-7), 3.86 (3H, s, H-18), 3.46 (2H, t, J 7.25 Hz, H-10), 2.74 (2H, t, J 7.23 Hz, H-11); δ_{C} (100 MHz, CD_3OD) 165.5 (C-9), 153.9 (C-3), 152.1 (C-8), 150.8 (C-15), 137.3 (C-6), 134.6 (C-12), 134.5 (C-1/5), 133.6 (C-13/17), 118.6 (C-2/4), 112.1 (C-14/16), 61.0 (C-18), 41.7 (C-10), 34.9 (C-11), 28.8 (C-7); m/z (ESI+) found 640.7936, $[\text{M}+\text{H}]^+$ $\text{C}_{18}\text{H}_{17}\text{Br}_4\text{N}_2\text{O}_4$ (^{79}Br) requires 640.7922; m.p. 67-69 $^\circ\text{C}$

2.1.7 Biology: Experimental

Cell lines and cell culture: SK-OV-3, TR175, and HeLa cell lines were obtained from Cell Services (CRUK LRI). Cell lines were grown in T75 flasks (NUNC™). SK-OV-3 cells were maintained in RPMI-1640 medium (Gibco) supplemented with 10% (v/v) FBS, at 37 °C in humidified air containing 5% CO₂. In a similar manner, TR175 cells were maintained in HAMS-F12 (Gibco) and HeLa cells were maintained in DMEM (Gibco).

MTS assay: Cell viability was assessed using the Promega CellTiter 96® AQueous One Solution Cell Proliferation Assay. Single cell suspensions were prepared and seeded into 96 well plates (96F Nunclon Delta microwell) with 3×10^3 cells/mL (90 µL/well). Cells were cultured for 24 h before the addition of agent in culture medium (10 µL) at the desired concentration. Drug samples were dissolved in DMSO (to form a 0.1 M stock solution) and diluted with the culture medium to the required concentrations. The final DMSO concentration did not exceed 0.1% to the total incubation solution (v/v) and a vehicle control was conducted with 0.1% DMSO concentration in each assay. Cells were incubated at 37 °C for 48 h. MTS reagent was aliquoted to each well (20 µL) and the plates were incubated at 37 °C for 2 h. Absorbance at 490 nm was determined for each well using a TECAN infinite M200. Each experimental point was performed in quadruplicate. Dose-response curves were generated using Microsoft Excel.

xCELLigence impedance assay HUVECs were isolated, cultured and defrosted immediately prior to use using standard procedures.⁴⁹ The background impedance of the E-plate 96 was determined with pre-warmed EGM-2 (50 µL), followed by addition of HUVEC cell suspension in EGM-2 (40 µL, 7.5×10^3 cells/well). Plates were returned to the Real-Time Cell Analyzer (RTCA) station and incubated for 5 h, with impedance measured every 10 min. Drug compound was then added in EGM-2 (10 µL, 10× concentrations to give appropriate 1× plate concentrations). The plates were returned to the RTCA and incubated for a further 40 h, with impedance measured every 40 s for 3 h, then every 30 min for 37 h. Data was obtained as cell index values which are calculated as measured impedance minus background impedance, divided by 15. These values were normalised using the cell index value obtained immediately prior to drug addition. Dose-response curves at the required

timepoint were generated and used to determine EC₅₀ values, which were calculated using a variable slope dose-response curve with Hill slope constrained to > -2.0 using GraphPad Prism version 5.0c for Mac, GraphPad Software, San Diego California USA, www.graphpad.com.

2.1.8 Appendix

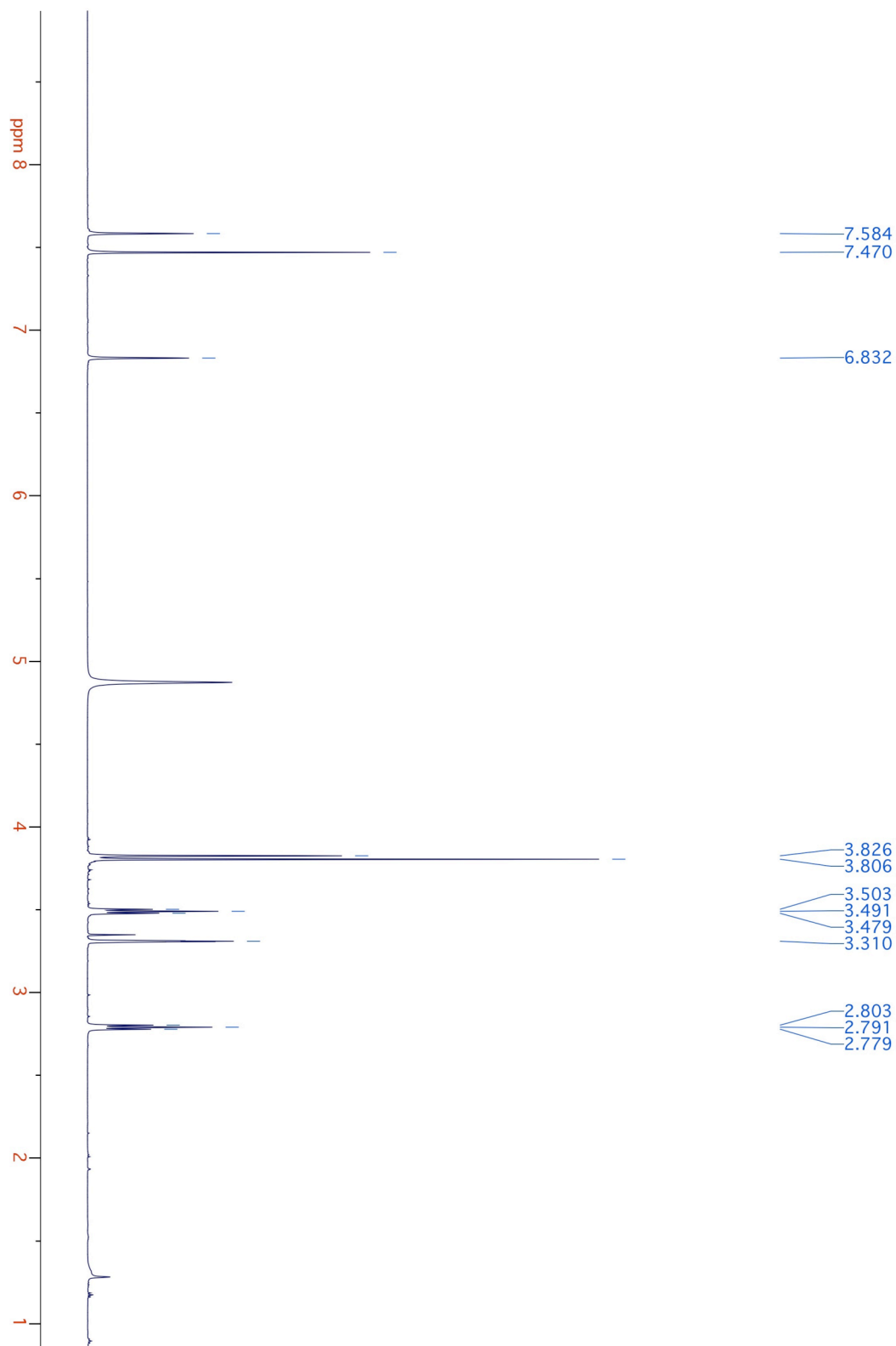
2.1.8.1 NMR Data of Natural Products

| Atom | Nat. 14 ¹³ C 62.8 MHz | Syn. 14 ¹³ C 150 MHz | Nat. 14 ¹ H 300 MHz | Syn. 14 ¹ H 600 MHz | Nat. 15 ¹³ C 62.8 MHz | Syn. 15 ¹³ C 100 MHz | Nat. 15 ¹ H 300 MHz | Syn. 15 ¹ H 400 MHz | Nat. 16 ¹³ C 125 MHz | Syn. 16 ¹³ C 100 MHz | Nat. 16 ¹ H 500 MHz | Syn. 16 ¹ H 400 MHz |
|------|--|---|--|--|--|---|--|--|---|---|--|--|
| 1 | 137.7 | 137.4 | – | – | 137.2 | 137.4 | – | – | 134.4 | 134.5 | 7.52 s | 7.52 s |
| 2 | 134.8 | 134.5 | 7.46 s | 7.47 s | 134.4 | 134.5 | 7.46 s | 7.47 s | 118.6 | 118.6 | – | – |
| 3 | 118.8 | 118.5 | – | – | 118.5 | 118.6 | – | – | 152.0 | 153.9 | – | – |
| 4 | 154.2 | 153.8 | – | – | 153.8 | 153.8 | – | – | 118.6 | 118.6 | – | – |
| 5 | 118.8 | 118.5 | – | – | 118.5 | 118.6 | – | – | 134.4 | 134.5 | 7.52 s | 7.52 s |
| 6 | 134.8 | 134.5 | 7.46 s | 7.47 s | 134.4 | 134.5 | 7.46 s | 7.47 s | 137.3 | 137.3 | – | – |
| 7 | 29.1 | 29.0 | 3.82 s | 3.83 s | 28.8 | 28.8 | 3.81 s | 3.83 s | 28.7 | 28.8 | 3.87 s | 3.87 s |
| 8 | 152.4 | 152.1 | – | – | 152.1 | 152.0 | – | – | 153.8 | 152.1 | – | – |
| 9 | 165.6 | 165.4 | – | – | 165.6 | 165.6 | – | – | 165.4 | 165.5 | – | – |
| 10 | 40.6 | 40.3 | 3.49 t | 3.49 t | 38.9 | 38.9 | 3.47 t | 3.48 t | 41.7 | 41.7 | 3.45 t | 3.46 t |
| 11 | 27.9 | 27.7 | 2.79 t | 2.79 t | 25.7 | 25.8 | 2.69 t | 2.70 t | 34.9 | 34.9 | 2.73 t | 2.74 t |
| 12 | 134.0 | 136.0 | – | – | 126.0 | 126.0 | – | – | 134.6 | 134.6 | – | – |
| 13 | 118.0 | 117.9 | 6.84 s | 6.82 s | 110.7 | 110.6 | 6.50 s | 6.50 s | 133.6 | 133.6 | 7.36 s | 7.36 s |
| 14 | 136.2 | 136.1 | 7.62 s | 7.57 s | 148.6 | 148.8 | – | – | 112.1 | 112.1 | – | – |
| 15 | 61.3 | 61.0 | 3.80 s | 3.80 s | 61.0 | 61.0 | 3.81 s | 3.82 s | 150.7 | 150.8 | – | – |
| 16 | – | – | – | – | – | – | – | – | 112.1 | 112.1 | – | – |
| 17 | – | – | – | – | – | – | – | – | 133.6 | 133.6 | 7.36 s | 7.36 s |
| 18 | – | – | – | – | – | – | – | – | 61.0 | 61.0 | 3.85 s | 3.86 s |

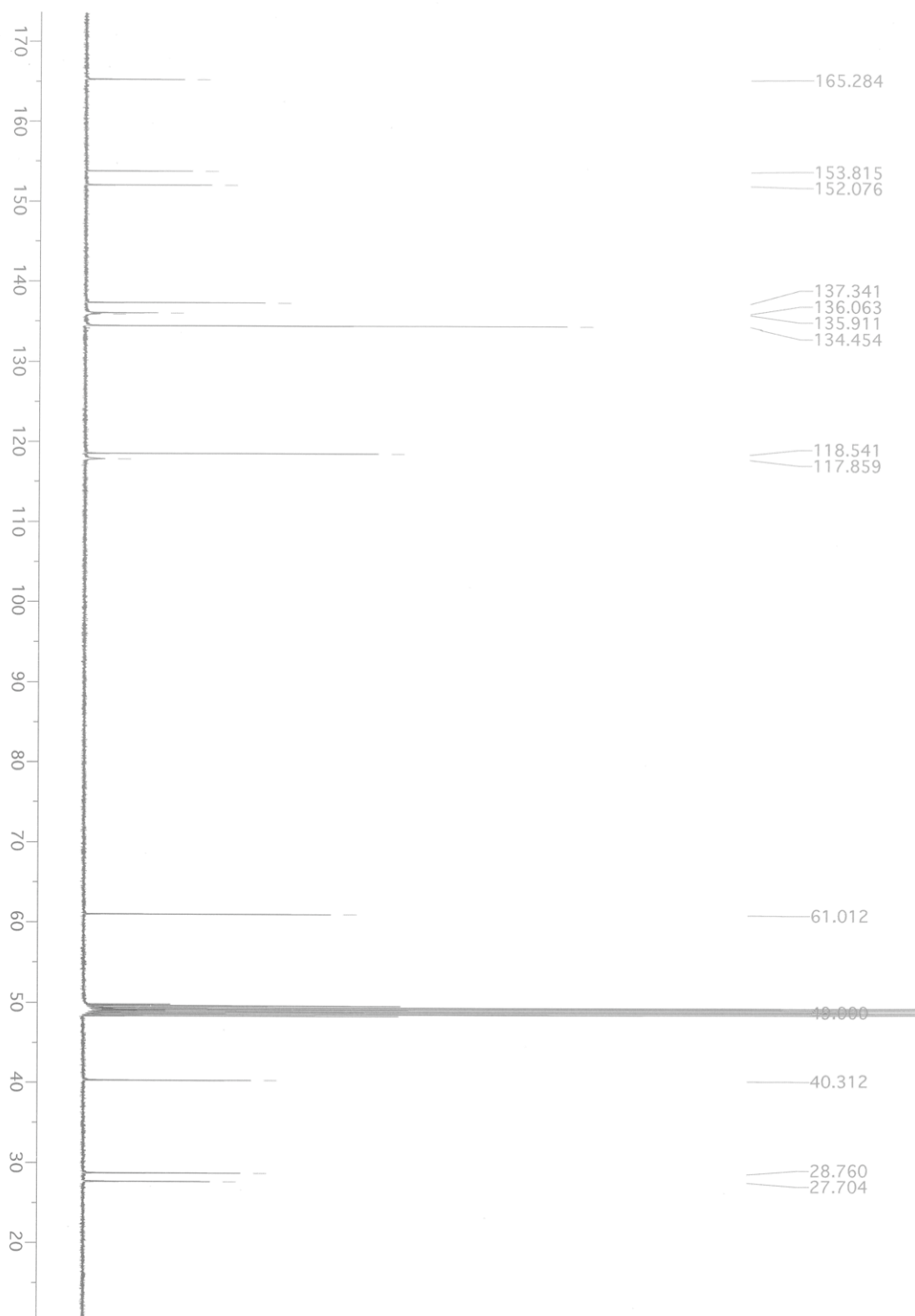
Table 3 Comparison of the NMR data (CD₃OD) of natural and synthetic (5)-bromoverongamine (**14**),¹ ianthelline (**15**),¹ and JBIR-44 (**16**).² Discrepancies in the original assignment are highlighted in bold.

2.1.8.2 NMR Spectra of Natural Products

^1H NMR (CD_3OD 600 MHz) spectrum of (5)-bromoverongamine (synthetic material)

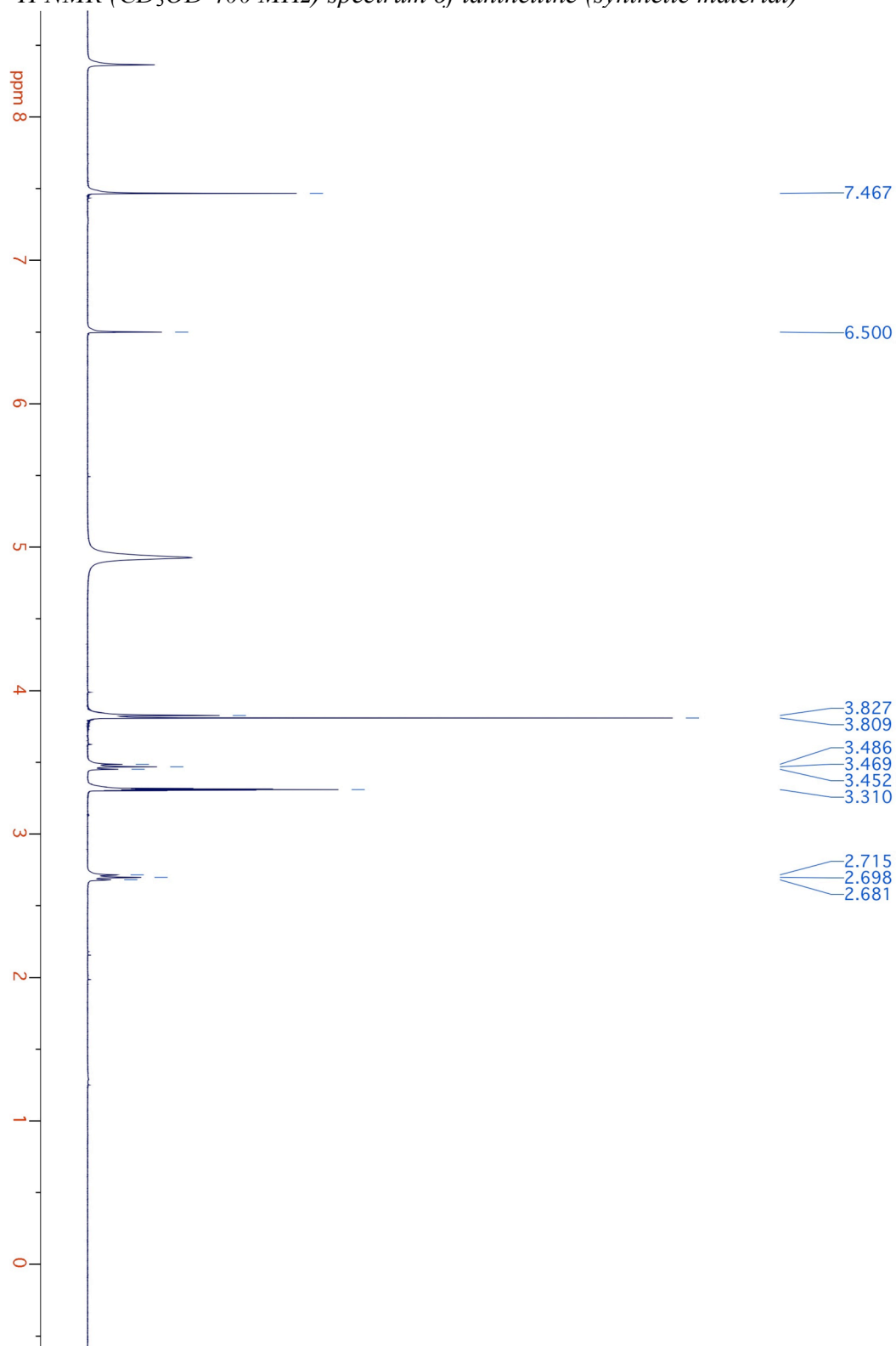


^{13}C NMR (CD_3OD 150 MHz) spectrum of (5)-bromoverongamine (synthetic material)

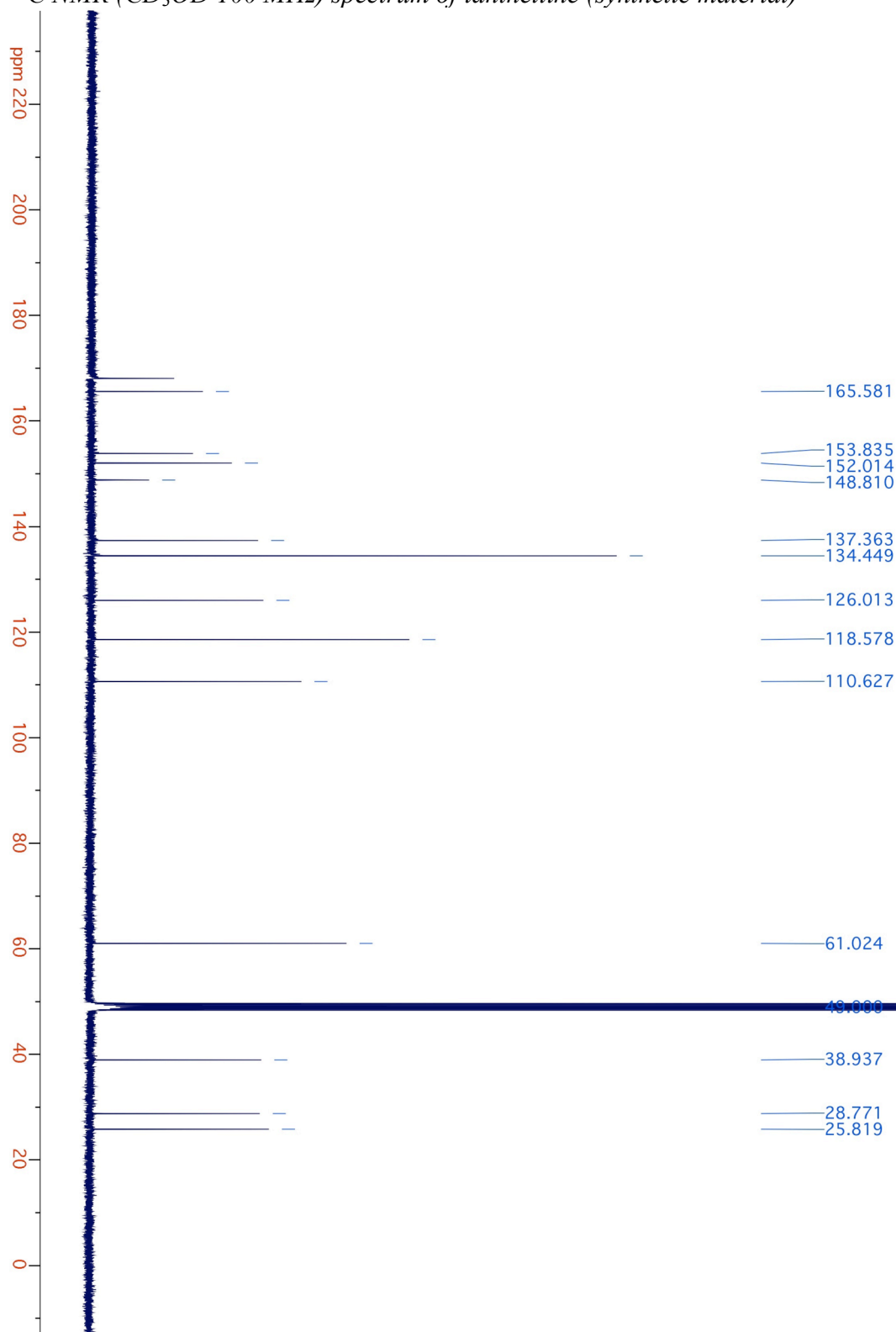


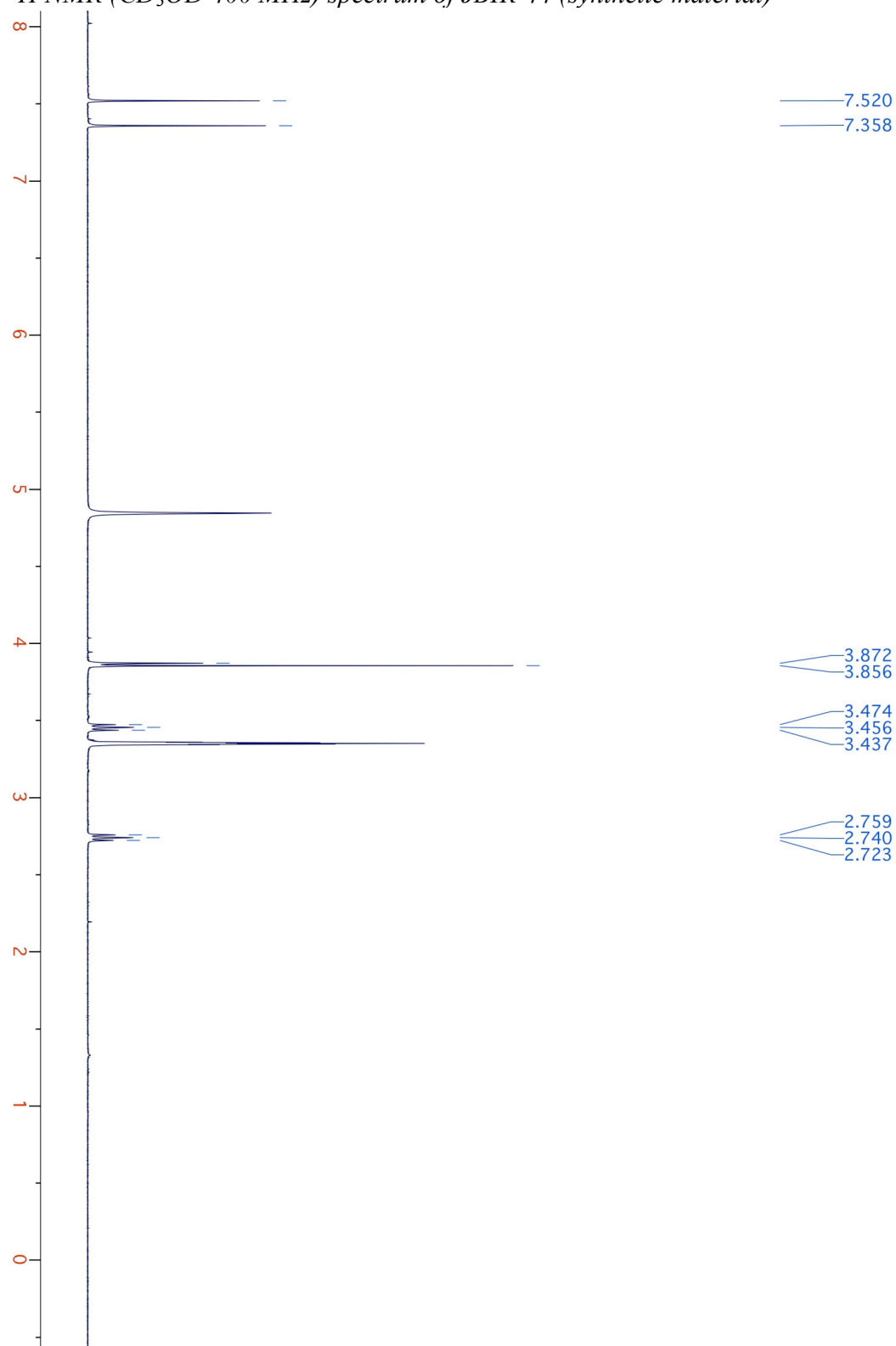


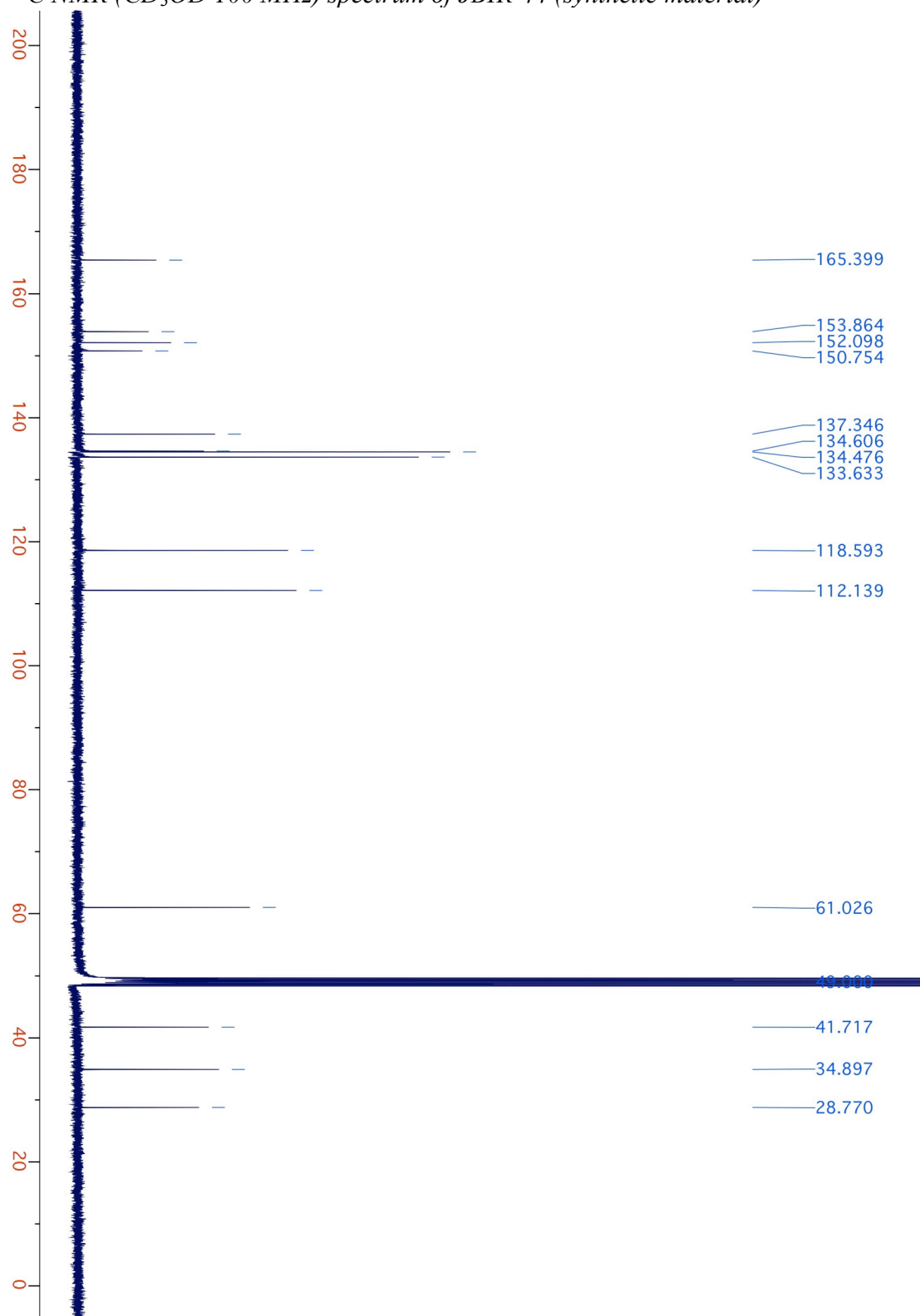
^1H NMR (CD_3OD 400 MHz) spectrum of ianthelline (synthetic material)



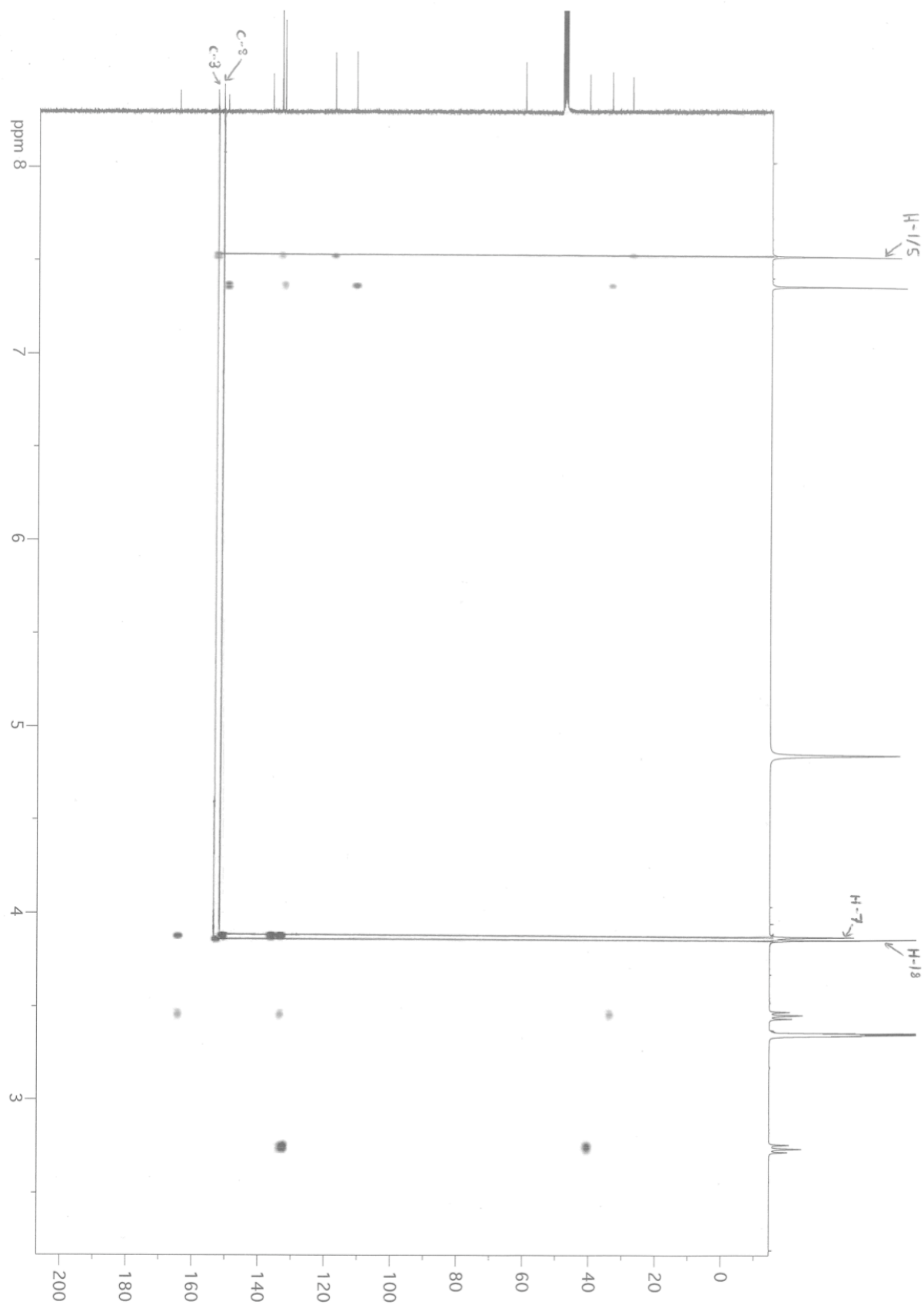
^{13}C NMR (CD_3OD 100 MHz) spectrum of ianthelline (synthetic material)

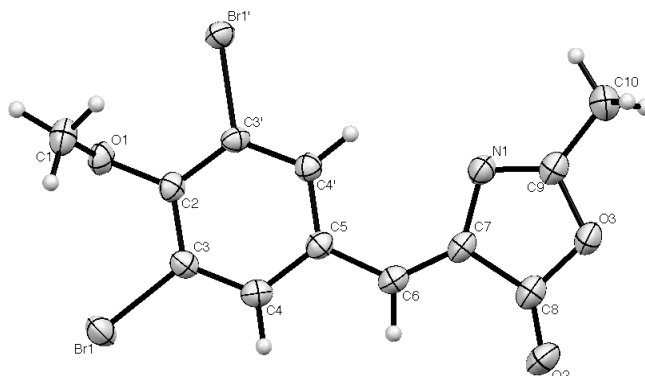


^1H NMR (CD_3OD 400 MHz) spectrum of JBIR-44 (synthetic material)

^{13}C NMR (CD_3OD 100 MHz) spectrum of JBIR-44 (synthetic material)

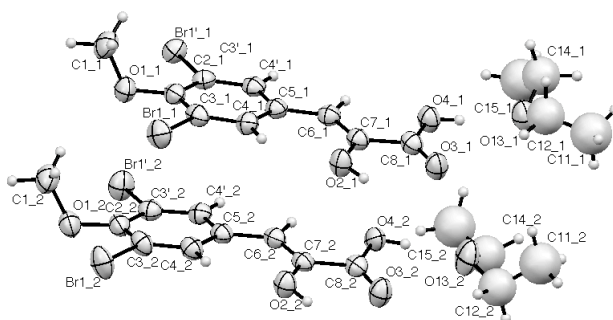
HMBC spectrum of JBIR-44 (synthetic material)



2.1.8.3 Crystal Structure Data**(Z)-4-(3,5-Dibromo-4-methoxybenzylidene)-2-methyloxazol-5(4H)-one (25)**

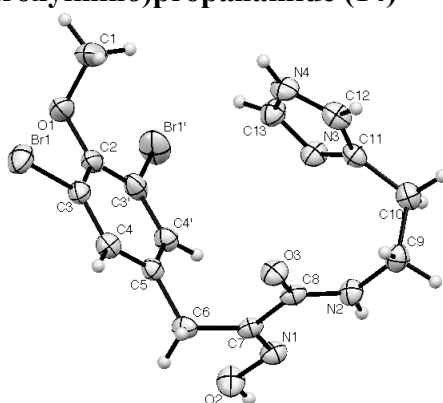
Crystal data and structure refinement for sl1031

| | |
|-----------------------------------|--|
| Identification code | sl1031 |
| Empirical formula | C ₁₂ H ₉ Br ₂ NO ₃ |
| Formula weight | 375.02 |
| Temperature | 180(2) K |
| Wavelength | 0.71073 Å |
| Crystal system | Monoclinic |
| Space group | P2(1)/c |
| Unit cell dimensions | a = 11.5810(3) Å α = 90° b = 14.3132 Å β = 94.95(3)° c = 7.6379 Å γ = 90° |
| Volume | 1261.35(8) Å ³ |
| Z | 4 |
| Density (calculated) | 1.975 Mg/m ³ |
| Absorption coefficient | 6.425 mm ⁻¹ |
| F(000) | 728 |
| Crystal size | 0.23 × 0.14 × 0.07 mm ³ |
| Theta range for data collection | 3.53 to 33.17° |
| Index ranges | -17 ≤ h ≤ 17, -21 ≤ k ≤ 21, -11 ≤ l ≤ 11 |
| Reflections collected | 18106 |
| Independent reflections | 4733 [R(int) = 0.0493] |
| Completeness to theta = 33.17° | 98.3% |
| Absorption correction | Semi-empirical from equivalents |
| Max. and min. transmission | 0.658 and 0.323 |
| Refinement method | Full-matrix least-squares on F ² |
| Data / restraints / parameters | 4733 / 0 / 165 |
| Goodness-of-fit on F ² | 1.036 |
| Final R indices [I > 2σ(I)] | R1 = 0.0328, wR2 = 0.0698 |
| R indices (all data) | R1 = 0.0504, wR2 = 0.0757 |
| Largest diff. peak and hole | 0.406 and -0.726 e. Å ⁻³ |

(Z)-3-(3,5-Dibromo-4-methoxyphenyl)-2-hydroxyacrylic acid (38)

Crystal data and structure refinement for sl1033

| | |
|-----------------------------------|---|
| Identification code | sl1033 |
| Empirical formula | C ₁₄ H ₁₈ Br ₂ O ₅ |
| Formula weight | 426.10 |
| Temperature | 180(2) K |
| Wavelength | 0.71073 Å |
| Crystal system | Monoclinic |
| Space group | P2(1)/n |
| Unit cell dimensions | a = 15.1400(3) Å α = 90° b = 15.0183(3) Å β = 101.805(1)° c = 15.3495(4) Å γ = 90° |
| Volume | 3416.31(13) Å ³ |
| Z | 8 |
| Density (calculated) | 1.657 Mg/m ³ |
| Absorption coefficient | 4.762 mm ⁻¹ |
| F(000) | 1696 |
| Crystal size | 0.42 × 0.23 × 0.12 mm ³ |
| Theta range for data collection | 3.55 to 27.89° |
| Index ranges | -19 ≤ h ≤ 19, -18 ≤ k ≤ 19, -19 ≤ l ≤ 20 |
| Reflections collected | 20026 |
| Independent reflections | 8006 [R(int) = 0.0372] |
| Completeness to theta = 27.89° | 98.2% |
| Absorption correction | Semi-empirical from equivalents |
| Max. and min. transmission | 0.451 and 0.354 |
| Refinement method | Full-matrix least-squares on F ² |
| Data / restraints / parameters | 8006 / 14 / 340 |
| Goodness-of-fit on F ² | 1.023 |
| Final R indices [I > 2σ(I)] | R1 = 0.0530, wR2 = 0.1249 |
| R indices (all data) | R1 = 0.0811, wR2 = 0.1424 |
| Largest diff. peak and hole | 1.127 and -0.702 e. Å ⁻³ |

(5)-Bromoverongamine. (*E*)-*N*-(2-(1*H*-Imidazol-5-yl)ethyl)-3-(3,5-dibromo-4-methoxyphenyl)-2-(hydroxyimino)propanamide (14)

Crystal data and structure refinement for sl1006

| | |
|-----------------------------------|--|
| Identification code | sl1006 |
| Empirical formula | C ₁₅ H ₁₆ Br ₂ N ₄ O ₃ |
| Formula weight | 460.14 |
| Temperature | 180(2) K |
| Wavelength | 0.71073 Å |
| Crystal system | Monoclinic |
| Space group | P2(1)/n |
| Unit cell dimensions | a = 8.9668(2) Å α = 90° b = 21.2760 Å β = 100.246(1)° c = 9.3347(2) Å γ = 90° |
| Volume | 1752.45(6) Å ³ |
| Z | 4 |
| Density (calculated) | 1.744 Mg/m ³ |
| Absorption coefficient | 4.647 mm ⁻¹ |
| F(000) | 912 |
| Crystal size | 0.23 × 0.18 × 0.12 mm ³ |
| Theta range for data collection | 3.60 to 30.01° |
| Index ranges | -12 ≤ h ≤ 12, -29 ≤ k ≤ 29, -12 ≤ l ≤ 12 |
| Reflections collected | 15914 |
| Independent reflections | 5050 [R(int) = 0.0586] |
| Completeness to theta = 30.01° | 98.7% |
| Absorption correction | Semi-empirical from equivalents |
| Max. and min. transmission | 0.580 and 0.362 |
| Refinement method | Full-matrix least-squares on F ² |
| Data / restraints / parameters | 5050 / 0 / 222 |
| Goodness-of-fit on F ² | 0.991 |
| Final R indices [I > 2σ(I)] | R1 = 0.0378, wR2 = 0.0927 |
| R indices (all data) | R1 = 0.0600, wR2 = 0.0991 |
| Largest diff. peak and hole | 0.587 and -0.955 e. Å ⁻³ |

2.1.9 References

- ¹ I. Thironet, D. Daloze, J. C. Braekman and P. Willemsen, *Nat. Prod. Lett.*, **1998**, *12*, 209.
- ² T. Fujiwara, J-H. Hwang, A. Kanamoto, H. Nagai, M. Takagi and K. Shin-ya, *J. Antibiot.*, **2009**, *62*, 393.
- ³ L. Arabshahi and F. J. Schmitz, *J. Org. Chem.*, **1987**, *52*, 3584.
- ⁴ G. C. Levy and G. L. Nelson, *J. Am. Chem. Soc.*, **1972**, *94*, 4897.
- ⁵ G. J. Karbatsos, R. A. Taller and F. M. Vane, *J. Am. Chem. Soc.*, **1963**, *85*, 2326.
- ⁶ L. Calcul, W. D. Inman, A. A. Morris, K. Tenney, J. Ratnam, J. H. McKerrow, F. A. Valeriote and P. Crews, *J. Nat. Prod.*, **2010**, *73*, 365.
- ⁷ A. S. Clare, *Biofouling*, **1996**, *9*, 211.
- ⁸ http://www.eurekalert.org/pub_releases/2009-06/oonr-nhc060409.php
- ⁹ N. Fusetani, *Nat. Prod. Rep.*, **2011**, *28*, 400; N. Fusetani, *Nat. Prod. Rep.*, **2004**, *21*, 94.
- ¹⁰ S. Ortlepp, M. Sjögren, M. Dahlström, H. Weber, R. Ebel, R. Edrada, C. Thoms, P. Schupp, L. Bohlin and P. Proksch, *Mar. Biotech.*, **2007**, *9*, 776.
- ¹¹ P. Proksch, A. Putz, S. Ortlepp, J. Kjer and M. Bayer, *Phytochem. Rev.*, **2010**, *9*, 475.
- ¹² M. Ishibashi, M. Tsuda, Y. Ohizumi, T. Sasaki and J. Kobayashi, *Experientia*, **1991**, *47*, 299.
- ¹³ J. Kobayashi, M. Tsuda, K. Agemi, H. Shigemori, M. Ishibashi, T. Sasaki and Y. Mikami, *Tetrahedron*, **1991**, *47*, 6617.
- ¹⁴ J. Jurek, W. Y. Yoshida and P. J. Scheuer, *J. Nat. Prod.*, **1993**, *56*, 1609.
- ¹⁵ J. N. Tabudravu and M. Jaspars, *J. Nat. Prod.*, **2002**, *65*, 1798.
- ¹⁶ E. O. Pordesimo and F. J. Schmitz, *J. Org. Chem.*, **1990**, *55*, 4704.
- ¹⁷ J. Kobayashi, K. Honma, T. Sasaki and M. Tsuda, *Chem. Pharm. Bull.*, **1995**, *43*, 403.
- ¹⁸ M. S. Buchanan, A. R. Carroll, G. A. Fechner, A. Boyle, M. M. Simpson, R. Addepalli, V. M. Avery, J. N. A. Hooper, N. Su, H. Chen and R. J. Quinn, *Bioorg. Med. Chem. Lett.*, **2007**, *17*, 6860.

- ¹⁹ M. S. Buchanan, A. R. Carroll, G. A. Fechner, A. Boyle, M. Simpson, R. Addepalli, V. M. Avery, J. N. A. Hooper, T. Cheung, H. Chen and R. J. Quinn, *J. Nat. Prod.*, **2008**, *71*, 1066.
- ²⁰ M. Y. Ahn, J. H. Jung, Y. J. Na and H. S. Kim, *Gynecol. Oncol.*, **2008**, *108*, 27.
- ²¹ D. H. Kim, J. Shin and H. J. Kwon, *Exp. Mol. Med.*, **2007**, *39*, 47.
- ²² S. K. Kottakota, J. J. Harburn, A. O'Shaughnessy, M. Gray, P. Konstanidis and D. E. Yakubu, 13th International Electronic Conference on Synthetic Organic Chemistry (ESOC-13), 1-30 November, **2009**.
- ²³ M. Litaudon and M. Guyot, *Tetrahedron Lett.*, **1986**, *27*, 4455.
- ²⁴ P. Ciminiello, E. Fattorusso, S. Magno and M. Pansini, *J. Nat. Prod.*, **1995**, *58*, 689.
- ²⁵ S. R. Kelly, E. Garo, P. R. Jensen, W. Fenical and J. R. Pawlik, *Aquat. Microb. Ecol.*, **2005**, *40*, 191.
- ²⁶ B. Liu and J. Zhou, *J. Comput. Chem.*, **2005**, *26*, 484.
- ²⁷ S. Nishiyama and S. Yamamura, *Bull. Chem. Soc. Jpn.*, **1985**, *58*, 3453; G. Zhu, F. Yang, R. Balachandran, P. Höök, R. B. Vallee, D. P. Curran and B. W. Day, *J. Med. Chem.*, **2006**, *49*, 2063.
- ²⁸ H. H. Wasserman and J. Wang, *J. Org. Chem.*, **1998**, *63*, 5581.
- ²⁹ J. García, R. Pereira and A. R. de Lera, *Tetrahedron Lett.*, **2009**, *50*, 5028.
- ³⁰ A. M. Godert, N. Angelino, A. Woloszynska-Read, S. R. Morey, S. R. James, A. R. Karpf and J. R. Sufrin, *Bioorg. Med. Chem. Lett.*, **2006**, *16*, 3330.
- ³¹ N. T. R. Boehlow, J. Harburn and C. D. Spilling, *J. Org. Chem.*, **2001**, *66*, 3111.
- ³² K. L. Bailey and T. F. Molinski, *Tetrahedron Lett.*, **2002**, *43*, 9657.
- ³³ K. J. Okamoto and J. Clardy, *Tetrahedron Lett.*, **1987**, *28*, 4969.
- ³⁴ E. Erleneyer, *Justus Liebigs Ann. Chem.*, **1893**, *275*, 1.
- ³⁵ E. L. Schumann, R. V. Heinzelman, M. E. Greig and W. Veldkamp, *J. Med. Chem.*, **1964**, *51*, 329.
- ³⁶ W. Nagai, K. L. Kirk and L. A. Cohen, *J. Org. Chem.*, **1973**, *38*, 1971; Y. St-Denis, S. Lévesque, B. Bachand, J. J. Edmunds, L. Leblond, P. Prévile, M. Tarazi, P. D. Winocour and M. A. Siddiqui, *Bioorg. Med. Chem. Lett.*, **2002**, *12*, 1181.

- ³⁷ J. A. Diers, H. K. Pennaka, J. Peng, J. J. Bowling, S. O. Duke and M. T. Hamann, *J. Nat. Prod.*, **2004**, 67, 2117.
- ³⁸ N. Ullah and K. M. Arafah, *Tetrahedron Lett.*, **2009**, 50, 158.
- ³⁹ B. M. Chanda and R. S. Sulake, *Tetrahedron Lett.*, **2005**, 46, 6461; P. Busca, F. Paradisi, E. Moynihan, A. R. Maguire and P. C. Engel, *Org. Biomol. Chem.*, **2004**, 2, 2684; H. N. C. Wong, Z. L. Xu, H. M. Chang and C. M. Lee, *Synthesis*, **1992**, 793.
- ⁴⁰ P. D. Leeson and B. Springthorpe, *Nat. Rev. Drug Discov.*, **2007**, 6, 881.
- ⁴¹ P. B. de la Mare and P. A. Newman, *J. Chem. Soc., Perkin Trans. 2*, **1984**, 231.
- ⁴² S. M. Johnson, S. Connelly, I. A. Wilson and J. W. Kelly, *J. Med. Chem.*, **2008**, 51, 6348.
- ⁴³ N. Ullah, S. A. Haladu and B. A. Mosa, *Tetrahedron Lett.*, **2011**, 52, 212.
- ⁴⁴ T. Kolasa and A. Chimiak, *Pol. J. Chem.*, **1981**, 55, 1163.
- ⁴⁵ G. F. Ruda, V. P. Alibu, C. Mitsos, O. Bidet, M. Kaiser, R. Brun, M. P. Barrett and I. H. Gilbert, *ChemMedChem*, **2007**, 2, 1169.
- ⁴⁶ J. Deles, E. Kolaczowska and A. Superson, *Pol. J. Chem.*, **1979**, 53, 1025.
- ⁴⁷ J. Shen, R. Woodward, J. P. Kedenburg, X. Liu, M. Chen, L. Fang, D. Sun and P. G. Wang, *J. Med. Chem.*, **2008**, 51, 7417.
- ⁴⁸ Yang, F. Ph.D. Thesis, University of Pittsburgh, **2006**.
- ⁴⁹ E. A. Jaffe, R. L. Nachman, C. G. Becker and C. R. Minick, *J. Clin. Invest.*, **1973**, 52, 2745.

CHAPTER 2 *Part II*

(5)-Bromoverongamine and JBIR-44: Structure-Activity Relationship Analysis

2.2.1 Introduction

Whether it is in industry or academia, the discovery of a novel bioactive natural product is commonly followed-up by a synthesis programme that serves to confirm the structural assignment and provide material for further biological studies. Once a robust synthesis route has been developed, a medicinal chemistry approach traditionally involving SAR analysis is adopted in order to establish the key pharmacophoric elements. Developing a pharmacophore model for a biological target is vital because it can be used in lead-optimisation and rational design scenarios, thereby accelerating the drug-discovery process.

Intriguingly, there is very little by way of SAR studies into bromotyrosine derivatives.¹ This is in spite of their rich bioactivity profiles and the relative ease in which their structural architectures can be accessed. Historically, brominated molecules, especially those containing multiple bromine atoms, would have been considered unattractive drug-leads due to their undesirable physicochemical properties. Understandably, these compounds run the risk of violating the molecular weight and LogP boundaries outlined in Lipinski's Rules.² Nevertheless, the use of bromine (and the other halogens) should not be disregarded when embarking on drug-discovery programmes.

Perhaps surprisingly, around half of the molecules entered into high-throughput screening programmes are halogenated³ and as a consequence of this, an ever-increasing number of drugs and drug candidates in development are halogenated structures. The vast majority of these contain fluorine and/or chlorine atoms.* In the past, the introduction of halogen atoms (particularly fluorine) has been used to block metabolically labile positions since carbon-halogen bonds are not readily metabolised by cytochrome p450 enzymes. Furthermore, halogenation is also known to improve a compound's oral permeability, blood-brain-barrier penetration, and selectivity for a particular target. In an attempt to improve potency, installation of a halogen atom at a tolerated site within a molecule is a common strategy employed by medicinal chemists. Until recently, it was believed that an increase in potency was purely due to a steric effect—the basis of this argument being that the halogen could exploit a

* From 1988 to 2006, 57% of halogenated drugs were fluorinated and 38% were chlorinated. In comparison, 4% of halogenated drugs contained bromine and only 1% contained iodine (*Curr. Drug Targets*, **2010**, *11*, 1).

hydrophobic pocket in the biological target and this additive binding would thus increase the affinity of the ligand to its target. In fact, it has now come to light that halogen atoms have the ability to engage with functional groups in a protein and form intermolecular bonding interactions. These electrostatic interactions are termed halogen bonds and although they are a familiar concept and have been extensively characterised in the area of supramolecular chemistry, investigations into the importance of this phenomenon in a biological setting is very much in its infancy.

In the simplest of terms, halogen bonding is analogous to hydrogen bonding and involves an interaction between an electronegative atom (*e.g.* O or N) and the electropositive cap (termed “sigma hole”) at the end region of halogen atoms (Cl, Br, I) along the C-X axis. As the halogen atom can be viewed as the electrophilic partner in this interaction, the strength of the halogen bond is positively correlated with the electrostatic potential of the cap; the strength of the interaction follows the trend $I > Br > Cl$.

The biological relevance of this interaction was first analysed in detail by Auffinger and co-workers. By surveying the Protein Data Bank (July 2004 release), they were able to identify 113 distinct halogen-protein interactions.⁴ In 2008, this number had risen to 248 and consisted of 47% $Cl \cdots O$, 22% $Br \cdots O$, and 31% $I \cdots O$ interactions with backbone carbonyl oxygens or side chain hydroxyl and carboxyl oxygens.⁵ In the same study, halogen bonding was shown to play an important role in inhibitor recognition and binding in protein kinases.

It is clearly evident that halogen bonding is a valid and important interaction that needs to be considered when working with halogenated molecules in a medicinal chemistry setting. To put this in context, IDD 594 is a highly selective aldolase reductase inhibitor⁶; this selectivity is necessary to avoid the toxicity associated with off-target effects that include inhibition of aldehyde reductase enzymes. Co-crystallisation of IDD 594 with aldose reductase revealed a short contact ($<3 \text{ \AA}$) that turned out to be responsible for the observed selectivity (Figure 23).

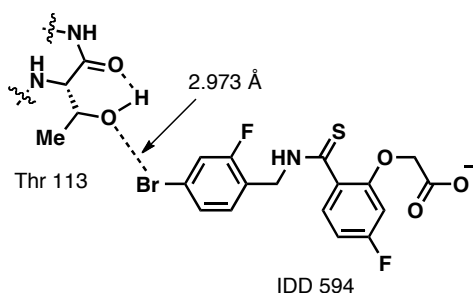


Figure 23 Halogen bonding of IDD 594 to aldolase reductase through Thr 113 residue.

In the Ley group, we are undertaking research in the area of halogen bonding after discovering that replacing *meta*-methoxy groups in the A-ring of the natural product combretastatin A-4 with halogen atoms leads to analogues that have equal or superior potency against cancer cells and HUVECs.⁷ Whilst these analogues retained both the antitubulin and antimitotic effects of the parent compound, intriguingly, the dibrominated compound (at 100 nM) caused the accumulation of interphase microtubules around the nucleus of HeLa cells (not shown). This phenomenon was also observed in MCF-7 cells that had been treated with ceratamine A (Chapter 1 Figure 9d); combretastatin A-4 did not elicit this response.

Curiously, the degree of biological activity exhibited by these analogues follows a distinct trend, for example, the antimitotic activity of the analogues increased in the order $F \ll Cl \approx OMe < Br < I$ (Figure 24). This trend correlates well with both halogen Van der Waal's radii and the calculated strength of halogen bonding. We believe the steric effect cannot be used to explain this trend because the Van der Waal's radii of bromine (1.85 Å) and iodine (1.98 Å) are smaller than that of a methoxy substituent (2.60 Å). Therefore, to account for these observations, we hypothesise that halogen bonding interactions can arise between tubulin and the dibromo and diiodo analogues which, in turn, increases the binding affinity.

Initial computational investigations into the binding of these halogenated combretastatin A-4 analogues to the tubulin heterodimer appear to support this hypothesis. Multiple rounds of energy minimisation of the ligand in the presence of the protein have shown that the free energy of binding for the diiodo analogue is greater than that for the dibromo analogue and combretastatin A-4. Furthermore, molecular docking supports this data, which shows that the halogenated portion of the

diiodo analogue is embedded further into the binding site when compared with the A-ring of combretastatin A-4 and other analogues.[†]

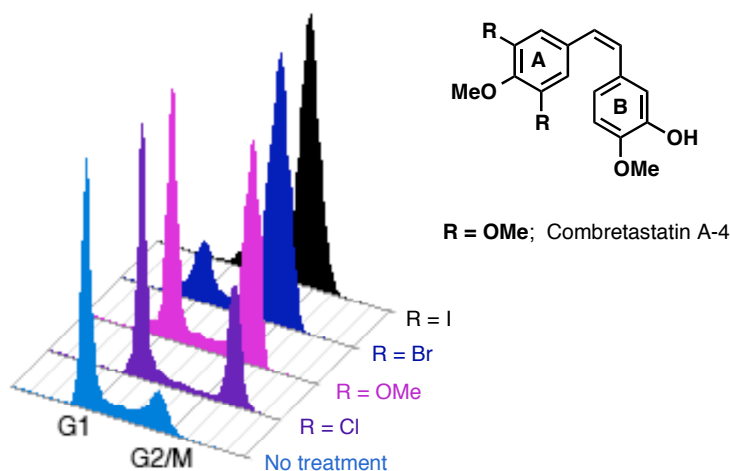


Figure 24 Antimitotic activity of analogues represented by histograms of DNA profiles showing G₁ and G₂/M populations.

To complement this research on the combretastatin A-4 analogues, we sought to investigate the importance of the 3,5-dibromo-4-methoxyaryl motif on the anticancer activities exhibited by the bromotyrosine derivatives in the first part of this chapter. To this end, we planned to synthesise analogues of (5)-bromoverongamine and JBIR-44 with the aryl ring substitution patterns (**40** to **44**) outlined in Figure 25. This library of compounds would enable us to probe the SAR of these natural products in a systematic fashion—to our knowledge, this traditional medicinal chemistry approach towards understanding the biological relevance of the 3,5-dibromo-4-methoxyaryl motif in bromotyrosine derivatives has not been reported in the literature.

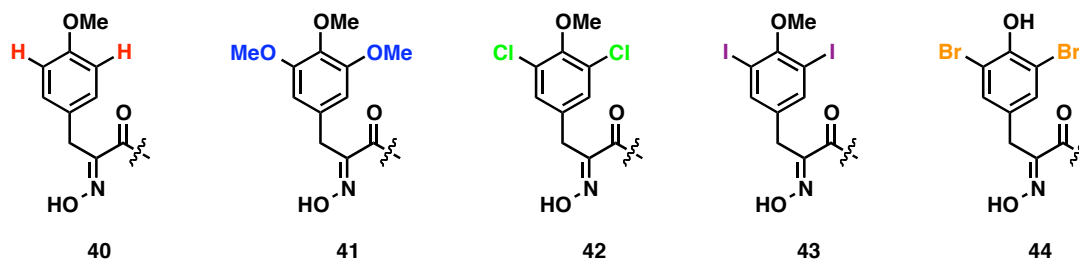


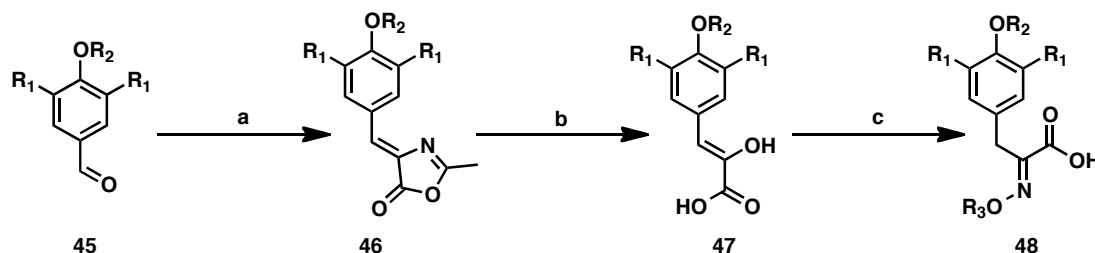
Figure 25 Desired phenyl ring substitutions on (5)-bromoverongamine and JBIR-44.

[†] Personal communication with Thomas M. Beale Esq.

2.2.2 Results and Discussion

It was our aim to synthesise these analogues in a similar vein to the natural products, whereby an α -oximino acid is coupled to the amine side chain, with the oxime functionality unmasked by removal of the PMB group (Scheme 8). Furthermore, it was envisaged that the collection of α -oximino acids which possessed the desired aryl ring substitutions could be accessed in short order by making use of the chemistry developed in the first part of this chapter (Scheme 19).

To recap, aldehydes of type **45** can be converted to the corresponding azlactones (**46**) using conditions described by Erlenmeyer. Finally, the phenylpyruvic acid derivatives (**47**), obtained from the acidic hydrolysis of **46**, can be condensed with a (*O*-protected) hydroxylamine to furnish the corresponding α -oximino acids (**48**). In this strategy, it is necessary for the 3,5-aryl substituents to be installed at the beginning of the synthesis and therefore the R_1 functionality in **48** is dependent on the starting aldehyde. Importantly, this route is not just limited to variations at R_1 ; diversity can also be introduced by modifying the phenolic substituent (R_2) or by using a range of *O*-protected hydroxylamines (R_3).



Scheme 19 General route to α -oximino acids of type **48**.

Reagents and conditions: (a) *N*-acetylglycine, NaOAc, Ac₂O, 120 °C; (b) 3 *N* HCl, reflux; (c) NH₂OR₃·HCl, NaOAc, EtOH.

The starting aldehydes necessary for the analogue syntheses are shown in Figure 26. 3,5-Dichloro-4-methoxybenzaldehyde (**51**) and 3,5-diiodo-4-methoxybenzaldehyde (**52**) were not available from commercial sources and therefore had to be synthesised.

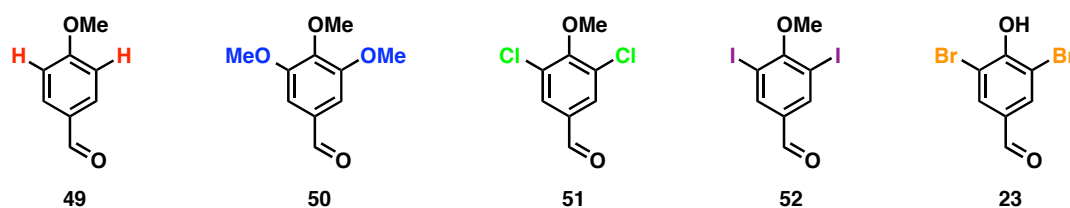
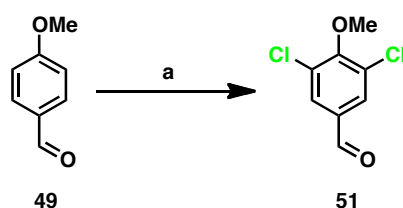


Figure 26 Starting aldehydes.

2.2.2.1 Synthesis of 3,5-Dichloro-4-methoxy Benzaldehyde (**51**)

3,5-Dichloro-4-methoxybenzaldehyde (**51**) is a naturally occurring halometabolite produced *de novo* from glucose by fungi of the phylum Basidiomycota.⁸ Yet, despite its structural simplicity, a convenient synthetic method to access **51** has yet to be reported. In 1923, Durrans was able to isolate **51** from a neat mixture of sulfuryl chloride (SO₂Cl₂) and anisaldehyde (**49**) that had been left at room temperature for three days (Scheme 20).⁹ Using this information as a start point, we began by investigating the chlorination of **49** and 4-hydroxybenzaldehyde (**53**) with sulfuryl chloride.



Scheme 20 Durrans' method for producing **51**.

Reagents and conditions: (a) SO₂Cl₂, rt, neat, 3 days.

Sulfuryl chloride is a source of Cl₂ and is often used instead of the gas because it is more convenient to handle. Although the reactivity of the halogens increases in the order I₂<Br₂<Cl₂<F₂, performing multiple electrophilic aromatic substitution reactions on a phenyl ring using chlorine is not trivial and can require forcing conditions and the presence of a catalyst.¹⁰ This is because the introduction of a second chlorine atom is disfavoured because of the deactivating effect the first chlorine atom imparts towards the next electrophilic substitution. In our case, it soon became apparent that whilst monochlorination of both substrates occurred rapidly, chlorination of the 3-chloroanisaldehyde (from **49**, results not shown) proved difficult. Therefore, the following discussion will describe the optimisation to find conditions to affect the *bis*-chlorination of **53** to 3,5-dichloro-4-hydroxybenzaldehyde (**54**) (Table 4). Once accessed, it was hoped **54** could then be methylated to access the desired aldehyde **51**.

In the beginning, **53** and SO₂Cl₂ (2.5 eq.) in CH₂Cl₂ were heated at 60 °C under microwave conditions for 10 minutes (Table 4, entry 1). By ¹H NMR analysis, the ratio of monochloro (**55**) to dichloro product (**54**) was 19.5:1. Next, the amount SO₂Cl₂ was increased in an attempt to improve this ratio (entries 2 and 3). From this experimentation, it was decided that 10 equivalents would be used for further

optimisation.[‡] By lengthening the reaction time to 2 hours (entry 4) and increasing the temperature to 80 °C (entry 5), the product ratio was eventually pushed in favour of the *bis*-chlorinated aldehyde **54**. An extended reaction time of 10 hours at 80 °C finally gave a more acceptable ratio of **55:54** (1:7); however, this reaction time was not ideal from the perspective of microwave chemistry.

Table 4 Conditions for the chlorination of **53** with sulfuryl chloride.

| | 53 | | 55 | + | 54 |
|-------|---------------------------------|---------------------------------------|-----------------|--------|---------------------------------|
| Entry | Solvent | SO ₂ Cl ₂ (eq.) | Temp/°C | Time/h | Ratio ^a 55:54 |
| 1 | CH ₂ Cl ₂ | 2.5 | 60 ^b | 0.2 | 19.5:1 |
| 2 | CH ₂ Cl ₂ | 7.5 | 60 ^b | 0.2 | 9.5:1 |
| 3 | CH ₂ Cl ₂ | 10 | 60 ^b | 0.2 | 7.2:1 |
| 4 | CH ₂ Cl ₂ | 10 | 60 ^b | 2 | 2.2:1 |
| 5 | CH ₂ Cl ₂ | 10 | 80 ^b | 2 | 1:1.33 |
| 6 | CH ₂ Cl ₂ | 10 | 80 ^b | 10 | 1:7 |
| 7 | MeCN | 10 | rt | 1.67 | 1:0.425 |
| 8 | MeCN | 10 | rt | 5 | 1:1.5 |
| 9 | MeCN | 10 | rt | 6 | 1:2.4 |
| 10 | MeCN | 10 | rt | 20 | 0:1 |
| 11 | MeCN | 2.5 | rt | 18 | 1.2:1 |
| 12 | MeCN | 2.5 | rt | 48 | 1:1 |
| 13 | EtOAc | 10 | 80 | 5 | 0:1 imp |
| 14 | EtOAc | 10 | 65 | 1 | 1:5.34 |
| 15 | EtOAc | 10 | 65 | 2 | 0:1 |
| 16 | EtOAc | 5 | 65 | 2 | 1:4.88 |
| 17 | EtOAc | 2.5 | 65 | 2 | 2.7:1 |

^a Product ratios were calculated by ¹H NMR; ^b Heated under microwave irradiation.

As chlorination is known to be much more rapid in polar solvents, acetonitrile was used in place of dichloromethane.¹¹ A rapid evolution of gas was observed upon the addition of SO₂Cl₂ to a solution of **53** in MeCN and in view of safety, the mixture was not heated (entries 7-10). Although full conversion to **54** was observed after 20 hours, a major impurity appeared to be present by ¹H NMR analysis.[§] This was confirmed when the mass recovery was far greater than anticipated following an aqueous work-up. The impurity was identified as 2,2,2-trichloroacetamide by X-ray crystallographic analysis. It is thought the chlorine liberated *in situ* reacted with the acetonitrile solvent

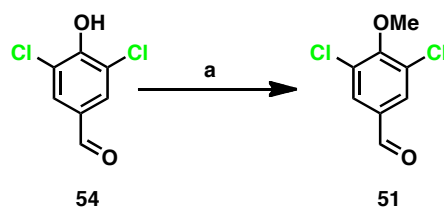
[‡] As these reactions were performed in sealed microwave vials, increasing the stoichiometry above 10 equivalents was prohibitive due to the volumes of SO₂Cl₂ that would have been required.

[§] This was characterised by two broad peaks at 6.62 and 6.30 in the ¹H NMR spectrum.

to form 2,2,2-trichloroacetonitrile which upon work-up, hydrolysed under the acidic conditions to give the corresponding acetamide. The stoichiometry of SO_2Cl_2 was reduced in an effort to limit this side reaction however this prevented full conversion to the *bis*-chlorinated product (entries 11 and 12).

In 2009, Terasaki and co-workers reported the chlorination of *para*-hydroxybenzoate esters with SO_2Cl_2 in ethyl acetate at 80 °C.¹² In our hands, full conversion of **53** to **54** was achieved by heating (conventional) the mixture to 80 °C for 5 hours in a sealed tube, however, a significant by-product was formed—this was derived from the aldehyde **54** and although not formally characterised was presumed to be the trichlorinated product (entry 13). Pleasingly, by reducing the temperature and reaction time, the formation of this by-product could be minimised without compromising the conversion of **53** to **54** (entries 14 and 15). Under these conditions (65 °C, 2 hours), attempts to lower the equivalents of SO_2Cl_2 without affecting the conversion proved unsuccessful (entries 16 and 17).

Methylation of the crude products from entries 6 and 15 was performed using the conditions described previously in Part I of this chapter (Scheme 21) to give **51** in 40% (entry 15) and 69% (entry 6) yields in two steps from 4-hydroxybenzaldehyde.**



Scheme 21 Methylation of the crude products from Table 4, entries 6 and 15.

Reagents and conditions: (a) MeI, K_2CO_3 , acetone, 60 °C, 3 h, 40% (entry 15) and 69% (entry 6) from **53**.

** Despite the lower yield, scale up of material was performed using the conditions described in entry 15. These conditions proved to be more convenient since the chlorination reactions could be run in parallel when using conventional heating.

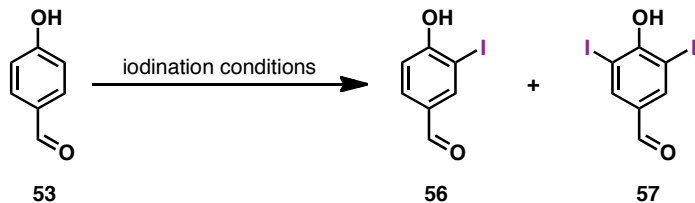
2.2.2.2 Synthesis of 3,5-Diiodo-4-methoxy Benzaldehyde (52)

As previously mentioned, electrophilic aromatic iodination is the least facile of the halogenation substitutions due to the low electrophilic strength of molecular iodine. With the exception of highly reactive substrates (anilines or phenolate anions), iodination of aromatic species often requires the use of an activated iodinating species. Common approaches involve the use of I^+ reagents,¹³ iodides,¹⁴ or molecular iodine in combination with an oxidising agent.¹⁵

Again, 4-hydroxybenzaldehyde (**53**) was chosen instead of anisaldehyde as the starting substrate given its greater propensity to undergo electrophilic substitution reactions. Of direct relevance to this, the mono and *bis*-iodination of phenols is heavily precedented in the literature. Research into this area has been driven in part by the importance of this process in the fields of radiopharmaceuticals¹⁶ and thyroid hormones.¹⁷

Starting with a mild and efficient iodination procedure, treatment of **53** with *bis*(pyridine)iodonium tetrafluoroborate (Barluenga's reagent) for 2 hours at room temperature exclusively gave **57** in 95% yield after purification (Table 5, entry 1).¹⁸ Although this transformation was high yielding, the cost of the iodinating reagent^{††} and need for purification meant an alternative procedure was desirable. Sudalai and co-workers developed a $NaIO_4/KI/NaCl$ system for the *in situ* generation of iodine monochloride that was shown to affect the *bis*-iodination of **53** in excellent yield after only 15 minutes at room temperature.¹⁹ In our hands, no conversion of **53** to either **56** or **57** was observed (by 1H NMR) after this timeframe (entry 2); however, after 24 h, partial conversion to the desired product **57** was evident (entry 3). Full conversion occurred after 96 hours and, following an aqueous work-up with sodium thiosulfate, **57** (>10 g) was obtained in 98% yield and excellent purity (entry 4).

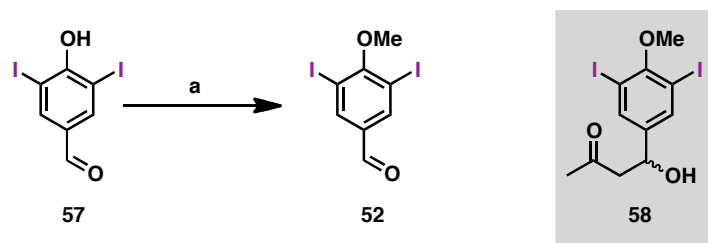
^{††}At the time of this research, the in-house preparation of *bis*(pyridine)iodonium tetrafluoroborate was not feasible as it involved the use of mercury(II) oxide. However, Davies and co-workers recently developed a safe and scalable preparation using silver as a substitute for mercury (*Org. Synth.*, **2010**, 87, 288).

Table 5 Conditions for the iodination of **53**.


| Entry | Reagent | Solvent | Temp/°C | Time/h | Ratio ^a 53:56:57 |
|-------|------------------------------------|---------------------------------|---------|--------|--------------------------------|
| 1 | I(Py) ₂ BF ₄ | CH ₂ Cl ₂ | rt | 2 | 0:0:1 |
| 2 | KI, NaIO ₄ , NaCl | AcOH/H ₂ O (9:1) | rt | 0.25 | No conversion |
| 3 | KI, NaIO ₄ , NaCl | AcOH/H ₂ O (9:1) | rt | 24 | 1:1.9:7.1 |
| 4 | KI, NaIO ₄ , NaCl | AcOH/H ₂ O (9:1) | rt | 96 | 0:0:1 |

^a Product ratios were calculated by ¹H NMR.

Methylation of **57** proceeded smoothly using the conditions described previously to give **52** in 90% yield after purification (Scheme 22). It is worth noting that a significant by-product formed when the reaction time was extended to 7.5 hours (*cf.* 3.5 hours). This was identified as the β-hydroxy carbonyl compound **58**—the aldol product of acetone with aldehyde **52**.

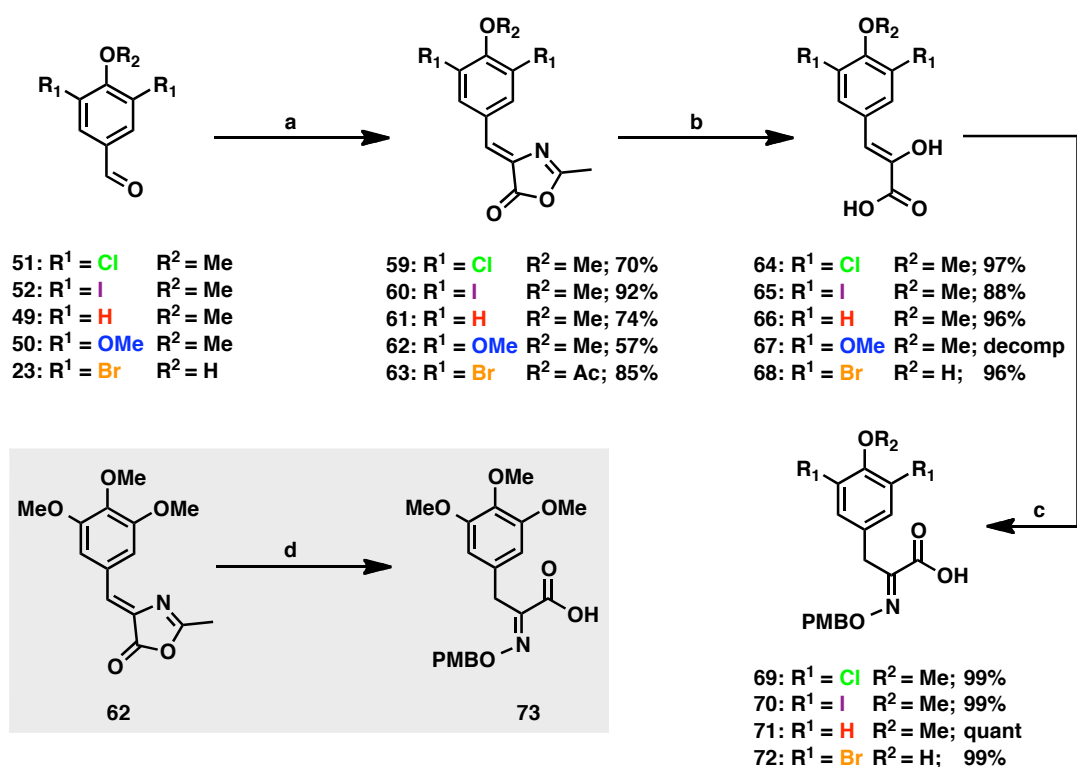
**Scheme 22** Methylation of **57**.

Reagents and conditions: (a) MeI, K₂CO₃, acetone, 60 °C, 3.5 h, 90%.

2.2.2.3 Synthesis of α-Oximino Acid Derivatives

With the required collection of aldehydes now in hand, the syntheses of the corresponding α-oximino acid derivatives **69** to **73** could be realised. Formation of the azlactones **59** to **63** was achieved using the previously described Erlenmeyer conditions. In the case of **63**, the 4-hydroxy functionality in the parent aldehyde (**23**)

was acetylated under the reaction conditions (Scheme 23).^{††} Although the acidic hydrolyses of azlactones **59** (22 hours), **60** (37 hours), **61** (17 hours), and **63** (10 hours) were high yielding, the trimethoxy azlactone **62** decomposed when subjected to these conditions (~2 hours). This was somewhat unexpected since Wong and co-workers reported the acidic hydrolysis of **62** to **67** using identical conditions (3 *N* HCl, 100 °C, 4 hours, 78%).²⁰ Nevertheless, the trimethoxy α -oximino acid **73** could be accessed directly from **62** following saponification of the azlactone with barium hydroxide and subsequent condensation with *O*-PMB hydroxylamine hydrochloride (**26**), albeit in a 30% yield. For the other substrates, condensation of *O*-PMB hydroxylamine hydrochloride with the phenylpyruvic acid derivatives **64**, **65**, **66** and **68** in the presence of sodium acetate gave the corresponding α -oximino acids **69** to **72** in excellent yields and purities.



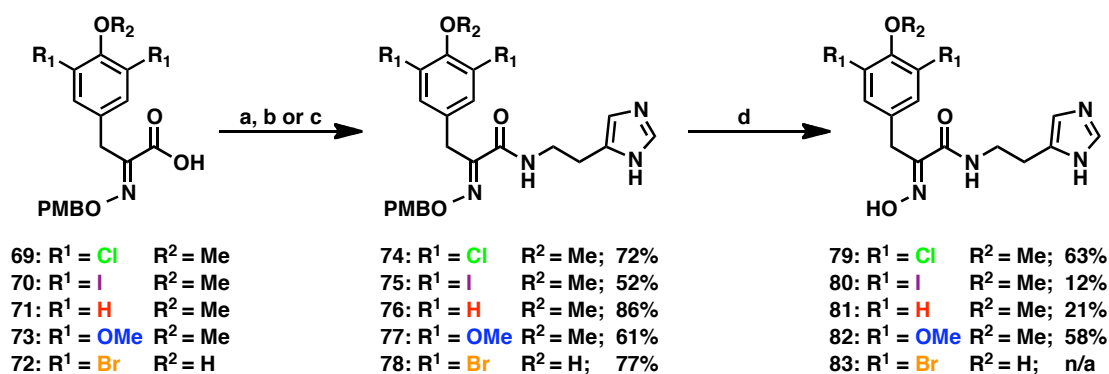
Scheme 23 Syntheses of α -oximino acids **69** to **73**.

Reagents and conditions: (a) *N*-acetyl glycine, NaOAc, Ac₂O, 120 °C; (b) 3 *N* HCl, reflux; **26**, NaOAc, EtOH, rt, 18 h; (d) Ba(OH)₂·8H₂O, 1,4-dioxane/H₂O (1:1), 60 °C, 30 min then **26**, 18 h, 30%.

^{††} This was inconsequential since hydrolysis of the acetyl group would occur in the next step.

2.2.2.4 Synthesis of (5)-Bromoverongamine Analogues

The histamine side chain of (5)-bromoverongamine (**14**) was appended to the collection of five α -oximino acid derivatives (**69** to **73**) to give the corresponding products **74** to **78** in good yields (Scheme 24). For the substrates, **74** to **77**, removal of the PMB group was achieved with aluminium trichloride and anisole in dichloromethane, giving **79** to **82** in moderate to low yields. Under these conditions it was not possible to deprotect **78** as it was not soluble in dichloromethane.^{§§} However, minimal conversion was observed (by LCMS) when the reaction was performed in neat anisole and at extended reaction times (24 hours), but it was not possible to isolate sufficient quantities of **83** for the purposes of characterisation or biological screening.



Scheme 24 (5)-Bromoverongamine analogue synthesis.

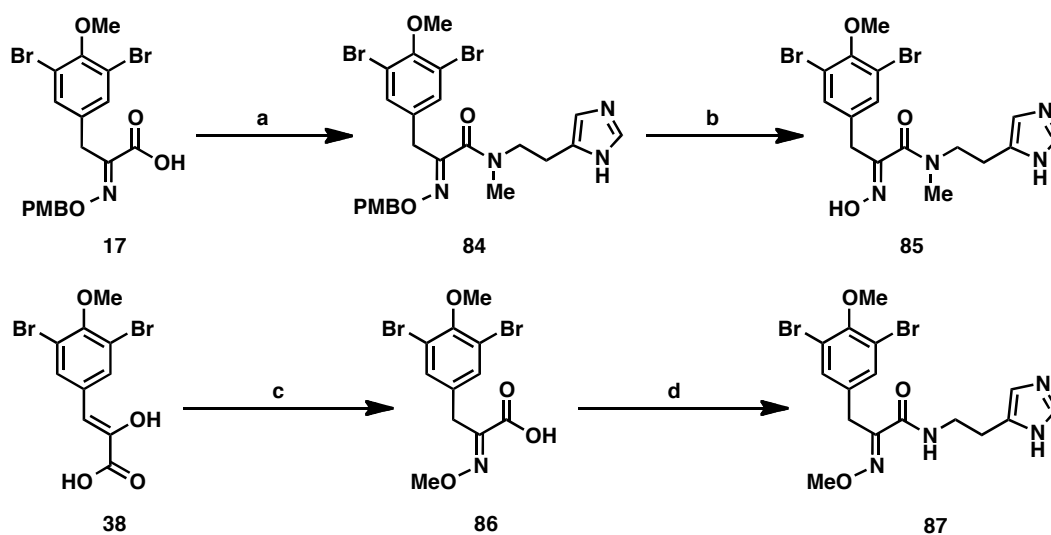
Reagents and conditions: (a) Histamine dihydrochloride, DCC, HOBT, *i*Pr₂EtN, CH₂Cl₂, rt, (for **69**, **71**, and **72**); (b) [®]T3P, histamine dihydrochloride *i*Pr₂EtN, CH₂Cl₂, 0 °C to rt (for **70**); CDI, THF, 0 °C, 1 h then histamine, CH₂Cl₂, (for **73**); (d) AlCl₃, anisole, CH₂Cl₂, rt, 5 min.

In addition to investigating aryl ring analogues of **14**, we also wanted to explore the biological effects of modifying other potentially relevant functionality within the natural product. As a starting point, we planned to synthesise **85** and **87** which would allow us to explore whether the oxime and/or amide hydrogens are involved in hydrogen bonding to a potential biological target.^{***}

^{§§} This may be due to the presence of the phenolic functionality.

^{***} It was reported in the first part of this chapter that the PMB protected congener (**29**) of (5)-bromoverongamine was more active than the natural product with this being attributed to an increase in lipophilicity. Therefore, masking the oxime with a methyl group should give further insight into whether the difference in activity was a result of increasing lipophilicity or as a result of nullifying the H-bond donating ability of the free oxime.

The α -oximino acid **17** was reacted with CDI and the resulting activated ester was treated with methylhistamine to give the tertiary amide **84** in 35% yield (Scheme 25). The previously mentioned Lewis acidic conditions cleaved the PMB group to furnish the *N*-methylated product **85** in a yield of 79%. It would not have been possible to access the *O*-methyl oxime **87** directly from the natural product because of the susceptibility of imidazole ring nitrogens towards methylation. Therefore a two-step procedure from **38** was required to circumvent this issue (Scheme 25). Accordingly, the phenylpyruvic acid derivative **38** was converted to the *O*-methyl oximino acid **86** with *O*-methylhydroxylamine hydrochloride in the presence of sodium acetate. Then, **86** was coupled with histamine dihydrochloride using DCC and HOBt to furnish *O*-methyl-(5)-bromoverongamine (**87**) in a yield of 60% over the two steps.

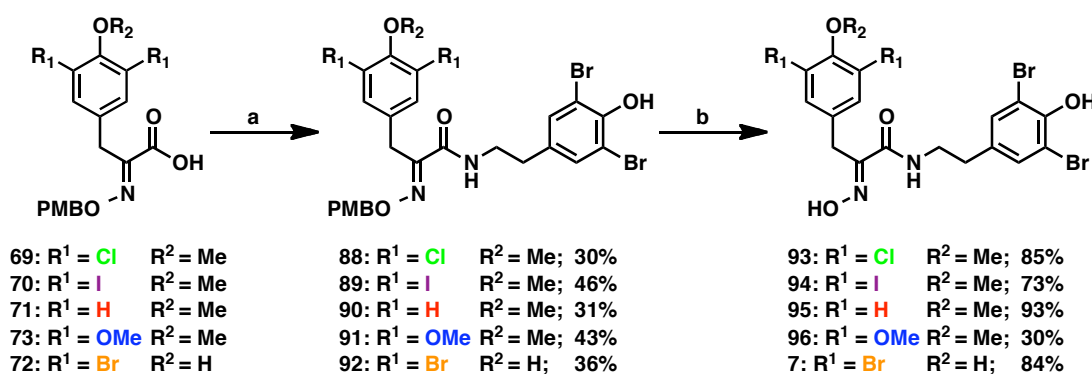


Scheme 25 Synthesis of **85** and **87**.

Reagents and conditions: (a) CDI, THF, rt, 1 h then 0 °C, methylhistamine, rt, 18 h, 35%; (b) AlCl_3 , anisole, CH_2Cl_2 , rt, 5 min, 79%; (c) *O*-methylhydroxylamine hydrochloride, NaOAc, EtOH, rt, 2 h, 97%; (d) histamine dihydrochloride, DCC, HOBt, $i\text{Pr}_2\text{EtN}$, CH_2Cl_2 , rt, 18 h, 62%.

2.2.2.5 Synthesis of JBIR-44 Analogues

To access the JBIR-44 analogues, the α -oximino acids **69** to **73** were coupled to 3,5-dibromotyramine hydrobromide using [®]T3P as the coupling agent (Scheme 26).^{†††} This gave the coupled products **89** to **92** in moderate yields (30-46%). These were consistent with the yield (42%) of the corresponding reaction that was used to access the natural product (Scheme 17). We hypothesised that a trans-esterification reaction between the phenolic functionality in the amine coupling partner and the activated ester of the α -oximino acid was responsible for these diminished yields although no evidence for the presence of this ester by-product was observed. Finally, removal of the PMB group gave the JBIR-44 analogues **7** and **93** to **96**.

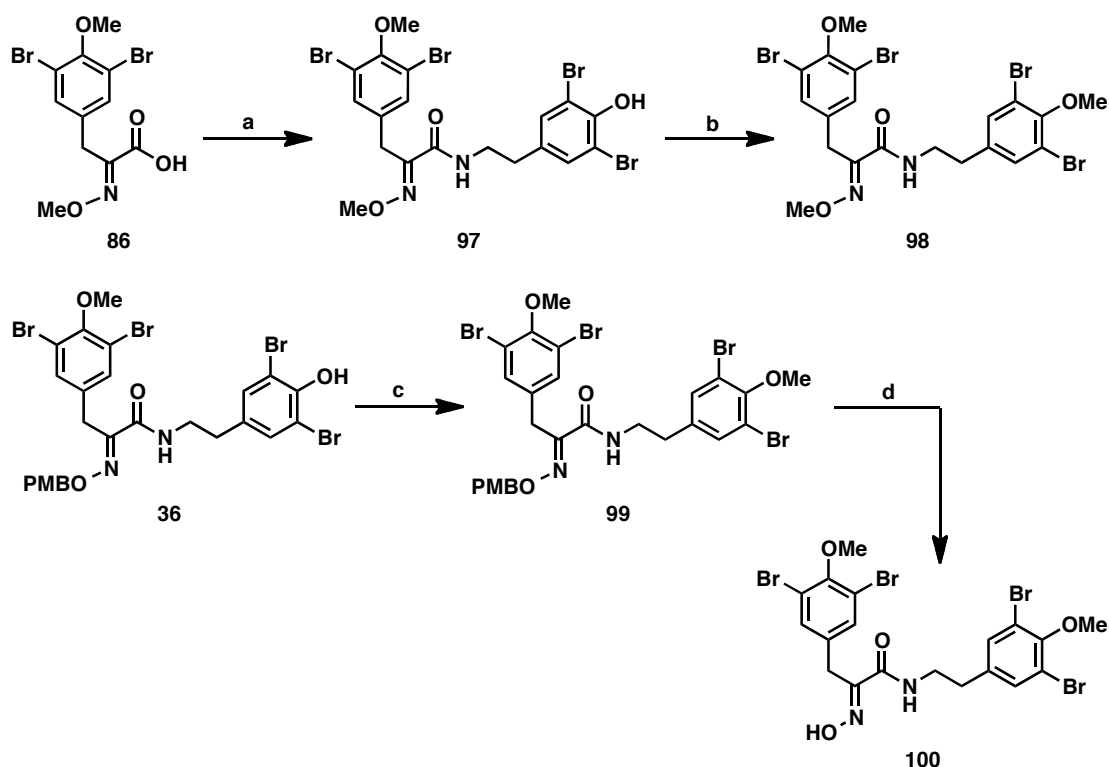


Scheme 26 JBIR-44 analogue synthesis.

Reagents and conditions: (a) [®]T3P, 3,5-dibromotyramine hydrobromide, *i*Pr₂EtN, CH₂Cl₂, 0 °C to rt; (b) AlCl₃, anisole, CH₂Cl₂, rt, 5 min.

With an established route towards JBIR-44 analogues, we also sought to synthesise a small number of analogues that would enable us to probe the effect of masking the hydrogen bond donating abilities of both the oxime and the phenolic functionality in the tyramine side chain. These compounds would also complement those produced within the (5)-bromoverongamine series.

^{†††} When these coupling reactions were performed with DCC/HOBt, purification of the products from the crude reaction mixture was labourious.



Scheme 27 Synthesis of analogues **98**, **99**, and **100**.

Reagents and conditions: (a) [®]T3P, 3,5-dibromotyramine hydrobromide, *i*Pr₂EtN, CH₂Cl₂/DMF (1:1), 0 °C to rt, 18 h, 36%; (b) MeI, K₂CO₃, acetone, reflux, 5 h, 93%; (c) MeI, K₂CO₃, acetone, reflux, 3 h, 89%; (d) AlCl₃, anisole, CH₂Cl₂, rt, 5 min, 94%.

Using the conditions mentioned previously, *O*-methyl oximino acid **86** was coupled to 3,5-dibromotyramine hydrobromide in 36% yield to give *O*-methyl oxime JBIR-44 (**97**) (Scheme 27). The phenolic oxygen in **97** was subsequently methylated with methyl iodide to furnish analogue **98**. In order to obtain the *O*-methylated phenol analogue **100**, *O*-PMB JBIR-44 (**36**) was treated with methyl iodide to give **99**. The PMB group could then be removed to access the desired analogue **100** in 84% over the two steps.

2.2.2.6 Biological Activity

Members of the two compound libraries pertaining to the (5)-bromoverongamine and JBIR-44 analogue series were screened against the ovarian cancer SK-OV-3 cell line. The primary aim of this initial screen was to identify whether any of the structural modifications incorporated into these analogues resulted in a significant decrease in cytotoxicity. Because the majority of these analogues differ from the parent compounds by a single modification, this would enable delineation of the key pharmacophoric elements of these molecules. On the other hand, the insight gained

from analogues with improved potency, along with those which retained the activity of the parent compound, would also prove valuable. Therefore, it was hoped that data from this initial assay could be used to design a second generation of superior analogues.

2.2.2.6.1 (5)-Bromoverongamine Series

The MTS results for the 12 analogues from the (5)-bromoverongamine series are shown in Table 6. To recap, in terms of cytotoxicity towards SK-OV-3 cells, the natural product **14** was less active ($EC_{50} > 50 \mu M$) than the PMB protected derivative **29** ($EC_{50} \sim 40 \mu M$). This trend was mirrored for the dichloro and diiodo analogues with the PMB derivatives **74** and **75** being more active than the free oximes **79** and **80**, respectively. The cytotoxic activity of the PMB derivatives was independent of the halogen substituent as **74** ($EC_{50} \sim 35 \mu M$) and **75** ($EC_{50} \sim 40 \mu M$) possessed a similar activity to the dibromo compound **29** ($EC_{50} \sim 40 \mu M$). In exploring the effect of the oxime protection further, the activity of the *O*-methyl oxime **87** ($EC_{50} > 50 \mu M$) was greater than that of the natural product (**14**) but lower than that of the PMB derivative (**29**). This observation supports the conclusion from the first part of this chapter, which stated that an increase in lipophilicity was the cause of the increase in cytotoxicity.

The trend in cytotoxicity of the corresponding free oximes appeared to follow the Van der Waal's radii and the halogen bonding capabilities of the halogen substituents; **74** was inactive with **75** ($EC_{50} \sim 50 \mu M$) more active than (5)-bromoverongamine (**14**). Interestingly, either replacing the halogens with methoxy substituents (**77** and **82**) or removing them altogether (**76** and **81**) resulted in a complete loss of activity. Furthermore, the drop in activity was also observed for compounds incorporating either an *N*-methyl group (**84** and **85**), or a phenolic functionality (**78**) indicated that these modifications were also unfavourable.

To summarise, none of the modifications in this series yielded analogues with superior activity to compounds **14** and **29**. However, we have found that the presence of halogen substituents at *C*-3 and *C*-5 is essential for conferring the observed cytotoxicity whereas all other modifications gave compounds with either reduced or no activity. In light of their moderate activity and the relationship between lipophilicity and cytotoxicity, it was decided that further investigations into the anticancer properties of this class of compounds were not warranted.

2.2.2.6.1 JBIR-44 Series

The MTS results for the 14 analogues from the JBIR-44 series are shown in Table 7. To recap, the natural product **16** displayed moderate activity (EC_{50} 22 μ M) against SK-OV-3 cells. On the other hand, the PMB derivative **36** was inactive.

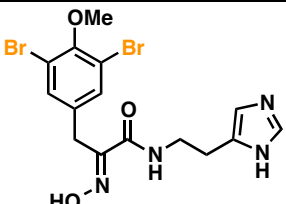
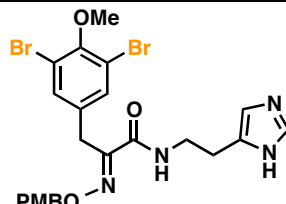
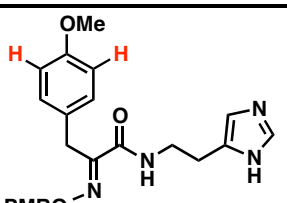
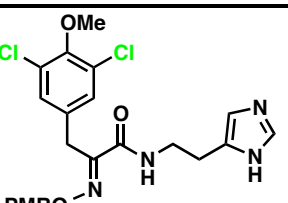
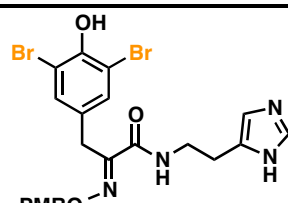
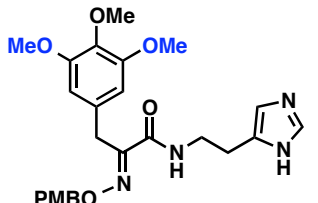
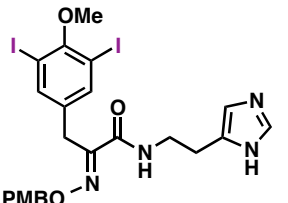
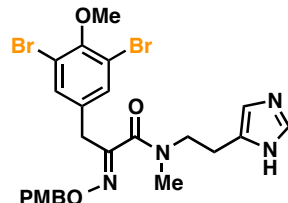
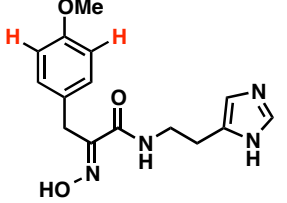
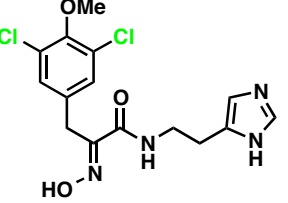
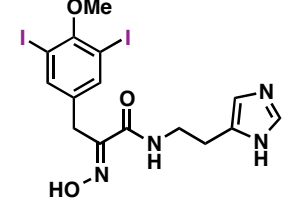
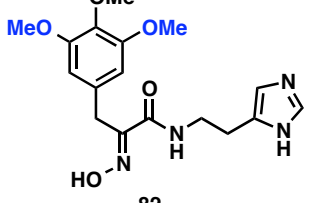
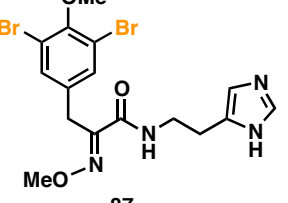
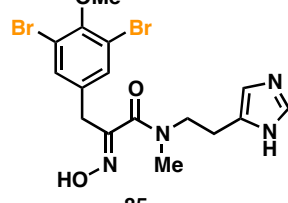
Both the dichloro (**93**) and diiodo (**94**) analogues of JBIR-44 were significantly less active than the natural product with EC_{50} values of ~ 60 μ M and ~ 55 μ M, respectively. Furthermore, the trimethoxy analogue **96** only caused a significant loss in cell viability at high concentrations (>60 μ M) and the dihydro analogue **95** was completely inactive. These results suggest that, whilst halogen substitution at C-2 and C-4 is superior to either methoxy or hydrogen, dibromo substitution is essential for optimal activity.

As expected, the PMB derivatives **88**, **89**, and **99** were completely inactive up to 100 μ M. Compounds **90** and **91** also showed poor activity causing only a 30% loss of cell viability at concentrations greater than 60 μ M. The only exception to this was the diphenol **92** which had an EC_{50} value of ~ 50 μ M. Following on from this, compounds **97** and **98**, possessing the *O*-methyl oximes, were also inactive.

Whereas methylation at the C-15 phenol of JBIR-44 caused no significant loss in activity (**100** EC_{50} 32 μ M), loss of the C-18 methyl group (**7**) had a detrimental impact on the cytotoxicity ($EC_{50} \sim 50$ μ M).

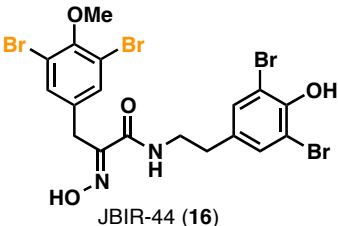
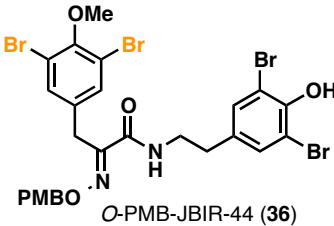
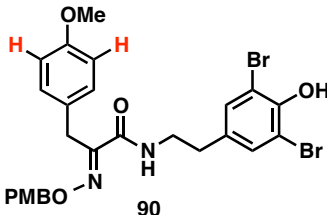
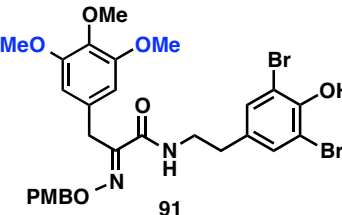
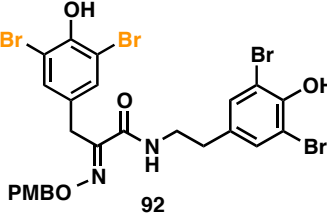
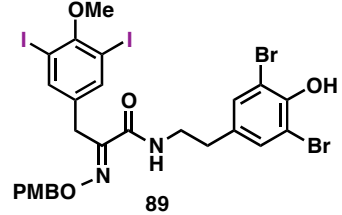
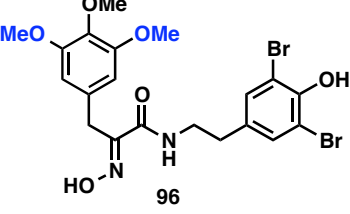
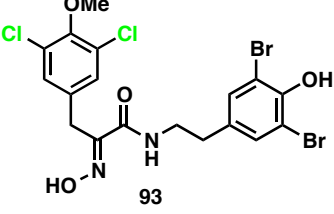
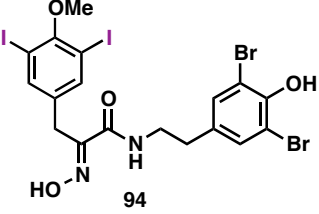
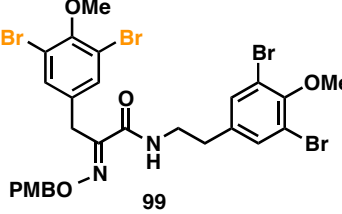
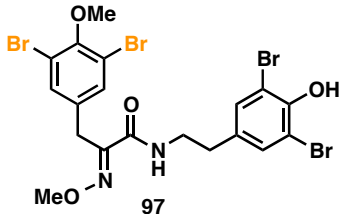
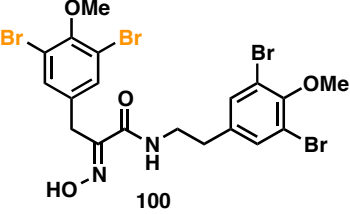
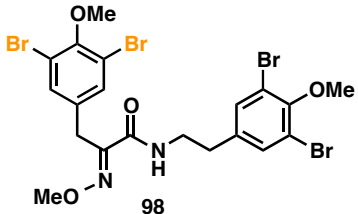
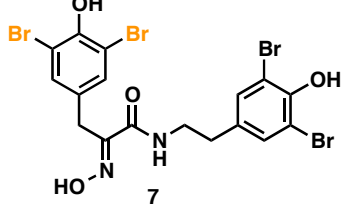
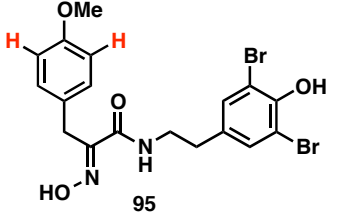
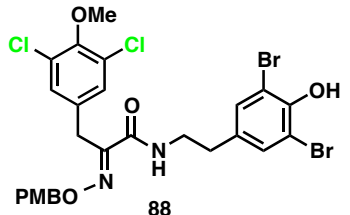
To summarise, we have shown that the oxime functionality in JBIR-44 is essential for eliciting a cytotoxic response since masking it with either a PMB or methyl group results in a significant loss in activity. In addition, out of the substituents examined, the presence of bromine at C-2 and C-4 is optimal. Furthermore, since methylation of the C-15 phenol was well tolerated, it would appear that there is scope for installing additional functionality at this position to give subsequent analogues with more favourable physicochemical properties.

Table 6 MTS assay results for the (5)-bromoverongamine series of analogues screened against SK-OV-3 cells. Drug incubations were for 48 h.

| | | |
|--|--|---|
|  <p>(5)-Bromoverongamine (14)</p> <p>$EC_{50} > 50 \mu M$</p> |  <p>O-PMB-(5)-Bromoverongamine (29)</p> <p>$EC_{50} 40 \mu M^a$</p> | |
|  <p>76</p> <p>N/A</p> |  <p>74</p> <p>$EC_{50} \sim 35 \mu M$</p> |  <p>78</p> <p>$EC_{50} > 50 \mu M$</p> |
|  <p>77</p> <p>N/A^b</p> |  <p>75</p> <p>$EC_{50} \sim 40 \mu M$</p> |  <p>84</p> <p>$EC_{50} > 50 \mu M$</p> |
|  <p>81</p> <p>N/A</p> |  <p>79</p> <p>N/A</p> |  <p>80</p> <p>$EC_{50} \sim 50 \mu M$</p> |
|  <p>82</p> <p>N/A</p> |  <p>87</p> <p>$EC_{50} > 50 \mu M$</p> |  <p>85</p> <p>N/A</p> |

^a Calculated from three independent experiments. ^b ~20% Decrease in cell viability observed at 100 μM .

Table 7 MTS assay results for the JBIR-44 series of analogues screened against SK-OV-3 cells. Drug incubations were for 48 h.

| | | | | | |
|---|--|--|---|--|--|
|  JBIR-44 (16) EC_{50} 22 μM^a | | |  O-PMB-JBIR-44 (36) N/A | | |
|  90 $EC_{50} > 50 \mu M$ | | |  91 $EC_{50} > 50 \mu M$ | | |
|  92 $EC_{50} \sim 50 \mu M$ | | |  89 N/A | | |
|  96 $EC_{50} > 50 \mu M$ | | |  93 $EC_{50} \sim 60 \mu M$ | | |
|  94 $EC_{50} \sim 55 \mu M$ | | |  99 N/A | | |
|  97 N/A | | |  100 $EC_{50} 32 \mu M^a$ | | |
|  98 N/A | | |  7 $EC_{50} \sim 50 \mu M$ | | |
|  95 N/A | | |  88 N/A | | |

^a Calculated from three independent experiments.

2.2.3 Conclusion and Future Work

We have developed an efficient route towards analogues of oxime-histamine and oxime-tyramine bromotyrosine-derived natural products that incorporate modifications on the aryl ring, the oxime, and the side chain. This has enabled us to conduct SAR analysis on both (5)-bromoverongamine (**14**) and JBIR-44 (**16**) analogues.

From these data, we can conclude that these two natural products display different anticancer profiles. In light of this, the preliminary SAR studies performed on the JBIR-44 analogues could be expanded upon in the future to probe this activity further. In addition, despite analogues of **14** not showing promise as an anticancer agent, based on its known activity, we hope to screen these compounds in antibacterial and antifungal assays in the future. Following on from this and, given the importance of the dibromomethoxyaryl moiety and the free oxime on the activity of these molecules, we also plan on synthesising a library of compounds derived from the coupling of non-naturally occurring amines to the α -oximino acid **17** with the hope that this would produce novel hits with more favourable physicochemical properties.

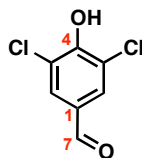
To conclude, this research further ignited our interest into these natural products and led us to explore the chemistry and biology of another class of bromotyrosine products: the spirocyclohexadienylisoxazoline derivatives.

2.2.4 Chemistry: Experimental

General Experimental Details

Refer to Section 2.1.6 for general experimental details.

3,5-Dichloro-4-hydroxybenzaldehyde (**54**)



Procedure 1

To a solution of 4-hydroxybenzaldehyde (**53**) (122 mg, 1.00 mmol) in CH_2Cl_2 (3 mL) in a 2-5 mL vial was added sulfuryl chloride (0.810 mL, 10.0 mmol). The vial was sealed and heated under microwave irradiation at 80 °C for 10 h. The reaction vessel was vented, after which a white precipitate formed. The mixture was evaporated to dryness *in vacuo* to furnish **54** and **55** (in a 7:1 ratio by ^1H NMR) as a white solid (187 mg). This was used without further purification.

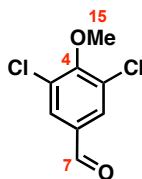
Procedure 2

To a solution of 4-hydroxybenzaldehyde (**53**) (500 mg, 4.09 mmol) in CH_2Cl_2 (6 mL) in a 20 mL vial was added sulfuryl chloride (3.32 mL, 41.0 mmol). The vial was sealed and heated at 65 °C for 2 h. The reaction vessel was vented and the mixture washed with H_2O (20 mL), dried and evaporated to dryness *in vacuo* to furnish **54** as a white solid (523 mg) which was used without further purification.

For characterisation purposes, a sample was purified by flash column chromatography (30% EtOAc/Hexane) to furnish **54** as a white solid.

R_f 0.40 (30% Et_2O /Petrol); ν_{max} (thin film)/ cm^{-1} 3343br, 1690s, 1486s, 1200s, 1144s; δ_{H} (400 MHz, CDCl_3) 9.81 (1H, s, H-7), 7.82 (2H, s, H-2/6), 6.41 (1H, br s, OH); δ_{C} (100 MHz, CDCl_3); 188.4 (C-7), 152.8 (C-4), 130.2 (C-1), 129.8 (C-2/6), 122.2 (C-3/5); m/z (ESI+) found 212.9484, $[\text{M}+\text{Na}]^+$ $\text{C}_7\text{H}_4\text{Cl}_2\text{O}_2\text{Na}$ requires 212.9481; *elem. anal.* $\text{C}_7\text{H}_4\text{Cl}_2\text{O}_2$ requires C 44.02%, H 2.11%, found C 43.69%, H 2.02%.

Consistent with literature data.²¹

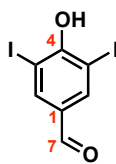
3,5-Dichloro-4-methoxybenzaldehyde (51)

A: To a stirred solution of a 7:1 mixture of **54** and **55** (187 mg, procedure 1) in acetone (5 mL) was added anhydrous K_2CO_3 (193 mg, 1.40 mmol). After 30 min, iodomethane (117 μ L, 1.88 mmol) was added and the reaction mixture was heated under reflux for 2.5 h. Upon cooling to room temperature, the solvent was removed *in vacuo*, the residue was partitioned between water (20 mL) and EtOAc (20 mL) and the organic layer separated. The aqueous phase was extracted with EtOAc (20 mL \times 3), the combined organic layers were dried and concentrated *in vacuo*. The residue was purified by flash column chromatography (5% Et₂O/Petrol) to furnish **51** (141 mg, 0.688 mmol, 69% over 2 steps from **53**) as a white solid.

B: To a stirred solution of **54** (523 mg, procedure 2) in acetone (15 mL) was added anhydrous K_2CO_3 (568 mg, 4.11 mmol). After 30 min, iodomethane (682 μ L, 11.0 mmol) was added and the reaction mixture was heated under reflux for 3 h. Upon cooling to room temperature, the solvent was removed *in vacuo*, the residue was partitioned between water (30 mL) and EtOAc (30 mL) and the organic layer separated. The aqueous phase was extracted with EtOAc (30 mL \times 3), the combined organic layers were dried and concentrated *in vacuo*. The residue was purified by flash column chromatography (5% Et₂O/Petrol) to furnish **51** (336 mg, 1.64 mmol, 40% over 2 steps from **53**) as a white solid.

R_f 0.45 (10% Et₂O/Petrol); ν_{max} (thin film)/cm⁻¹ 2856w, 1691s, 1586s, 1556s, 1266s; δ_H (400 MHz, CDCl₃) 9.86 (1H, s, H-7), 7.82 (2H, s, H-2/6), 3.97 (3H, s, H-15); δ_C (100 MHz, CDCl₃) 188.6 (C-7), 157.3 (C-4), 133.1 (C-1), 130.6 (C-3/5), 130.0 (C-2/6), 61.0 (C-15); m.p. 63-65 °C (lit.,²² 60 °C). *elem. anal.* C₈H₆Cl₂O₂ requires C 46.86%, H 2.95%, found C, 46.78%, H, 2.93%.

Consistent with literature data.²²

4-Hydroxy-3,5-diiodobenzaldehyde (57)**Procedure 1**

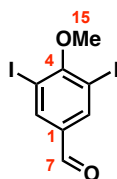
To a stirred solution of 4-hydroxybenzaldehyde (**53**) (3.51 g, 28.7 mmol), sodium periodate (6.16 g, 28.8 mmol), and sodium chloride (3.36 g, 57.5 mmol) in AcOH/H₂O (9:1, 100 mL) was added potassium iodide (9.55 g, 57.5 g) portionwise. After 96 h, EtOAc (500 mL) and 10% sodium thiosulfate solution (500 mL) were added. The organic layer was separated and the aqueous phase was extracted with EtOAc (500 mL). The combined organic layers were washed with 10% sodium thiosulfate solution (500 mL), brine (500 mL), dried and evaporated to dryness *in vacuo* to furnish **57** (10.5 g, 28.1 mmol, 98%) as a white solid.

Procedure 2

To a stirred solution of 4-hydroxybenzaldehyde (**53**) (78.0 mg, 0.639 mmol) in CH₂Cl₂ (5 mL) at 0 °C was added *bis*(pyridine)iodonium tetrafluoroborate (500 mg, 1.34 mmol). After 1 h, H₂O (20 mL) was added and the aqueous phase was extracted with CH₂Cl₂ (20 mL × 3) and the combined organic layers were dried and concentrated *in vacuo*. The residue was purified by flash column chromatography (20-100% EtOAc/Petrol) to furnish **57** (228 mg, 0.610 mmol, 95%) as a white solid.

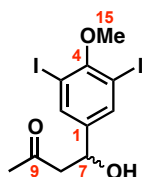
R_f 0.34 (30% EtOAc/Petrol); ν_{\max} (thin film)/cm⁻¹ 3181br, 1665s, 1563m, 1456m, 1095s; δ_H (400 MHz, CDCl₃) 9.74 (1H, s, H-7), 8.20 (2H, s, H-2/6), 6.28 (1H, br s, OH); δ_C (100 MHz, *d*₆-DMSO) 189.1 (C-7), 160.6 (C-4), 140.6 (C-1), 132.1 (C-2/6), 86.4 (C-3/5); *elem. anal.* C₇H₄I₂O₂ requires C 22.49%, H 1.08 %, found C 22.20 %, H 1.10 %.

Consistent with literature data.²³

3,5-Diiodo-4-methoxybenzaldehyde (52)

To a stirred solution of **57** (4.00 g, 10.7 mmol) in acetone (60 mL) at room temperature was added anhydrous K_2CO_3 (2.21 g, 16.0 mmol). After 30 min, iodomethane (1.33 mL, 21.4 mmol) was added and the reaction mixture was heated at reflux for 3.5 h, after which a further portion of iodomethane (1.33 mL, 21.4 mmol) was added. After 1.5 h, the mixture was cooled to room temperature, concentrated *in vacuo*, the residue was partitioned between water (250 mL) and EtOAc (150 mL) and the organic layer separated. The aqueous phase was extracted with EtOAc (150 mL \times 3) and the combined organic layers were dried and concentrated *in vacuo*. The residue was purified by flash column chromatography (5-10% EtOAc/Petrol) to furnish **52** (3.75 g, 9.67 mmol, 90%) as a white solid.

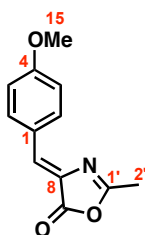
R_f 0.69 (10% EtOAc/Petrol); ν_{max} (thin film)/ cm^{-1} 2938w, 2859w, 1689s, 1673s, 1536s, 1184s; δ_H (400 MHz, $CDCl_3$) 9.77 (1H, s, H-7), 8.22 (2H, s, H-2/6), 3.88 (3H, s, H-15); δ_C (100 MHz, $CDCl_3$) 187.8 (C-7), 163.5 (C-4), 141.0 (C-1), 135.2 (C-2/6), 91.2 (C-3/5), 60.8 (C-15); m/z (ESI+) found 410.8343, $[M+Na]^+$ $C_8H_6I_2O_2Na$ requires 410.8349; m.p. 126-128 $^{\circ}C$ (lit.,²⁴ 124 $^{\circ}C$); *elem. anal.* $C_8H_6I_2O_2$ requires C 24.77 %, H 1.56 %, found C 24.44%, H 1.53%.

(\pm)-4-(3,5-Diiodo-4-methoxyphenyl)-4-hydroxybutan-2-one (58)

R_f 0.14 (20% EtOAc/Petrol); ν_{max} (thin film)/ cm^{-1} 3600-3300br, 2936w, 1706s, 1535w, 1461s, 1249s, 992s; δ_H (400 MHz, $CDCl_3$) 7.70 (2H, s, H-2/6), 5.00-4.96 (1H, m, H-7), 3.78 (3H, s, H-15), 3.61 (1H, d, J 3.3 Hz, OH), 2.82-2.68 (2H, m, H-8) 2.15 (3H, s, H-10); δ_C (100 MHz, $CDCl_3$) 208.1 (C-9), 157.7 (C-4), 142.6 (C-1), 137.0 (C-2/6), 90.4 (C-3/5), 67.5 (C-7), 60.5 (C-15), 51.6 (C-8), 30.6 (C-10).

General Procedure 1: Erlenmeyer Azlactone Synthesis

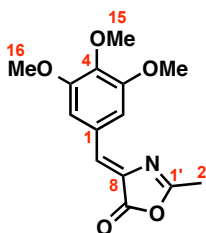
A stirred mixture of aldehyde (1 eq.), *N*-acetylglycine (1.3 eq.), sodium acetate (1.3 eq.) and acetic anhydride (5 eq.) were heated under reflux until the starting aldehyde was fully consumed (TLC). Upon cooling to room temperature, the mixture was partitioned between H₂O and CH₂Cl₂, the organic layer was separated, washed with H₂O and brine, dried and concentrated *in vacuo*. The residue was purified by flash column chromatography to furnish the desired azlactone product.

(*Z*)-4-(4-Methoxybenzylidene)-2-methyloxazol-5(4*H*)-one (61)

Following general procedure 1 using aldehyde **49**: Purified by flash column chromatography (50% CH₂Cl₂/Petrol) to furnish **61** (478 mg, 2.20 mmol, 88%) as a yellow solid.

R_f 0.32 (70% CH₂Cl₂/Petrol); ν_{\max} (thin film)/cm⁻¹ 1796m, 1769s, 1748m, 1658s, 1590s, 1159s; δ_H (400 MHz, CDCl₃) 8.03 (2H, d, *J* 8.9 Hz, H-2/6), 7.07 (1H, s, H-7), 6.93 (2H, d, *J* 8.9 Hz, H-3/5), 3.84 (3H, s, H-15), 2.36 (3H, s, H-2'); δ_C (100 MHz, CDCl₃) 168.0 (C-1'), 164.8 (C-9), 161.9 (C-4), 134.1 (C-2/6), 131.3 (C-7), 130.3 (C-8), 126.0 (C-1), 114.3 (C-3/5), 55.3 (C-15), 15.5 (C-2'); *m/z* (ESI+) found 218.0822, [M+H]⁺ C₁₂H₁₁NO₃ requires 218.0817; m.p. 110-112 °C (lit.,²⁵ 109.5-110 °C); *elem. anal.* C₁₂H₁₁NO₃ requires C 66.35 %, H 5.10 %, N 6.45 %, found C 66.22 %, H 5.09 %, N 6.46 %.

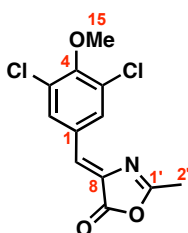
Consistent with literature data.²⁶

(Z)-2-Methyl-4-(3,4,5-trimethoxybenzylidene)oxazol-5(4H)-one (62)

Following general procedure 1 using aldehyde **50**: Purified by flash column chromatography (70-100% CH₂Cl₂/Petrol) to furnish **62** (514 mg, 1.85 mmol, 70%) as a pale yellow solid.

R_f 0.54 (30% EtOAc/Petrol); ν_{\max} (thin film)/cm⁻¹ 3005w, 1794m, 1763s, 1654m, 1424s, 1251s; δ_H (400 MHz, CDCl₃) 7.36 (2H, s, H-2/6), 6.99 (1H, s, H-7), 3.89 (3H, s, H-15), 3.88 (6H, s, H-16), 2.36 (3H, s, H-2'); δ_C (100 MHz, CDCl₃) 167.7 (C-1'), 165.5 (C-9), 153.0 (C-3/5), 140.8 (C-4), 131.5 (C-8), 131.2 (C-7), 128.4 (C-1), 109.4 (C-2/6), 60.9 (C-15), 56.0 (C-16) 15.6 (C-2'); m/z (ESI+) found 278.1035, [M+H]⁺ C₁₄H₁₆NO₅ requires 278.1028; m.p. 154-156 °C (lit.,²⁰ 157-158.5 °C); *elem. anal.* C₁₄H₁₅NO₅ requires C 60.64%, H 5.45%, N 5.05%, found C 60.55%, H 5.47%, N 5.11%.

Consistent with literature data.²⁰

(Z)-4-(3,5-Dichloro-4-methoxybenzylidene)-2-methyloxazol-5(4H)-one (59)

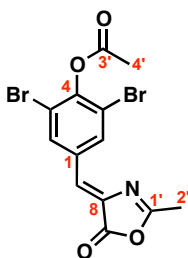
Following general procedure 1 using aldehyde **51**: Purified by flash column chromatography (50% CH₂Cl₂/Petrol) to furnish **59** (355 mg, 1.24 mmol, 71%) as a pale yellow solid.

R_f 0.37 (10% EtOAc/Petrol); ν_{\max} (thin film)/cm⁻¹ 2940w, 1803m, 1791s, 1763s, 1656s, 1601s, 1257s; δ_H (400 MHz, CDCl₃) 8.04 (2H, s, H-2/6), 6.91 (1H, s, H-7), 3.95 (3H, s, H-15), 2.42 (3H, s, H-2'); δ_C (100 MHz, CDCl₃) 167.2 (C-1'), 167.0 (C-9), 154.1 (C-4), 133.7 (C-8), 132.1 (C-2/6), 130.5 (C-1), 129.8 (C-3/5), 127.4 (C-7), 60.9 (C-15), 15.7 (C-2'); m/z (ESI+) found 286.0044, [M+H]⁺ C₁₂H₁₀Cl₂NO₃ (³⁵Cl)

requires 286.0038; m.p. 186-188 °C; *elem. anal.* C₁₂H₉Cl₂NO₃ requires C 50.38%, H 3.17%, N 4.90% found C 50.14%, H 3.08%, N 4.60%.

Crystals of **59** were obtained by slow evaporation of CDCl₃. The structure was confirmed by X-ray crystallographic analysis and given the unique identifier sl1029.

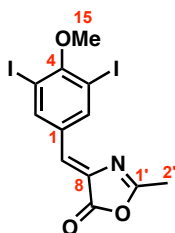
(Z)-2,6-Dibromo-4-((2-methyl-5-oxooxazol-4(5H)-ylidene)methyl)phenyl acetate (63)



Following general procedure 1 using aldehyde **23**: Purified by flash column chromatography (50% CH₂Cl₂/Petrol) to furnish **63** (650 mg, 1.61 mmol, 85%) as a pale yellow solid.

R_f 0.50 (100% CH₂Cl₂); *v*_{max} (thin film)/cm⁻¹ 3070w, 1804m, 1759s, 1662m, 1168s, 892s; *δ*_H (400 MHz CDCl₃) 8.27 (2H, s, H-2/6), 6.90 (1H, s, H-7), 2.42 (3H, s, H-2'), 2.40 (3H, s, H-4'); (100 MHz, CDCl₃) 167.7 (C-1'), 166.79 (C-3'), 166.77 (C-9), 147.6 (C-4), 135.2 (C-2/6), 134.4 (C-1), 133.5 (C-8), 126.5 (C-7), 118.1 (C-3/5), 20.4 (C-4'), 15.7 (C-2'); m.p. 188-190 °C (lit.,²⁷ 187-189 °C); *elem. anal.* C₁₃H₉Br₂NO₄ requires C 38.74%, H 2.25%, N 3.48% found C 38.69%, H 2.19%, N 3.34%.

Consistent with literature data.²⁷

(Z)-4-(3,5-Diiodo-4-methoxybenzylidene)-2-methyloxazol-5(4H)-one (60)

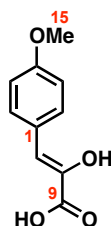
Following general procedure 1 using aldehyde **52**: Purified by flash column chromatography (50% CH₂Cl₂/Petrol) to furnish **60** (1.10 g, 2.35 mmol, 92%) as a pale yellow solid.

R_f 0.40 (10% EtOAc/Petrol); ν_{\max} (thin film)/cm⁻¹ 1808m, 1764s, 1663s, 1456m, 1254s; δ_H (400 MHz, CDCl₃) 8.48 (2H, s, H-2/6), 6.88 (1H, s, H-7), 3.90 (3H, s, H-15), 2.43 (3H, s, H-2'); δ_C (100 MHz, CDCl₃) 167.1 (C-1'), 167.0 (C-9), 160.7 (C-4), 143.0 (C-2/6), 133.5 (C-8), 132.9 (C-1), 126.7 (C-7), 90.7 (C-3/5), 60.8 (C-15), 15.7 (C-2'); m/z (ESI+) found 469.8755, $[M+H]^+$ C₁₂H₁₀I₂NO₃ requires 469.8750; m.p. 161-163 °C (lit.,²⁸ 169.5-171 °C); *elem. anal.* C₁₂H₉I₂NO₃ requires C 30.73%, H 1.93%, N 2.99%, found C 30.71%, H 1.91%, N 2.83%.

Consistent with literature data.²⁸

General Procedure 2: Azlactone Hydrolysis

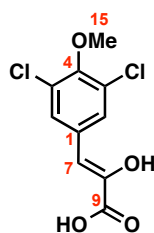
A stirred suspension of azlactone in aqueous HCl (3 N, 10 mL per mmol of substrate) was heated under reflux and the reaction progress monitored by ^1H NMR analysis. Upon completion, the mixture was cooled to room temperature and the precipitate was isolated by filtration, washed with H_2O and dried *in vacuo* to furnish the desired phenylpyruvic acid.

(Z)-2-Hydroxy-3-(4-methoxyphenyl)acrylic acid (66)

Following general procedure 2 using azlactone **61**: furnished **66** (755 mg, 3.89 mmol, 94%) as a brown solid which was used without further purification.

ν_{max} (thin film)/ cm^{-1} 3457m, 3000-2500br, 1658s, 1238s; δ_{H} (600 MHz, CD_3OD) 7.71 (2H, d, J 8.7 Hz, H-2/6), 6.88 (2H, d, J 8.7 Hz, H-3/5), 6.46 (1H, s, H-7), 3.79 (3H, s, H-15); δ_{C} (125 MHz, CD_3OD) 168.6 (C-9), 160.5 (C-4), 140.5 (C-8), 132.2 (C-2/6), 129.0 (C-1), 114.7 (C-3/5), 111.8 (C-7), 55.6 (C-15); *elem. anal.* $\text{C}_{10}\text{H}_{10}\text{O}_4$ requires C 61.85 %, H 5.19 %, found C 61.95 %, H 5.18 %.

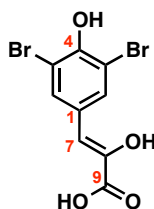
Consistent with literature data.²⁶

(Z)-3-(3,5-Dichloro-4-methoxyphenyl)-2-hydroxyacrylic acid (64)

Following general procedure 2 using azlactone **59**: furnished **64** (308 mg, 1.17 mmol, 97%) as a pale yellow solid which was used without further purification.

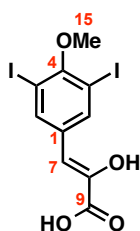
ν_{\max} (thin film)/cm⁻¹ 3475w, 3091w, 2944w, 2580w, 1682s, 1646s, 1423s, 1145s; δ_{H} (400 MHz, CD₃OD) 7.75 (2H, s, H-2/6), 6.33 (1H, s, H-7), 3.86 (3H, s, H-15); δ_{C} (100 MHz, CD₃OD) 167.5 (C-9), 152.0 (C-4), 143.8 (C-8), 134.4 (C-1), 130.7 (C-2/6), 130.0 (C-3/5), 108.1 (C-7), 61.2 (C-15); m.p. 191-193 °C (lit.,²⁹ 190 °C); *elem. anal.* C₁₀H₈Cl₂O₄ requires C 45.66%, H 3.07%, found C, 45.43%, H, 3.03%.

Consistent with literature data.²⁹

(Z)-3-(3,5-Dibromo-4-hydroxyphenyl)-2-hydroxyacrylic acid (68)

Following general procedure 2 using azlactone **63**: furnished **68** (396 mg, 1.17 mmol, 94%) as a white solid which was used without further purification.

ν_{\max} (thin film)/cm⁻¹ 3465m, 3100-2800br, 1678s, 1648s, 1584m, 1475s; δ_{H} (400 MHz CD₃OD) 7.92 (2H, s, H-2/6), 6.32 (1H, s, H-7); (100 MHz, CD₃OD) 167.8 (C-9), 151.3 (C-4), 142.4 (C-8), 134.2 (C-2/6), 131.1 (C-1), 111.9 (C-3/5), 108.7 (C-7); *elem. anal.* C₉H₆Br₂O₄ requires C 31.99%, H 1.79%, found C 32.29%, H 1.84%.

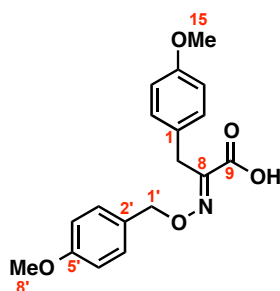
(Z)-3-(3,5-Diiodo-4-methoxyphenyl)-2-hydroxyacrylic acid (65)

Following general procedure 2 using azlactone **60**: furnished **65** (2.24 g, 5.02 mmol, 88%) as a beige solid which was used without further purification.

ν_{\max} (thin film)/ cm^{-1} 3509w, 3200-2500br, 1683s, 1650s, 1242s; δ_{H} (600 MHz, CD_3OD) 8.23 (2H, s, H-2/6), 6.30 (1H, s, H-7), 3.82 (3H, s, H-15); δ_{C} (125 MHz, CD_3OD) 167.5 (C-9), 159.0 (C-4), 143.6 (C-8), 141.8 (C-2/6), 136.6 (C-1), 107.4 (C-7), 90.7 (C-3/5), 61.2 (C-15); *elem. anal.* $\text{C}_{10}\text{H}_8\text{I}_2\text{O}_4$ requires C 26.93%, H 1.81%, found C 27.19%, H 1.76%.

General Procedure 3: α -Oximino acid synthesis

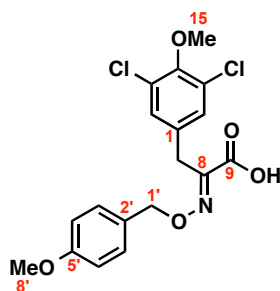
To a stirred solution of the phenylpyruvic acid (1 eq.) and *O*-*para*-methoxybenzyl hydroxylamine hydrochloride (1 eq.) in EtOH (10 mL per mmol of substrate) was added sodium acetate (3 eq.). After 18 h, H₂O was added, the mixture was acidified (pH 0) by the addition of aqueous HCl (3 *N*) and extracted with EtOAc (3 \times 100 mL). The combined organic extracts were dried and evaporated to dryness *in vacuo* to furnish the desired α -oximino acid.

(*E*)-2-(((4-Methoxybenzyl)oxy)imino)-3-(4-methoxyphenyl)propanoic acid (71)

Following general procedure 3 using phenylpyruvic acid **66**: furnished **71** (593 mg, 1.80 mmol, 98%) as a white solid which was used without further purification.

R_f 0.46 (10% MeOH/CH₂Cl₂); ν_{\max} (thin film)/cm⁻¹ 2939w, 1706s, 1614m, 1514s, 1240s; δ_H (500 MHz, CDCl₃) 7.27 (2H, d, J 8.3 Hz, H-3'/7'), 7.17 (2H, d, J 8.6 Hz, H-H-2/6), 6.91 (2H, d, J 8.7 Hz, H-4'/6'), 6.78 (2H, d, J 8.7 Hz, H-3/5), 5.22 (2H, s, H-1'), 3.834 (2H, s, H-7), 3.830 (3H, s, H-8'), 3.77 (3H, s, H-15); δ_C (125 MHz, CDCl₃) 162.5 br (C-9), 159.9 (C-5'), 158.4 (C-4), 150.1 (C-8), 130.3 (C-2/6), 130.2 (C-3'/7'), 127.8 (C-2'), 127.0 (C-1), 114.0 (C-4'/6'), 113.9 (C-3/5), 78.1 (C-1'), 55.3 (C-8'), 55.2 (C-15), 29.4 (C-7); m/z (ESI+) found 352.1174, [M+Na]⁺ C₁₈H₁₉NO₅Na requires 352.1161.

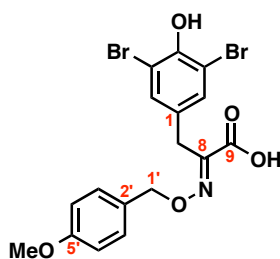
(E)-3-(3,5-Dichloro-4-methoxyphenyl)-2-(((4-methoxybenzyl)oxy)imino)propanoic acid (69)



Following general procedure 3 using phenylpyruvic acid **64**: furnished **69** (298 mg, 0.748 mmol, 99%) as a white solid which was used without further purification.

R_f 0.42 (10% MeOH/CH₂Cl₂); ν_{\max} (thin film)/cm⁻¹ 3670w, 2988m, 2902m, 1698m, 1513m, 1478m, 1257s, 983s; δ_H (400 MHz, CDCl₃) 7.28 (2H, d, J 8.7 Hz, H-3'/7'), 7.16 (2H, s, H-2/6), 6.92 (2H, d, J 8.7 Hz, H-4'/6'), 5.25 (2H, s, H-1'), 3.86 (3H, s, H-15), 3.83 (3H, s, H-8'), 3.79 (2H, s, H-7); δ_C (100 MHz, CDCl₃) 163.2 (C-9), 160.1 (C-5'), 151.2 (C-4), 148.6 (C-8), 132.4 (C-1), 130.4 (C-3'/7'), 129.6 (C-2/6), 129.1 (C-3/5), 127.4 (C-2'), 114.2 (C-4'/6'), 78.5 (C-1'), 60.6 (C-15), 55.3 (C-8'), 29.3 (C-7); m/z (ESI+) found 420.0398, $[M+Na]^+$ C₁₈H₁₇Cl₂NO₅Na (³⁵Cl) requires 420.0381.

(E)-3-(3,5-Dibromo-4-hydroxyphenyl)-2-(((4-methoxybenzyl)oxy)imino)propanoic acid (72)

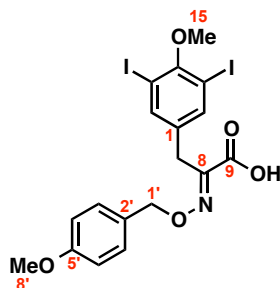


Following general procedure 3 using phenylpyruvic acid **68**: furnished **72** (459 mg, 0.97 mmol, 100%) as a white solid which was used without further purification.

R_f 0.27 (10% MeOH/CH₂Cl₂); ν_{\max} (thin film)/cm⁻¹ 3492s, 3300-2900br, 1694s, 1474s, 1239s, 1009s; δ_H (400 MHz, CDCl₃) 7.34 (2H, s, H-2/6), 7.28 (2H, d, J 8.7 Hz, H-3'/7'), 6.93 (2H, d, J 8.7 Hz, H-4'/6'), 5.78 (1H, s, OH), 5.24 (2H, s, H-1'), 3.83, (3H, s, H-8'), 3.77 (2H, s, H-7); δ_C (125 MHz, CDCl₃); 161.8 (C-9), 160.1 (C-5'), 148.9 (C-8), 148.3 (C-4), 132.8 (C-2/6), 130.4 (C-3'/7'), 129.4 (C-1), 127.3 (C-2'),

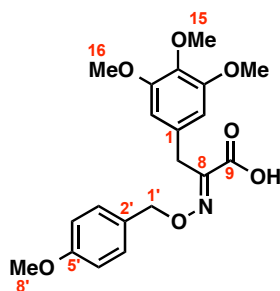
114.2 (C-4'/6'), 109.6 (C-3/5), 78.5 (C-1'), 55.3 (C-8'), 28.7 (C-7) m/z (ESI+) found 471.9419, $[M+H]^+$ $C_{17}H_{16}Br_2NO_5$ (^{79}Br) requires 471.9395; m.p. 130-132 °C.

(*E*)-3-(3,5-Diiodo-4-methoxyphenyl)-2-(((4-methoxybenzyl)oxy)imino)propanoic acid (70)



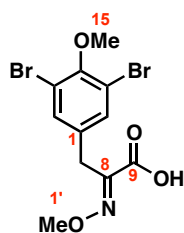
Following general procedure 3 using phenylpyruvic acid **65**: furnished **70** (549 mg, 0.945 mmol, 99%) as a white solid which was used without further purification.

R_f 0.32 (10% MeOH/ CH_2Cl_2); ν_{max} (thin film)/ cm^{-1} 3600-3200br, 2946w, 2837w, 1695s, 1513s, 1416s, 1246s; δ_H (400 MHz, $CDCl_3$) 7.64 (2H, s, H-2/6), 7.29 (2H, d, J 8.7 Hz, H-3'/7'), 6.94 (2H, d, J 8.7 Hz, H-4'/6'), 5.24 (2H, s, H-1'), 3.83, (3H, s, H-8'), 3.82 (3H, s, H-15), 3.76 (2H, s, H-7); δ_C (100 MHz, $CDCl_3$) 161.8 (C-9), 160.1 (C-5'), 157.9 (C-4), 148.7 (C-8), 140.5 (C-2/6), 134.6 (C-1), 130.4 (C-3'/7'), 127.3 (C-2'), 114.3 (C-4'/6'), 90.3 (C-3/5), 78.6 (C-1'), 60.7 (C-15), 55.3 (C-8'), 28.4 (C-7); m/z (ESI+) found 603.9091, $[M+H]^+$ $C_{18}H_{17}I_2NO_5Na$ requires 603.9094; m.p. 122-124 °C.

(E)-2-(((4-Methoxybenzyl)oxy)imino)-3-(3,4,5-trimethoxyphenyl)propanoic acid (73)

A mixture of azlactone **62** (278 mg, 1.00 mmol) and Ba(OH)₂·8H₂O (2.21 g, 7.00 mmol) in dioxane/ H₂O (1:1, 15 mL) was stirred at 60 °C. After 1 h, *O*-para-methoxybenzyl hydroxylamine hydrochloride (190 mg, 1.00 mmol) was added, and the mixture was stirred vigorously at the same temperature. After 18 h, the reaction mixture was cooled to 0 °C and acidified (pH 0) with aqueous HCl (3 N). The mixture was extracted with EtOAc (3 × 50 mL) and the combined organic extracts were dried and concentrated *in vacuo*. The residue was purified by flash column chromatography (1-10% MeOH/CH₂Cl₂) to furnish **73** (125 mg, 0.32 mmol, 32%) as a white solid.

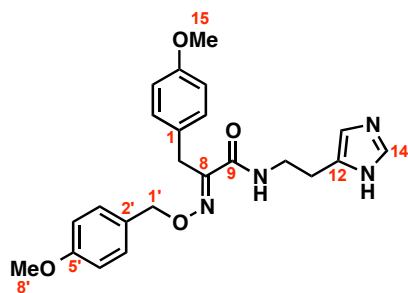
R_f 0.31 (10% MeOH/CH₂Cl₂); *v*_{max} (thin film)/cm⁻¹ 3700-3200br, 2949s, 1714w, 1611m, 1589s, 1121s; *δ*_H (400 MHz, CDCl₃) 7.28 (2H, d, *J* 8.6 Hz, H-3'/7'), 6.84 (2H, d, *J* 8.7 Hz, H-4'/6'), 6.46 (2H, s, H-2/6), 5.24 (2H, s, H-1'), 3.83 (2H, s, H-7), 3.82 (3H, s, H-8'), 3.80 (3H, s, H-15), 3.71 (6H, s, H-16); *δ*_C (125 MHz, CDCl₃) 163.0 (C-9), 160.0 (C-5'), 153.1 (C-3/5), 149.6 (C-8), 136.8 (C-4), 130.5 (C-1), 130.0 (C-3'/7'), 127.6 (C-2'), 114.0 (C-4'/6'), 106.3 (C-2/6), 78.3 (C-1'), 60.8 (C-15), 55.9 (C-16), 55.3 (C-8'), 30.5 (C-7); *m/z* (ESI+) found 412.1386, [M+Na]⁺ C₂₀H₂₃NO₇Na requires 412.1372.

(E)-3-(3,5-Dibromo-4-methoxyphenyl)-2-(methoxyimino)propanoic acid (86)

To a stirred solution of **38** (109 mg, 0.310 mmol) and *O*-methyl hydroxylamine hydrochloride (25.9 mg, 0.310 mmol) in EtOH (3.10 mL) was added sodium acetate (76.3 mg, 0.930 mmol). After 2 h, the mixture was acidified (pH 0) with aqueous HCl (3 *N*). The mixture was extracted with EtOAc (3 × 30 mL) and the combined organic extracts were dried and evaporated to dryness *in vacuo* to furnish **86** (115 mg, 0.302 mmol, 97%) as a white solid which was used without further purification.

R_f 0.26 (10% MeOH/CH₂Cl₂); ν_{\max} (thin film)/cm⁻¹ 2942w, 1706s, 1472s, 1259s, 1043s; δ_H (400 MHz, CDCl₃) 7.38 (2H, s, H-2/6), 4.12 (3H, s, H-1'), 3.83 (3H, s, H-15), 3.79 (2H, s, H-7); δ_C (100 MHz, CDCl₃) 165.0 (C-9), 152.9 (C-4), 148.4 (C-8), 133.7 (C-1), 133.1 (C-2/6), 117.9 (C-3/5), 64.0 (C-1'), 60.5 (C-15), 29.1 (C-7) *m/z* (ESI+) found 379.9146, [M+H]⁺ C₁₁H₁₂Br₂NO₄ (⁷⁹Br) requires 379.9133.

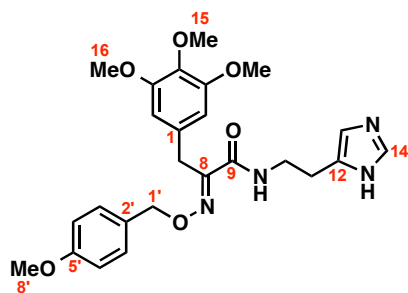
(E)-N-(2-(1H-Imidazol-4-yl)ethyl)-2-(((4-methoxybenzyl)oxy)imino)-3-(4-methoxyphenyl)propanamide (76)



To a stirred solution of acid **71** (126 mg, 0.383 mmol) in CH_2Cl_2 (6 mL) was added *N,N'*-dicyclohexylcarbodiimide (95.0 mg, 0.460 mmol) and *N*-hydroxybenzotriazole (62.0 mg, 0.459 mmol). After stirring for 5 min, histamine dihydrochloride (98.0 mg, 0.532 mmol) and *i*Pr₂EtN (184 μL , 1.07 mmol) were added. After 24 h, the mixture was concentrated *in vacuo* and the residue partitioned between H_2O (40 mL) and EtOAc (40 mL). The organic layer was separated and the aqueous layer was extracted with EtOAc (3 \times 40 mL). The combined organic extracts were washed with brine (100 mL), dried and concentrated *in vacuo*. The residue was purified by flash column chromatography (1-2% MeOH/ CH_2Cl_2) to furnish **76** (140 mg, 0.331 mmol, 86%) as a white foam.

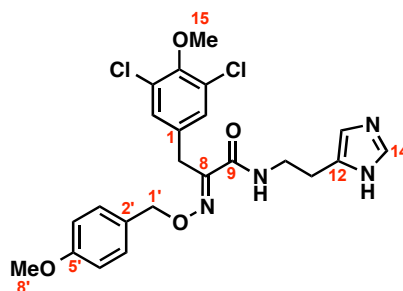
R_f 0.43 (10% MeOH/ CH_2Cl_2); ν_{max} (thin film)/ cm^{-1} 3324w, 2928m, 2850m, 1676m, 1625m, 1575m, 1509s, 1243s, 1034s; δ_{H} (500 MHz, CDCl_3) 7.53 (1H, s, H-14), 7.24 (2H, d, J 8.6 Hz, H-3'/7'), 7.18 (2H, d, J 8.6 Hz, H-2/6), 6.88 (2H, d, J 8.7 Hz, H-4'/6'), 6.76 (2H, d, J 8.6 Hz, H-3/5), 6.74 (1H, s, H-13), 5.11 (2H, s, H-1'), 3.85 (2H, s, H-7), 3.82 (3H, s, H-8'), 3.76 (3H, s, H-15), 3.57 (2H, apparent q, J 6.4 Hz, H-10), 2.83 (2H, t, J 6.6 Hz, H-11); δ_{C} (125 MHz, CDCl_3) 162.8 (C-9), 159.5 (C-5'), 158.1 (C-4), 152.6 (C-8), 134.6 (C-14), 130.4 (C-2/6), 129.9 (C-3'/7'), 129.0 (C-2'), 128.3 (C-1), 113.8 (C-4'/6'), 113.7 (C-3/5), 76.9 (C-1'), 55.3 (C-8'), 55.2 (C-15), 39.0 (C-10), 29.1 (C-7), 27.1 (C-11); m/z (ESI+) found 423.2038, $[\text{M}+\text{H}]^+$ $\text{C}_{23}\text{H}_{27}\text{N}_4\text{O}_4$ requires 423.2032.

Peaks corresponding to C-12 and C-13 were not visible.

(E)-N-(2-(1H-Imidazol-4-yl)ethyl)-2-(((4-methoxybenzyl)oxy)imino)-3-(3,4,5-trimethoxyphenyl)propanamide (77)

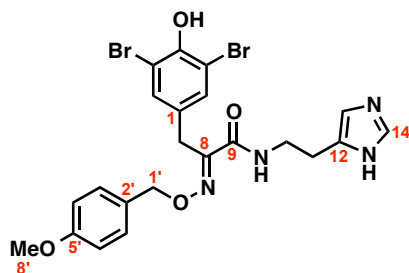
To a stirred solution of **73** (300 mg, 0.770 mmol) in THF (10 mL) was added CDI (150 mg, 0.925 mmol). After 1 h the solution was cooled to 0 °C and histamine (85.6 mg, 0.770 mmol) and CH₂Cl₂ (10 mL) were added, after which the reaction was warmed to room temperature and stirred for 18 h. The mixture was concentrated *in vacuo* and the residue partitioned between H₂O (20 mL) and CH₂Cl₂ (20 mL). The organic layer was separated and the aqueous layer was extracted with CH₂Cl₂ (3 × 20 mL). The combined organic extracts were washed with brine (20 mL), dried and concentrated *in vacuo*. The residue was purified by flash column chromatography (5–10 % MeOH/CH₂Cl₂) to furnish **77** (228 mg, 0.473 mmol, 61%) as a white foam.

R_f 0.57 (10% MeOH/CH₂Cl₂); ν_{\max} (thin film)/cm⁻¹ 3343w, 3114w, 2939w, 2836w, 1663s, 1513s, 1240s, 1119s; δ_H (400 MHz, CDCl₃) 9.52 (1H, br s, NH), 7.56 (1H, s, H-14) 7.24 (2H, d, J 8.6 Hz, H-3'/7'), 6.89 (2H, d, J 8.7 Hz, H-4'/6'), 6.75 (1H, s, H-13), 6.47 (2H, s, H-2/6), 5.11 (2H, s, H-1'), 3.83 (2H, s, H-7), 3.78 (3H, s, H-8'), 3.77 (3H, s, H-15), 3.67 (6H, s, H-16), 3.58 (2H, apparent q, J 6.4 Hz, H-10), 2.82 (2H, t, J 6.6 Hz, H-11); δ_C (125 MHz, CDCl₃) 162.8 (C-9), 159.7 (C-5'), 152.9 (C-3/5), 152.0 (C-8), 136.3 (C-4), 135.7 br (C-12), 134.7 (C-14), 131.8 (C-1), 130.1 (C-3'/7'), 128.7 (C-2'), 116.0 br (C-13), 113.8 (C-4'/6'), 106.4 (C-2/6), 77.1 (C-1'), 60.8 (C-15), 55.9 (C-16), 55.3 (C-8'), 39.1 (C-10), 30.2 (C-7), 27.0 (C-11); m/z (ESI⁺) found 483.2238, $[M+H]^+$ C₂₅H₃₁N₄O₆ requires 483.2244.

(E)-N-(2-(1H-Imidazol-4-yl)ethyl)-3-(3,5-dichloro-4-methoxyphenyl)-2-(((4-methoxybenzyl)oxy)imino)propanamide (74)

To a stirred solution of acid **69** (71.8 mg, 0.180 mmol) in CH_2Cl_2 (3 mL) was added *N,N'*-dicyclohexylcarbodiimide (44.7 mg, 0.217 mmol) and *N*-hydroxybenzotriazole (29.2 mg, 0.216 mmol). After stirring for 5 min, histamine dihydrochloride (36.5 mg, 0.198 mmol) and *i*Pr₂EtN (77 μL , 0.436 mmol) were added. After 18 h, the mixture was concentrated *in vacuo* and the residue partitioned between H_2O (30 mL) and EtOAc (30 mL). The organic layer was separated and the aqueous layer was extracted with EtOAc (3 \times 30 mL). The combined organic extracts were washed with brine (100 mL), dried and concentrated *in vacuo*. The residue was purified by flash column chromatography (1-5% MeOH/ CH_2Cl_2) to furnish **74** (64.1 mg, 0.130 mmol, 72%) as a white foam.

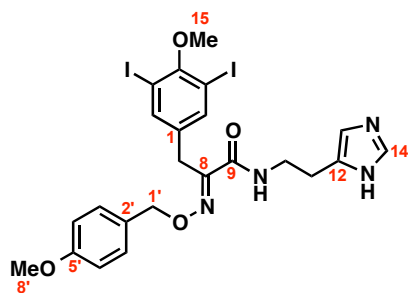
R_f 0.52 (10% MeOH/ CH_2Cl_2); ν_{max} (thin film)/ cm^{-1} 3300-2800br, 2935w, 1662s, 1612m, 1514s, 1478s, 1248s, 995s δ_{H} (400 MHz CDCl_3) 8.54 (1H, br s, NH), 7.59 (1H, s, H-14), 7.24 (2H, d, J 8.6 Hz, H-3'/7'), 7.16 (2H, s, H-2/6), 6.88 (2H, d, J 8.7 Hz, H-4'/6'), 6.79 (1H, s, H-13), 5.11 (2H, s, H-1'), 3.83 (3H, s, H-15), 3.80 (3H, s, H-8'), 3.78 (2H, s, H-7), 3.59 (2H, apparent q, J 6.4 Hz, H-10), 2.84 (2H, t, J 6.6 Hz, H-11); δ_{C} (100 MHz, CDCl_3) 162.3 (C-9), 159.7 (C-5'), 150.9 (C-8), 150.7 (C-4), 135.8 br (C-12), 134.7 (C-14), 133.7 (C-1), 130.1 (C-3'/7'), 129.7 (C-2/6), 128.8 (C-3/5), 128.4 (C-2'), 115.8 br (C-13), 114.0 (C-4'/6'), 77.3 (C-1'), 60.6 (C-15), 55.3 (C-8'), 39.1 (C-10), 28.8 (C-7), 27.0 (C-11); m/z (ESI⁺) found 491.1270, $[\text{M}+\text{H}]^+$ $\text{C}_{23}\text{H}_{25}\text{Cl}_2\text{N}_4\text{O}_4$ (^{35}Cl) requires 491.1253.

(E)-N-(2-(1H-Imidazol-4-yl)ethyl)-3-(3,5-dibromo-4-hydroxyphenyl)-2-(((4-methoxybenzyl)oxy)imino)propanamide (78)

To a stirred solution of acid **72** (100 mg, 0.211 mmol) in CH_2Cl_2 (5 mL) were added *N,N'*-dicyclohexylcarbodiimide (52.3 mg, 0.253 mmol) and *N*-hydroxybenzotriazole (34.3 mg, 0.254 mmol). After stirring for 5 min, histamine dihydrochloride (46.8 mg, 0.254 mmol) and *i* Pr_2EtN (99 μL , 0.575 mmol) were added. After 18 h, the solvent was removed *in vacuo* and the residue partitioned between H_2O (30 mL) and EtOAc (30 mL). The organic layer was separated and the aqueous layer was extracted with EtOAc (3 \times 30 mL). The combined organic extracts were washed with brine (100 mL), dried and concentrated *in vacuo*. The residue was purified by flash column chromatography (1-10% MeOH/ CH_2Cl_2) to furnish **78** (91.5 mg, 0.162 mmol, 77%) as a white foam.

R_f 0.47 (10% MeOH/ CH_2Cl_2); ν_{max} (thin film)/ cm^{-1} 3137w, 2933w, 1660s, 1612m, 1514s, 1247s, 1007s; δ_{H} (400 MHz, CD_3OD) 7.62 (1H, s, H-14), 7.27 (2H, s, H-2/6), 7.23 (2H, d, J 8.7 Hz, H-3'/7'), 6.88 (2H, d, J 8.7 Hz, H-4'/6'), 6.83 (1H, s, H-13), 5.12 (2H, s, H-1'), 3.77 (3H, s, H-8'), 3.70 (2H, s, H-7), 3.49 (2H, t, J 7.1 Hz, H-10), 2.80 (2H, t, J 7.1 Hz, H-11); δ_{C} (100 MHz, CD_3OD) 164.6 (C-9), 161.2 (C-5'), 152.9 (C-8), 151.1 (C-4), 136.0 (C-14), 135.7 br (C-12), 133.9 (C-2/6), 131.3 (C-1), 131.2 (C-3'/7'), 130.0 (C-2'), 117.8 br (C-13), 115.0 (C-4'/6'), 112.1 (C-3/5), 78.3 (C-1'), 55.7 (C-8'), 40.3 (C-10), 29.3 (C-7), 27.6 (C-11); m/z (ESI+) found 565.0097, $[\text{M}+\text{H}]^+$ $\text{C}_{22}\text{H}_{23}\text{Br}_2\text{N}_4\text{O}_4$ (^{79}Br) requires 565.0086.

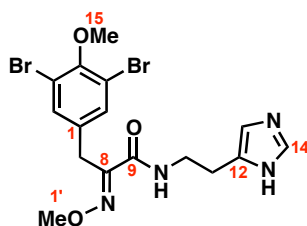
(E)-N-(2-(1H-Imidazol-4-yl)ethyl)-3-(3,5-diiodo-4-methoxyphenyl)-2-(((4-methoxybenzyl)oxy)imino)propanamide (75)



To a stirred solution of **70** (226 mg, 0.389 mmol), histamine dihydrochloride (107 mg, 0.583 mmol) and *i*Pr₂EtN (204 μ L, 1.17 mmol) in CH₂Cl₂ (5 mL) at 0 °C was added [®]T3P (347 μ L of a 50% w/w solution in EtOAc, 0.584 mmol) dropwise. After 1 h the reaction mixture was warmed to room temperature and stirred for 18 h upon which H₂O (20 mL) and CH₂Cl₂ (20 mL) were added and the organic phase removed. The aqueous layer was extracted with CH₂Cl₂ (20 mL \times 2) and the combined organic layers were dried and concentrated *in vacuo*. The residue was purified by flash column chromatography (1-10% MeOH/CH₂Cl₂) to furnish **75** (137 mg, 0.203 mmol, 52%).

R_f 0.52 (10% MeOH/CH₂Cl₂); ν_{max} (thin film)/cm⁻¹ 2934w, 2836w, 1660s, 1513s, 1460s, 1246s; δ_{H} (500 MHz, CDCl₃) 7.64 (2H, s, H-2/6), 7.59 (1H, s, H-14), 7.25 (2H, d, *J* 8.4 Hz, H-3'/7'), 6.91 (2H, d, *J* 8.5 Hz, H-4'/6'), 6.79 (1H, s, H-13), 5.11 (2H, s, H-1'), 3.81 (3H, s, H-8'), 3.79 (3H, s, H-15), 3.75 (2H, s, H-7), 3.59 (2H, apparent q, *J* 6.4 Hz, H-10), 2.84 (2H, t, *J* 6.6 Hz, H-11); δ_{C} (125 MHz, CDCl₃); 162.3 (C-9), 159.6 (C-5'), 157.2 (C-4), 150.9 (C-8), 140.5 (C-2/6), 136.1 (C-1), 135.8 (br, C-12), 134.7 (C-14), 130.2 (C-3'/7'), 128.4 (C-2'), 115.9 (br, C-13), 114.1 (C-4'/6'), 90.1 (C-3/5), 76.7 (C-1'), 60.6 (C-15), 55.3 (C-8'), 39.1 (C-10), 28.1 (C-7), 27.1 (C-11); *m/z* (ESI⁺) found 674.9982, [M+H]⁺ C₂₃H₂₅I₂N₄O₄ requires 674.9965.

(E)-N-(2-(1*H*-Imidazol-4-yl)ethyl)-3-(3,5-dibromo-4-methoxyphenyl)-2-(methoxyimino)propanamide (87)



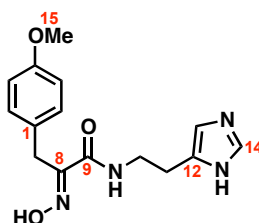
To a stirred solution of acid **86** (39.7 mg, 0.104 mmol) in CH₂Cl₂ (4 mL) were added *N,N'*-dicyclohexylcarbodiimide (25.8 mg, 0.125 mmol) and *N*-hydroxybenzotriazole (16.9 mg, 0.125 mmol). After stirring for 5 min, histamine dihydrochloride (23.0 mg, 0.125 mmol) and *i*Pr₂EtN (49 μ L, 0.285 mmol) were added. After 18 h, the solvent was removed *in vacuo* and the residue partitioned between H₂O (20 mL) and EtOAc (20 mL). The organic layer was separated and the aqueous layer was extracted with EtOAc (3 \times 20 mL). The combined organic extracts were washed with brine (50 mL), dried and concentrated *in vacuo*. The residue was purified by flash column chromatography (1-10% MeOH/CH₂Cl₂) to furnish **87** (30.6 mg, 64.5 μ mol, 62%) as a white foam.

R_f 0.45 (10% MeOH/CH₂Cl₂); ν_{\max} (thin film)/cm⁻¹ 2939w, 1660m, 1542w, 1472s; δ_H (400 MHz, CD₃OD) 7.59 (1H, s, H-14), 7.43 (2H, s, H-2/6), 6.84 (1H, s, H-13), 4.02 (3H, s, H-1'), 3.81 (3H, s, H-15), 3.80 (2H, s, H-7), 3.49 (2H, t, *J* 7.2 Hz, H-10), 2.80 (2H, t, *J* 7.2 Hz, H-11); δ_C (100 MHz, CD₃OD) 164.5 (C-9), 154.0 (C-4), 152.4 (C-8), 136.8 (C-1), 136.1 (C-14), 135.9 (C-13), 134.4 (C-2/6), 118.7 (C-3/5), 117.8 br (C-12), 63.6 (C-1'), 61.0 (C-15), 40.5 (C-10), 29.4 (C-7), 27.7 (C-11); *m/z* (ESI⁺) found 472.9845, [M+H]⁺ C₁₆H₁₉Br₂N₄O₃ (⁷⁹Br) requires 472.9824.

General Procedure 4: PMB removal

To a stirred solution of PMB protected substrate (1 eq.) and anisole (10 eq.) in CH_2Cl_2 (5 mL per 0.2 mmol substrate) was added aluminium trichloride (10 eq.). After 5 min, the mixture was basified by the addition of a saturated aqueous solution of NaHCO_3 followed by the addition of a saturated aqueous solution of Rochelle's salt. After stirring for 10 min, the aqueous phase was extracted with CH_2Cl_2 and the combined organic layers were dried and concentrated *in vacuo*. The residue was purified by flash column chromatography.

(E)-N-(2-(1*H*-Imidazol-4-yl)ethyl)-2-(hydroxyimino)-3-(4-methoxyphenyl)propanamide (81)

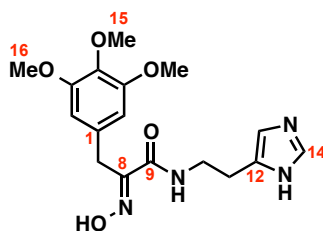


Following general procedure 4 using substrate **76**: residue purified by flash column chromatography (10-20% MeOH/ CH_2Cl_2) furnished **81** (3.00 mg, 9.92 μmol , 21%) as a white solid.

R_f 0.12 (10% MeOH/ CH_2Cl_2); ν_{max} (thin film)/ cm^{-1} 3400-3100br, 2925w, 1652s, 1509s, 1462s, 1245s; δ_{H} (400 MHz, CD_3OD) 7.55 (1H, s, H-14), 7.16 (2H, d, J 8.8 Hz, H-2/6), 6.79 (1H, s, H-13), 6.78 (2H, d, J 8.6 Hz, H-3/5), 3.82 (2H, s, H-7), 3.74 (3H, s, H-15), 3.47 (2H, t, J 7.2 Hz, H-10), 2.77 (2H, t, J 7.2 Hz, H-11); δ_{C} (125 MHz, CD_3OD) 165.9 (C-9), 159.6 (C-4), 153.6 (C-8), 136.0 (C-14), 131.1 (C-2/6), 130.1 (C-1), 114.7 (C-3/5), 55.6 (C-15), 40.2 (C-10), 29.0 (C-7), 27.0 (C-11); m/z (ESI+) found 303.1463, $[\text{M}+\text{H}]^+$ $\text{C}_{15}\text{H}_{19}\text{N}_4\text{O}_3$ requires 303.1457.

Peaks corresponding to C-12 and C-13 were not visible.

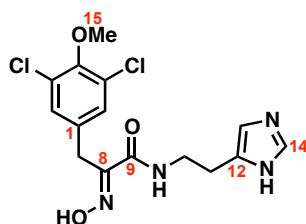
(*E*)-*N*-(2-(1*H*-Imidazol-4-yl)ethyl)-2-(hydroxyimino)-3-(3,4,5-trimethoxyphenyl)propanamide (82)



Following general procedure 4 using substrate **77**: residue purified by flash column chromatography (10-20% MeOH/CH₂Cl₂) furnished **82** (19.5 mg, 53.8 μmol, 58%) as a white foam.

R_f 0.14 (10% MeOH/CH₂Cl₂); *ν*_{max} (thin film)/cm⁻¹ 3300-3100br, 2925w, 2853w, 1737w, 1655m, 1590s, 1421s, 1120s; *δ*_H (500 MHz, CD₃OD) 7.57 (1H, s, H-14), 6.81 (1H, s, H-13), 6.59 (2H, s, H-2/6), 3.85 (2H, s, H-7), 3.80 (6H, s, H-16), 3.72 (3H, H-15), 3.48 (2H, t, *J* 7.2 Hz, H-10), 2.78 (2H, t, *J* 7.2 Hz, H-11); *δ*_C (125 MHz, CD₃OD) 165.9 (C-9), 154.3 (C-3/5), 153.2 (C-8), 137.5 (C-4), 136.1 (C-14), 136.1 br (C-12), 134.2 (C-1), 117.8 (br, C-13), 107.5 (C-2/6), 61.1 (C-15), 56.5 (C-16), 40.3 (C-10), 30.1 (C-11), 27.7 (C-7); *m/z* (ESI+) found 363.1678, [M+H]⁺ C₁₇H₂₃N₄O₅ requires 363.1668.

(*E*)-*N*-(2-(1*H*-Imidazol-4-yl)ethyl)-3-(3,5-dichloro-4-methoxyphenyl)-2-(hydroxyimino)propanamide (79)

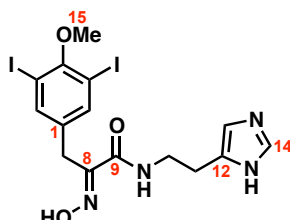


Following general procedure 4 using substrate **74**: residue purified by flash column chromatography (5-10% MeOH/CH₂Cl₂) furnished **79** (9.50 mg, 25.6 μmol, 63%) as a white solid.

R_f 0.20 (10% MeOH/CH₂Cl₂); *ν*_{max} (thin film)/cm⁻¹ 3400-3200br, 2926w, 1659m, 1529m, 1478s, 1265s, 994s; *δ*_H (400 MHz, CD₃OD) 7.57 (1H, s, H-14), 7.27 (2H, s, H-2/6), 6.83 (1H, s, H-13), 3.82 (5H, s, H-15 and H-7), 3.49 (2H, t, *J* 7.2 Hz, H-10), 2.79 (2H, t, *J* 7.2 Hz, H-11); *δ*_C (100 MHz, CD₃OD) 165.3 (C-9), 152.1 (C-8), 151.9

(C-4), 136.3 (C-1), 136.1 (C-14), 136.0 br (C-12), 130.7 (C-2/6), 129.9 (C-3/5), 117.9 br (C-13), 61.1 (C-15), 40.3 (C-10), 28.9 (C-7), 27.7 (C-11); m/z (ESI+) found 371.0676, $[M+H]^+$ $C_{15}H_{17}Cl_2N_4O_3$ (^{35}Cl) requires 371.0678.

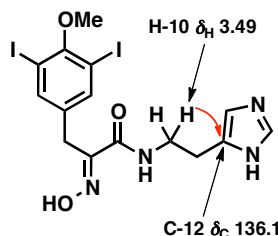
(*E*)-*N*-(2-(1*H*-Imidazol-4-yl)ethyl)-3-(3,5-diiodo-4-methoxyphenyl)-2-(hydroxyimino)propanamide (80)

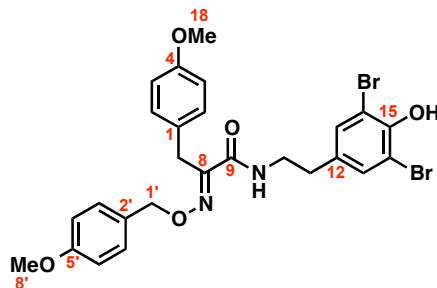


Following general procedure 4 using substrate **75**: residue purified by flash column chromatography (2-10% MeOH/ CH_2Cl_2) furnished **80** (12.7 mg, 22.9 μ mol, 12%) as a white solid.

R_f 0.38 (10% MeOH/ CH_2Cl_2); ν_{max} (thin film)/ cm^{-1} 3342w, 2930w, 1670s, 1642m, 1460s; δ_H (500 MHz, CD_3OD) 7.71 (2H, s, H-2/6), 7.57 (1H, s, H-14), 6.83 (1H, s, H-13), 3.79 (2H, s, H-7), 3.78 (3H, s, H-15), 3.49 (2H, t, J 7.2 Hz, H-10), 2.79 (2H, t, J 7.2 Hz, H-11); δ_C (125 MHz, CD_3OD); 165.3 (C-9), 158.8 (C-4), 152.2 (C-8), 141.6 (C-2/6), 138.2 (C-1), 136.1 (C-14) 136.1 (hidden, C-12) 117.8 (br, C-13), 90.7 (C-3/5), 61.1 (C-15), 40.3 (C-10), 28.2 (C-7), 27.7 (C-11); m/z (ESI+) found 554.9412, $[M+H]^+$ $C_{15}H_{17}I_2N_4O_3$ requires 554.9390.

In the HMBC spectrum, there is a coupling between H-10 (δ_H 3.49) and the signal δ_C 136.1. As C-14 is 5 bonds away from H-10, this interaction is attributed to the 3 bond coupling with C-12.

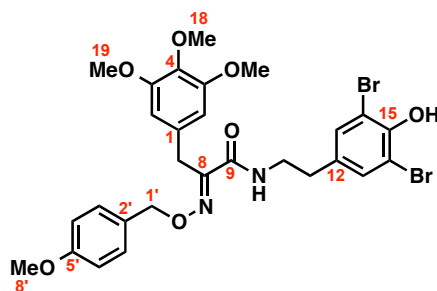


(E)-N-(3,5-Dibromo-4-hydroxyphenethyl)-2-(((4-methoxybenzyl)oxy)imino)-3-(4-methoxyphenyl)propanamide (90)

To a stirred solution of acid **71** (83.5 mg, 0.254 mmol), amine **20** (105 mg, 0.279 mmol) and *i*Pr₂EtN (165 μ L, 0.961 mmol) in CH₂Cl₂/DMF (1:1, 6 mL) at 0 °C was added [®]T3P (197 μ L of a 50% w/w solution in EtOAc, 0.330 mmol) dropwise. After 1 h the reaction mixture was warmed to room temperature and stirred for 18 h upon which H₂O (20 mL) and CH₂Cl₂ (20 mL) were added and the organic phase removed. The aqueous layer was extracted with CH₂Cl₂ (20 mL \times 2) and the combined organic layers were dried and concentrated *in vacuo*. The residue was purified by flash column chromatography (20-50% Et₂O/Petrol) to furnish **90** (47.0 mg, 77.5 μ mol, 31%) as a colourless oil.

R_f 0.39 (50% Et₂O/Petrol); ν_{\max} (thin film)/cm⁻¹ 3400-3100w, 2933w, 1664m, 1611m, 1509s, 1244s; δ_{H} (400 MHz, CDCl₃) 7.27 (2H, s, H-13/17), 7.22 (2H, d, *J* 8.7 Hz, H-3'/7'), 7.17 (2H, d, *J* 8.8 Hz, H-2/6), 6.88 (2H, d, *J* 8.7 Hz, H-4'/6'), 6.77 (2H, d, *J* 8.8 Hz, H-3/5), 5.49 (1H, br s, OH), 5.11 (2H, s, H-1'), 3.85 (2H, s, H-7), 3.83 (3H, s, H-8'), 3.77 (3H, s, H-18), 3.47 (2H, apparent q, *J* 6.7 Hz, H-10), 2.71 (2H, t, *J* 7.0 Hz, H-11); δ_{C} (100 MHz, CDCl₃) 162.7 (C-9), 159.6 (C-5'), 158.1 (C-4), 152.5 (C-8), 148.1 (C-15), 133.5 (C-12), 132.2 (C-13/17), 130.3 (C-2/6), 129.8 (C-3'/7'), 128.8 (C-2'), 128.2 (C-1), 113.9 (C-4'/6'), 113.8 (C-3/5), 109.9 (C-14/16), 77.0 (C-1'), 55.3 (C-8'), 55.2 (C-18), 40.4 (C-10), 34.3 (C-11), 29.0 (C-7); *m/z* (ESI+) found 605.0283, [M+H]⁺ C₂₆H₂₇Br₂N₂O₅ (⁷⁹Br) requires 605.0287.

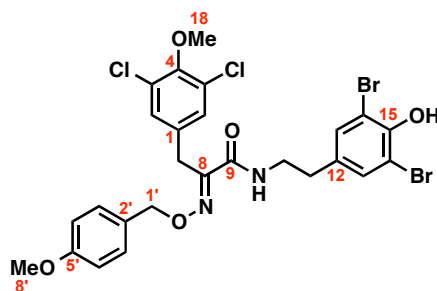
(E)-N-(3,5-Dibromo-4-hydroxyphenethyl)-2-(((4-methoxybenzyl)oxy)imino)-3-(3,4,5-trimethoxyphenyl)propanamide (91)



To a stirred solution of acid **73** (139 mg, 0.357 mmol), amine **20** (160 mg, 0.426 mmol) and *i*Pr₂EtN (232 μ L, 1.35 mmol) in CH₂Cl₂/DMF (1:1, 8 mL) at 0 °C was added [®]T3P (275 μ L of a 50% w/w solution in EtOAc, 0.463 mmol) dropwise. After 1 h the reaction mixture was warmed to room temperature and stirred for 18 h upon which H₂O (30 mL) and CH₂Cl₂ (30 mL) were added and the organic phase removed. The aqueous layer was extracted with CH₂Cl₂ (30 mL \times 2) and the combined organic layers were dried and concentrated *in vacuo*. The residue was purified by flash column chromatography (40-80% Et₂O/Petrol) to furnish **91** (103 mg, 0.155 mmol, 43%) as a white foam.

R_f 0.28 (70% Et₂O/Petrol); ν_{\max} (thin film)/cm⁻¹ 3348br, 2936w, 1663s, 1611w, 1590s, 1513s, 1242s, 1124s; δ_H (400 MHz, CDCl₃) 7.28 (2H, s, H-13/17), 7.23 (2H, d, *J* 8.7 Hz, H-3'/7'), 6.87 (2H, d, *J* 8.7 Hz, H-4'/6'), 6.76 (1H, t, *J* 6.1 Hz, NH), 6.49 (2H, s, H-2/6), 5.95 (1H, s, OH), 5.13 (2H, s, H-1'), 3.84 (2H, s, H-7), 3.81 (3H, s, H-8'), 3.79 (3H, s, H-18), 3.70 (6H, s, H-19), 3.49 (2H, apparent q, *J* 7.0 Hz, H-10), 2.73 (2H, t, *J* 7.0 Hz, H-11); δ_C (100 MHz, CDCl₃) 162.6 (C-9), 159.7 (C-5'), 152.9 (C-3/5), 151.9 (C-8), 148.1 (C-15), 136.5 (C-4), 133.4 (C-12), 132.2 (C-13/17), 131.6 (C-1), 130.0 (C-3'/7'), 128.6 (C-2'), 113.9 (C-4'/6'), 109.9 (C-14/16), 106.5 (C-2/6), 77.2 (C-1'), 60.7 (C-18), 55.9 (C-19), 55.3 (C-8'), 40.5 (C-10), 34.3 (C-11), 30.1 (C-7); *m/z* (ESI+) found 665.0491, [M+H]⁺ C₂₈H₃₁Br₂N₂O₇ (⁷⁹Br) requires 665.0498.

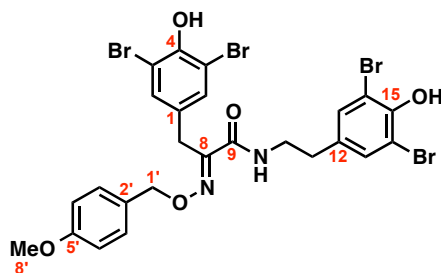
(E)-N-(3,5-Dibromo-4-hydroxyphenethyl)-3-(3,5-dichloro-4-methoxyphenyl)-2-(((4-methoxybenzyl)oxy)imino)propanamide (88)



To a stirred solution of acid **69** (100 mg, 0.251 mmol), amine **20** (94.3 mg, 0.251 mmol) and *i*Pr₂EtN (172 μ L, 1 mmol) in CH₂Cl₂/DMF (1:1, 5 mL) at 0 °C was added [®]T3P (194 μ L of a 50% w/w solution in EtOAc, 0.326 mmol) dropwise. After 1 h the reaction mixture was warmed to room temperature and stirred for 20 h upon which H₂O (30 mL) and EtOAc (30 mL) were added and the organic phase removed. The aqueous layer was extracted with EtOAc (30 mL \times 2) and the combined organic layers were washed with brine, dried and concentrated *in vacuo*. The residue was purified by flash column chromatography (20-60% Et₂O/Petrol) to furnish **88** (50.5 mg, 74.8 μ mol, 30%) as a white foam.

*R*_f 0.48 (50% Et₂O/Petrol); ν_{max} (thin film)/cm⁻¹ 3399br, 2934m, 1665s, 1611m, 1513s, 1476s, 1246s, 996s; δ_{H} (400 MHz CDCl₃) 7.29 (2H, s, H-13/17), 7.22 (2H, d, *J* 8.7 Hz, H-3'/7'), 7.19 (2H, s, H-2/6), 6.89 (2H, d, *J* 8.7 Hz, H-4'/6'), 6.73 (1H, t, *J* 6.0, NH), 5.86 (1H, br s, OH), 5.12 (2H, s, H-1'), 3.85 (3H, s, H-18), 3.82 (3H, s, H-8'), 3.80 (2H, s, H-7) 3.50 (2H, apparent q, *J* 6.7 Hz, H-10), 2.74 (2H, t, *J* 7.0 Hz, H-11); δ_{C} (100 MHz, CDCl₃) 162.2 (C-9), 159.8 (C-5'), 150.9 (C-8), 150.8 (C-4), 148.1 (C-15), 133.5 (C-1), 133.3 (C-12), 132.2 (C-13/17), 130.1 (C-3'/7'), 129.7 (C-2/6), 128.9 (C-3/5), 128.3 (C-2'), 114.0 (C-4'/6'), 109.9 (C-14/16), 77.5 (C-1'), 60.6 (C-18), 55.3 (C-8'), 40.5 (C-10), 34.3 (C-11), 28.8 (C-7); *m/z* (ESI⁺) found 672.9539, [M+H]⁺ C₂₆H₂₅Br₂Cl₂N₂O₅ (⁷⁹Br, ³⁵Cl) requires 672.9507.

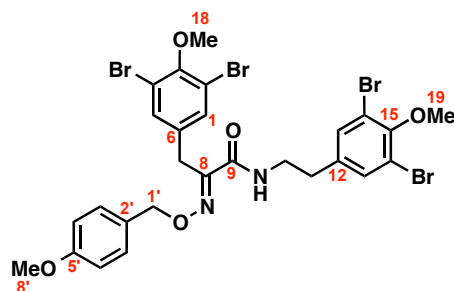
(E)-N-(3,5-Dibromo-4-hydroxyphenethyl)-3-(3,5-dibromo-4-hydroxyphenyl)-2-(((4-methoxybenzyl)oxy)imino)propanamide (92)



To a stirred solution of acid **72** (123 mg, 0.260 mmol), amine **20** (117 mg, 0.311 mmol) and *i*Pr₂EtN (176 μ L, 1.02 mmol) in CH₂Cl₂/DMF (1:1, 8 mL) at 0 °C was added [®]T3P (201 μ L of a 50% w/w solution in EtOAc, 0.338 mmol) dropwise. After 1 h the reaction mixture was warmed to room temperature and stirred for 16 h upon which H₂O (30 mL) and EtOAc (30 mL) were added and the organic phase removed. The aqueous layer was extracted with EtOAc (30 mL \times 2) and the combined organic layers were washed with brine, dried and concentrated *in vacuo*. The residue was purified by flash column chromatography (20-50% Et₂O/Petrol) to furnish **92** (69.4 mg, 92.5 μ mol, 36%) as a white foam.

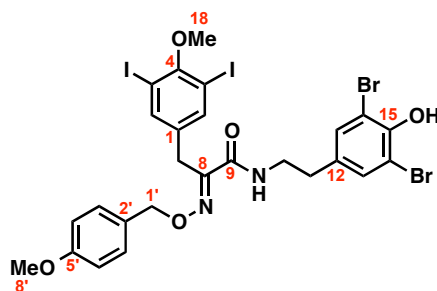
*R*_f 0.33 (50% Et₂O/Petrol); ν_{max} (thin film)/cm⁻¹ 3489w, 3401w, 2936w, 1663s, 1611m, 1514s, 1474s, 1242s; δ_{H} (400 MHz, CDCl₃) 7.36 (2H, s, H-13/17), 7.28 (2H, s, H-2/6), 7.23 (2H, d, *J* 8.7 Hz, H-3'/7'), 6.90 (2H, d, *J* 8.7 Hz, H-4'/6'), 6.74 (1H, t, *J* 6.0 Hz, NH), 5.89 (1H, s, OH), 5.83 (1H, s, OH), 5.12 (2H, s, H-1'), 3.82 (3H, s, H-8'), 3.77 (2H, s, H-7), 3.50 (2H, q, *J* 6.7 Hz, H-10), 2.74 (2H, t, *J* 7.0 Hz, H-11); δ_{C} (100 MHz, CDCl₃) 162.2 (C-9), 159.7 (C-5'), 151.2 (C-8), 148.1 (C-4), 147.9 (C-15), 133.3 (C-12), 132.8 (C-13/17), 132.2 (C-2/6), 130.7 (C-1), 130.1 (C-3'/7'), 128.3 (C-2'), 114.1 (C-4'/6'), 109.9 (C-3/5), 109.5 (C-14/16), 77.4 (C-1'), 55.3 (C-8'), 40.5 (C-10), 34.2 (C-11), 28.4 (C-7); *m/z* (ESI⁺) found 746.8324, [M+H]⁺ C₂₅H₂₃Br₄N₂O₅ (⁷⁹Br) requires 746.8340.

(E)-N-(3,5-Dibromo-4-methoxyphenethyl)-3-(3,5-dibromo-4-methoxyphenyl)-2-(((4-methoxybenzyl)oxy)imino)propanamide (99)



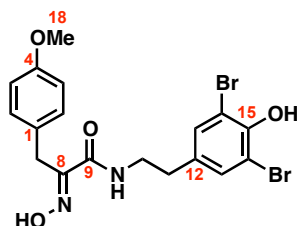
To a stirred solution of **36** (91.0 mg, 0.119 mmol) in acetone (4 mL) at room temperature was added anhydrous K_2CO_3 (24.5 mg, 0.177 mmol). The resulting mixture was stirred for 20 min, then treated with iodomethane (14.8 μ L, 0.238 mmol) and stirred at reflux for a further 3 h. After this time, acetone and excess iodomethane were removed *in vacuo* and the resulting residue was partitioned between EtOAc (20 mL) and H_2O (20 mL). The organic layer was separated and the aqueous layer was extracted with EtOAc (3 x 20 mL). The combined organic extracts were washed with brine, dried and concentrated *in vacuo*. The residue was purified by flash column chromatography (30-50% Et₂O/Petrol) to furnish **99** (82.5 mg, 0.106 mmol, 89%) as a colourless oil.

R_f 0.50 (50% Et₂O/Petrol); ν_{max} (thin film)/cm⁻¹ 2929w, 1670m, 1513s, 1470s, 1250s; δ_H (400 MHz CDCl₃) 7.41 (2H, s, H-1/5), 7.35 (2H, s, H-13/17), 7.23 (2H, d, J 8.7 Hz, H-3'/7'), 6.90 (2H, d, J 8.7 Hz, H-4'/6'), 6.74 (1H, t, J 6.0, NH), 5.13 (2H, s, H-1'), 3.88 (3H, s, H-19), 3.84 (3H, s, H-18), 3.82 (3H, s, H-8'), 3.80 (2H, s, H-7), 3.51 (2H, apparent q, J 6.9 Hz, H-10), 2.76 (2H, t, J 7.1 Hz, H-11); δ_C (100 MHz, CDCl₃) 162.2 (C-9), 159.8 (C-5'), 152.9 (C-15), 152.7 (C-3), 150.9 (C-8), 137.5 (C-12), 134.7 (C-6), 133.5 (C-1/5), 132.9 (C-13/17), 130.1 (C-3'/7'), 128.3 (C-2'), 118.2 (C-14/16), 117.7 (C-2/4), 114.1 (C-4'/6'), 77.5 (C-1'), 60.6 (C-19), 60.5 (C-18), 55.3 (C-8'), 40.4 (C-10), 34.5 (C-11), 28.6 (C-7); m/z (ESI⁺) found 774.8666, $[M+H]^+$ C₂₇H₂₇Br₄N₂O₅ (⁷⁹Br) requires 774.8653.

(E)-N-(3,5-Dibromo-4-hydroxyphenethyl)-3-(3,5-diiodo-4-methoxyphenyl)-2-(((4-methoxybenzyl)oxy)imino)propanamide (89)

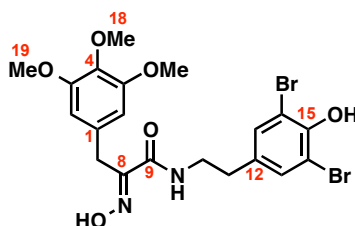
To a stirred solution of acid **70** (50.7 mg, 87.3 μmol), amine **20** (32.8 mg, 87.3 μmol) and *i*Pr₂EtN (60.6 μL , 0.349 mmol) in CH₂Cl₂/DMF (1:1, 3 mL) at 0 °C was added [®]T3P (67.5 μL of a 50% w/w solution in EtOAc, 0.113 mmol) dropwise. After 1 h the reaction mixture was warmed to room temperature and stirred for 20 h upon which H₂O (30 mL) and EtOAc (30 mL) were added and the organic phase removed. The aqueous layer was extracted with EtOAc (30 mL \times 2) and the combined organic layers were washed with brine, dried and concentrated *in vacuo*. The residue was purified by flash column chromatography (20-60% Et₂O/Petrol) to furnish **89** (34.4 mg, 40.1 μmol , 46%) as a colourless oil.

R_f 0.45 (50% Et₂O/PE 40-60); ν_{max} (thin film)/cm⁻¹ 3396br, 2928m, 1663s, 1611m, 1513s, 1460s, 1245s; δ_{H} (400 MHz CDCl₃) 7.66 (2H, s, H-2/6), 7.29 (2H, H-13/17), 7.24 (2H, d, *J* 8.7 Hz, H-3'/7'), 6.92 (2H, d, *J* 8.7 Hz, H-4'/6'), 6.72 (1H, t, *J* 6.0, NH), 5.87 (1H, br s, OH), 5.12 (2H, s, H-1'), 3.83 (3H, s, H-8'), 3.81 (3H, s, H-18), 3.77 (2H, s, H-7), 3.50 (2H, apparent q, *J* 6.7 Hz, H-10), 2.74 (2H, t, *J* 7.0 Hz, H-11); δ_{C} (100 MHz, CDCl₃) 162.2 (C-9), 159.7 (C-5'), 157.4 (C-4), 150.9 (C-8), 148.1 (C-15), 140.5 (C-2/6), 135.9 (C-1), 133.4 (C-12), 132.2 (C-13/17), 130.1 (C-3'/7'), 128.3 (C-2'), 114.1 (C-4'/6'), 109.9 (C-14/16), 90.1 (C-3/5), 77.4 (C-1'), 60.6 (C-18), 55.3 (C-8'), 40.5 (C-10), 34.3 (C-11), 28.1 (C-7); *m/z* (ESI⁺) found 856.8209, [M+H]⁺ C₂₆H₂₅Br₂I₂N₂O₅ (⁷⁹Br) requires 856.8220.

(E)-N-(3,5-Dibromo-4-hydroxyphenethyl)-2-(hydroxyimino)-3-(4-methoxyphenyl)propanamide (95)

Following general procedure 4 using substrate **90**: residue purified by flash column chromatography (20-50% Et₂O/Petrol) furnished **95** (23.0 mg, 47.3 μ mol, 93%) as a white solid.

R_f 0.20 (50% Et₂O/Petrol); ν_{\max} (thin film)/cm⁻¹ 3400-3200br, 2973w, 2932w, 1655s, 1627m, 1509s, 1242s, 1036s; δ_H (400 MHz, CD₃OD) 7.31 (2H, s, H-13/17), 7.13 (2H, d, J 8.8 Hz, H-2/6), 6.77 (2H, d, J 8.8 Hz, H-3/5), 3.82 (2H, s, H-7), 3.74 (3H, s, H-18), 3.40 (2H, t, J 7.2 Hz, H-10), 2.67 (2H, t, J 7.2 Hz, H-11); δ_C (100 MHz, CD₃OD) 166.0 (C-9), 159.6 (C-4), 153.6 (C-8), 150.7 (C-15), 134.6 (C-12), 133.6 (C-13/17), 131.0 (C-2/6), 130.0 (C-1), 114.8 (C-3/5), 112.1 (C-14/16), 55.6 (C-18), 41.5 (C-10), 34.9 (C-11), 29.0 (C-7); m/z (ESI⁺) found 484.9720, $[M+H]^+$ C₁₈H₁₉Br₂N₂O₄ (⁷⁹Br) requires 484.9712.

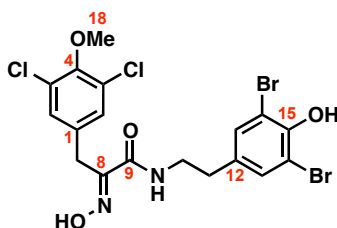
(E)-N-(3,5-Dibromo-4-hydroxyphenethyl)-2-(hydroxyimino)-3-(3,4,5-trimethoxyphenyl)propanamide (96)

Following general procedure 4 using substrate **91**: residue purified by flash column chromatography (40-100% Et₂O/Petrol) furnished **96** (19.2 mg, 35.2 μ mol, 30%) as a white solid.

R_f 0.24 (70% Et₂O/Petrol); ν_{\max} (thin film)/cm⁻¹ 3400-3100br, 2934w, 2838w, 1658s, 1626m, 1591s, 1421s, 1122s; δ_H (400 MHz, CDCl₃) 7.53 (1H, br s, NOH), 7.27 (2H, s, H-13/17), 6.71 (1H, t, J 6.1 Hz, NH), 6.59 (2H, s, H-2/6), 5.79 (1H, br s, OH), 3.91 (2H, s, H-7), 3.83 (6H, s, H-19), 3.81 (3H, s, H-18), 3.51 (2H, apparent q, J 6.7 Hz, H-10), 2.73 (2H, t, J 7.1 Hz, H-11); δ_C (100 MHz, CDCl₃) 162.7 (C-9), 153.7 (C-8),

153.1 (C-3/5), 148.1 (C-15), 136.7 (C-4), 133.3 (C-12), 132.2 (C-13/17), 131.5 (C-1), 109.9 (C-14/16), 106.5 (C-2/6), 60.8 (C-18), 56.1 (C-19), 40.5 (C-10), 34.3 (C-11), 29.4 (C-7); m/z (ESI+) found 544.9938, $[M+H]^+$ $C_{20}H_{23}Br_2N_2O_6$ (^{79}Br) requires 544.9923.

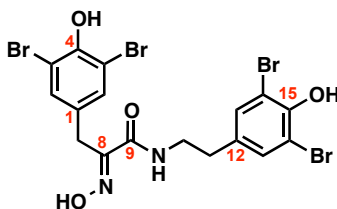
(E)-N-(3,5-Dibromo-4-hydroxyphenethyl)-3-(3,5-dichloro-4-methoxyphenyl)-2-(hydroxyimino)propanamide (93)



Following general procedure 4 using substrate **88**: residue purified by flash column chromatography (20-50% Et₂O/Petrol) furnished **93** (18.8 mg, 33.9 μ mol, 85%) as a colourless oil.

R_f 0.28 (50% Et₂O/Petrol); ν_{max} (thin film)/cm⁻¹ 3399w, 3218br, 2934w, 1659m, 1625m, 1530m, 1476s, 1265s, 994s; δ_H (400 MHz CD₃OD) 7.32 (2H, s, H-2/6), 7.27 (2H, s, H-13/17), 3.83 (5H, s, H-7 and H-18), 3.41 (2H, t, J 7.2 Hz, H-10), 2.70 (2H, t, J 7.2 Hz, H-11); δ_C (100 MHz, CD₃OD) 165.4 (C-9), 152.1 (C-8), 151.9 (C-4), 150.7 (C-15), 136.2 (C-1), 134.6 (C-12), 133.6 (C-13/17), 130.7 (C-2/6), 129.9 (C-3/5), 112.1 (C-14/16), 61.1 (C-18), 41.7 (C-10), 34.9 (C-11), 28.9 (C-7); m/z (ESI+) found 552.8926, $[M+H]^+$ $C_{18}H_{17}Br_2Cl_2N_2O_4$ (^{79}Br , ^{35}Cl) requires 552.8932.

(E)-N-(3,5-Dibromo-4-hydroxyphenethyl)-3-(3,5-dibromo-4-hydroxyphenyl)-2-(hydroxyimino)propanamide (7)



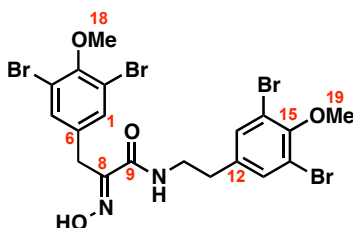
Following general procedure 4 using substrate **92**: residue purified by flash column chromatography (20-50% Et₂O/Petrol) furnished **7** (17.0 mg, 27.0 μ mol, 84%) as a white solid.

R_f 0.21 (50% Et₂O/Petrol); ν_{max} (thin film)/cm⁻¹ 3500-3000br, 2929w, 1659m, 1536m, 1474s, 1408m, 1241s; δ_H (400 MHz, CD₃OD) 7.39 (2H, s, H-2/6), 7.31 (2H, s, H-

13/17), 3.78 (2H, s, H-7), 3.40 (2H, q, J 7.3 Hz, H-10), 2.69 (2H, t, J 7.3 Hz, H-11); δ_{C} (100 MHz, CD_3OD) 165.5 (C-9), 152.6 (C-8), 150.8 (C-15), 150.7 (C-4), 134.6 (C-12), 133.9 (C-2/6), 133.6 (C-13/17), 132.2 (C-1), 112.1 (C-3/5), 112.0 (C-14/16), 41.8 (C-10), 34.9 (C-11), 28.4 (C-7); m/z (ESI+) found 626.7786, $[\text{M}+\text{H}]^+$ $\text{C}_{17}\text{H}_{15}\text{Br}_4\text{N}_2\text{O}_4$ (^{79}Br) requires 626.7765.

Consistent with literature data.³⁰

(*E*)-*N*-(3,5-Dibromo-4-methoxyphenethyl)-3-(3,5-dibromo-4-methoxyphenyl)-2-(hydroxyimino)propanamide (100)

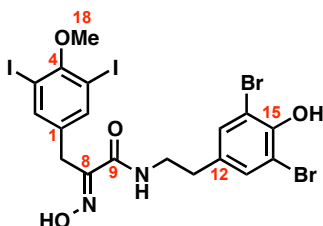


Following general procedure 4 using substrate **99**: residue purified by flash column chromatography (20-30% Et_2O /Petrol) furnished **100** (55.5 mg, 84.3 μmol , 94%) as a white solid.

R_f 0.40 (50% Et_2O /Petrol); ν_{max} (thin film)/ cm^{-1} 3206br, 2928w, 1657m, 1532m, 1471s, 1420s, 1258s; δ_{H} (400 MHz CDCl_3) 8.38 (1H, s, OH), 7.49 (2H, s, H-1/5), 7.32 (2H, s, H-13/17), 6.77 (1H, t, J 6.1, NH), 3.89 (2H, s, H-7), 3.87 (3H, s, H-19), 3.85 (3H, s, H-18), 3.50 (2H, apparent q, J 6.8 Hz, H-10), 2.75 (2H, t, J 7.1 Hz, H-11); δ_{C} (100 MHz, CDCl_3) 162.8 (C-9), 152.8 (C-15), 152.7 (C-3), 152.1 (C-8), 137.3 (C-12), 134.7 (C-6), 133.5 (C-1/5), 132.8 (C-13/17), 118.1 (C-14/16), 117.8 (C-2/4), 60.62 (C-19), 60.55 (C-18), 40.4 (C-10), 34.4 (C-11), 27.9 (C-7); m/z (ESI+) found 654.8087, $[\text{M}+\text{H}]^+$ $\text{C}_{19}\text{H}_{19}\text{Br}_4\text{N}_2\text{O}_4$ (^{79}Br) requires 654.8078.

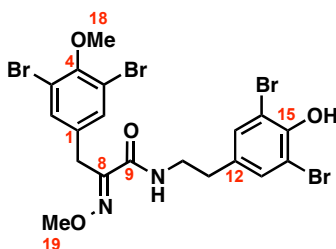
Crystals of **100** were obtained by slow evaporation of a solution of Et_2O /Hexane. The structure was confirmed by X-ray crystallographic analysis and given the unique identifier sl1005.

(E)-N-(3,5-Dibromo-4-hydroxyphenethyl)-3-(3,5-diiodo-4-methoxyphenyl)-2-(hydroxyimino)propanamide (94)



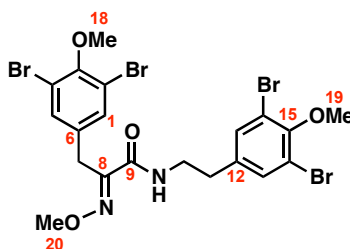
Following general procedure 4 using substrate **89**: residue purified by flash column chromatography (20-50% Et₂O/Petrol) furnished **94** (14.8 mg, 20.1 μ mol 73%) as a white solid.

R_f 0.29 (50% Et₂O/Petrol); ν_{\max} (thin film)/cm⁻¹ 3400-3200br, 2933w, 1655s, 1623m, 1532s, 1460s, 1241s, 990s; δ_H (400 MHz CD₃OD) 7.73 (2H, s, H-2/6), 7.32 (2H, H-13/17), 3.79 (2H, s, H-7), 3.78 (3H, s, H-18), 3.41 (2H, t, J 7.3 Hz, H-10), 2.70 (2H, t, J 7.3 Hz, H-11); δ_C (100 MHz, CD₃OD) 165.4 (C-9), 158.8 (C-4), 152.2 (C-8), 150.8 (C-15), 141.6 (C-2/6), 138.2 (C-1), 134.6 (C-12), 133.6 (C-13/17), 112.2 (C-14/16), 90.7 (C-3/5), 61.1 (C-18), 41.8 (C-10), 34.9 (C-11), 28.2 (C-7); m/z (ESI+) found 736.7612, $[M+H]^+$ C₁₈H₁₇Br₂I₂N₂O₄ (⁷⁹Br) requires 736.7644.

(E)-N-(3,5-Dibromo-4-hydroxyphenethyl)-3-(3,5-dibromo-4-methoxyphenyl)-2-(methoxyimino)propanamide (97)

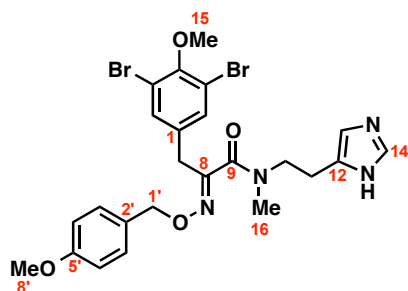
To a stirred solution of acid **86** (55.7 mg, 0.146 mmol), amine **20** (65.8 mg, 0.175 mmol) and *i*Pr₂EtN (99.0 μ L, 0.575 mmol) in CH₂Cl₂/DMF (1:1, 3 mL) at 0 °C was added [®]T3P (113 μ L of a 50% w/w solution in EtOAc, 0.19 mmol) dropwise. After 18 h, H₂O (10 mL) and CH₂Cl₂ (10 mL) were added and the organic phase removed. The aqueous layer was extracted with CH₂Cl₂ (10 mL \times 2) and the combined organic layers were dried and concentrated *in vacuo*. The residue was purified by flash column chromatography (10-30% Et₂O/Petrol) to furnish **97** (34.2 mg, 52.0 μ mol, 36%).

R_f 0.13 (20% Et₂O/Petrol); ν_{max} (thin film)/cm⁻¹ 3676m, 2988s, 2901s, 1666m, 1525m, 1407m; δ_{H} (400 MHz, CDCl₃) 7.43 (2H, s, H-2/6), 7.29 (2H, s, H-13/17), 6.77 (1H, t, *J* 5.9 Hz, NH), 5.80 (1H, s, OH), 4.02 (3H, s, H-19), 3.85 (3H, s, H-18), 3.82 (2H, s, H-7), 3.51 (2H, apparent q, *J* 6.0 Hz, H-10), 2.75 (2H, t, *J* 7.1 Hz, H-11); δ_{C} (100 MHz, CDCl₃) 162.2 (C-9), 152.7 (C-4), 150.7 (C-8), 148.2 (C-15), 134.8 (C-1), 133.41 (C-12), 133.37 (C-2/6), 132.3 (C-13/17), 117.9 (C-3/5), 109.9 (C-14/16), 63.4 (C-19), 60.6 (C-18), 40.6 (C-10), 34.4 (C-11), 28.5 (C-7); *m/z* (ESI+) found 654.8085, [M+H]⁺ C₁₉H₁₉Br₄N₂O₄ (⁷⁹Br) requires 654.8078.

(E)-N-(3,5-Dibromo-4-methoxyphenethyl)-3-(3,5-dibromo-4-methoxyphenyl)-2-(methoxyimino)propanamide (98)

To a stirred solution of **97** (18.0 mg, 27.4 μmol) in acetone (2 mL) at room temperature was added anhydrous K_2CO_3 (5.7 mg, 41.2 μmol). The resulting mixture was stirred for 20 min, then treated with iodomethane (17.1 μL , 0.274 mmol) and stirred at reflux 5 h. After this time, acetone and excess iodomethane were removed *in vacuo* and the resulting residue was partitioned between EtOAc (20 mL) and H_2O (20 mL). The organic layer was separated and the aqueous layer was extracted with EtOAc (3 x 20 mL). The combined organic extracts were washed with brine, dried and concentrated *in vacuo*. The residue was purified by flash column chromatography (30-50% Et_2O /Petrol) to furnish **98** (17.2 mg, 25.6 μmol , 93%) as a colourless oil.

R_f 0.58 (50% Et_2O /Petrol); ν_{max} (thin film)/ cm^{-1} 3404w, 2931w, 1668m, 1520m, 1471s, 1420s, 1258s; δ_{H} (400 MHz CDCl_3) 7.43 (2H, s, H-1/5), 7.34 (2H, s, H-13/17), 6.77 (1H, br s, NH), 4.01 (3H, s, C-20), 3.87 (3H, s, H-19), 3.85 (3H, s, H-18), 3.81 (2H, s, H-7) 3.51 (2H, apparent q, J 6.8 Hz, H-10), 2.76 (2H, t, J 7.1 Hz, H-11); δ_{C} (125 MHz, CDCl_3) 162.2 (C-9), 152.8 (C-15), 152.7 (C-3), 150.6 (C-8), 137.4 (C-12), 134.7 (C-6), 133.3 (C-1/5), 132.9 (C-13/17), 118.1 (C-14/16), 117.8 (C-2/4), 63.3 (C-20), 60.61 (C-19), 60.55 (C-18), 40.4 (C-10), 34.4 (C-11), 28.4 (C-7); m/z (ESI+) found 668.8251, $[\text{M}+\text{H}]^+$ $\text{C}_{20}\text{H}_{21}\text{Br}_4\text{N}_2\text{O}_4$ (^{79}Br) requires 668.8235.

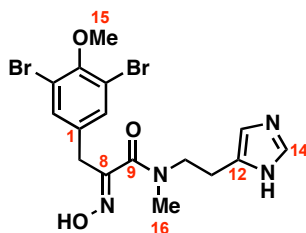
(E)-N-(2-(1H-Imidazol-5-yl)ethyl)-3-(3,5-dibromo-4-methoxyphenyl)-2-(((4-methoxybenzyl)oxy)imino)-N-methylpropanamide (84)

To a solution of acid **17** (283 mg, 0.581 mmol) in THF (3 mL) at room temperature was added CDI (104 mg, 0.641 mmol). After 1 h the solution was cooled to 0 °C and a solution of methylhistamine³¹ (73.0 mg, 0.583 mmol) in THF (2 mL) was added dropwise. The reaction was warmed to rt and stirred for 18 h after which the solvent was removed *in vacuo* and the residue partitioned between H₂O (20 mL) and EtOAc (20 mL). The organic layer was separated and the aqueous layer was extracted with EtOAc (3 × 20 mL). The combined organic extracts were washed with brine (20 mL), dried and concentrated *in vacuo*. The residue was purified by flash column chromatography (3-10% MeOH/CH₂Cl₂) to furnish **84** (122 mg, 0.205 mmol, 35%) as a yellow oil.

R_f 0.78 (10% MeOH/CH₂Cl₂); ν_{\max} (thin film)/cm⁻¹ 3207br, 2968w, 2931w, 1627s, 1613s, 1513s, 1471s, 1248s; The product exists as a rotameric mixture (ratio of 1.15:1) at room temperature in CDCl₃. Major Rotamer: δ_H (400 MHz CDCl₃) 9.96 (1H, br s, NH), 7.51 (1H, s, H-14), 7.32 (2H, s, H-2/6), 7.22 (2H, d, J 8.6 Hz, H-3'/7'), 6.86 (2H, d, J 8.6 Hz, H-4'/6'), 6.74 (1H, s, H-13), 5.07 (2H, s, H-1'), 3.81 (3H, s, H-15), 3.78 (3H, s, H-8'), 3.76 (2H, s, H-7), 3.62 (2H, t, J 7.3 Hz, H-10), 2.80 (2H, t, J 7.3 Hz, H-11), 2.76 (3H, s, H-16). Minor Rotamer: δ_H (400 MHz CDCl₃) 9.96 (1H, br s, NH), 7.51 (1H, s, H-14), 7.38 (2H, s, H-2/6), 7.18 (2H, d, J 8.6 Hz, H-3'/7'), 6.82 (2H, d, J 8.6 Hz, H-4'/6'), 6.60 (1H, s, H-13), 5.07 (2H, s, H-1'), 3.79 (3H, s, H-8'), 3.75 (3H, s, H-15), 3.68 (2H, s, H-7), 3.56 (2H, t, J 7.3 Hz, H-10), 2.88 (3H, s, H-16), 2.68 (2H, t, J 7.3 Hz, H-11); m/z (ESI+) found 593.0396, [M+H]⁺ C₂₄H₂₆Br₂N₄O₄ (⁷⁹Br) requires 593.0399.

Using VT ¹H NMR, the peaks coalesced at 120 °C although the peak corresponding to H-14 was lost. Multiple peaks were lost in the VT ¹³C NMR at 120 °C. At 25 °C the ¹³C NMR was too complex to accurately interpret (see Section 2.2.6.1).

(*E*)-*N*-(2-(1*H*-Imidazol-5-yl)ethyl)-3-(3,5-dibromo-4-methoxyphenyl)-2-(hydroxyimino)-*N*-methylpropanamide (85**)**



Following general procedure 4 using substrate **84**: Residue purified by flash column chromatography (10-20% MeOH/CH₂Cl₂) to furnish **85** (12.6 mg, 26.6 μmol, 79%) as a pale yellow oil.

R_f 0.16 (10% MeOH/CH₂Cl₂); *v*_{max} (thin film)/cm⁻¹ 3400-3100br, 2971w, 1611s, 1543m, 1471s, 1259s, 987s; The product exists as a rotameric mixture (ratio of 1.15:1) at room temperature in CD₃OD. Major Rotamer δ_H (400 MHz CD₃OD) 7.59 (1H, s, H-14), 7.50 (2H, s, H-2/6), 6.81 (1H, s, H-13), 3.79 (3H, s, H-15), 3.73 (2H, s, H-7), 3.59 (2H, t, *J* 7.5 Hz, H-10), 2.93 (3H, s, H-16), 2.77-2.72 (2H, m, H-11). Minor Rotamer δ_H (400 MHz CD₃OD) 7.58 (1H, s, H-14), 7.49 (2H, s, H-2/6), 6.80 (1H, s, H-13), 3.82 (3H, s, H-15), 3.83 (2H, s, H-7), 3.59 (2H, t, *J* 7.5 Hz, H-10), 2.89 (3H, s, H-16), 2.77-2.72 (2H, m, H-11); *m/z* (ESI+) found 472.9818, [M+H]⁺ C₁₆H₁₉Br₂N₄O₃ (⁷⁹Br) requires 478.9824.

Due to the rotameric nature of **85** and the limited amount of material obtained, the ¹³C NMR spectrum was too complex to accurately interpret. The ¹H NMR spectrum is provided in Section 2.2.6.1.

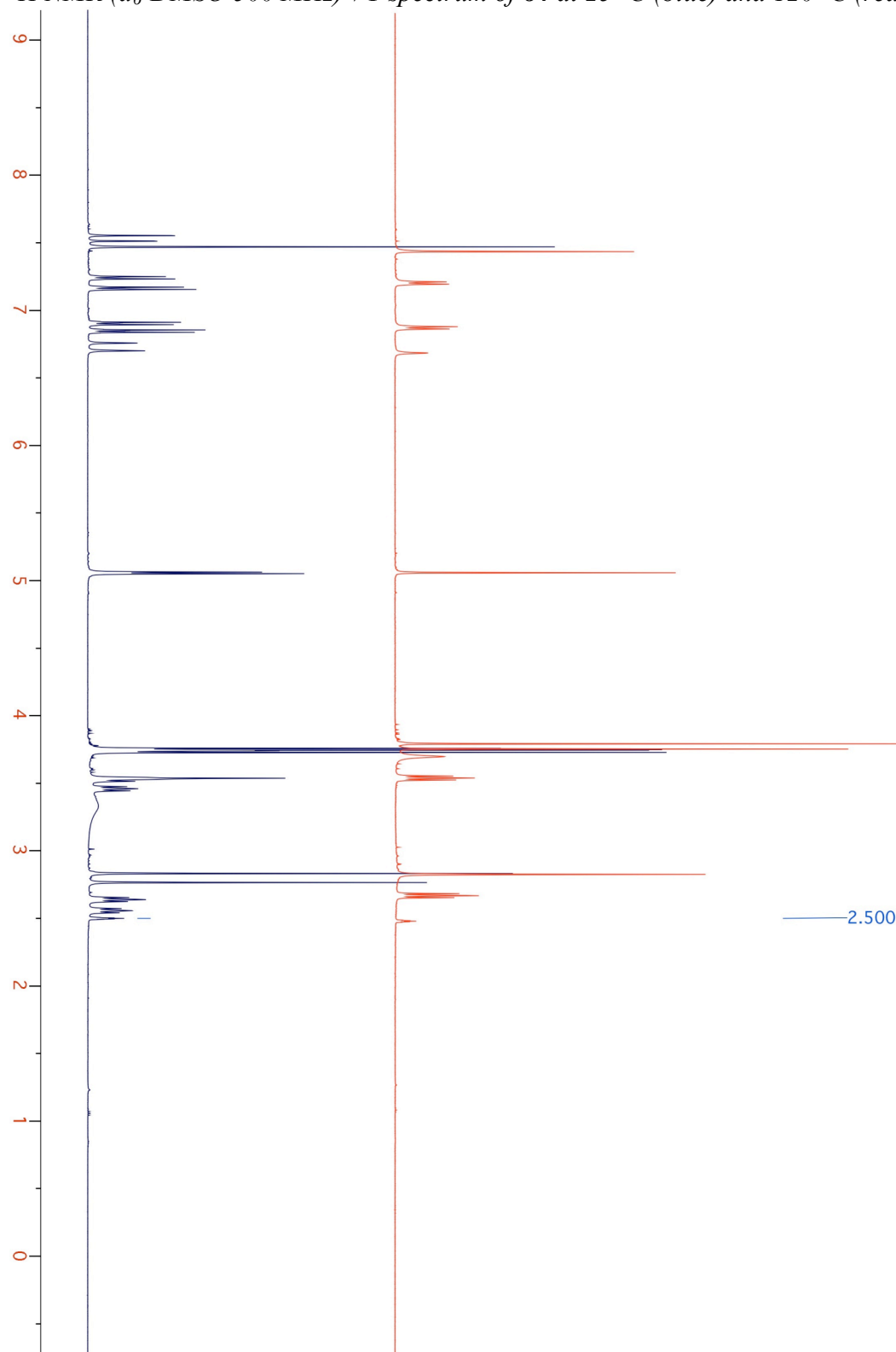
2.2.5 Biology: Experimental

Refer to Section 2.1.7 for experimental details.

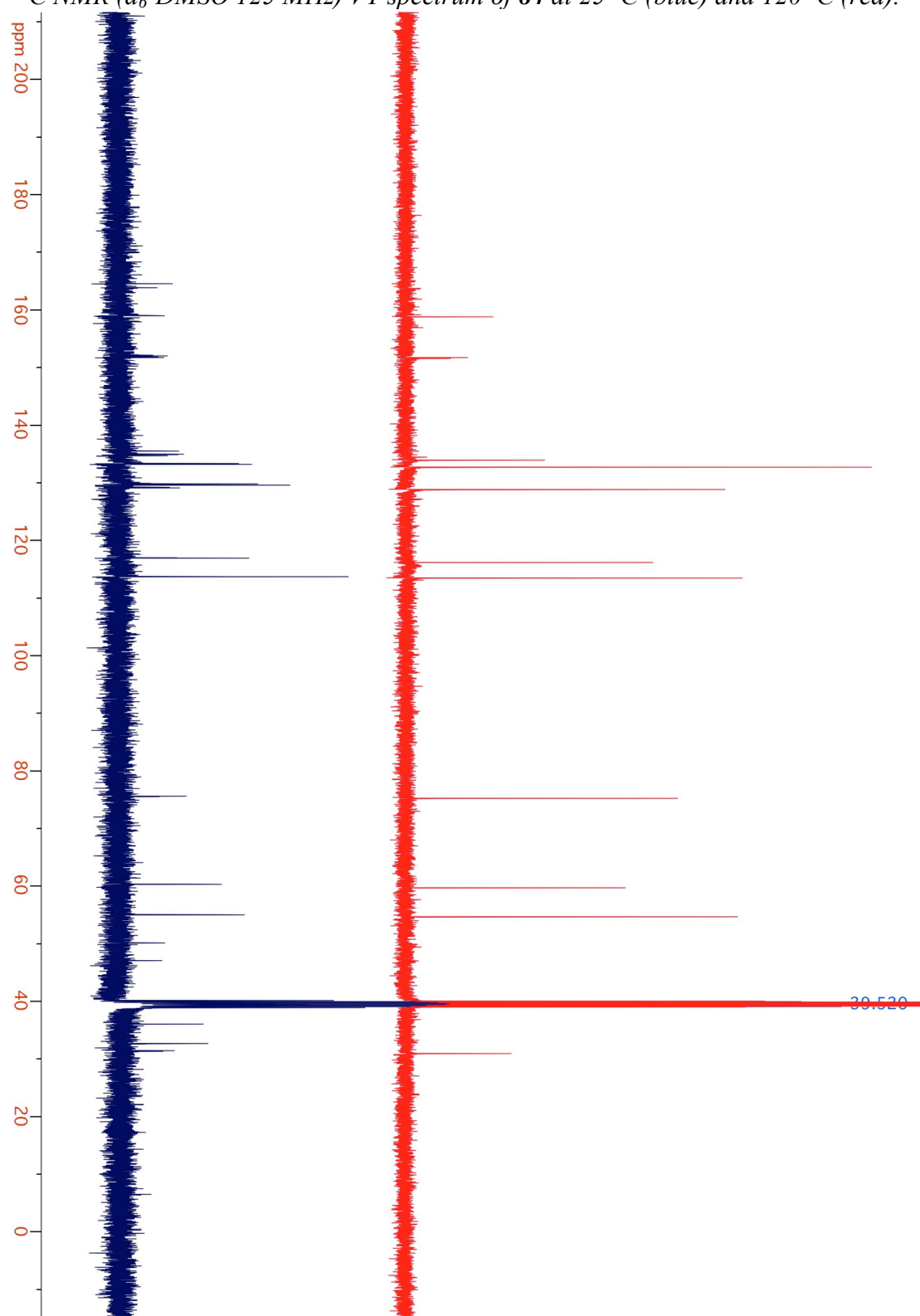
2.2.6 Appendix

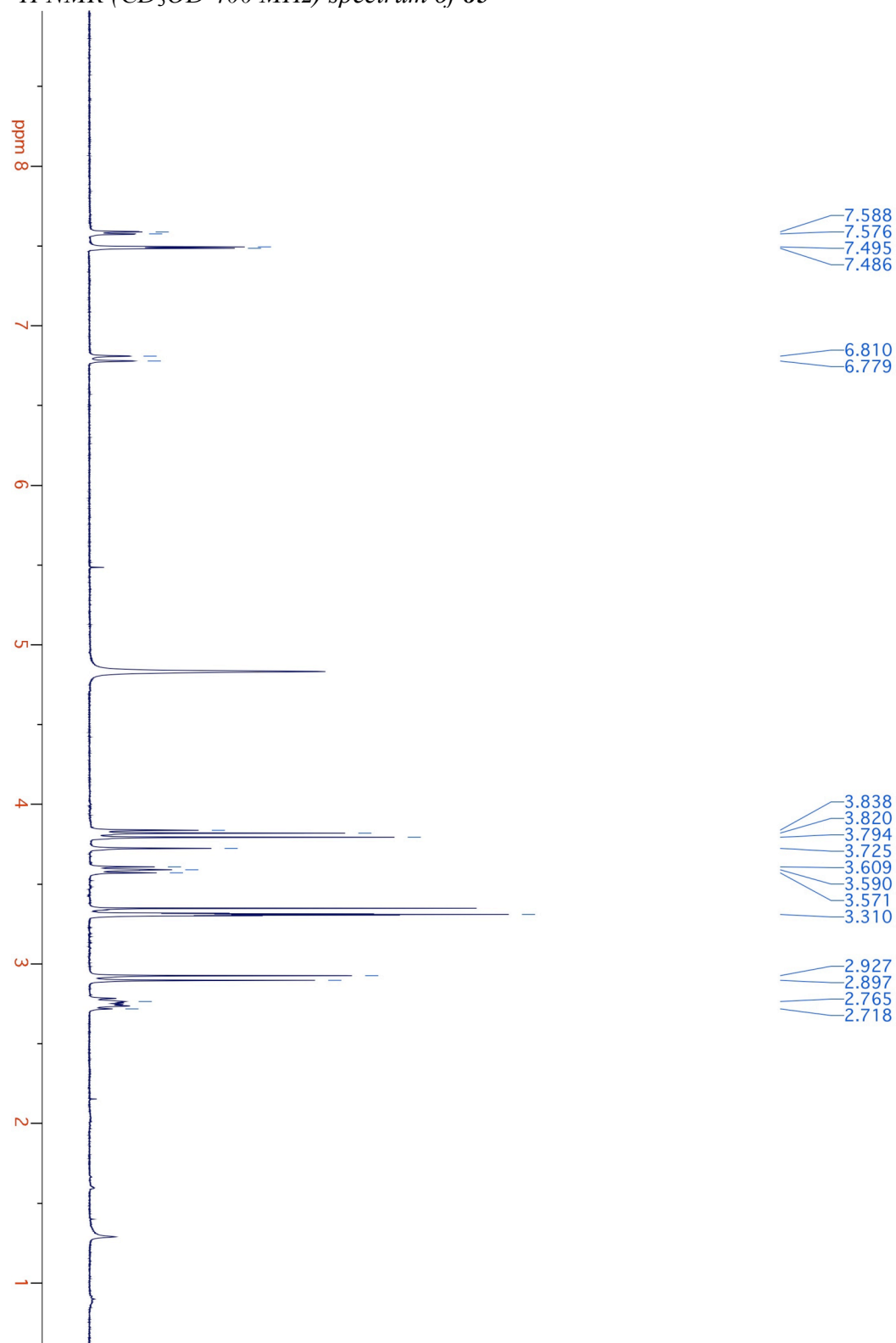
2.2.6.1 NMR Spectra

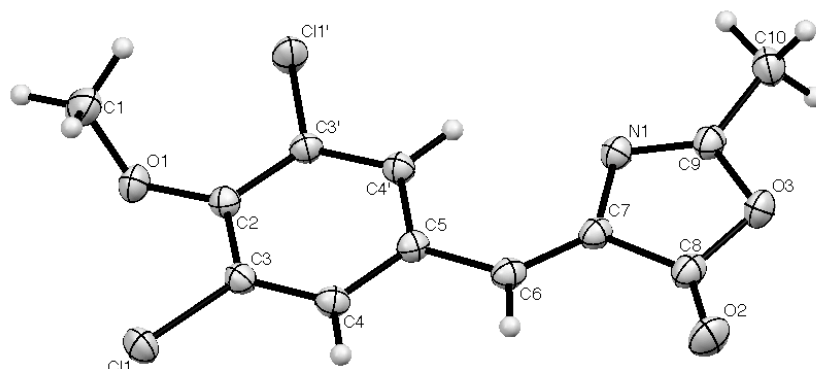
^1H NMR (d_6 -DMSO 500 MHz) VT spectrum of **84** at 25 °C (blue) and 120 °C (red).



^{13}C NMR (d_6 -DMSO 125 MHz) VT spectrum of **84** at 25 °C (blue) and 120 °C (red).



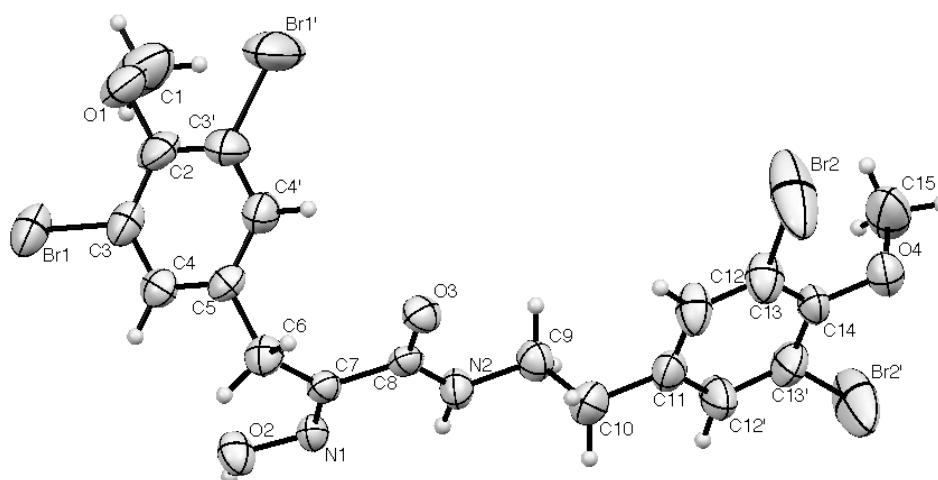
^1H NMR (CD_3OD 400 MHz) spectrum of **85**

2.2.6.2 Crystal Structure Data**(Z)-4-(3,5-Dichloro-4-methoxybenzylidene)-2-methyloxazol-5(4H)-one (59)**

Crystal data and structure refinement for sl1029

| | |
|-----------------------------------|--|
| Identification code | sl1029 |
| Empirical formula | C ₁₂ H ₉ Cl ₂ NO ₃ |
| Formula weight | 286.10 |
| Temperature | 180(2) K |
| Wavelength | 0.71073 Å |
| Crystal system | Triclinic |
| Space group | P-1 |
| Unit cell dimensions | a = 7.2007(1) Å α = 102.473(1)° b = 7.6943(2) Å β = 98.169(1)° c = 11.6371(2) Å γ = 104.107(1)° |
| Volume | 597.49(2) Å ³ |
| Z | 2 |
| Density (calculated) | 1.590 Mg/m ³ |
| Absorption coefficient | 0.541 mm ⁻¹ |
| F(000) | 292 |
| Crystal size | 0.35 × 0.28 × 0.21 mm ³ |
| Theta range for data collection | 3.75 to 33.13° |
| Index ranges | -11 ≤ h ≤ 11, -11 ≤ k ≤ 11, -16 ≤ l ≤ 17 |
| Reflections collected | 11625 |
| Independent reflections | 4517 [R(int) = 0.0220] |
| Completeness to theta = 33.13° | 99.3% |
| Absorption correction | Semi-empirical from equivalents |
| Max. and min. transmission | 0.898 and 0.860 |
| Refinement method | Full-matrix least-squares on F ² |
| Data / restraints / parameters | 4517 / 0 / 165 |
| Goodness-of-fit on F ² | 1.055 |
| Final R indices [I > 2σ(I)] | R1 = 0.0314, wR2 = 0.0805 |
| R indices (all data) | R1 = 0.0378, wR2 = 0.0844 |
| Largest diff. peak and hole | 0.396 and -0.336 e. Å ⁻³ |

(*E*)-*N*-(3,5-Dibromo-4-methoxyphenethyl)-3-(3,5-dibromo-4-methoxyphenyl)-2-(hydroxyimino)propanamide (100)



Crystal data and structure refinement for sl1005

| | |
|-----------------------------------|--|
| Identification code | sl1005 |
| Empirical formula | C ₁₉ H ₁₈ Br ₄ N ₂ O ₄ |
| Formula weight | 657.99 |
| Temperature | 180(2) K |
| Wavelength | 0.71073 Å |
| Crystal system | Orthorhombic |
| Space group | P2 ₁ ca |
| Unit cell dimensions | a = 14.775(3) Å α = 90° b = 13.554(3) Å β = 90° c = 22.852(5) Å γ = 90° |
| Volume | 4576.7(16) Å ³ |
| Z | 8 |
| Density (calculated) | 1.910 Mg/m ³ |
| Absorption coefficient | 7.062 mm ⁻¹ |
| F(000) | 2544 |
| Crystal size | 0.30 × 0.10 × 0.02 mm ³ |
| Theta range for data collection | 3.61 to 25.00° |
| Index ranges | -16 ≤ h ≤ 17, -13 ≤ k ≤ 13, -27 ≤ l ≤ 26 |
| Reflections collected | 20333 |
| Independent reflections | 3820 [R(int) = 0.0554] |
| Completeness to theta = 25.00° | 94.7% |
| Absorption correction | Semi-empirical from equivalents |
| Max. and min. transmission | 0.853 and 0.581 |
| Refinement method | Full-matrix least-squares on F ² |
| Data / restraints / parameters | 3820 / 0 / 264 |
| Goodness-of-fit on F ² | 1.052 |
| Final R indices [I > 2σ(I)] | R1 = 0.0991, wR2 = 0.2477 |
| R indices (all data) | R1 = 0.1280, wR2 = 0.2690 |
| Largest diff. peak and hole | 2.219 and -2.715 e. Å ⁻³ |

2.2.7 References

- ¹ A. A. Sallam, S. Ramasahayam, S. A. Meyer and K. A. El Sayed, *Bioorg. Med. Chem.*, **2010**, *18*, 7446; S. Ortlepp, M. Sjögren, M. Dahlström, H. Weber, R. Ebel, R. Edrada, C. Thoms, P. Schupp, L. Bohlin and P. Proksch, *Mar. Biotech.*, **2007**, *9*, 776; G. M. Nicholas, L. L. Eckman, S. Ray, R. O. Hughes, J. A. Pfefferkorn, S. Barluenga, K. C. Nicolaou and C. A. Bewley, *Bioorg. Med. Chem. Lett.*, **2002**, *12*, 2487; K. C. Nicolaou, R. Hughes, J. A. Pfefferkorn, S. Barluenga and A. J. Roecker, *Chem. Eur. J.*, **2001**, *7*, 4280.
- ² C. A. Lipinski, F. Lombardo, B. W. Dominy and P. J. Feeney, *Adv. Drug. Deliver. Rev.*, **1997**, *23*, 3.
- ³ P. Metrangolo and G. Resnati, *Science*, **2008**, *321*, 981.
- ⁴ P. Auffinger, F. A. Hays, E. Westhof and P. S. Ho, *P. Natl. Acad. Sci. USA*, **2004**, *101*, 16789.
- ⁵ Y. Lu, T. Shi, Y. Wang, H. Yang, X. Yan, X. Luo, H. Jiang and W. Zhu, *J. Med. Chem.*, **2009**, *52*, 2854.
- ⁶ E. I. Howard, R. Sanishvili, R. E. Cachau, A. Mitschler, B. Chevrier, P. Barth, V. Lamour, M. Van Zandt, E. Sibley, C. Bon, D. Moras, T. R. Schneider, A. Joachimiak and A. Podjarny, *Proteins: Struct. Funct. Bioinf.*, **2004**, *55*, 792.
- ⁷ T. M. Beale, R. M. Myers, J. W. Shearman, D. S. Charnock-Jones, J. D. Brenton, F. V. Gergely and S. V. Ley, *Med. Chem. Commun.*, **2010**, *1*, 202.
- ⁸ H. J. Swarts, P. J. M. Teunissen, F. J. M. Verhagen, J. A. Field and J. B. P. A. Wijnberg, *Mycol. Res.*, **1997**, *101*, 372; E. de Jong, A. E. Cazemier, J. A. Field and J. A. M. de Bont, *Appl. Environ. Microbiol.*, **1994**, *60*, 271; E. de Jong, J. A. Field, H-E. Spinnler, J. B. P. A. Wijnberg and J. A. M. de Bont, *Appl. Environ. Microbiol.*, **1994**, *60*, 264.
- ⁹ T. H. Durrans, *J. Chem. Soc., Trans.*, **1923**, *123*, 1424.
- ¹⁰ F. A. Carey and R. J. Sundberg, *Advanced Organic Chemistry Part A: Structure and Mechanisms*, Springer, New York, 2008, pp. 800-802.
- ¹¹ L. M. Stock and A. Himoe, *J. Am. Chem. Soc.*, **1961**, *83*, 4605; M. Zhang and C. R. F. Lund, *J. Phys. Chem. A*, **2002**, *106*, 10294.
- ¹² M. Terasaki and M. Makino, *J. Health Sci.*, **2009**, *55*, 631.

- ¹³ T. Sugiyama, *Bull. Chem. Soc. Jpn.*, **1981**, *54*, 2847; J. Barluenga, J. M. González, M. A. Garcia-Martin, P. J. Campos and G. Asensio, *J. Org. Chem.*, **1993**, *58*, 2058.
- ¹⁴ K. J. Edgar and S. N. Falling, *J. Org. Chem.*, **1990**, *55*, 5287.
- ¹⁵ H. Suzuki, *Org. Synth.*, **1971**, *51*, 94; N.-W. Sy and B. A. Lodge, *Tetrahedron Lett.*, **1989**, *30*, 3769; Y. Noda and M. Kashima, *Tetrahedron Lett.*, **1997**, *38*, 6225;
- ¹⁶ R. H. Seevers and R. E. Counsell, *Chem. Rev.*, **1982**, *82*, 575.
- ¹⁷ M. E. Hart, K. L. Suchland, M. Miyakawa, J. R. Bunzow, D. K. Grandy and T. S. Scanlan, *J. Med. Chem.*, **2006**, *49*, 1101.
- ¹⁸ J. Barluenga, J. M. González, P. J. Campos and G. Asensio, *Angew. Chem. Int. Ed.*, **1985**, *24*, 319.
- ¹⁹ L. Emmanuvel, R. K. Shukla, A. Sudalai, S. Gurunath and S. Sivaram, *Tetrahedron Lett.*, **2006**, *47*, 4793.
- ²⁰ H. N. C. Wong, Z. L. Xu, H. M. Chang and C. M. Lee, *Synthesis*, **1992**, 793.
- ²¹ M. Takahashi, H. Konishi, S. Iida, K. Nakamura, S. Yamamura and S. Nishiyama, *Tetrahedron*, **1999**, *55*, 5295.
- ²² A. A. Taha, *Phytochemistry*, **2000**, *55*, 921.
- ²³ Y. B. Kiran, T. Konakahara and N. Sakal, *Synthesis*, **2008**, 2327.
- ²⁴ J. H. Wilkinson, L. F. Wiggins, D. J. C. Wood, F. Bell, I. F. B. Smyth, C. E. Dalgliesh, R. J. W. Le Fèvre and J. Northcott, *J. Chem. Soc.*, **1949**, 2370.
- ²⁵ H. Hoshina, H. Tsuru, K. Kubo, T. Igarashi and T. Sakurai, *Heterocycles*, **2000**, *53*, 2261.
- ²⁶ P. Busca, F. Paradisi, E. Moynihan, A. R. Maguire and P. C. Engel, *Org. Biomol. Chem.*, **2004**, *2*, 2684.
- ²⁷ T. Shiba and H. J. Cahnmann, *J. Org. Chem.*, **1964**, *29*, 3061.
- ²⁸ R. I. Meltzer and J. R. Stanaback, *J. Org. Chem.*, **1961**, *26*, 1977.
- ²⁹ I. Kamiya, S. Murata and K. Yamabe, *Bull. Chem. Soc. Jpn.*, **1984**, *57*, 1740.
- ³⁰ S. Ortlepp, M. Sjögren, M. Dahlström, H. Weber, R. Ebel, R. Edrada, C. Thoms, P. Schupp, L. Bohlin and P. Proksch, *Mar. Biotech.*, **2007**, *9*, 776.
- ³¹ R. Mechoulam and A. Hirshfeld, *Tetrahedron*, **1967**, *23*, 239

CHAPTER 3

Total Syntheses of Subereamollines A and B

Compound Numbering

In this chapter, the numbering of the carbon atoms in subereamolline A and B is based on the convention outlined by Abou-Shoer and co-workers (Figure 27).¹

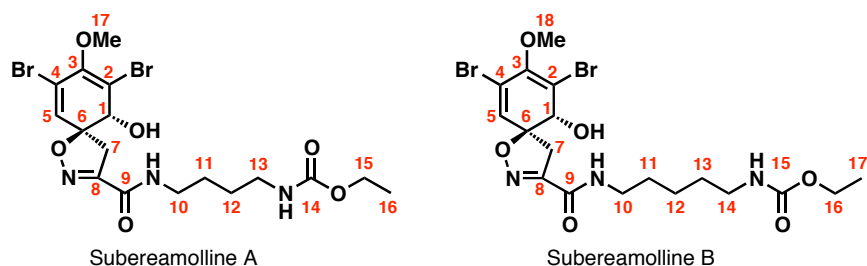


Figure 27 Atom labeling of subereamolline A and B.

Stereochemistry

Throughout this chapter, absolute stereochemistry is represented by bold and hashed wedged bonds; bold and hashed bar bonds represent relative stereochemistry; wavy bonds are used for cases where the relative stereochemistry is unknown.

3.1 Spirocyclohexadienylisoxazoline Bromotyrosine

Derivatives

3.1.1 Structure

Bromotyrosine derivatives in this class are characterised by their signature asymmetric spirocyclohexadienylisoxazoline (SHI) motif. Aerothionin (**1**), the first member of this class to be discovered, was optically active ($[\alpha]_D +252^\circ$) and contained two SHI units connected by a four-carbon chain linker (Figure 28).² The relative stereochemistry between the C-1 hydroxyl group and the oxygen in the isoxazoline ring of the SHI moiety was assumed to be *trans* by analogy with (+)-aerophysinin-1 (**2**).³ However, it took another ten years to unravel the absolute configuration since crystals of **1** were unstable to X-rays. Using circular dichroism* to verify the crystallographic analysis solved this problem.⁴

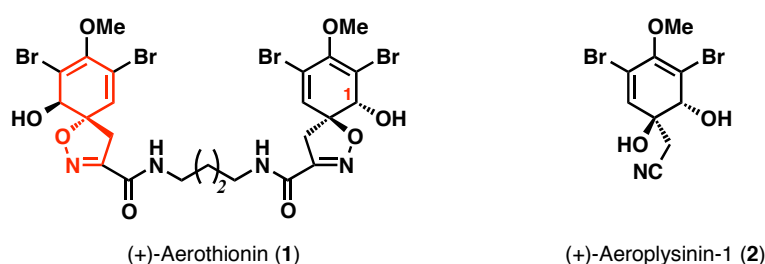
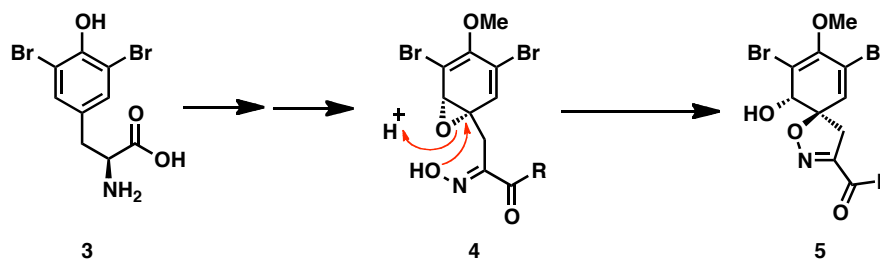


Figure 28 Structure of (+)-aerothionin (**1**) and (+)-aerophysinin-1 (**2**). The SHI motif is highlighted in red.

As alluded to in Section 1.3.2, the relative stereochemistry between C-1 and C-6 (*trans*) is conserved amongst all compounds in this class as a consequence of their biosynthesis. The arene oxide **4**, derived from dibromotyrosine (**3**), undergoes intramolecular nucleophilic attack from the hydroxyl group of the oxime to construct the SHI motif in **5** (Scheme 28).⁵ The stereospecific nature of this epoxide opening leads to the observed *trans* relative configuration.



Scheme 28 Proposed biosynthesis of the SHI motif.

* The SHI motif has a distinctive CD spectra resulting from the helicity imparted by skewed diene and the *trans* relationship of the oxygens.

In a peculiarity that is not frequently observed in nature, this arene oxide biosynthetic pathway can produce both enantioforms of the SHI motif, depending on the genera of sponge. For example, purealidin J (**6**) and pseudoceratinine A (**7**) are enantiomers of one another and were isolated from *Psammaphysilla purpurea*⁶ and *Pseudoceratina verrucosa*,⁷ respectively (Figure 29). The reason why both enantiomers are biosynthesised is not known, however, derivatives possessing the same SHI motif as **6** appear to be much more abundant in nature.⁸ Since these isoxazoline derivatives are believed to be precursors for aeropylsinin-1 (**2**) (Section 1.3.3) one could hypothesise that enzymatic degradation of the more common enantioform, would lead to the more biologically relevant enantiomer of **2**. Indeed, under the proposed degradative pathway (Scheme 4) derivatives containing the same SHI motif as **6** would give (+)-**2**.

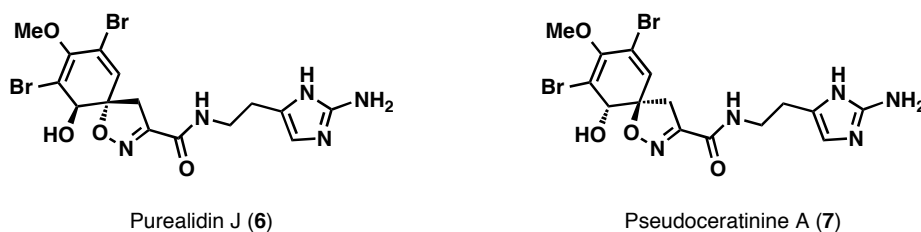


Figure 29 Structures of purealidin J (**6**) and pseudoceratinine A (**7**).

The structural similarities shared between bromotyrosine isoxazolines means that comparison of NMR spectra, optical rotations and CD spectra is often used to aid the structural elucidation of new derivatives. Despite this, mistakes can still be made and this is typified by the case of zamamistatin (Figure 30). Isolated by Uemura and co-workers, zamamistatin was optically active ($[\alpha]_D +248^\circ$) and its ESIMS exhibited 1:4:6:4:1 quintet ion peak at m/z 697, 699, 701, 703 and 705, indicating the presence of four bromine atoms. In combination with NMR data, the natural product was determined to be a symmetrical dimer with the unprecedented structure **8**.⁹

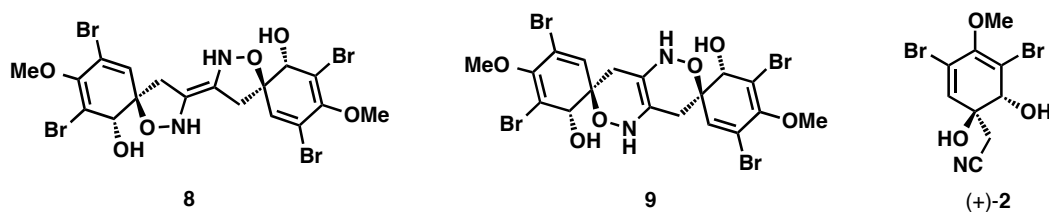


Figure 30 Proposed structures of zamamistatin (**8** and **9**) along with the actual structure (**2**).

In 2006, Kigoshi and co-workers re-isolated zamamistatin and revised the structure to **9**, based on the NMR spectra of synthetic models.¹⁰ Later, they discovered the IR spectra indicated the presence of a nitrile (2258 cm^{-1}) and closer inspection of the

ESIMS revealed the presence of a triplet ion peak at m/z 361.9 (initially thought to be $[M/2+Na]^+$) along with the quintet peak (at a concentration of 15 μ M).¹¹ However, running the same sample at a lower concentration (0.15 μ M) caused the larger, quintet ion peak to disappear. Based on these observations, zamamistatin was actually determined to be (+)-aeroplysinin-1 (**2**). Once again, this example emphasises the value of total synthesis in being able to confirm or invalidate the proposed structures of new natural products.

3.1.2 Biological Activity

The bioactivity profile exhibited by this class of products is less diverse than their oxime counterparts. To account for this observation, it is theorised that these isoxazoline metabolites serve as pro-toxins that are enzymatically degraded to give more active compounds; the evidence for this theory was reviewed in Section 1.3.3. However, the metabolic expenditure required to biosynthesise these parent compounds—over 60 have been isolated to date—would suggest they also have a protective role. In fact, some of these derivatives have been shown to exhibit cytotoxic activities in cancer cell lines.

11-Oxo-aerotherionin (**10**) (Figure 31) showed selective cytotoxicity against HCT 116 (colon cancer) cells over a range of 120 nM to 1.2 μ M.¹² Fistularin-3 (**13**), whose stereochemistry at C-10 and C-18 has not been established, inhibited cell growth in epidermoid, prostate and leukaemia cell lines (IC₅₀ 3.6, 3.8 and 1.2 μ M, respectively).¹³ Araplysillin-1 (**11**), araplysillin-2 (not shown), purealidin S (**15**) and purealidin Q (**14**) were cytotoxic against ovarian tumour A2780 (EC₅₀ 18.6, 14.8, 7.4 and 2.5 μ M, respectively) and leukaemia K562 cell lines (EC₅₀ 28, 43, 6.0 and 1.5 μ M, respectively).¹⁴ In a separate study, **14** along with purealidin P (**12**) proved to be cytotoxic against murine lymphoma K1210 (EC₅₀ 1.3 and 3.9 μ M, respectively) and human epidermal carcinoma KB (nasopharynx) (EC₅₀ 1.6 and 10.6 μ M, respectively) cell lines.⁶

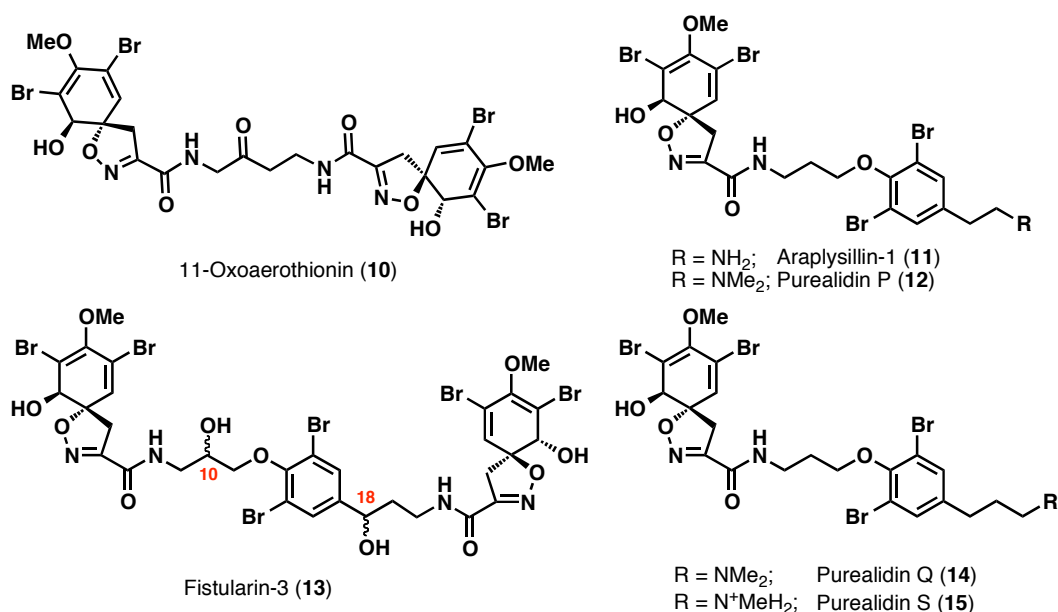


Figure 31 Structures of cytotoxic bromotyrosine-derived isoxazolines.

3.2 Subereamollines A and B

3.2.1 Isolation and Biological Activity

The isolation of subereamollines A (**16**) and B (**17**) (Figure 32) was reported by Abou-Shoer and co-workers in 2008 following the reinvestigation of the crude extract from the Red Sea sponge *Suberea mollis*.¹ Owing to the small quantities isolated (4.9 mg of **16** and 2.0 mg of **17**), investigation into their biological properties was limited. Neither **16** nor **17** exhibited antioxidant activity, however, **16** was found to possess modest antimicrobial activity against *Staphylococcus aureus* (3 mm inhibition zone at a concentration of 3 mg/mL). Furthermore, it was not reported if their cytotoxic activities had been investigated and as a result, the subereamollines were attractive synthetic targets since they are structurally related to the cytotoxic isoxazoline natural products shown in Figure 31.

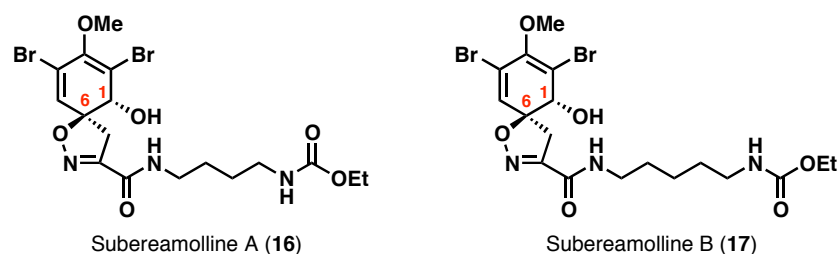


Figure 32 Subereamollines A (**16**) and (**17**).

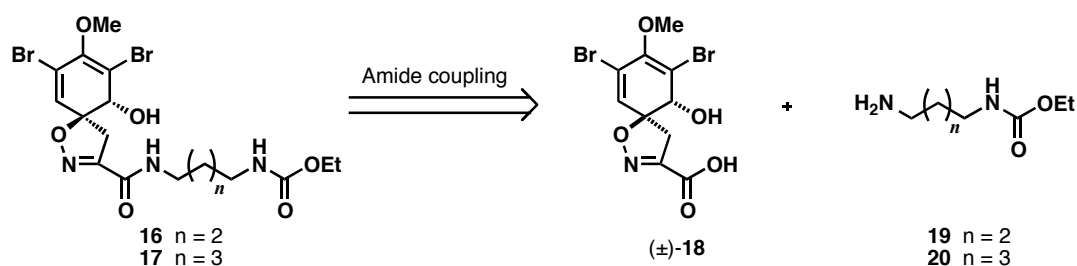
In terms of structure, both **16** and **17** contain a 2,4-dibromo-1-hydroxy-3-methoxyspirocyclohexadienylisoxazole moiety attached to a linear carbamate

containing side chain *via* an amide linkage. Although not explicitly stated in the isolation paper, the absolute stereochemistries at C-1 and C-6 were determined to be (*R*) and (*S*) based on the optical rotations of **16** $\{[\alpha]_{\text{D}} +156.5$ (*c* 0.55, MeOH) $\}$ and **17** $\{[\alpha]_{\text{D}} +22.9$ (*c* 6.25, CH₂Cl₂) $\}$. These optical rotations correlated with (+)-aerotherionin (**1**) $\{[\alpha]_{\text{D}} +210$ (*c* 1.7, MeOH) $\}$ (Figure 28).⁴

In addition to achieving the total syntheses of **16** and **17**, it was also our aim to develop a strategy that incorporated a method for obtaining both enantiomers of the natural products in excellent enantiopurity. This was desirable for two reasons: firstly, it would be possible to investigate whether any observed bioactivity was dependent on the stereochemistry of the SHI motif; secondly, it is more than likely that the “unnatural” enantiomer is also produced in nature given the occurrence of **6** and **7** (Figure 29).

3.2.2 Synthetic Strategy

The total syntheses of natural products from the same SHI class of bromotyrosine-derivatives as **16** and **17** have previously been reported in the literature.¹⁵ The universal strategy in synthesising these molecules has involved coupling the SHI motif to the appropriate side chain to form the key amide bond. Therefore, in a similar strategy, it was envisaged that **16** and **17** could be accessed from coupling the spiroisoxazoline acid (\pm)-**18** with amine **19** or **20**, respectively (Scheme 29).



Scheme 29 Retrosynthetic analysis of **16** and **17**.

Interestingly, (–)-**18** has been isolated from the marine sponge *Pseudoceratina* sp. as an optically pure isomer with its absolute configuration defined as 1*S*,6*R* by CD analysis.¹⁶ To date, only Day and co-workers have reported the synthesis of (\pm)-**18**, and, while it was successfully employed as an intermediate in their synthesis of purealin, the DCC/HOBt mediated amidation only proceeded in 54%.¹⁷ Nevertheless, this was a significant improvement on the prior art since amidation reactions had previously been performed directly on the methyl ester **21** (Figure 33).¹⁵

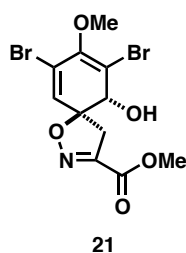
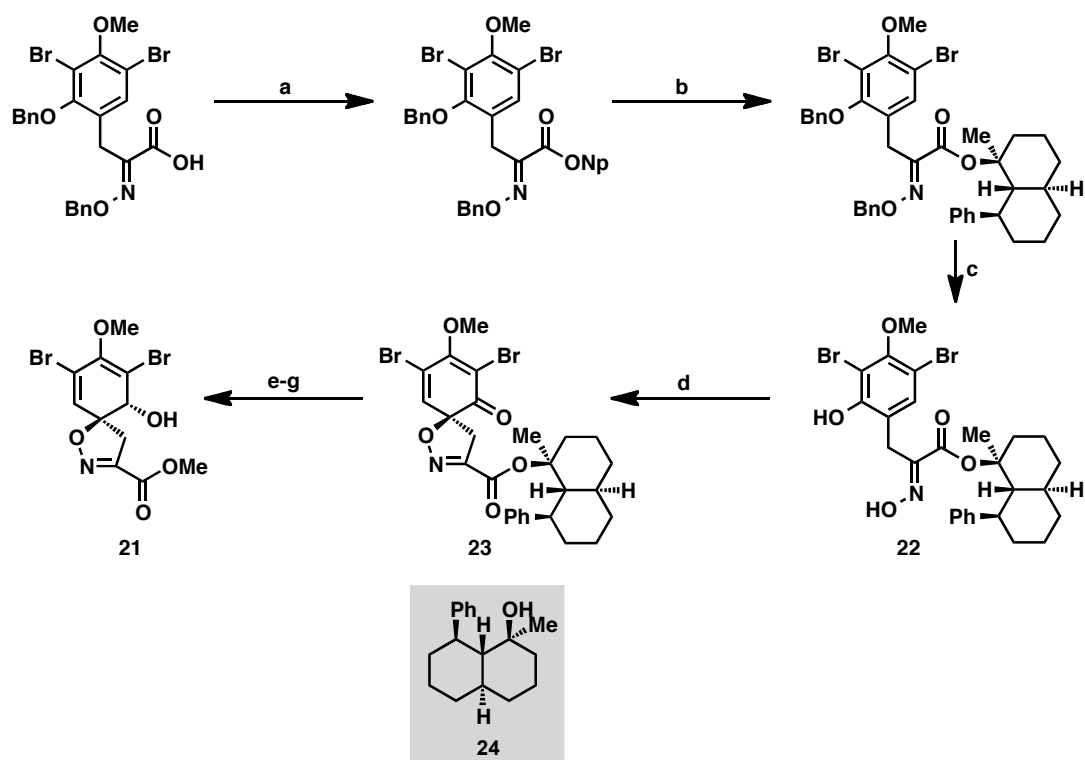


Figure 33 Structure of methyl ester **21**.

Hoshino and co-workers achieved the first synthesis of optically active **21** by developing an asymmetric oxidative spirocyclisation which employed a chiral auxiliary (**24**) derived from a phenyl decalol (Scheme 30).¹⁸ Spirocyclisation of oxime ester **22** upon treatment with PhIO and CSA furnished **23** in a yield of 83% and a diastereomeric excess of between 70–80% as determined by ¹H NMR analysis. Following removal of the chiral auxiliary with TFA and conversion of the resulting acid to the methyl ester, diastereoselective reduction of the ketone using Zn(BH₄)₂ furnished the desired, optically enriched, methyl ester **21**. Whilst this represented the first asymmetric synthesis of this SHI structural motif, the method required a multi-step synthesis of the chiral auxiliary and only delivered the final product in moderate enantiopurity (84% *ee*).

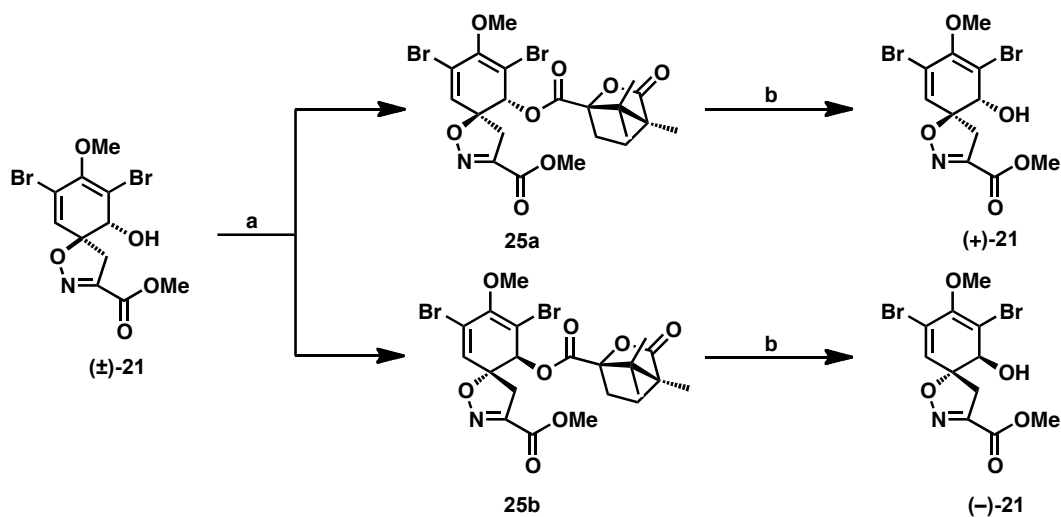
In an alternative approach developed by Nishiyama and co-workers, a racemic mixture of **21** was resolved by derivatisation with (–)-camphanic chloride to give the corresponding diastereomeric camphanate esters **25a** and **25b**, which could then be separated by silica gel chromatography. Subsequent methanolysis provided enantiopure (+)- and (–)-**21**, which were used to achieve the first syntheses of optically pure (+)- and (–)-aerOTHIONIN (**1**).¹⁹

After assessing the merits of these two methods it was clear that the stereoselective spirocyclisation was not viable for our purpose. Despite the fact that resolution can deliver enantiopure material, we also wanted to investigate an alternative method for separation of the racemic products which would avoid the need for additional synthetic manipulations. Therefore, it was decided to investigate the possibility of separating the natural product racemates themselves either by resolution or preparative chiral HPLC. Furthermore, we envisaged that a combination of these methods would enable the absolute configuration at C-1 and C-6 to be unambiguously assigned.



Scheme 30 Hoshino synthesis of optically active **21**.

Reagents and conditions: (a) *p*-nitrophenol, DCC, CH₂Cl₂, 91%; (b) **24**, MeLi, HMPA, PhMe, 0 °C, 85%; (c) H₂, Pd-black, AcOH/1,4-dioxane (1:1), 90%; (d) PhIO, CSA, CH₂Cl₂, -78 °C, 83%, (70-80% *de*); (e) TFA, CH₂Cl₂, 0 °C; (f) DCC, DMAP, MeOH, CH₂Cl₂, 71% over 2 steps, 84% *ee* after recrystallisation; (g) Zn(BH₄)₂, CH₂Cl₂/Et₂O (3:2).



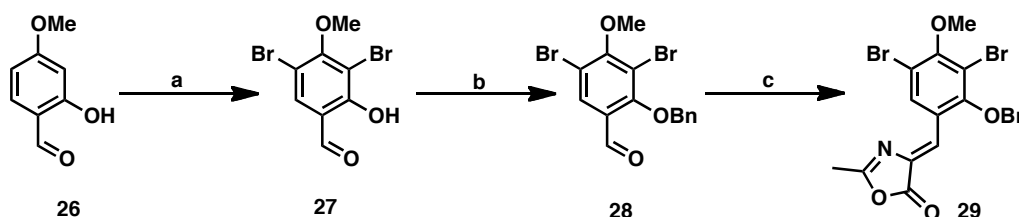
Scheme 31 Nishiyama synthesis of optically pure **21**.

Reagents and conditions: (a) (-)-camphanic chloride, py, CH₂Cl₂, **25a**, 46%; **25b**, 47%; (b) K₂CO₃, MeOH, (+)-**21** quant, (-)-**21** quant.

3.3 Results and Discussion

3.3.1 Synthesis of Spiroisoxazoline Acid 18

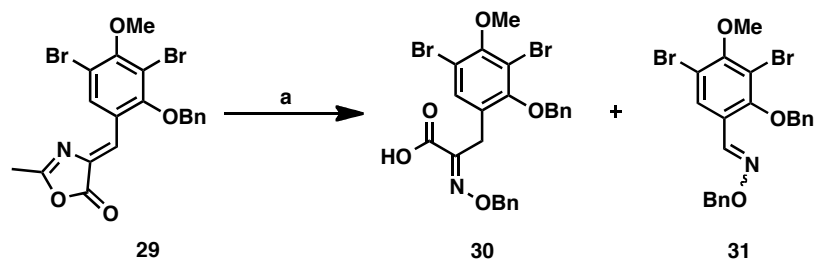
Beginning with the commercially available 2-hydroxy-4-methoxybenzaldehyde (**26**), bromination with *N*-bromosuccinimide afforded **27**. Subsequent benzyl protection of the phenol furnished aldehyde **28** in 92% yield over 2 steps (Scheme 32). This was then converted into the corresponding azlactone **29** by heating with *N*-acetylglycine and sodium acetate in the presence of acetic anhydride (Erlenmeyer conditions).²⁰



Scheme 32 Synthesis of azlactone **29**.

Reagents and conditions: (a) NBS, DMF, 0 °C, 50 min, 93%; (b) BnCl, NaI, K₂CO₃, DMF, rt, 13 h, 99%; (c) *N*-acetylglycine, NaOAc, Ac₂O, 120 °C, 6 h, 90%.

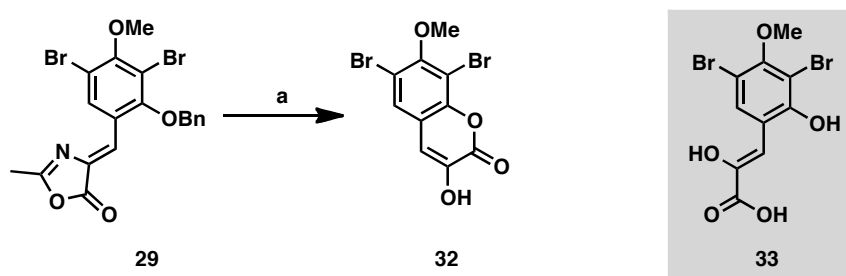
Saponification of the crude azlactone (**29**) with barium hydroxide and subsequent condensation with *O*-benzylhydroxylamine furnished the carboxylic acid **30** which could be isolated by trituration from hexane and diethyl ether. As mentioned in Section 2.1.4.1, the modest yield of 49% is common for transformations of this nature and likewise, could not be improved upon even when **29** had been either recrystallised or purified by flash chromatography. Furthermore, following trituration TLC analysis showed numerous by-products in the mother liquor. The major by-product was isolated by chromatography and discovered to be oxime **31** (22%). It is postulated that this may have arisen from the hydrolysis of **29** back to its parent aldehyde (**28**), under the basic conditions, and subsequent condensation with the *O*-benzylhydroxylamine.

Scheme 33 Saponification of **29**.

Reagents and conditions: (a) Ba(OH)₂·8H₂O, 1,4-dioxane/H₂O (1:1), 60 °C, 1 h then *O*-benzylhydroxylamine, 16 h, **30**, 49%; **31**, 22%

As mentioned in Chapter 2, azlactones are known to hydrolyse efficiently under acidic conditions²¹ to give phenylpyruvic acid derivatives which can then be converted to their corresponding oxime acids.²² When azlactone **29** was subjected to the hydrolysis conditions (3 *N* HCl, reflux), ¹H and ¹³C NMR analysis of the product showed that in addition to the hydrolysis of the azlactone, debenzylation of the phenolic oxygen had also occurred. This led us to suspect the product was the phenylpyruvic acid **33** (Scheme 34).

Fortunately, it was possible to crystallise the product from diethyl ether and X-ray crystallographic analysis revealed the structure to be the known enol coumarin **32** (Figure 34).[†] Therefore, it is believed that under the reaction conditions **33** undergoes acid catalysed lactonisation to produce **32**. Since sufficient quantities of **30** were obtained from the method described in Scheme 33, the use of an alternative phenolic protecting group was not investigated.

Scheme 34 Formation of coumarin **32**.

Reagents and conditions: (a) 3 *N* HCl, reflux, 24 h, 68%.

[†] This coumarin had previously been synthesised by Spilling and co-workers and used as an intermediate in the synthesis of purealidin N (*J. Org. Chem.* **2005**, 70, 6398).

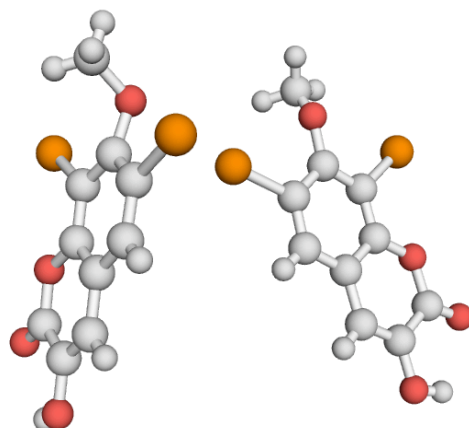
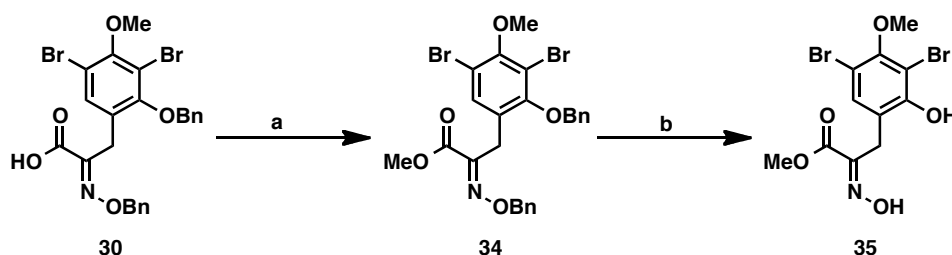


Figure 34 X-ray crystal structure of coumarin **32**.

The oxidative cyclisation precursor, oxime methyl ester **35**, could be obtained in two steps from **30**. Firstly, treatment of **30** with trimethylsilyldiazomethane gave the corresponding methyl ester **34** (Scheme 35). Subsequently, the benzyl groups were removed *via* hydrogenolysis over palladium black to furnish the cyclisation precursor **35**.



Scheme 35 Synthesis of cyclisation precursor **35**.

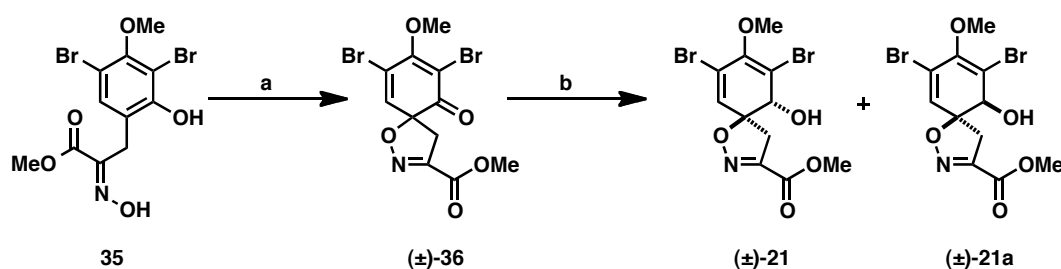
Reagents and conditions: (a) TMSCHN₂, PhMe/MeOH (3:1), 0 °C to rt, 1 h, 95%; (b) Pd-black, H₂, 1,4-dioxane/AcOH (1:1), rt, 3 h, 92%

Several conditions known to affect the oxidative cyclisation of oxime **35** to the spiroisoxazoline (±)-**36** have been reported in the literature. Nishiyama and co-workers found that treatment of **35** with thallium(III) trifluoroacetate furnished **36** in 27% yield whilst other oxidizing agents including bromine and 2,4,4,6-tetrabromo-2,5-cyclohexadien-1-one were ineffective.²³ To circumvent the toxicity issues associated with thallium salts, they subsequently developed an electroorganic oxidation whereby subjecting **35** to constant potential electrolysis[‡] in the presence of tetrabutylammonium perchlorate furnished **36** in 68% yield.²⁴ For this transformation, *N*-bromosuccinimide²⁵ and iodobenzene diacetate²⁶ mediated cyclisations have also

[‡] Electrolysis in which a constant voltage is applied.

been reported and, from a synthesis perspective, were the most appealing due to their practicality, low toxicity and good yields. Furthermore, since **36** is unstable to silica gel chromatography,²⁵ a procedure that gave the crude material in good purity following a standard aqueous work-up was desirable. In our hands, iodobenzene diacetate proved to be the reagent of choice (Scheme 36).[§] Spilling and co-workers reported the use of PS-iodobenzene diacetate to affect the same transformation in quantitative yield.²⁷ Unfortunately, this reagent was not readily accessible and the use of a commercially available PS-4-hydroxyiodobenzene diacetate gave no conversion.

Following work-up the crude mixture was taken on directly to the next step where diastereoselective reduction of (\pm)-**36** with $\text{Zn}(\text{BH}_4)_2$ ²⁸ furnished the desired *trans*-isomer (\pm)-**21** and the undesired *cis*-isomer (\pm)-**21a** in diastereomeric ratio of 2.03:1 (by ^1H NMR). Purification of the crude mixture gave (\pm)-**21** and (\pm)-**21a** in a yield of 32% and 16%, respectively, over 2 steps from oxime **35**.



Scheme 36 Oxidative cyclisation of **35** and subsequent reduction.

Reagents and conditions: (a) $\text{PhI}(\text{OAc})_2$, MeCN, 0 °C, 1 h; (b) $\text{Zn}(\text{BH}_4)_2$, CH_2Cl_2 , rt, 10 min, (\pm)-**21**, 32% from **35**; (\pm)-**21a**, 16% from **35**.

At this point, we were able to obtain X-ray quality crystals of (\pm)-**21** and (\pm)-**21a** by slow evaporation from diethyl ether to confirm the relative stereochemistry of each isomer (Figure 35). It is worth mentioning that previously the relative stereochemistries of (\pm)-**21** and (\pm)-**21a** had originally been established by comparison of their ^1H NMR spectra with those of aerothionin (**1**) and *cis,cis*-aerothionin.²⁹

[§] Removal of the succinimide by-product from the NBS-mediated cyclisation proved to be laborious.

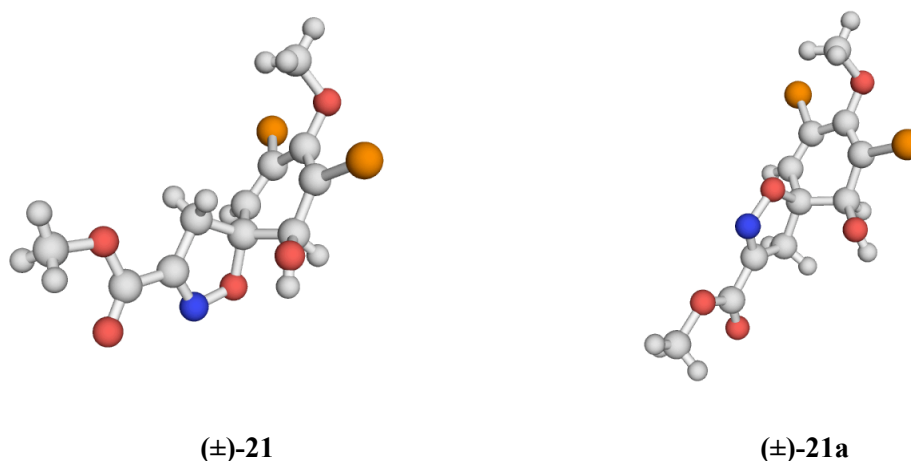
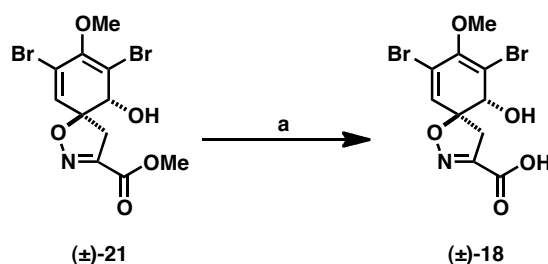


Figure 35 X-ray crystal structures of (±)-21 and (±)-21a.

The methyl ester of (±)-21 was then saponified with lithium hydroxide to furnish spiroisoxazoline acid (±)-18 in an overall yield of 11% in 9 steps from the commercially available aldehyde 26 (Scheme 37).

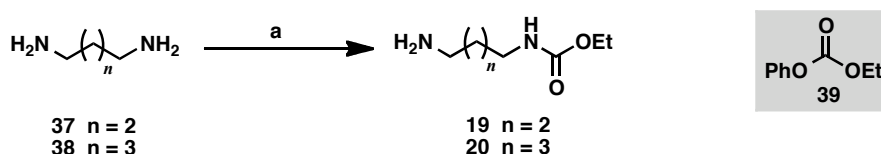


Scheme 37 Saponification of methyl ester (±)-21.

Reagents and conditions: (a) LiOH·H₂O, MeOH/H₂O (3:1), rt, 1 h, 99%.

3.3.2 Synthesis of Amines 19 and 20

The amine coupling partners could be synthesised in one step from the commercially available diamines putrescine (37) and cadaverine (38). Addition of the carbamylating agent ethyl phenyl carbonate (39)³⁰ in EtOH to 37 and 38 minimised *bis*-carbamylation and furnished the amine coupling partners 19 and 20 in 80% and 82% yield, respectively (Scheme 38).

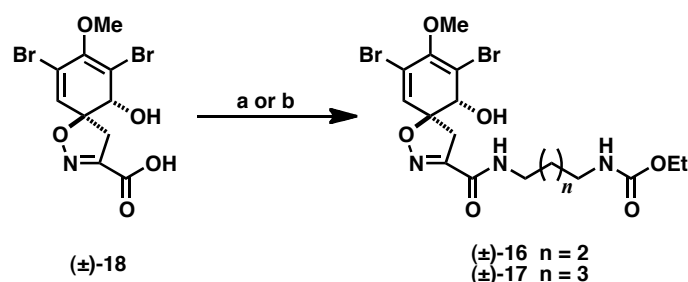


Scheme 38 Synthesis of amine coupling partners.

Reagents and conditions: (a) 39, EtOH, rt, 12 h, 19, 80%; 20, 82%.

3.3.3 Synthesis of Subereamollines A and B

With both the acid and amine coupling partners in hand, the syntheses of (±)-**16** and (±)-**17** could be realised. The spiroisoxazoline (±)-**18** was coupled to amines **19** and **20** in the presence of DCC and HOBT to afford the natural products (±)-subereamolline A (**16**) and B (**17**), respectively, in 91% and 75% yield (Scheme 39). Despite giving the natural products in good yield the use of DCC as coupling agent was far from ideal since careful chromatography was required to remove the dicyclohexylurea (DCU) by-product.



Scheme 39 Synthesis of (±)-**16** and (±)-**17**.

Reagents and conditions: (a) DCC, HOBT, amine **19** or **20**, *i*Pr₂EtN, CH₂Cl₂, rt, 18h, (±)-**16**, 91%; (±)-**17**, 75%; (b) [®]T3P, amine **19** or **20**, *i*Pr₂EtN, CH₂Cl₂, 0 °C, 2 h, (±)-**16**, 96%; (±)-**17**, 97%.

Upon reinvestigation of this coupling step, it was found that the coupling agent [®]T3P furnished **16** and **17** in 96% and 97% yields, respectively. In addition, purification was simplified by the fact that the polyphosphate by-product could be extracted from the product during an aqueous work-up.

The ¹H and ¹³C NMR spectra of synthetic **16** and **17** matched those of the natural materials (see Appendix).¹ We have also established that the originally reported ¹³C chemical shift assignments of C-2 (δ_C 122.9 ppm) and C-4 (δ_C 114.3 ppm) should be switched on the basis of COLOC NMR experiments reported for related spirocyclised products.³¹ This is also supported by the HMBC correlations in the natural products (Figure 36).

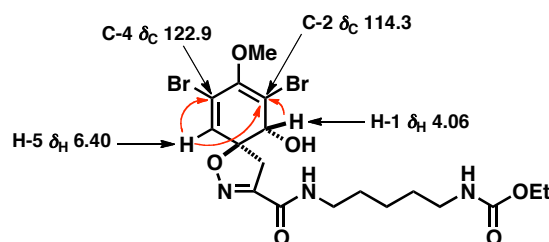
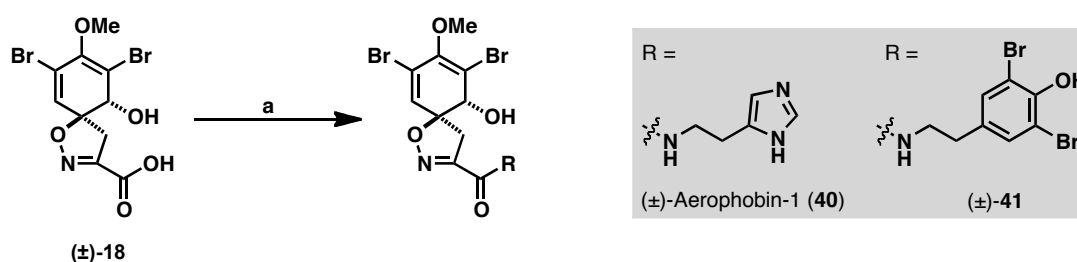


Figure 36 ^1H ^{13}C HMBC correlations for subereamolline B (**17**).

In the HMBC spectra of the natural and synthetic samples of **16** and **17**, the quaternary carbon (δ_{C} 114.3 ppm) couples strongly to the protons H-1 (δ_{H} 4.07 and 4.06 ppm, respectively) and H-5 (δ_{H} 6.42 and 6.40 ppm, respectively). However, the quaternary carbon (δ_{C} 122.9 ppm) only couples to H-5. Therefore the original assignments for C-2 (δ_{C} 122.9 ppm) and C-4 (δ_{C} 114.3 ppm) proposed by Abou-Shoer and co-workers should be reversed.

3.3.4 Side Chain Variations

In a continuation of our studies on the oxime-type bromotyrosine derivatives, we sought to append the (5)-bromoverongamine and JBIR-44 side chains to the spiro acid (\pm)-**18**. These spirocyclised analogues (**40** and **41**) would provide additional insight into the biological importance of the oxime functionality in these compounds.** Accordingly, (\pm)-**18** was coupled to histamine dihydrochloride and 3,5-dibromotyramine hydrobromide with $^{\text{®}}$ T3P to give (\pm)-aerophobin-1 (**40**) and (\pm)-**41**,^{††} respectively (Scheme 40). Multiple attempts to improve the low yields were unsuccessful but sufficient quantities for screening could still be obtained by this method.



Scheme 40 Synthesis of (\pm)-aerophobin-1 (**40**) and (\pm)-**41**.

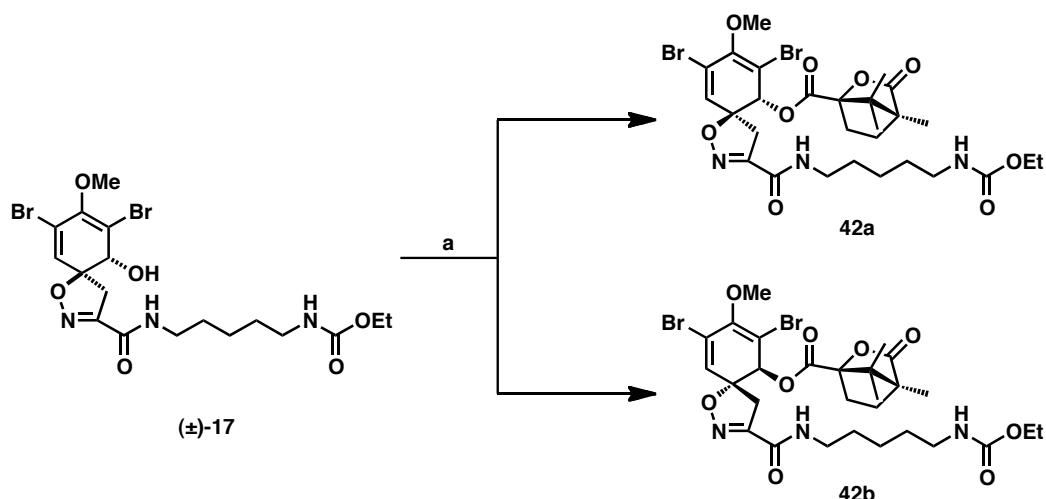
Reagents and conditions: (a) $^{\text{®}}$ T3P, amine, $i\text{Pr}_2\text{EtN}$, CH_2Cl_2 , 0 $^\circ\text{C}$, 2 h, (\pm)-**40**, 20%; (\pm)-**41**, 11%.

** The presence of the C-1 hydroxyl means that **40** and **41** are not direct spirocyclised analogues of (5)-bromoverongamine and JBIR-44.

^{††} Although this compound has not yet been isolated from a natural source, we hypothesise that **41** is a naturally occurring bromotyrosine-derivative given its structural similarity to **11**, **12**, **14**, and **15**.

3.3.5 Separation of Racemic Subereamollines A and B

With the natural products in hand, we then wanted to investigate how best to separate the racemates. In our first attempt, (\pm)-**17** could be derivatised with (–)-camphanic chloride;^{‡‡} however, all efforts to separate the respective diastereoisomers **42a** and **42b** by normal-phase chromatography were in vain (Scheme 41). The use of other chiral derivatising agents was not explored since this had been previously investigated for the separation of (\pm)-**21** by Nishiyama and co-workers¹⁹



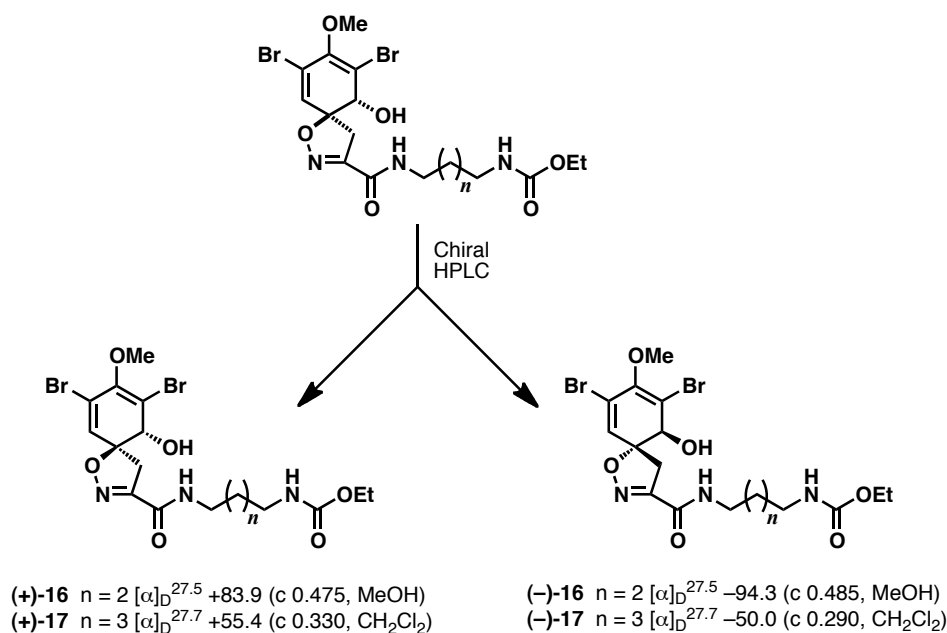
Scheme 41 Derivatisation of (\pm)-**17** with (–)-camphanic chloride.

Reagents and conditions: (a) (–)-camphanic chloride, DMAP, CH₂Cl₂, 0 °C to rt, 6 h.

Pleasingly, the enantiomeric forms of (\pm)-**16** and (\pm)-**17** were separated using preparative chiral HPLC (CHIRALPAK AD-H column and 10% *i*PrOH in hexane at a flow rate of 5 mL/min) (Scheme 42). In both cases, the first compound to elute was the naturally occurring enantiomer. The optical rotations of (+)-**16** (R_t = 40.3 min) and (+)-**17** (R_t = 48.3 min) agreed with those observed for natural **16** and **17**.^{§§} To our knowledge this is the first reported use of chiral HPLC to separate compounds in this class of natural products. Furthermore, this method could deliver the quantities of enantiopure material required for the cytotoxicity testing.

^{‡‡} Due to the complex nature of the ¹H and ¹³C NMR spectra, this was confirmed by HRMS.

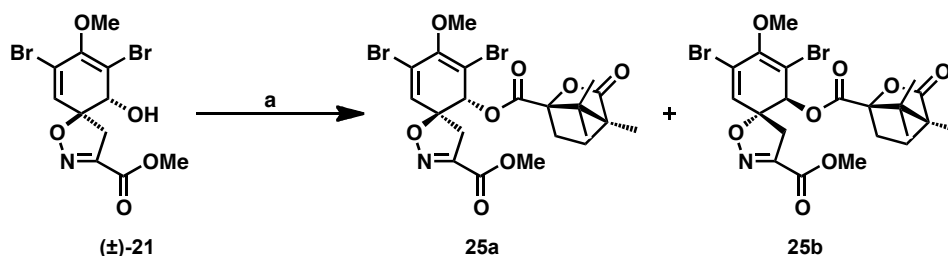
^{§§} The optical rotation for (+)-**17** reported by Abou-Shoer and co-workers was [α]_D +22.9 (c 6.25, CH₂Cl₂). Due to the fact that only 2.0 mg were isolated, we believe there was a typographical error in the reported concentration.



Scheme 42 Preparative chiral HPLC separations of (±)-**16** and (±)-**17**.

3.3.6 Confirmation of the Absolute Stereochemistries at C-1 and C-6

In order to confirm the absolute stereochemistries at C-1 and C-6 it was necessary to synthesise the natural products from an optically pure intermediate whose absolute configuration was known. As discussed in Section 3.2.2, Nishiyama reported the synthesis of the enantiomeric forms of methyl ester **21** by resolution with (–)-camphanic chloride (Scheme 31). Furthermore, in this research the absolute stereostructures of the spiroisoxazolines (+)- and (–)-**21** were unambiguously assigned.^{***} Therefore, we initially adopted this method to access (+)- and (–)-**21**. Racemic methyl ester **21** could be coupled to (–)-camphanic chloride in the presence of DMAP to give, as expected, a 1:1 diastereomeric mixture of **25a** and **25b** by ¹H NMR (Scheme 43).



Scheme 43 Derivatisation of (±)-**21**.

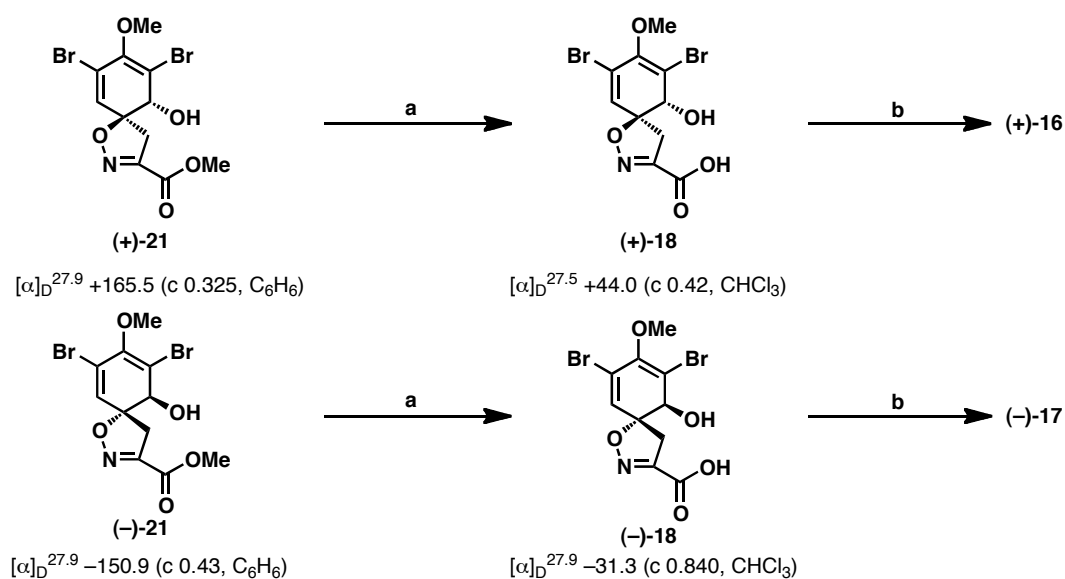
Reagents and conditions: (a) (–)-camphanic chloride, DMAP, CH₂Cl₂, 0 °C to rt, 6 h.

^{***} This was achieved by using both enantiomers to synthesise (+)- and (–)-aeroplysinin-1 (**2**), the absolute configurations of which had previously been determined by X-ray crystallography.

The diastereoisomers **25a** and **25b** were reported to be “easily separable” by silica gel chromatography although the eluting conditions were not described. A screen of solvent systems found that, by analytical TLC, two elutions with CH₂Cl₂/EtOAc (99:1) gave visible separation of **25a** (*R_f* 0.50) and **25b** (*R_f* 0.45). However, attempts to separate these compounds on a synthetically useful scale were unsuccessful as it was not possible to prevent co-elution of the two diastereoisomers.

This problem was circumvented since it was possible to obtain (+)-**21** (*R_t* = 30.9 min) and (–)-**21** (*R_t* = 32.9 min) by chiral HPLC separation of (±)-**21** (CHIRALPAK AD-H column and 4% *i*PrOH in hexane at a flow rate of 5 mL/min). A sample of both (+)-**21** and (–)-**21** was converted to the corresponding camphanate esters (**25a** and **25b**) using the conditions described in Scheme 43. As expected, the ¹H NMR spectra of these derivatives matched those reported in the literature thus confirming the absolute structure of the HPLC material.¹⁹

Saponification of (+)-**21** and (–)-**21** under the conditions described in Scheme 37 furnished the corresponding carboxylic acids (+)-**18** and (–)-**18** (Scheme 44). These were then coupled with amines **19** and **20** and expected to give (+)-**16** and (–)-**17**, respectively. This was confirmed by analytical HPLC (CHIRALPAK AD-H column and 10% *i*PrOH in hexane at a flow rate of 1 mL/min) thus proving the original stereochemical assignments at C-1 and C-6 (see appendix for HPLC traces). Furthermore, this analysis also showed that, saponification of the methyl ester with lithium hydroxide did not erode the stereochemistry.



Scheme 44 Synthesis of (+)-16 and (-)-17 from enantiopure methyl ester.

Reagents and conditions: (a) DCC, HOBT, $i\text{Pr}_2\text{EtN}$, CH_2Cl_2 , rt, 18 h; (b) $\text{LiOH}\cdot\text{H}_2\text{O}$, $\text{MeOH}/\text{H}_2\text{O}$ (3:1), rt, 1 h.

3.3.7 Biological Screening

The racemic and enantiomeric forms of the subereamollines were screened against ovarian (SK-OV-3) and cervical (HeLa) cell lines (Table 8). However, following 48 h treatment, none of the compounds were active up to a concentration of 100 μM . Coumarin **32**, oxime **35**, (\pm)-aerophobin-1 (**40**) and (\pm)-**41** were also inactive against SK-OV-3 cells.

Table 8 MTS assay results for compounds screened against SK-OV-3 and HeLa cells. Drug incubations were for 48 h.

| Cell Line | Compound | | | | | | 32 | 35 | (\pm)- 40 | (\pm)- 41 |
|----------------|----------------------|----------------------|----------------|----------------|----------------|----------------|-----------|-----------|----------------------|----------------------|
| | (\pm)- 16 | (\pm)- 17 | (+)- 16 | (-)- 16 | (+)- 17 | (-)- 17 | | | | |
| SK-OV-3 | N/A | N/A | N/A | N/A | N/A | N/A | N/A | N/A | N/A | N/A |
| HeLa | N/A | N/A | N/A | N/A | N/A | N/A | – | – | – | – |

N/A (not active); – (not tested)

Aerophobin-1 (**40**) has been isolated as a major component from a number of Verongida sponges.³² Interestingly, it was shown to have moderate cytotoxic activity against ovarian A2780 (ID_{50} 45 μM) and leukaemia K562 (ID_{50} 51 μM) cells¹⁴ but was inactive against murine lymphoma L1210 and human epidermoid carcinoma KB cells.⁶

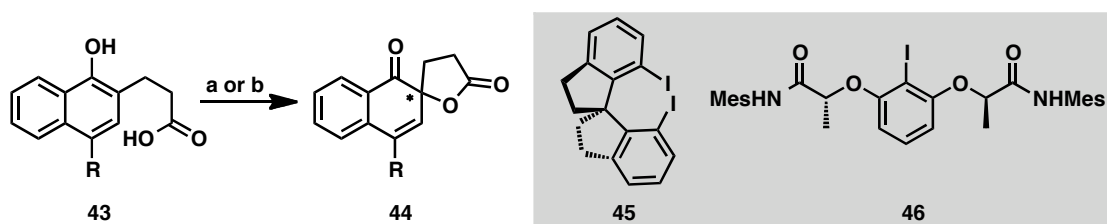
It is perhaps surprising that (\pm)-**41** showed no activity since other SHI products with modified dibromotyramine appendages have exhibited cytotoxicity across a range of cell lines (Section 3.1.2). However, it is apparent that loss of the oxime functionality and aromaticity/planarity in the phenyl ring is unfavourable (*cf.* activity of JBIR-44 in Section 2.1.4.6).

3.4 Conclusion and Future Work

In conclusion, the first total syntheses of the bromotyrosine-derived natural products subereamolline A and B have been achieved and, in addition, the enantiomeric forms of **16** and **17** were obtained by chiral HPLC. This approach not only delivered enantiopure material but also removed the need to for additional synthetic operations and represents a significant improvement upon previous syntheses of products from this class of bromotyrosine derivatives. Furthermore, the absolute stereochemistries at C-1 and C-6 in the naturally occurring enantiomers (+)-**16** and (+)-**17** were confirmed to be *R* and *S*, respectively. Disappointingly, none of the compounds tested were cytotoxic and this may reflect the theory that the SHI class of derivatives serve to act as pro-toxins to more biologically active agents.

A significant challenge which still needs to be addressed in the syntheses of these molecules is the development of a catalytic enantioselective oxidative spirocyclisation of the oxime **35** to the spiroisoxazoline **36**. In the age of organocatalysis, the use of a chiral auxiliary (Scheme 30) is dated and leaves much to be desired. A truly asymmetric cyclisation would not only be more elegant but it would also increase atom efficiency and have the potential to impart greater asymmetric induction. Ideally, the catalyst should be based on a reagent with precedent in being able to efficiently affect the spirocyclisation in a racemic fashion. Of direct relevance to this, the last few years has seen the emergence of catalytic chiral hypervalent iodine precatalysts that rely on co-oxidants for their activation *in situ*.³³ In pioneering work by Kita and co-workers, precatalyst **45** in the presence of *m*CPBA and acetic acid could dearomatise 1-naphthol derivatives (**43**) to their corresponding spirolactones (**44**) in up to 69% *ee*^{†††} (Scheme 45).³⁴ In a continuation of this work, Ishihara and co-workers developed a *C*₂-symmetric chiral iodoarene catalyst (**46**) capable of performing the same transformation in up to 94% yield and 92% *ee*.³⁵

^{†††} When a stoichiometric amount of the corresponding iodine(III) reagent of **46** was used, higher enantioselectivities (up to 86% *ee*) were observed.



Scheme 45 Enantioselective oxidative spirocyclisation.

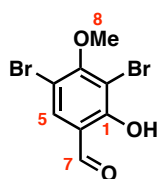
Reagents and conditions: (a) **45** (15 mol%), *m*CPBA, AcOH, up to 70% yield and 69% *ee*; (b) **46** (10–15 mol%), *m*CPBA, up to 94% and 92% *ee*.

In these examples, the catalyst optimisation was carried out on 1-naphthyl derivatives and attempts to perform the spirocyclisation of simple phenol derivatives with the optimised precatalyst **46** proved unsuccessful.³⁵ Furthermore, to our knowledge, the use of chiral hypervalent iodine catalysts to affect the oxidative spirocyclisation of oximes to spiroisoxazolines had not been investigated. Both of these issues need to be addressed and therefore, further investigations exploring the feasibility of this strategy for constructing chiral spiroisoxazolines would be of great value.

3.5 Chemistry: Experimental

General Experimental Details

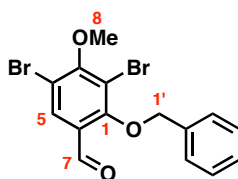
Refer to Section 2.1.6 for general experimental details. In addition, specific optical rotations were recorded on a Perkin-Elmer 343 digital polarimeter using a sodium lamp (589 nm) as the light source. Concentrations (c) are quoted in g per 100 ml. Chiral HPLC was performed on an HP Agilent 1100.

3,5-Dibromo-2-hydroxy-4-methoxybenzaldehyde (27)

To a stirred solution of 2-hydroxy-4-methoxybenzaldehyde (**26**) (8.10 g, 53.2 mmol) in DMF (20 mL) at 0 °C was added *N*-bromosuccinimide (19.0 g, 107 mmol) in DMF (40 mL) dropwise over 30 min. After stirring at 0 °C for a further 20 min Et₂O (600 mL) was added and the mixture was washed with H₂O (500 mL × 2), 10% aqueous Na₂S₂O₃ (400 mL × 3), brine (500 mL), dried, and evaporated to dryness *in vacuo* to furnish **27** (15.3 g, 49.4 mmol, 93%) as a white solid.

R_f 0.32 (10% Et₂O/Petrol); ν_{\max} (thin film)/cm⁻¹ 3052w, 1651s, 1417m, 1289s, 1193s; δ_H (400 MHz, CDCl₃) 11.72 (1H, s, OH), 9.79 (1H, s, H-7), 7.73 (1H, s, H-5), 3.97 (3H, s, H-8); δ_C (100 MHz, CDCl₃) 194.1 (C-7), 161.2 (C-3), 159.5 (C-1), 136.3 (C-5), 118.7 (C-6), 107.9 (C-4), 107.8 (C-2), 61.0 (C-8).

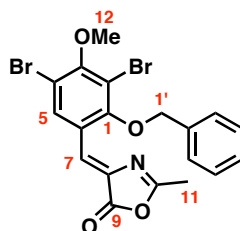
Consistent with literature data.²⁵

2-(Benzyloxy)-3,5-dibromo-4-methoxybenzaldehyde (28)

To a stirred solution of **27** (11.2 g, 36.1 mmol), sodium iodide (5.41 g, 36.1 mmol), anhydrous K_2CO_3 (12.0 g, 86.8 mmol) in DMF (58 mL) was added benzyl chloride (4.18 mL, 36.3 mmol). The mixture was stirred for 13 h before partitioning between H_2O (500 mL) and Et_2O (500 mL). The aqueous phase was extracted with Et_2O (500 mL \times 2) and the combined organic layers were washed with 5% LiCl solution (300 mL \times 2), H_2O (500 mL \times 2), brine (500 mL), dried, and evaporated to dryness *in vacuo* to furnish **27** (14.3 g, 35.7 mmol, 99%) as a white solid.

R_f 0.49 (10% Et_2O /Petrol); ν_{max} (thin film)/ cm^{-1} 1689s, 1577m, 1366s, 1161s; δ_H (400 MHz, $CDCl_3$) 9.94 (1H, s, H-7), 7.99 (1H, s, H-5), 7.40 (5H, m, H-3'/7', H-4'/6' and H-7'), 5.13 (2H, s, H-1'), 3.98 (3H, s, H-8); δ_C (100 MHz, $CDCl_3$) 187.1 (C-7), 160.4 (C-3), 159.3 (C-1), 134.9 (C-2'), 131.6 (C-5), 129.2 (C-4'/6'), 128.91 (C-5'), 128.87 (C-3'/7'), 128.4 (C-6), 115.4 (C-4), 114.5 (C-2), 78.1 (C-1'), 61.0 (C-8); m/z (ESI+) found 420.9044, $[M+Na]^+$ $C_{15}H_{12}Br_2O_3Na$ (^{79}Br) requires 420.9045; m.p. 85-87 $^{\circ}C$ (lit.,³⁶ 91-93 $^{\circ}C$).

Consistent with literature data.³⁶

(Z)-4-(2-(Benzyloxy)-3,5-dibromo-4-methoxybenzylidene)-2-methyloxazol-5(4H)-one (29)

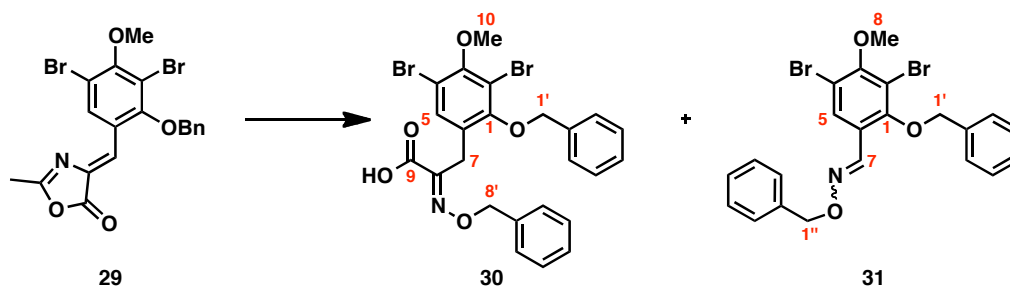
A stirred slurry of **28** (6.40 g, 16.0 mmol), sodium acetate (1.31 g, 16.0 mmol) and *N*-acetylglycine (1.87 g, 16.0 mmol) in acetic anhydride (30 mL, 317 mmol) was heated to 120 °C for 6 h. The reaction mixture was allowed to cool to room temperature and the resulting precipitate isolated by filtration. The filtrand was dissolved in CH₂Cl₂ (200 mL), washed with H₂O (200 mL), dried, and evaporated to dryness *in vacuo* to furnish **29** (6.93 g, 14.4 mmol, 90%) as an orange solid which was used without further purification.

For characterisation purposes, a sample was purified by flash column chromatography (50% CH₂Cl₂/Petrol) to furnish **29** as a bright yellow solid.

R_f 0.65 (20% EtOAc/Petrol); ν_{\max} (thin film)/cm⁻¹ 2944w, 1802s, 1655s, 1599s, 1192s; δ_{H} (400 MHz, CDCl₃) 8.87 (1H, s, H-5), 7.44-7.36 (5H, m, H-3'/7', H-4'/6' and H-7'), 7.23 (1H, s, H-7), 4.99 (2H, s, H-1'), 3.95 (3H, s, H-12), 2.39 (3H, s, H-11); δ_{C} (100 MHz, CDCl₃) 167.0 (C-10), 166.8 (C-9), 157.1 (C-3), 156.4 (C-1), 135.2 (C-2'), 134.7 (C-5), 133.3 (C-8), 128.9 (C-4'/6'), 128.71 (C-5'), 128.69 (C-3'/7'), 126.3 (C-6), 122.7 (C-7), 114.7 (C-4), 113.8 (C-2), 77.3 (C-1'), 60.8 (C-12), 15.6 (C-11); *m/z* (ESI+) found 479.9464, [M+H]⁺ C₁₉H₁₆Br₂NO₄ (⁷⁹Br) requires 479.9446; m.p. 128-131 °C (lit.,²⁶ 174-176 °C); *elem. anal.* C₁₉H₁₅Br₂NO₄ requires C 47.43%, H 3.14%, N 2.91% found C 47.06%, H 3.10%, N 2.80%.

Consistent with literature data.²⁶

(E)-3-(2-(Benzyloxy)-3,5-dibromo-4-methoxyphenyl)-2-((benzyloxy)imino)propanoic acid (30)



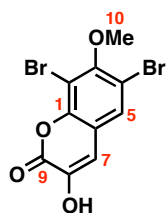
A solution of **29** (4.00 g, 8.31 mmol) and Ba(OH)₂·8H₂O (18.3 g, 58.0 mmol) in 1,4-dioxane (60 mL) and H₂O (60 mL) was heated to 60 °C. After 1 h *O*-benzylhydroxylamine (3.07 g, 24.9 mmol) was added and the mixture was stirred for a further 16 h. The reaction mixture was cooled to 0 °C, acidified to pH 0 with 3 *N* HCl and extracted with CH₂Cl₂ (250 mL × 3). The combined organic layers were dried, evaporated to dryness *in vacuo* and the resulting residue triturated with petroleum ether to furnish **30** (2.31 g, 4.10 mmol, 49%) as an off white solid. The mother liquor was concentrated *in vacuo* and the resulting residue was purified by flash column chromatography (10% Et₂O/Petrol) to furnish **31** (924 mg, 1.83 mmol, 22%) as a white solid.

30: *R*_f 0.59 (10% MeOH/CH₂Cl₂); ν_{max} (thin film)/cm⁻¹ 2991br, 1701s, 1455s, 1427s, 1216s, 993s; δ_{H} (400 MHz, CDCl₃) 7.50-7.48 (2H, m, H-10'/14'), 7.39-7.33 (6H, m, Ph-H), 7.21-7.19 (2H, m, Ph-H), 7.16 (1H, s, H-5), 5.22 (2H, s, H-1'), 5.01 (2H, s, H-8'), 3.89 (2H, s, H-7), 3.88 (3H, s, H-10); δ_{C} (100 MHz, CDCl₃) 163.4 (C-9), 154.3 (C-1), 154.1 (C-3), 149.3 (C-8), 136.4 (C-9'), 135.6 (C-2'), 131.9 (C-5), 128.7 (C-6), 128.6 (Ph-C), 128.4 (Ph-C), 128.3 (C-5' or C-12'), 128.2 (Ph-C), 128.03 (C-5' or C-12'), 127.96 (Ph-C), 114.6 (C-4), 112.8 (C-2), 78.4 (C-1'), 74.7 (C-8'), 60.6 (C-10), 25.3 (C-7); *m/z* (ESI⁺) found 583.9688, [M+Na]⁺ C₂₄H₂₁Br₂NO₅Na (⁷⁹Br) requires 583.9679 *m.p.* 159-161 °C.

Consistent with literature data.²⁶

2-(Benzyloxy)-3,5-dibromo-4-methoxybenzaldehyde O-benzyl oxime (31)

R_f 0.84 (30% Et₂O/Petrol); ν_{\max} (thin film)/cm⁻¹ 2945w, 1599w, 1580w, 1457m, 1365s, 1155s, 943s; δ_H (400 MHz, CDCl₃) 8.40 (1H, s, H-7), 8.20 (1H, s, H-5), 7.59-7.43 (10H, s, Ph-H), 5.36 (2H, s, H-1'), 5.05 (2H, s, H-1''), 4.04 (3H, s, H-8); δ_C (100 MHz, CDCl₃) 156.0 (C-3), 154.4 (C-1), 142.8 (C-7), 137.0 (C-2'), 135.4 (C-2''), 128.9 (Ph-C), 128.28 (Ph-C), 128.25 (Ph-C), 128.14 (Ph-C), 128.06 (Ph-C), 128.02 (Ph-C), 127.7 (Ph-C), 124.7 (C-6), 114.6 (C-4), 113.6 (C-2), 76.4 (C-1'), 76.2 (C-1''), 60.4 (C-8); m.p. 69-71 °C; *elem. anal.* C₂₂H₁₉Br₂NO₃ requires C 52.30%, H 3.79%, N 2.77%, found C 51.85%, H 3.79%, N 2.76%.

6,8-Dibromo-3-hydroxy-7-methoxy-2H-chromen-2-one (32)

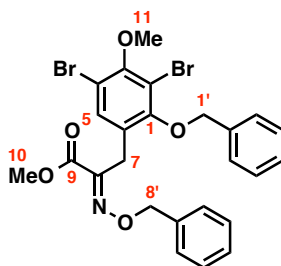
A suspension of azlactone **29** (428 mg, 0.890 mmol) and 3 *N* HCl (20 mL) were heated to reflux for 20 h. The mixture was cooled to room temperature and the white precipitate was isolated by filtration, washed with H₂O (20 mL) and dried *in vacuo* to furnish **32** (211 mg, 0.603 mmol, 68%) as an off-white solid.

ν_{max} (thin film)/cm⁻¹ 3358m, 1699s, 1471m, 1251s, 1148s; δ_{H} (400 MHz, *d*₆-DMSO) 10.70 (1H, s, OH), 7.92 (1H, s, H-5), 7.07 (1H, s, H-7), 3.83 (3H, s, H-10); δ_{C} (100 MHz, *d*₆-DMSO) 157.2 (C-9), 152.5 (C-3), 146.0 (C-1), 141.7 (C-8), 128.5 (C-5), 119.7 (C-2), 113.3 (C-7), 112.2 (C-4), 105.3 (C-6), 60.7 (C-10).

Consistent with literature data.²⁷

Crystals of **32** were obtained by slow evaporation of Et₂O. The structure was confirmed by X-ray crystallographic analysis and given the unique identifier sl1037.

(E)-Methyl-3-(2-(benzyloxy)-3,5-dibromo-4-methoxyphenyl)-2-((benzyloxy)imino)propanoate (34)

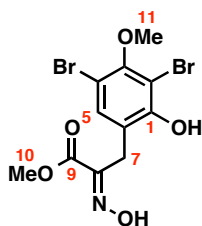


To a stirred solution of **30** (307 mg, 0.545 mmol) in toluene/MeOH (3:1, 8 mL) at 0 °C was added trimethylsilyldiazomethane (2.0 M in hexane, 409 μ L, 0.818 mmol) dropwise. The mixture was stirred for 1 h at room temperature and quenched by the addition of 3 N HCl (100 μ L). The solvent was removed *in vacuo* and the residue partitioned between H₂O (30 mL) and EtOAc (30 mL). The aqueous phase was extracted with EtOAc (30 mL \times 2) and the combined organic layers were dried and evaporated to dryness *in vacuo* to furnish **34** (300 mg, 0.520 mmol, 95%) as an off white solid.

R_f 0.31 (20% Et₂O/Petrol); ν_{\max} (thin film)/cm⁻¹ 1724s, 1421m, 1207s, 998s; δ_H (400 MHz, CDCl₃) 7.52-7.49 (2H, m, H-10'/14'), 7.41-7.31 (6H, m, Ph-H), 7.23-7.21 (2H, m, Ph-H), 7.20 (1H, s, H-5), 5.26 (2H, s, H-1'), 4.97 (2H, s, H-8'), 3.92 (2H, s, H-7), 3.89 (3H, s, H-11), 3.72 (3H, s, H-10); δ_C (100 MHz, CDCl₃) 163.6 (C-9), 154.2 (C-1), 153.8 (C-3), 149.9 (C-8), 136.5 (C-9'), 135.9 (C-2'), 132.0 (C-5), 128.6 (C-6), 128.5 (Ph-C), 128.33 (Ph-C), 128.27 (C-5' or C-12'), 128.2 (Ph-C), 128.1 (C-5' or C-12'), 127.8 (Ph-C), 114.4 (C-4), 112.7 (C-2), 78.0 (C-1'), 74.4 (C-8'), 60.5 (C-11), 52.8 (C-10), 26.4 (C-7); m/z (ESI+) found 576.0048, $[M+H]^+$ C₂₅H₂₄Br₂NO₅ (⁷⁹Br) requires 576.0021; m.p. 97-99 °C (lit.,²⁶ 97-99 °C).

Consistent with literature data.¹⁷

(E)-Methyl-3-(3,5-dibromo-2-hydroxy-4-methoxyphenyl)-2-(hydroxyimino)propanoate (35)

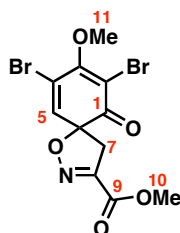


A mixture of **34** (100 mg, 0.173 mmol) and palladium black (18 mg, 0.169 mmol) in dioxane/AcOH (1:1, 2.46 mL) was stirred under an H₂ atmosphere for 3 h. The mixture was filtered through a pad of celite and the solvent removed *in vacuo*. The residue was taken up in EtOAc (15 mL), washed with water (15 mL) dried, and concentrated *in vacuo*. The residue was purified by flash column chromatography (25% EtOAc/Hexanes) to furnish **35** (63 mg, 0.159 mmol, 93%) as a white solid.

R_f 0.37 (30% EtOAc/Hexanes); ν_{\max} (thin film)/cm⁻¹ 3267br, 1730s, 1593w, 1015s; δ_H (400 MHz, CDCl₃) 7.40 (1H, s, H-5), 3.92 (2H, s, H-7), 3.90 (3H, s, H-11), 3.85 (3H, s, H-10); δ_C (100 MHz, CDCl₃) 164.4 (C-9), 153.8 (C-3), 151.5 (C-1), 149.9 (C-8), 133.4 (C-5), 119.4 (C-4), 107.6 (C-2), 60.5 (C-11), 53.4 (C-10), 25.5 (C-7); m/z (ESI+) found 395.9100, [M+H]⁺ C₁₁H₁₂Br₂NO₅ (⁷⁹Br) requires 395.9082; m.p. 148-150 °C (lit.,²⁶ 150-152 °C).

The ¹³C chemical shift for C-6 is not visible, however, this is consistent with literature data.²⁵

Methyl 7,9-dibromo-8-methoxy-10-oxo-1-oxa-2-azaspiro[4.5]deca-2,6,8-triene-3-carboxylate (36**)**



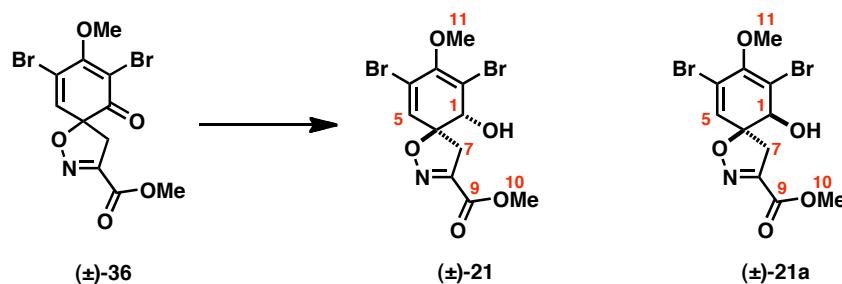
To a stirred solution of **35** (397 mg, 1.00 mmol) in MeCN (45 mL) at 0 °C was added iodobenzene diacetate (354 mg, 1.10 mmol). After 2 h, H₂O (50 mL) was added and the mixture stirred for a further 10 min at room temperature. The mixture was extracted with CH₂Cl₂ (200 mL × 2) and the combined organic extracts were dried and evaporated to dryness *in vacuo* to furnish (±)-**36** as an orange oil (523 mg) which was used without further purification.

For characterisation purposes, a sample was purified by flash column chromatography (10-40% EtOAc/Hexane) to furnish (±)-**36** as a white solid.

R_f 0.62 (40% EtOAc/Hexanes); ν_{\max} (thin film)/cm⁻¹ 1725s, 1679m, 1239s, 732s; δ_H (400 MHz, CDCl₃) 6.77 (1H, s, H-5), 4.18 (3H, s, H-10), 3.91 (3H, s, H-11), 3.62 (1H, d, J 17.8 Hz, H-7a), 3.29 (1H, d, J 17.8 Hz, H-7b); δ_C (100 MHz, CDCl₃) 188.6 (C-1), 163.2 (C-9), 159.6 (C-3), 149.9 (C-8), 135.9 (C-5), 120.9 (C-4), 106.7 (C-2), 86.8 (C-6), 62.1 (C-11), 53.1 (C-10), 44.4 (C-7).

Consistent with literature data.¹⁸

Methyl 7,9-dibromo-10-hydroxy-8-methoxy-1-oxa-2-azaspiro[4.5]deca-2,6,8-triene-3-carboxylate (21)



To a stirred solution of crude (±)-**36** (523 mg) in CH_2Cl_2 (5 mL) at room temperature was added a freshly prepared solution of $\text{Zn}(\text{BH}_4)_2$ ²⁸ (0.21 M in Et_2O , 1.73 mL, 0.363 mmol). After 10 min, H_2O (0.4 mL) was added and the mixture stirred for a further 20 min. Following the addition of anhydrous MgSO_4 , the mixture was filtered and concentrated *in vacuo*. The residue was purified by careful flash column chromatography (10-20% EtOAc / Petrol) to furnish (±)-**21** (127 mg, 0.320 mmol, 32% over 2 steps) and (±)-**21a** (64 mg, 0.161 mmol, 16% over 2 steps from **35**) as pale yellow oils.

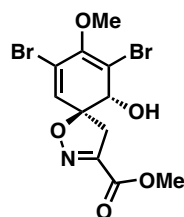
(5*S,10*R**)-Methyl 7,9-dibromo-10-hydroxy-8-methoxy-1-oxa-2-azaspiro[4.5]deca-2,6,8-triene-3-carboxylate (21)**

R_f 0.53 (40% EtOAc / Petrol); ν_{max} (thin film)/ cm^{-1} 3370br, 2958w, 1732s, 1604m, 1578m, 1431m, 1268s; δ_{H} (400 MHz, $(\text{CD}_3)_2\text{CO}$) 6.51 (1H, s, H-5), 5.38 (1H, d, J 8.1 Hz, OH), 4.22 (1H, d, J 8.1 Hz, H-1), 3.84 (1H, d, J 18.2 Hz, H-7a), 3.83 (3H, s, H-11), 3.73 (3H, s, H-10), 3.21 (1H, d, J 18.2 Hz, H-7b); δ_{C} (100 MHz, $(\text{CD}_3)_2\text{CO}$) 161.1 (C-9), 152.4 (C-8), 148.7 (C-3), 132.0 (C-5), 122.1 (C-4), 113.7 (C-2), 92.4 (C-6), 75.1 (C-1), 60.2 (C-11), 52.8 (C-10), 39.9 (C-7); m.p. 134-136 °C; m/z (ESI+) found 395.9099, $[\text{M}+\text{H}]^+$ $\text{C}_{11}\text{H}_{12}\text{Br}_2\text{NO}_5$ (^{79}Br) requires 395.9082.

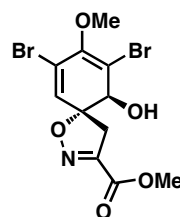
Consistent with literature data.²³

Crystals of (±)-**21** were obtained by slow evaporation of Et_2O . The structure was confirmed by X-ray crystallographic analysis and given the unique identifier sl1040.

The enantiomers were separated using preparative chiral HPLC (CHIRALPAK AD-H column and 4% *i*PrOH in hexane at a flow rate of 5 mL/min). Retention times: (+)-**21** = 30.9 min; (–)-**21** = 32.9 min.



(+)-**21** $[\alpha]_D^{27.9} +165.5$ (*c* 0.325, C₆H₆)
 {lit. $[\alpha]_D^{26} +217.1$ (*c* 1.0, C₆H₆)}



(–)-**21** $[\alpha]_D^{27.9} -150.9$ (*c* 0.43, C₆H₆)
 {lit. $[\alpha]_D^{26} -210.3$ (*c* 1.0, C₆H₆)}

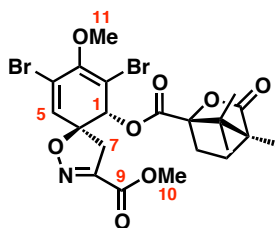
(5*S,10*S**)-Methyl 7,9-dibromo-10-hydroxy-8-methoxy-1-oxa-2-azaspiro[4.5]deca-2,6,8-triene-3-carboxylate (**21a**)**

R_f 0.47 (40% EtOAc/Petrol); ν_{\max} (thin film)/cm^{–1} 3433br, 2938w, 1725s, 1597m, 1575m, 1441s, 1248s; δ_H (400 MHz, (CD₃)₂CO) 6.61 (1H, s, H-5), 5.00 (1H, d, *J* 8.5 Hz, OH), 4.56 (1H, d, *J* 8.4 Hz, H-1), 3.82 (3H, s, H-11), 3.71 (3H, s, H-10), 3.48 (1H, d, *J* 17.9 Hz, H-7a), 3.40 (1H, d, *J* 17.9 Hz, H-7b); δ_C (100 MHz, (CD₃)₂CO) 161.2 (C-9), 152.3 (C-8), 148.4 (C-3), 132.8 (C-5), 121.1 (C-4), 115.5 (C-2), 91.4 (C-6), 75.2 (C-1), 60.1 (C-11), 52.8 (C-10), 43.3 (C-7); m.p. 125–127 °C; *m/z* (ESI+) found 395.9073, [M+H]⁺ C₁₁H₁₂Br₂NO₅ (⁷⁹Br) requires 395.9082.

Consistent with literature data.²³

Crystals of (±)-**21a** were obtained by slow evaporation of Et₂O. The structure was confirmed by X-ray crystallographic analysis and given the unique identifier sl1041.

(5*S*,10*R*)-Methyl 7,9-dibromo-8-methoxy-10-(((1*R*,4*R*)-4,7,7-trimethyl-3-oxo-2-oxabicyclo[2.2.1]heptane-1-carbonyl)oxy)-1-oxa-2-azaspiro[4.5]deca-2,6,8-triene-3-carboxylate (25a)

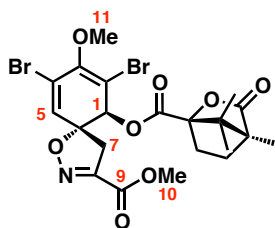


To a stirred solution of (+)-**21** (9.20 mg, 23.2 μmol) in CH_2Cl_2 (2 mL) and DMAP (8.50 mg, 69.6 μmol) at 0 $^\circ\text{C}$ was added a solution of (–)-camphanic chloride (10.1 mg, 46.6 μmol) in CH_2Cl_2 (2 mL) dropwise. Upon warming to room temperature the mixture was stirred for 18 h after which H_2O (15 mL) was added. The organic layer was separated and the aqueous phase was extracted with CH_2Cl_2 (20 mL \times 2). The combined organic layers were dried and concentrated *in vacuo*. The residue was purified by flash column chromatography (25% EtOAc/Petrol) to furnish **25a** (5.1 mg, 8.84 μmol , 38%) as a colourless oil.

R_f 0.50 (1% EtOAc/ CH_2Cl_2 , 2 elutions); ν_{max} (thin film)/ cm^{-1} 2967w, 2936w, 1789s, 1746s, 1728s, 1443m, 1259s, 1050s; δ_{H} (400 MHz, CDCl_3) 6.40 (1H, s, H-5), 6.07 (1H, s, H-1), 3.90 (3H, s, H-11), 3.77 (H-10), 3.60 (1H, d, J 18.2 Hz, H-7a), 3.05 (1H, d, J 18.2 Hz, H-7b), 2.48–2.41 (1H, m, camph CH_2), 2.09–2.02 (1H, m, camph CH_2), 1.96–1.89 (1H, m, camph CH_2), 1.70–1.64 (1H, m, camph CH_2), 1.11 (3H, s, camph CH_3), 1.04 (3H, s, camph CH_3), 1.02 (3H, s, camph CH_3); δ_{C} (100 MHz, CDCl_3) 177.7, 166.5, 159.9, 151.6, 150.1, 130.6, 121.2, 106.8, 90.8, 74.8, 60.3, 60.3, 55.0, 54.6, 53.1, 39.5, 31.0, 28.8, 16.9, 16.6, 9.7; m/z (ESI+) found 575.9890, $[\text{M}+\text{H}]^+$ $\text{C}_{21}\text{H}_{24}\text{Br}_2\text{NO}_8$ (^{79}Br) requires 575.9869.

Consistent with literature data.¹⁹

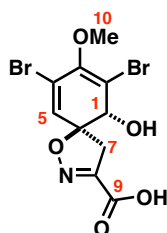
(5*R*,10*S*)-Methyl 7,9-dibromo-8-methoxy-10-(((1*R*,4*R*)-4,7,7-trimethyl-3-oxo-2-oxabicyclo[2.2.1]heptane-1-carbonyl)oxy)-1-oxa-2-azaspiro[4.5]deca-2,6,8-triene-3-carboxylate (25b)



To a stirred solution of (–)-**21** (6.00 mg, 15.1 μmol) in CH_2Cl_2 (2 mL) and DMAP (5.50 mg, 45.0 μmol) at 0 $^\circ\text{C}$ was added a solution of (–)-camphanic chloride (6.50 mg, 30.0 μmol) in CH_2Cl_2 (2 mL) dropwise. Upon warming to room temperature the mixture was stirred for 18 h after which H_2O (15 mL) was added. The organic layer was separated and the aqueous phase was extracted with CH_2Cl_2 (20 mL \times 2). The combined organic layers were dried and concentrated *in vacuo*. The residue was purified by flash column chromatography (25% EtOAc/Petrol) to furnish **25b** (4.00 mg, 6.93 μmol , 46%) as a colourless oil.

R_f 0.45 (1% EtOAc/ CH_2Cl_2 , 2 elutions); ν_{max} (thin film)/ cm^{-1} 2966w, 2937w, 1790s, 1748s, 1728s, 1443m, 1258s, 1051s; δ_{H} (400 MHz, CDCl_3) 6.42 (1H, s, H-5), 6.12 (1H, s, H-1), 3.90 (3H, s, H-11), 3.77 (H-10), 3.67 (1H, d, J 18.2 Hz, H-7a), 3.03 (1H, d, J 18.2 Hz, H-7b), 2.41–2.34 (1H, m, camph CH_2), 2.15–2.08 (1H, m, camph CH_2), 1.97–1.90 (1H, m, camph CH_2), 1.74–1.68 (1H, m, camph CH_2), 1.11 (3H, s, camph CH_3), 1.09 (3H, s, camph CH_3), 0.97 (3H, s, camph CH_3); δ_{C} (125 MHz, CDCl_3) 177.5, 166.3, 159.8, 151.5, 149.8, 130.8, 120.7, 107.2, 90.9, 74.3, 60.4, 60.3, 54.8, 54.5, 53.2, 39.2, 31.3, 29.0, 16.7, 16.5, 9.6; m/z (ESI+) found 575.9879, $[\text{M}+\text{H}]^+$ $\text{C}_{21}\text{H}_{24}\text{Br}_2\text{NO}_8$ (^{79}Br) requires 575.9869.

Consistent with literature data.¹⁹

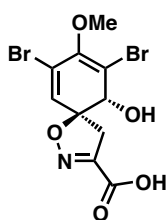
(5*S,10*R**)-7,9-Dibromo-10-methoxy-1-oxa-2-azaspiro[4.5]deca-2,6,8-triene-3-carboxylic acid (18)**

To a solution of (\pm)-**21** (100 mg, 0.252 mmol) in H₂O/MeOH (1:3, 15 ml) was added lithium hydroxide monohydrate (32.0 mg, 0.763 mmol). After 70 min 3 *N* HCl (1.5 mL) was added followed by H₂O (25 mL). The mixture was extracted with EtOAc (25 mL \times 2) and the combined organic extracts were dried and evaporated to dryness *in vacuo* to furnish (\pm)-**18** (96 mg, 0.251 mmol, quant.) as a light brown foam which was used without further purification

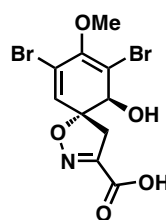
ν_{max} (thin film)/cm⁻¹ 3402br, 2978w, 2935w, 1709s, 1598m, 1431m, 1255s; δ_{H} (600 MHz, CD₃OD) 6.43 (1H, s, H-5), 4.11 (1H, s, H-1) 3.75 (1H, d, *J* 18.3 Hz, H-7a), 3.73 (3H, s, H-10) 3.10 (1H, d, *J* 18.3 Hz, H-7b); δ_{C} (150 MHz, CD₃OD) 162.6 (C-9), 153.8 (C-3), 149.3 (C-8), 132.2 (C-5), 122.8 (C-4), 114.1 (C-2), 93.1 (C-6), 75.5 (C-1), 60.4 (C-10), 43.3 (C-7).

Consistent with literature data.¹⁷

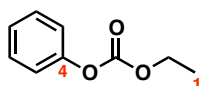
The enantiopure esters (+)-**21** and (–)-**21** were converted to the corresponding enantiopure acids (+)-**18** and (–)-**18** by the procedure described above.



(+)-**18** [α]_D^{27.5} +44.0 (*c* 0.42, CHCl₃)

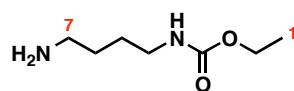


(–)-**18** [α]_D^{28.1} –31.3 (*c* 0.84, CHCl₃)

Ethyl phenyl carbonate (39)

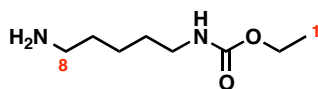
Phenol (94.0 mg, 1.00 mmol), diethylpyrocarbonate (174 μ L, 1.18 mmol) and magnesium perchlorate (22.3 mg, 0.100 mmol) were heated at 40 $^{\circ}$ C for 3 h. Following this, the mixture was partitioned between H₂O (10 mL) and EtOAc (10 mL). The organic layer was separated and the aqueous phase was extracted with EtOAc (3 \times 10 mL). The combined organic layers were combined, dried and concentrated *in vacuo*. The residue was purified by flash column chromatography (5% Et₂O/Petrol) to furnish **39** (163 mg, 0.981 mmol, 98%) as a colourless oil.

R_f 0.35 (5% Et₂O/Petrol); ν_{\max} (thin film)/cm⁻¹ 1756s, 1240s, 1203s, 1015s; δ_H (400 MHz, CDCl₃) δ 7.41-7.36 (2H, m, H-6/8), 7.26-7.17 (3H, m, H-5/9 and H-7), 4.32 (2H, q, J 7.1 Hz, H-2), 1.39 (3H, t, J 7.1 Hz, H-1); δ_C (100 MHz, CDCl₃) δ 153.6 (C-3), 151.1 (C-4), 129.4 (C-6/8), 125.9 (C-7), 121.0 (C-5/9), 64.8 (C-2), 14.2 (C-1).

Ethyl (4-aminobutyl)carbamate (19)

To a stirred solution of butane-1,4-diamine (**37**) (943 mg, 10.7 mmol) in absolute EtOH (13 mL) at room temperature was added a solution of phenyl ethyl carbonate (**39**) (1.77 g, 10.7 mmol) in absolute EtOH (2 mL) dropwise. After 12 h, the mixture was concentrated *in vacuo* and the residue was taken up in H₂O (25 mL) and acidified to pH 2-3 by the dropwise addition of 3 *N* HCl. The aqueous phase was washed with CH₂Cl₂ (50 mL × 3), basified by the addition of 10% aqueous sodium hydroxide solution and extracted with CH₂Cl₂ (50 mL × 3). The combined organic layers were dried and evaporated to dryness *in vacuo* to furnish **19** (1.36 g, 8.49 mmol, 79%) as a pale yellow oil.

R_f 0.10 (12% MeOH/CH₂Cl₂); ν_{\max} (thin film)/cm⁻¹ 3328w, 2954w, 1683s, 1531s; δ_H (400 MHz, CDCl₃) 4.96 (1H, br, NH), 4.09 (2H, q, J 6.8 Hz, H-2), 3.16 (2H, br, H-4), 2.71 (2H, t, J 6.7 Hz, H-7), 1.57-1.43 (4H, m, H-5 and H-6), 1.22 (3H, t, J 7.0 Hz, H-1), 1.03 (2H, br, NH₂); δ_C (125 MHz, CDCl₃) 156.6 (C-3), 60.4 (C-2), 41.7 (C-7), 40.6 (C-4), 30.7 (C-6), 27.3 (C-5), 14.5 (C-1); m/z (ESI+) found 161.1287, [M+H]⁺ C₇H₁₇N₂O₂ requires 161.1285.

Ethyl (5-aminopentyl)carbamate (20)

To a stirred solution of pentane-1,5-diamine (**38**) (2.19 mL, 18.7 mmol) in absolute EtOH (70 mL) at room temperature was added phenyl ethyl carbonate (**39**) (3.10 g, 18.7 mmol) in absolute EtOH (5 mL) dropwise. After 12 h the mixture was concentrated *in vacuo* and the residue was taken up in H₂O (50 mL) and acidified to pH 2-3 by the dropwise addition of 3 N HCl. The aqueous phase was washed with CH₂Cl₂ (100 mL × 3), basified by the addition of 10% aqueous sodium hydroxide solution and extracted with CH₂Cl₂ (100 mL × 3). The combined organic layers were dried and evaporated to dryness *in vacuo* to furnish **20** (2.67 g, 15.3 mmol, 82%) as a pale yellow oil.

R_f 0.11 (12% MeOH/CH₂Cl₂); ν_{\max} (thin film)/cm⁻¹ 3316w, 2932w, 1690s, 1540s, 1255s; δ_H (400 MHz, CDCl₃) 4.99 (1H, br, NH), 4.01 (2H, q, J 7.0 Hz, H-2), 3.07 (2H, apparent q, J 6.5 Hz, H-4), 2.60 (2H, t, J 6.9 Hz, H-8), 1.46-1.34 (4H, m, H-5 and H-7), 1.27-1.24 (2H, m, H-6), 1.22 (2H, br, NH₂), 1.14 (3H, t, J 7.0 Hz, H-1); δ_C (100 MHz, CDCl₃) 156.6 (C-3), 60.3 (C-2), 41.8 (C-8), 40.6 (C-4), 33.1 (C-7), 29.7 (C-5), 23.8 (C-6), 14.5 (C-1); m/z (ESI+) found 175.1447, $[M+H]^+$ C₈H₁₉N₂O₂, requires 175.1440.

General Procedures for coupling acid 18 to amines 19 and 20**Procedure 1**

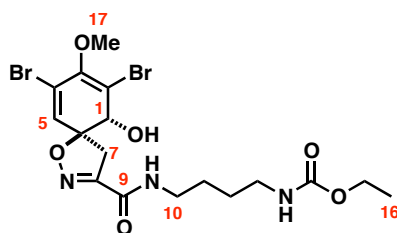
To a stirred solution of (\pm)-**18** (1 eq.) and HOBt (1.3 eq.) in CH₂Cl₂ (10 mL per 0.1 mmol substrate) at 0 °C was added a solution of DCC (1.3 eq.) in CH₂Cl₂ (1 mL per 0.1 mmol DCC). After 10 min, a solution of amine (1.3 eq.) in CH₂Cl₂ (2 mL per 0.1 mmol amine) was added in one portion and the mixture was stirred at room temperature. After 18 h, H₂O and CH₂Cl₂ were added and the organic phase separated. The aqueous layer was extracted with CH₂Cl₂ (\times 2) and the combined organic layers were dried and concentrated *in vacuo*. The residue was purified by flash column chromatography.

Procedure 2

To a stirred solution of (\pm)-**18** (1 eq.), amine (1 eq.) and *i*Pr₂EtN (2.5 eq.) in CH₂Cl₂ (5 mL per 0.1 mmol substrate) at 0 °C was added [®]T3P (1.2 eq. of a 50% w/w solution in EtOAc) dropwise. After 2 h, H₂O and CH₂Cl₂ were added and the organic phase separated. The aqueous layer was extracted with CH₂Cl₂ (\times 2) and the combined organic layers were dried and concentrated *in vacuo*. The residue was purified by flash column chromatography.

Ethyl (4-((5S,10R)-7,9-dibromo-10-hydroxy-8-methoxy-1-oxa-2-azaspiro[4.5]deca-2,6,8-triene-3-carboxamido)butyl)carbamate (16).

Subereamolline A.

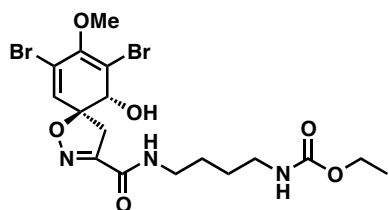


Procedure 1: Purified by flash column chromatography (20-60% EtOAc/Petrol) to furnish (±)-subereamolline A (**16**) (31.3 mg, 59.6 μ mol, 91%) as a colourless oil.

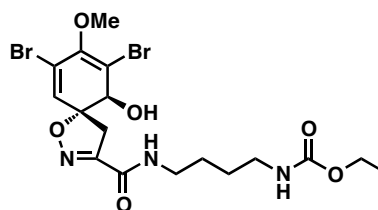
Procedure 2: Purified by flash column chromatography (40-60% EtOAc/Petrol) to furnish (±)-subereamolline A (**16**) (58.0 mg, 0.110 mmol, 96%) as a colourless oil.

R_f 0.42 (60% EtOAc/Petrol); ν_{\max} (thin film)/ cm^{-1} 3330br, 2936w, 1658s, 1536m, 1438m, 1260m; δ_H (500 MHz, CD_3OD) 6.42 (1H, s, H-5), 4.08 (1H, s, H-1), 4.05 (2H, q, J 7.1 Hz, H-15), 3.77 (1H, d, J 18.3 Hz, H-7a), 3.73 (3H, s, H-17), 3.29 (2H, t, J 6.9 Hz, H-10), 3.11 (2H, t, J 6.7 Hz, H-13), 3.10 (1H, d, J 18.1 Hz, H-7b), 1.60-1.49 (4H, m, H-11 and H-12), 1.22 (3H, t, J 7.1 Hz, H-16); δ_C (125 MHz, CD_3OD) 161.5 (C-9), 159.2 (C-14), 155.3 (C-8), 149.3 (C-3), 132.3 (C-5), 122.7 (C-4), 114.1 (C-2), 92.3 (C-6), 75.5 (C-1), 61.6 (C-15), 60.4 (C-17), 41.2 (C-13), 40.2 (C-7), 40.1 (C-10), 28.3 (C-12), 27.6 (C-11), 15.0 (C-16); m/z (ESI+) found 545.9872, $[\text{M}+\text{Na}]^+$ $\text{C}_{17}\text{H}_{23}\text{Br}_2\text{N}_3\text{O}_6\text{Na}$ (^{79}Br) requires 545.9851.

The enantiomers were separated using preparative chiral HPLC (CHIRALPAK AD-H column and 10% *i*PrOH in hexane at a flow rate of 5 mL/min). Retention times: (+)-**16** = 40.3 min; (–)-**16** = 43.6 min

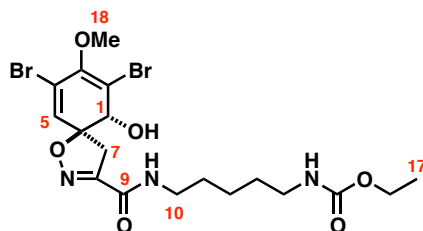


(+)-**16** $[\alpha]_D^{27.5} +83.9$ (c 0.475, MeOH)
{lit. $[\alpha]_D +156.5$ (c 0.55, MeOH)}



(–)-**16** $[\alpha]_D^{27.5} -94.3$ (c 0.485, MeOH)

Ethyl (5-((5*S*,10*R*)-7,9-dibromo-10-hydroxy-8-methoxy-1-oxa-2-azaspiro[4.5]deca-2,6,8-triene-3-carboxamido)pentyl)carbamate (17**).
Subereamolline B.**

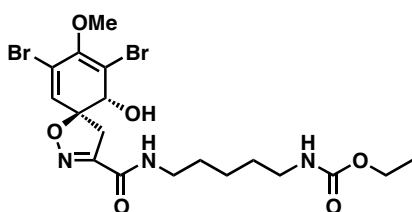


Procedure 1: Purified by flash column chromatography (20-60% EtOAc/Petrol) to furnish (±)-subereamolline B (**17**) (18.0 mg, 33.4 μmol, 75%) as a colourless oil.

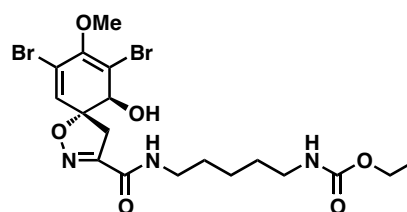
Procedure 2: Purified by flash column chromatography (40-60% EtOAc/Petrol) to furnish (±)-subereamolline B (**17**) (70.0 mg, 0.130 mmol, 97%) as a colourless oil.

R_f 0.45 (60% EtOAc/Petrol); ν_{\max} (thin film)/cm⁻¹ 3349br, 2934w, 1663s, 1536s, 1439m, 1260m; δ_H (500 MHz, CD₃OD) 6.42 (1H, s, H-5), 4.08 (1H, s, H-1), 4.05 (2H, q, J 7.1 Hz, H-16), 3.77 (1H, d, J 18.3 Hz, H-7a), 3.73 (3H, s, H-18), 3.28 (2H, t, J 7.1 Hz, H-10), 3.10-3.07 (2H, m, H-14), 3.09 (1H, hidden d, J 18.5 Hz, H-7b), 1.60-1.54 (2H, m, H-11), 1.54-1.48 (2H, m, H-13), 1.39-1.33 (2H, m, H-12), 1.22 (3H, t, J 7.1 Hz, H-17); δ_C (125 MHz, CD₃OD) 161.5 (C-9), 159.2 (C-15), 155.3 (C-8), 149.3 (C-3), 132.3 (C-5), 122.7 (C-4), 114.1 (C-2), 92.3 (C-6), 75.5 (C-1), 61.6 (C-16), 60.4 (C-18), 41.5 (C-14), 40.3 (C-7), 40.2 (C-10), 30.6 (C-13), 30.0 (C-11), 25.1 (C-12), 15.0 (C-17); m/z (ESI+) found 560.0029, $[M+Na]^+$ C₁₈H₂₅Br₂N₃O₆Na (⁷⁹Br) requires 560.0008.

The enantiomers were separated using preparative chiral HPLC (CHIRALPAK AD-H column and 10% *i*PrOH in hexane at a flow rate of 5 mL/min). Retention times: (+)-**17** = 48.3 min; (–)-**17** = 52.9 min



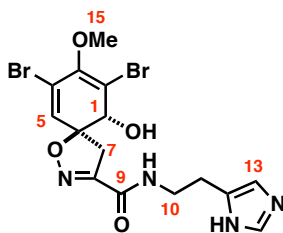
(+)-**17** [α]_D^{27.7} +55.4 (*c* 0.33, CH₂Cl₂)
{lit. [α]_D +22.9 (*c* 6.25, CH₂Cl₂)}



(–)-**17** [α]_D^{27.6} –50.0 (*c* 0.29, CH₂Cl₂)

(5*S*^{*},10*R*^{*})-*N*-(2-(1*H*-Imidazol-5-yl)ethyl)-7,9-dibromo-10-hydroxy-8-methoxy-1-oxa-2-azaspiro[4.5]deca-2,6,8-triene-3-carboxamide (40).

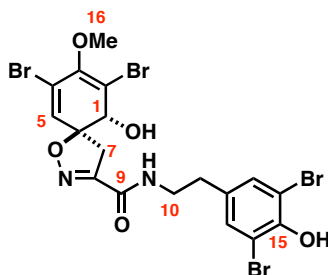
(±)-Aerophobin-1.



To a stirred solution of (±)-**18** (49.0 mg, 0.128 mmol), histamine dihydrochloride (23.6 mg, 0.128 mmol), *i*Pr₂EtN (100 μL, 0.581 mmol) in CH₂Cl₂ (1.2 mL) at 0 °C was added [®]T3P (190 μL of a 50% w/w solution in EtOAc, 0.320 mmol). After 2 h, H₂O (10 mL) and CH₂Cl₂ (10 mL) were added. The organic layer was separated, the aqueous layer extracted with CH₂Cl₂ (2 × 10 mL) and the combined organic extracts were dried and concentrated *in vacuo*. The residue was purified by flash column chromatography (5-10% MeOH/CH₂Cl₂) to furnish **40** (12.2 mg, 25.6 μmol, 20%) as a colourless oil.

*R*_f 0.26 (10% MeOH/CH₂Cl₂); *v*_{max} (thin film)/cm⁻¹ 3244br, 2922w, 2851w, 1658s, 1540s; δ_H (600 MHz, CD₃OD) 7.67 (1H, s, H-14), 6.90 (1H, s, H-13), 6.43 (1H, s, H-5), 4.06 (1H, s, H-1), 3.76 (1H, d, *J* 18.2 Hz, H-7a), 3.72 (3H, s, H-15), 3.52 (2H, t, *J* 7.2 Hz, H-10), 3.09 (1H, d, *J* 18.2 Hz, H-7b), 2.83 (2H, t, *J* 7.2 Hz, H-11); δ_C (150 MHz, CD₃OD) 161.5 (C-9), 155.2 (C-8), 149.3 (C-3), 136.1 (C-14), 134.7 (C-12), 132.2 (C-5), 122.8 (C-4), 117.6 (br, C-13), 114.2 (C-2), 92.3 (C-6), 75.5 (C-1), 60.4 (C-15), 40.4 (C-10), 40.1 (C-7), 27.6 (C-11); *m/z* (ESI+) found 474.9625, [M+H]⁺ C₁₅H₁₇Br₂N₄O₄ (⁷⁹Br) requires 474.9617.

(5*S,10*R**)-7,9-Dibromo-*N*-(3,5-dibromo-4-hydroxyphenethyl)-10-hydroxy-8-methoxy-1-oxa-2-azaspiro[4.5]deca-2,6,8-triene-3-carboxamide (**41**)**



To a stirred solution of (\pm)-**18** (52.0 mg, 0.136 mmol), 4-(2-aminoethyl)-2,6-dibromophenol hydrobromide (61.3 mg, 0.163 mmol) and *i*Pr₂EtN (104 μ L, 0.604 mmol) in CH₂Cl₂ (4 mL) at 0 °C was added [®]T3P (105 μ L of a 50% w/w solution in EtOAc, 0.177 mmol) dropwise. After 18 h H₂O (10 mL) and EtOAc (10 mL) were added and the organic phase separated. The aqueous layer was extracted with EtOAc (10 mL \times 2) and the combined organic layers were dried and concentrated *in vacuo*. The residue was purified by flash column chromatography (40-70% EtOAc/Petrol) to furnish **41** (9.7 mg, 14.7 μ mol, 11 %) as a colourless oil

R_f 0.23 (30% EtOAc/Petrol); ν_{max} (thin film)/cm⁻¹ 3330br, 2927m, 2852w, 1655s, 1595m, 1541s, 1475s, 735s; δ_{H} (500 MHz, CD₃OD) 7.36 (2H, s, H-13/17), 6.41 (1H, s, H-5), 4.09 (1H, s, H-1), 3.76 (1H, d, *J* 18.3 Hz, H-7a), 3.73 (3H, s, H-16), 3.45 (2H, t, *J* 7.2 Hz, H-10), 3.06 (1H, d, *J* 18.3 Hz, H-7b), 2.74 (2H, t, *J* 7.2 Hz, H-11); δ_{C} (125 MHz, CD₃OD) 161.5 (C-9), 155.2 (C-8), 150.9 (C-15), 149.3 (C-3), 134.4 (C-12), 133.7 (C-13/17), 132.2 (C-5), 122.8 (C-4), 114.2 (C-2), 112.2 (C-14/16), 92.4 (C-6), 75.5 (C-1), 60.4 (C-16), 41.8 (C-10), 40.1 (C-7), 34.8 (C-11); *m/z* (ESI⁺) found 656.7902, [M+H]⁺ C₁₈H₁₇Br₄N₂O₅ (⁷⁹Br) requires 656.7871.

3.6 Biology: Experimental

Refer to Section 2.1.6 for experimental details.

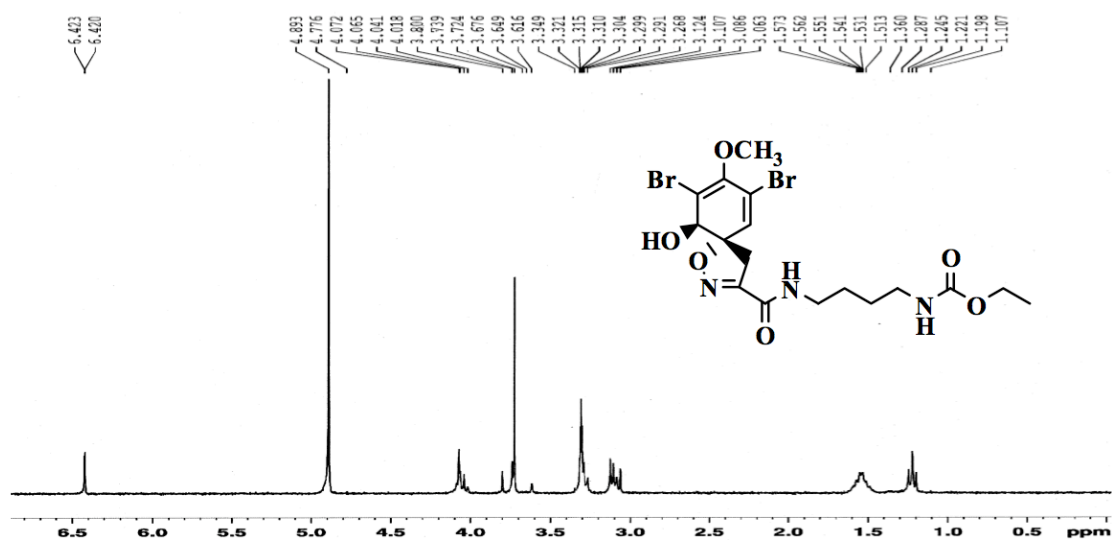
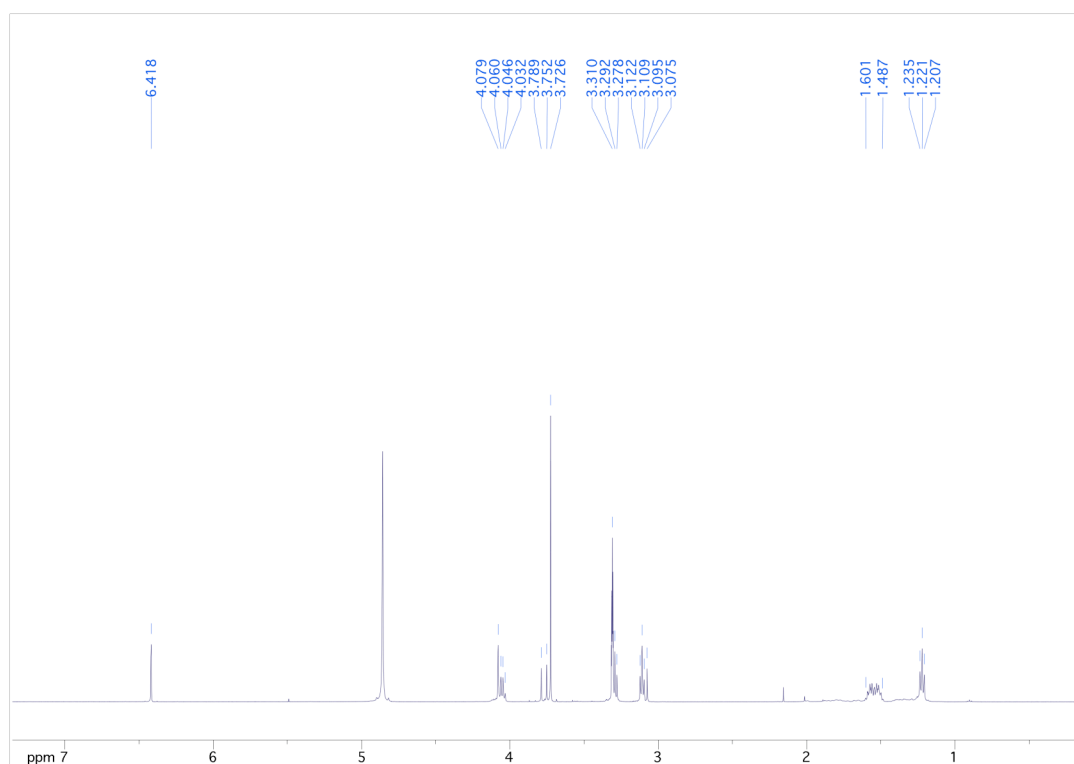
3.7 Appendix

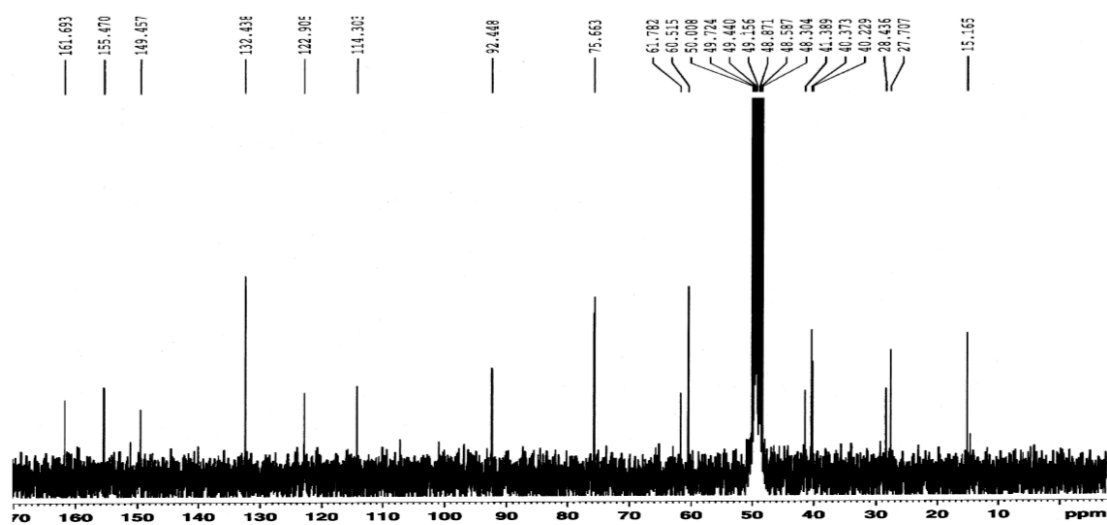
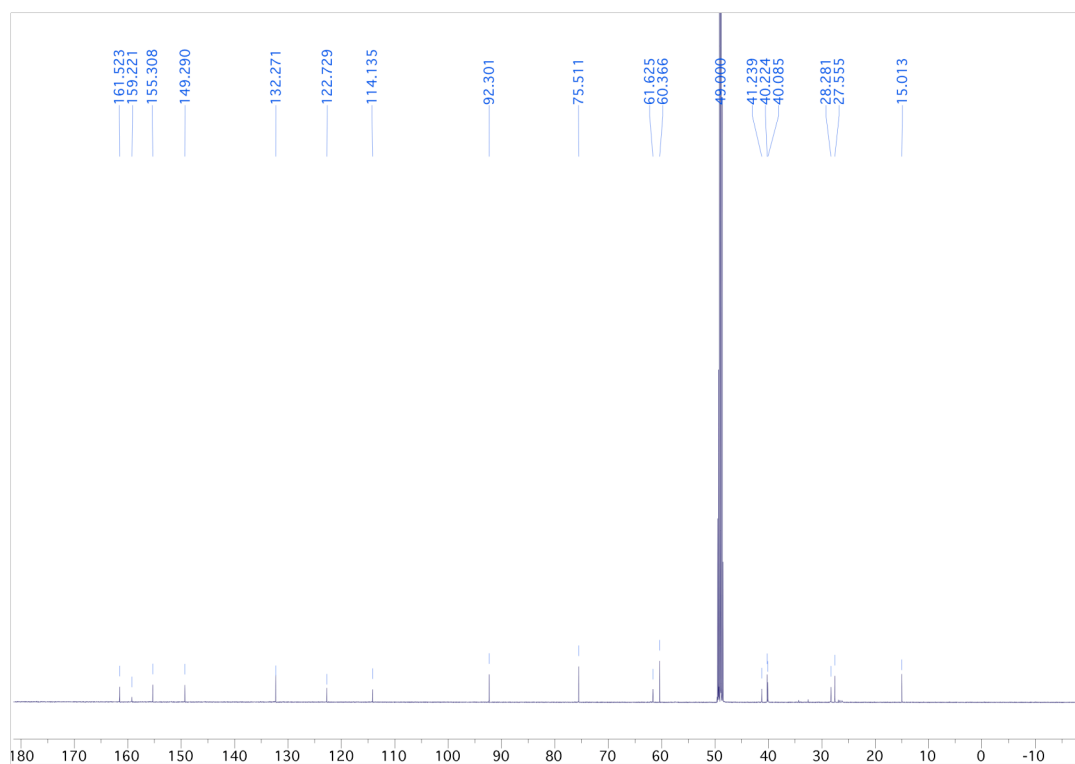
3.7.1 NMR Data of Natural Products

| Atom | Nat. 16 ¹³ C 75 MHz | Syn. 16 ¹³ C 125 MHz | Nat. 16 ¹ H 300 MHz | Syn. 16 ¹ H 500 MHz | Nat. 17 ¹³ C 75 MHz | Syn. 17 ¹³ C 125 MHz | Nat. 17 ¹ H 300 MHz | Syn. 17 ¹ H 500 MHz |
|-----------|---|--|---|---|---|--|---|---|
| 1 | 75.6 | 75.5 | 4.07 s | 4.08 s | 75.6 | 75.5 | 4.06 s | 4.08 s |
| 2 | 122.9 | 114.1 | – | – | 122.9 | 114.1 | – | – |
| 3 | 149.4 | 149.3 | – | – | 149.4 | 149.3 | – | – |
| 4 | 114.3 | 122.7 | – | – | 114.3 | 122.7 | – | – |
| 5 | 132.4 | 132.3 | 6.42 s | 6.42 s | 132.4 | 132.3 | 6.40 s | 6.42 s |
| 6 | 92.4 | 92.3 | – | – | 92.4 | 92.4 | – | – |
| 7 | 40.3 | 40.2 | 3.77 d 3.09 d | 3.77 d 3.10 d | 40.4 | 40.3 | 3.77 d 3.09 d | 3.77 d 3.09 d |
| 8 | 155.4 | 155.3 | – | – | 155.4 | 155.3 | – | – |
| 9 | 161.1 | 161.5 | – | – | 161.6 | 161.5 | – | – |
| 10 | 40.2 | 40.1 | 3.30 m | 3.29 t | 40.3 | 40.2 | 3.30 m | 3.28 t |
| 11 | 27.7 | 27.6 | 1.54 m | 1.60-1.49 m | 30.1 | 30.0 | 1.53 m | 1.54 m |
| 12 | 28.4 | 28.3 | 1.54 m | 1.60-1.49 m | 25.2 | 25.1 | 1.36 m | 1.39-1.33 m |
| 13 | 41.3 | 41.2 | 3.11 m | 3.11 t | 30.7 | 30.6 | 1.53 m | 1.54-1.48 m |
| 14 | 160.0 | 159.2 | – | – | 41.6 | 41.5 | 3.08 m | 3.10-3.07 m |
| 15 | 61.7 | 61.6 | 4.04 q | 4.05 q | 159.0 | 159.2 | – | – |
| 16 | 15.1 | 15.0 | 1.22 q | 1.22 t | 61.7 | 61.6 | 4.03 q | 4.05 q |
| 17 | 60.4 | 60.4 | 3.72 s | 3.73 s | 15.1 | 15.0 | 1.22 t | 1.22 t |
| 18 | – | – | – | – | 60.5 | 60.4 | 3.72 s | 3.73 s |

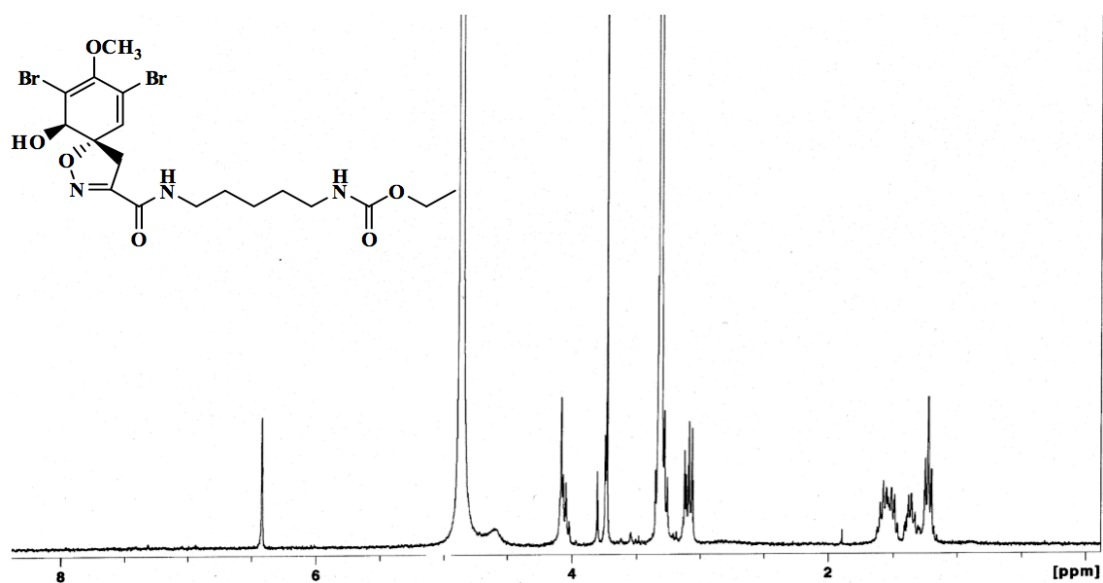
Table 9 Comparison of the NMR data (CD₃OD) of natural and synthetic subereamolline A (**16**) and (**17**).¹ Discrepancies in the original assignment are highlighted in bold.

3.7.2 NMR Spectra of Natural Products

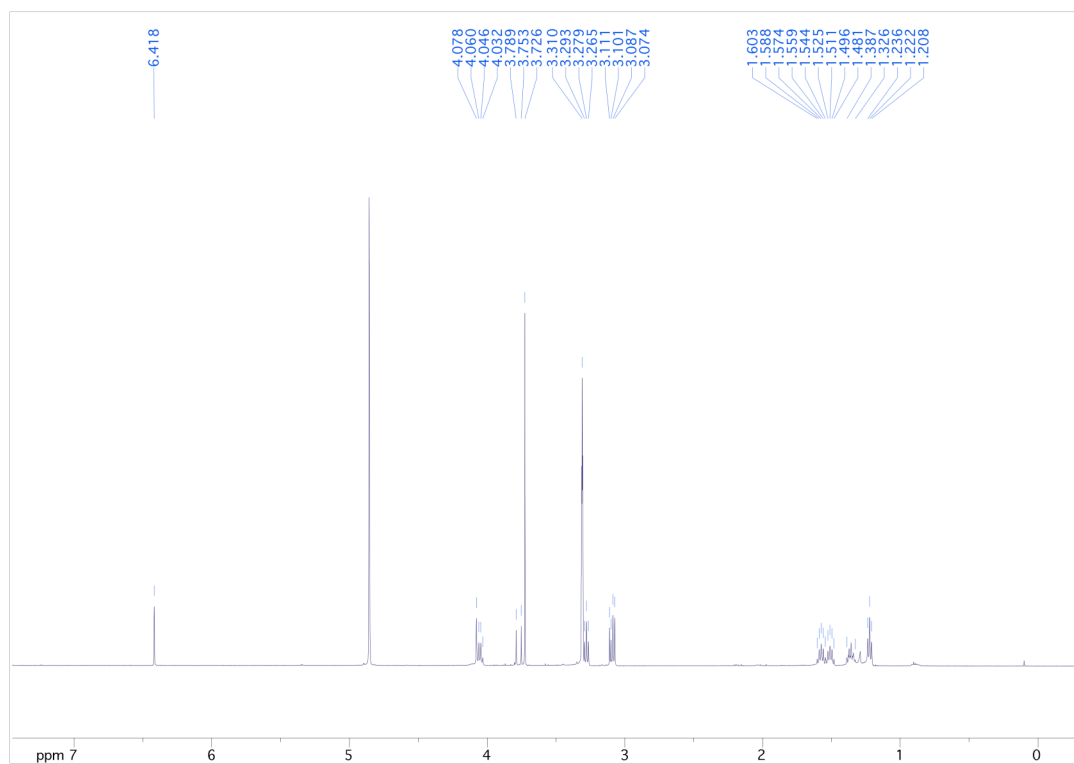
 ^1H NMR (CD_3OD 300 MHz) spectrum of subereamolline A (natural material) ^1H NMR (CD_3OD 500 MHz) spectrum of subereamolline A (synthetic material)

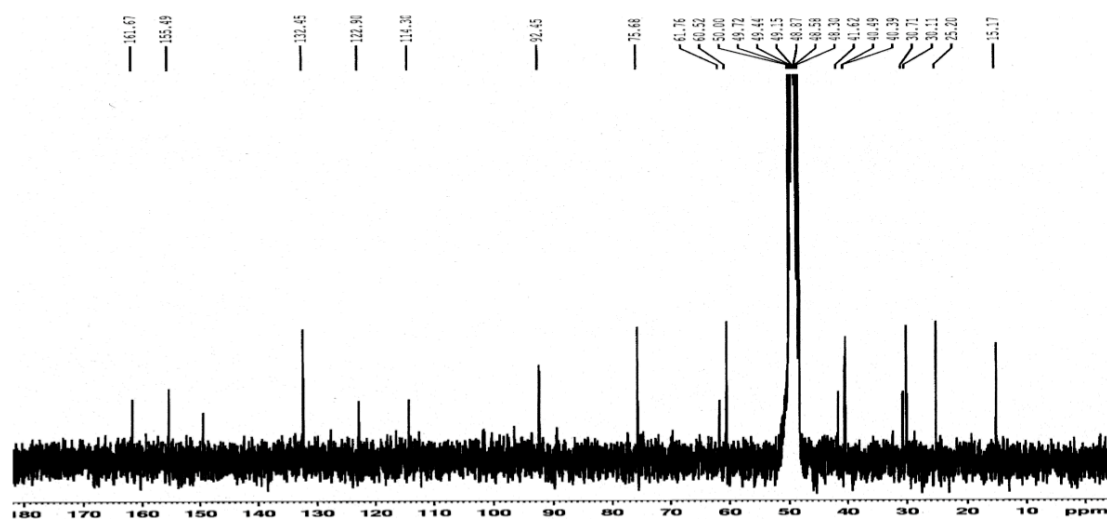
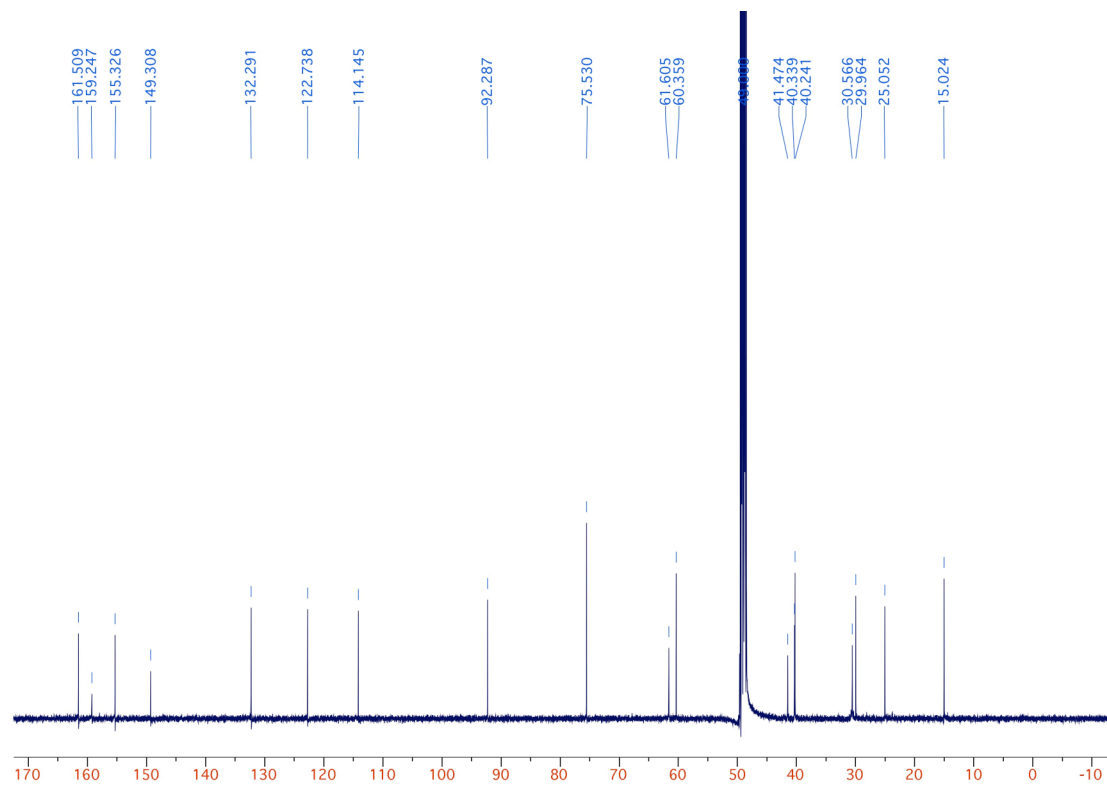
^{13}C NMR (CD_3OD 75 MHz) spectrum of subereamolline A (natural material) ^{13}C NMR (CD_3OD 125 MHz) spectrum of subereamolline A (synthetic material)

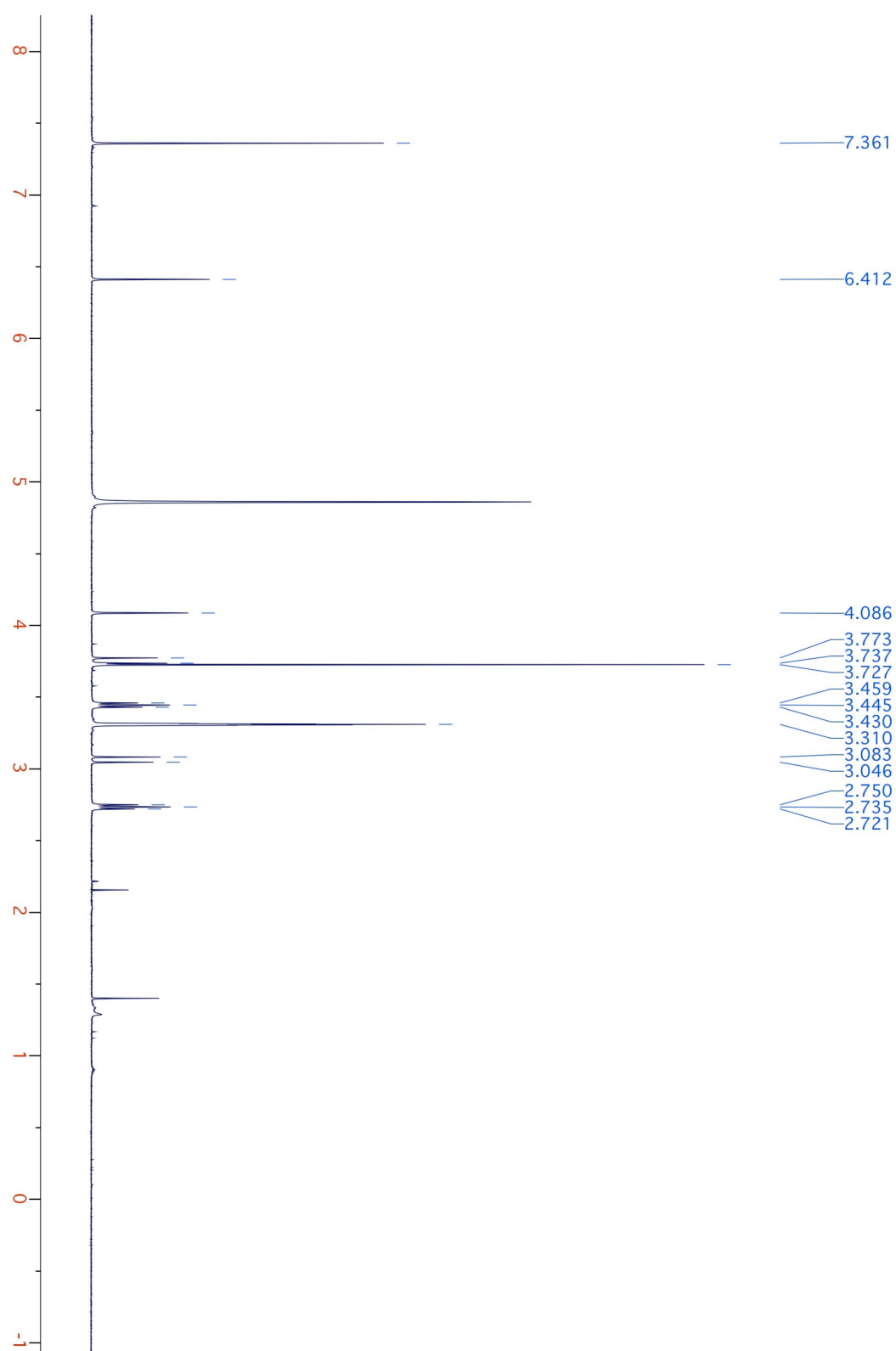
^1H NMR (CD_3OD 300 MHz) spectrum of subereamolline B (natural material)



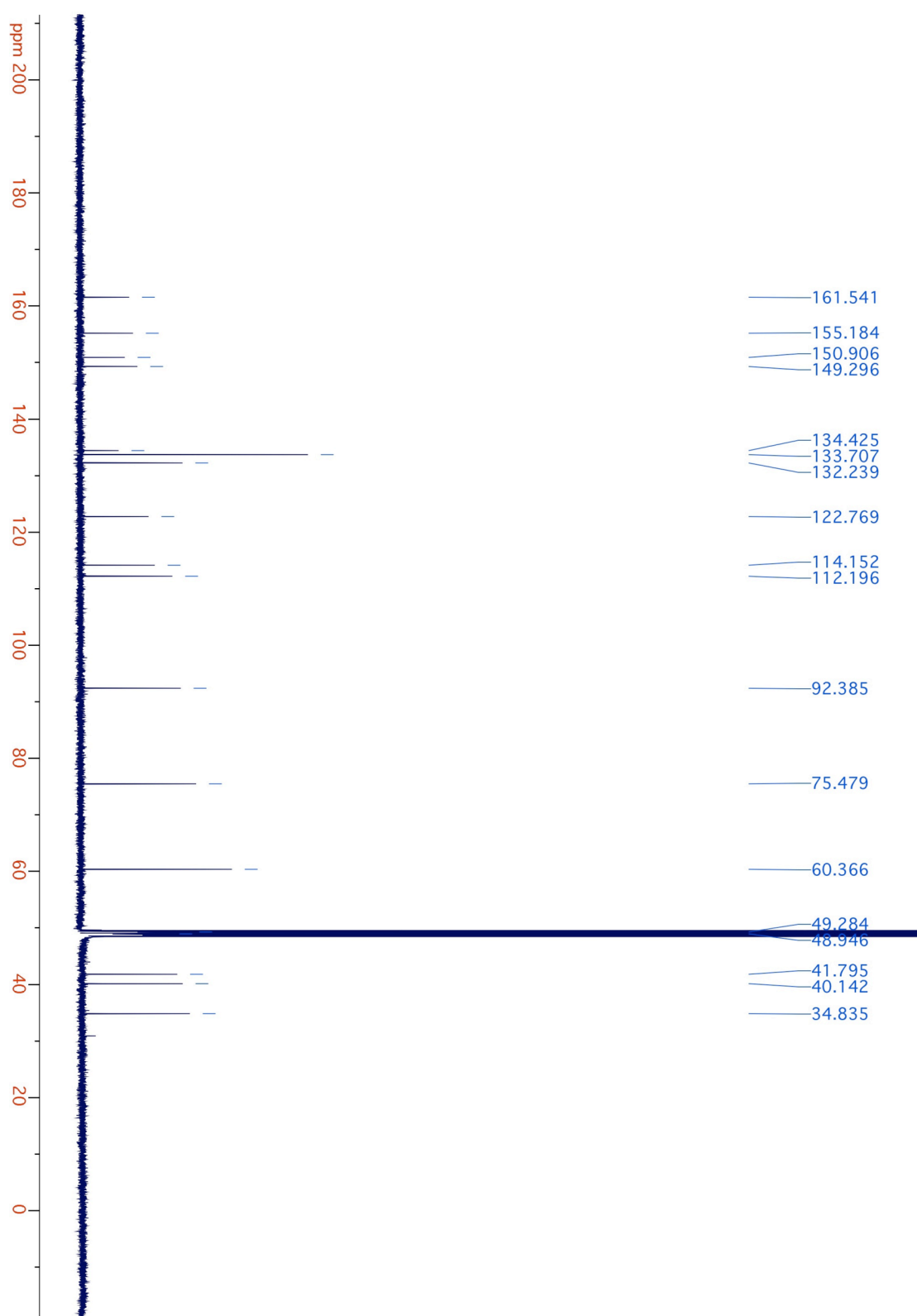
^1H NMR (CD_3OD 500 MHz) spectrum of subereamolline A (synthetic material)



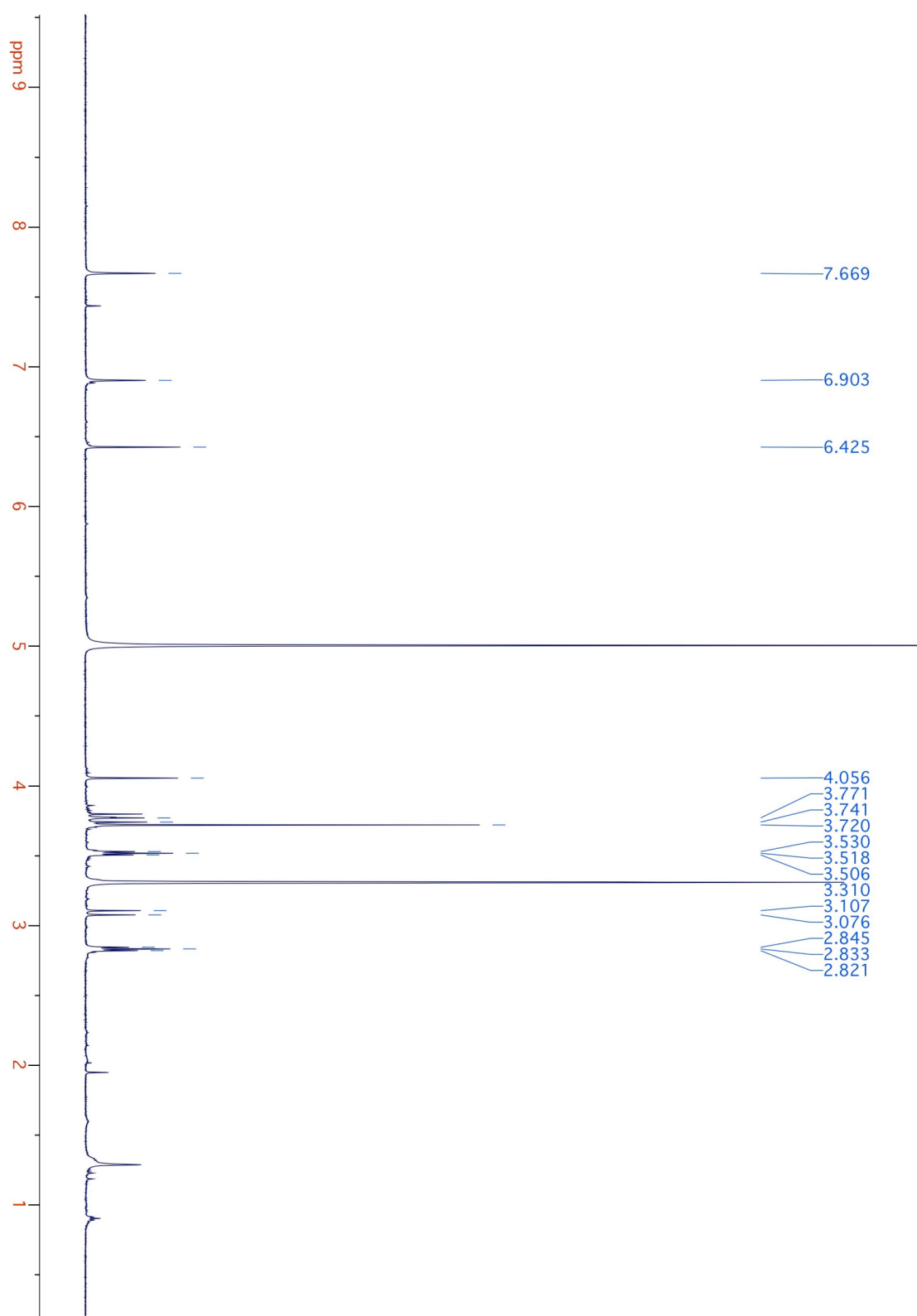
^{13}C NMR (CD_3OD 75 MHz) spectrum of subereamolline B (natural material) ^{13}C NMR (CD_3OD 125 MHz) spectrum of subereamolline B (synthetic material)

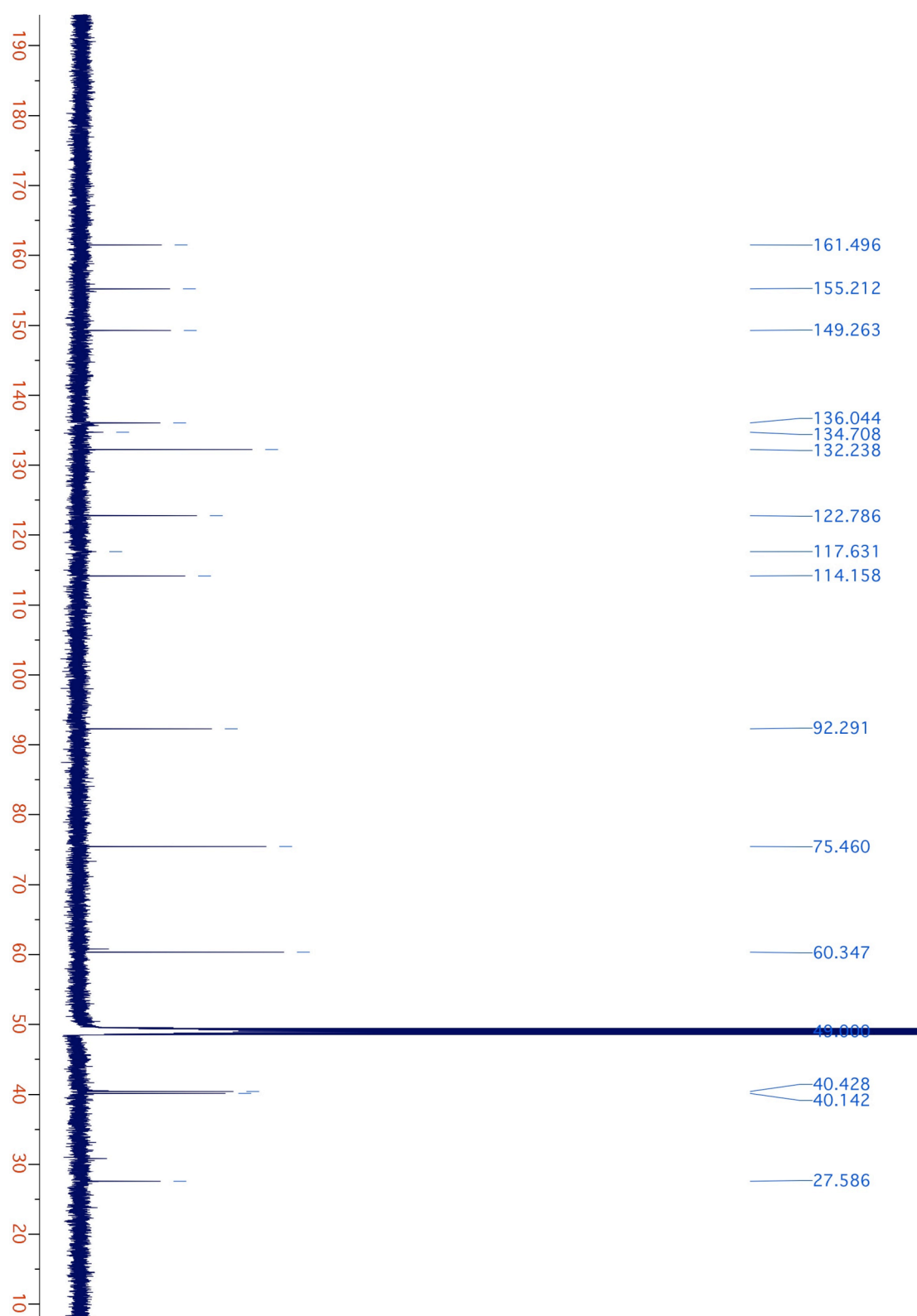
^1H NMR (CD_3OD 500 MHz) spectrum of **41**

^{13}C NMR (CD_3OD 125 MHz) spectrum of **41**



^1H NMR (CD_3OD 600 MHz) spectrum of aerophobin-1 (synthetic material)

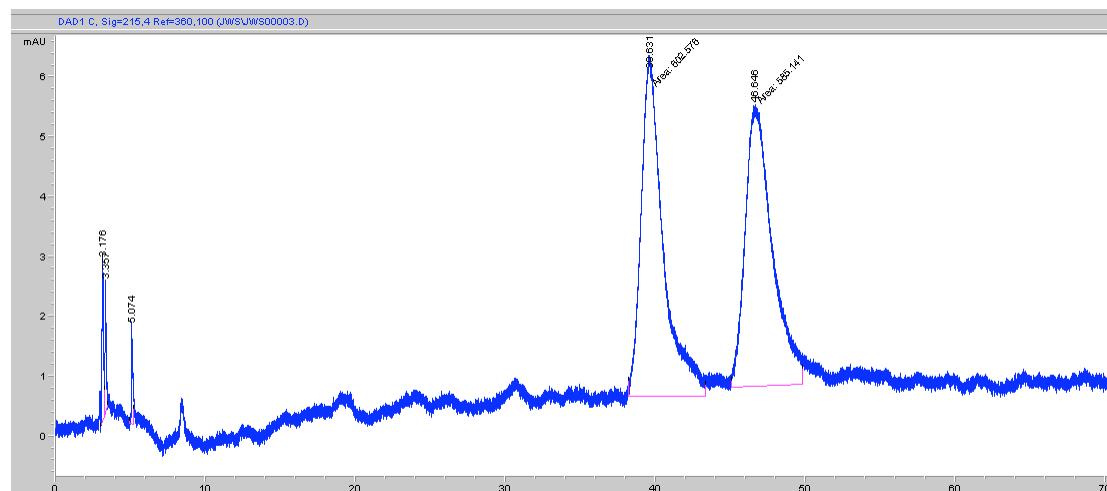


^1H NMR (CD_3OD 150 MHz) spectrum of aerophobin-1 (synthetic material)

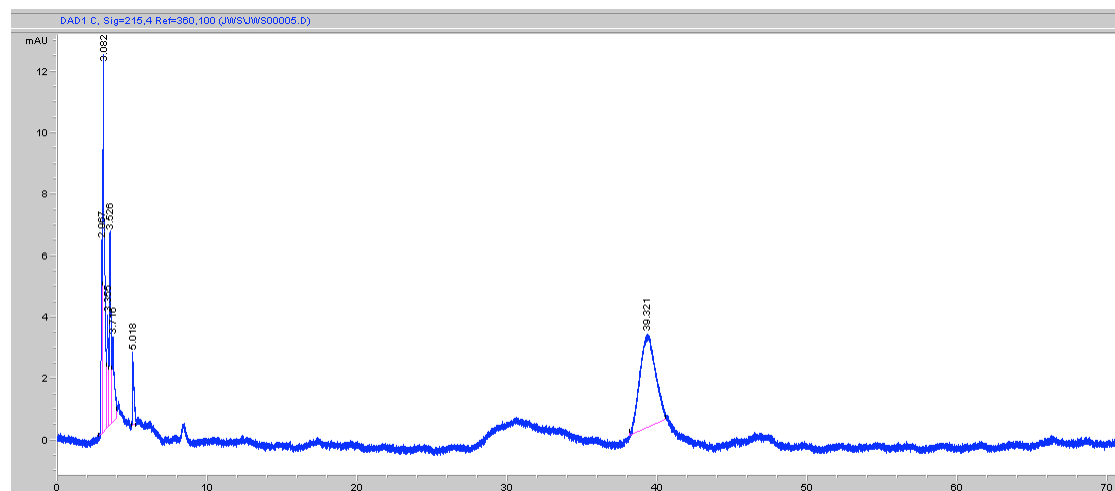
3.7.3 Analytical Chiral HPLC Traces

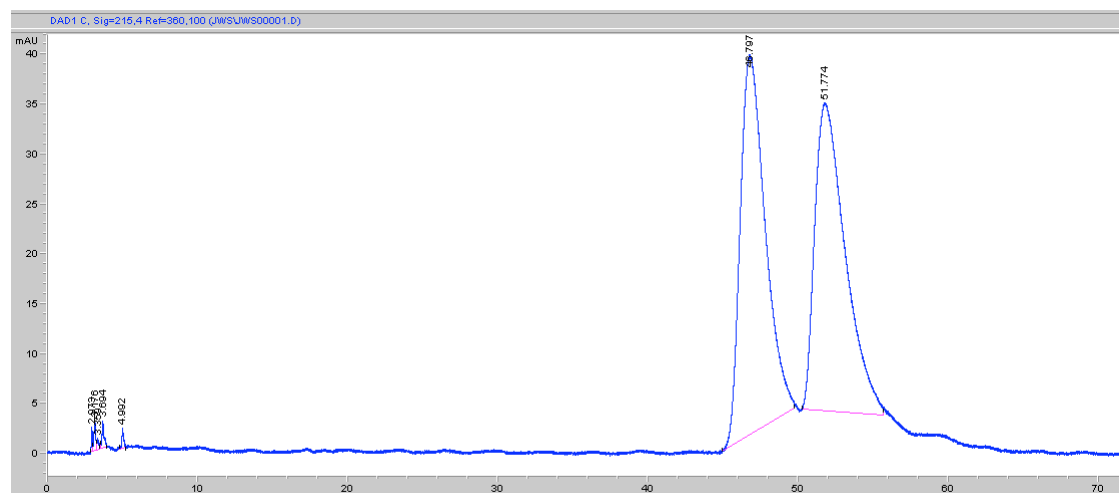
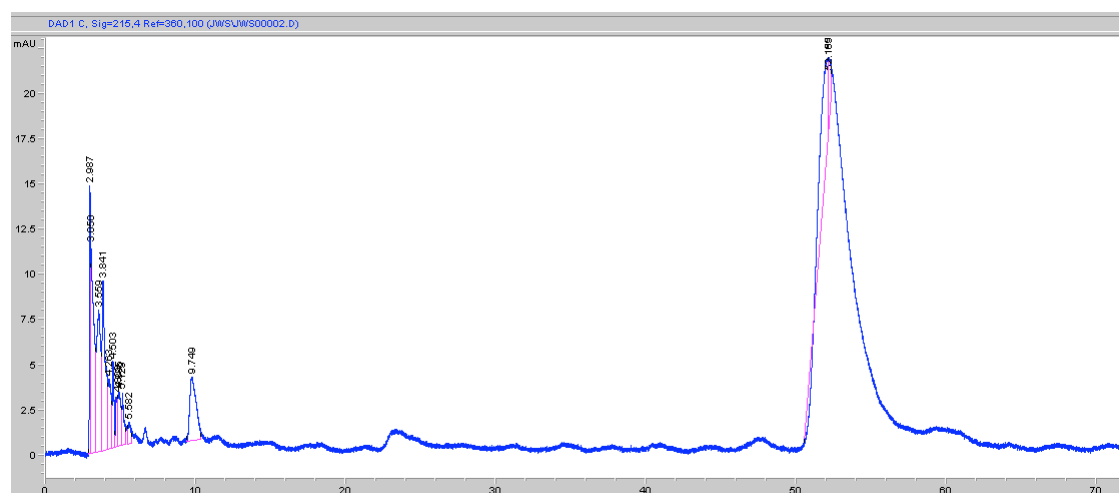
The following HPLC analyses were performed on an analytical CHIRALPAK AD-H column. Conditions: 10% *i*PrOH in hexane at a flow rate of 1 mL/min.

Trace for (\pm)-**16**

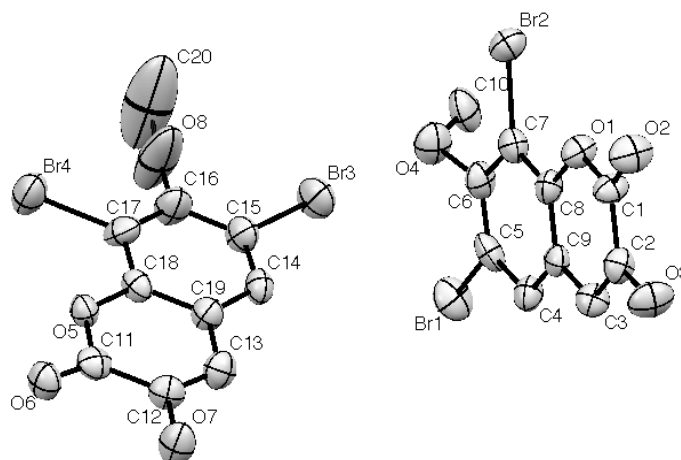


Trace for (+)-**16** synthesised from (+)-**18**



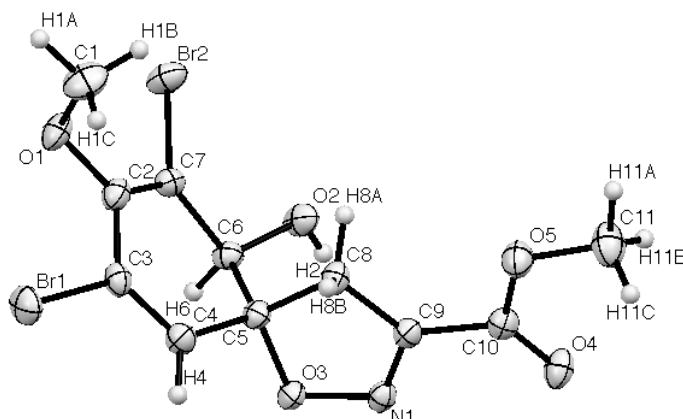
Trace for (±)-17*Trace for (–)-17 synthesised from (–)-18*

3.7.4 Crystal Structure Data

6,8-Dibromo-3-hydroxy-7-methoxy-2*H*-chromen-2-one (32)

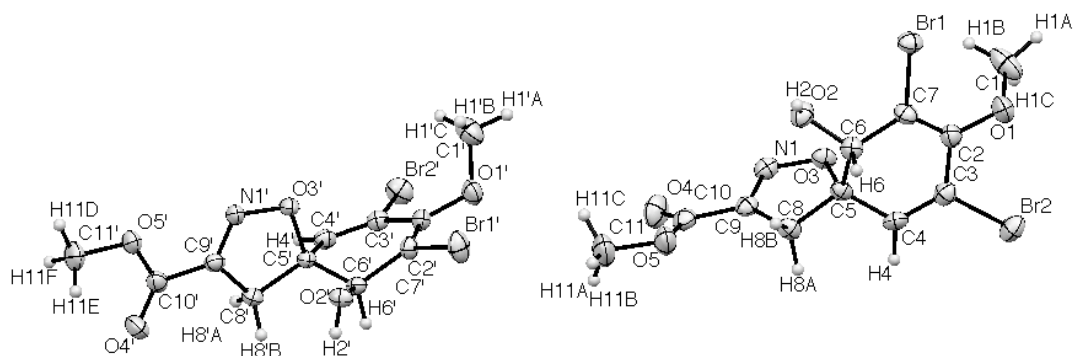
Crystal data and structure refinement for sl1037

| | |
|-----------------------------------|--|
| Identification code | sl1037 |
| Empirical formula | C ₁₀ H ₆ Br ₂ O ₄ |
| Formula weight | 349.97 |
| Temperature | 250(2) K |
| Wavelength | 0.71073 Å |
| Crystal system | Orthorhombic |
| Space group | Pna2(1) |
| Unit cell dimensions | a = 8.9710(2) Å α = 90° b = 10.6189(2) Å β = 90° c = 22.6185(6) Å γ = 90° |
| Volume | 2154.69(8) Å ³ |
| Z | 8 |
| Density (calculated) | 2.158 Mg/m ³ |
| Absorption coefficient | 7.518 mm ⁻¹ |
| F(000) | 1344 |
| Crystal size | 0.28 × 0.05 × 0.05 mm ³ |
| Theta range for data collection | 2.12 to 27.47° |
| Index ranges | -11 ≤ h ≤ 11, -12 ≤ k ≤ 13, -18 ≤ l ≤ 28 |
| Reflections collected | 11137 |
| Independent reflections | 2504 [R(int) = 0.0477] |
| Completeness to theta = 27.47° | 98.9% |
| Absorption correction | Semi-empirical from equivalents |
| Max. and min. transmission | 0.734 and 0.464 |
| Refinement method | Full-matrix least-squares on F ² |
| Data / restraints / parameters | 2504 / 1 / 291 |
| Goodness-of-fit on F ² | 1.074 |
| Final R indices [I > 2σ(I)] | R1 = 0.0462, wR2 = 0.1169 |
| R indices (all data) | R1 = 0.0587, wR2 = 0.1354 |
| Largest diff. peak and hole | 1.430 and -0.968 e. Å ⁻³ |

(5*S,10*R**)-Methyl 7,9-dibromo-10-hydroxy-8-methoxy-1-oxa-2-azaspiro[4.5]deca-2,6,8-triene-3-carboxylate (21)**

Crystal data and structure refinement for sl1040

| | |
|-----------------------------------|--|
| Identification code | sl1040 |
| Empirical formula | C ₁₁ H ₁₁ Br ₂ NO ₅ |
| Formula weight | 397.03 |
| Temperature | 180(2) K |
| Wavelength | 0.71073 Å |
| Crystal system | Triclinic |
| Space group | P-1 |
| Unit cell dimensions | a = 6.5189(1) Å α = 65.732(1)° b = 10.7194(2) Å β = 77.573(1)° c = 11.0482(2) Å γ = 80.693° |
| Volume | 684.99(2) Å ³ |
| Z | 2 |
| Density (calculated) | 1.925 Mg/m ³ |
| Absorption coefficient | 5.932 mm ⁻¹ |
| F(000) | 388 |
| Crystal size | 0.21 × 0.12 × 0.07 mm ³ |
| Theta range for data collection | 3.51 to 33.74° |
| Index ranges | -10 ≤ h ≤ 10, -16 ≤ k ≤ 16, -17 ≤ l ≤ 17 |
| Reflections collected | 12983 |
| Independent reflections | 5457 [R(int) = 0.0494] |
| Completeness to theta = 33.74° | 99.4% |
| Absorption correction | Semi-empirical from equivalents |
| Max. and min. transmission | 0.663 and 0.447 |
| Refinement method | Full-matrix least-squares on F ² |
| Data / restraints / parameters | 5457 / 0 / 177 |
| Goodness-of-fit on F ² | 1.010 |
| Final R indices [I > 2σ(I)] | R1 = 0.0379, wR2 = 0.0876 |
| R indices (all data) | R1 = 0.0590, wR2 = 0.0972 |
| Largest diff. peak and hole | 0.590 and -1.088 e. Å ⁻³ |

(5*S,10*S**)-Methyl 7,9-dibromo-10-hydroxy-8-methoxy-1-oxa-2-azaspiro[4.5]deca-2,6,8-triene-3-carboxylate (21a)**

Crystal data and structure refinement for sl1041

| | |
|-----------------------------------|--|
| Identification code | sl1041 |
| Empirical formula | C ₁₁ H ₁₁ Br ₂ NO ₅ |
| Formula weight | 397.03 |
| Temperature | 180(2) K |
| Wavelength | 0.71073 Å |
| Crystal system | Monoclinic |
| Space group | P-2(1)/c |
| Unit cell dimensions | a = 10.9772(1) Å α = 90° b = 25.2605(3) Å β = 104.60(3)° c = 10.1567(2) Å γ = 90° |
| Volume | 2725.4(3) Å ³ |
| Z | 8 |
| Density (calculated) | 1.935 Mg/m ³ |
| Absorption coefficient | 5.963 mm ⁻¹ |
| F(000) | 1552 |
| Crystal size | 0.23 × 0.12 × 0.05 mm ³ |
| Theta range for data collection | 3.55 to 30.97° |
| Index ranges | -15 ≤ h ≤ 15, -36 ≤ k ≤ 36, -14 ≤ l ≤ 14 |
| Reflections collected | 30388 |
| Independent reflections | 8610 [R(int) = 0.0660] |
| Completeness to theta = 30.97° | 99.3% |
| Absorption correction | Semi-empirical from equivalents |
| Max. and min. transmission | 0.737 and 0.400 |
| Refinement method | Full-matrix least-squares on F ² |
| Data / restraints / parameters | 8610 / 0 / 347 |
| Goodness-of-fit on F ² | 1.014 |
| Final R indices [I > 2sigma(I)] | R1 = 0.0471, wR2 = 0.0928 |
| R indices (all data) | R1 = 0.0937, wR2 = 0.1063 |
| Largest diff. peak and hole | 0.988 and -0.631 e. Å ⁻³ |

3.8 References

- ¹ M. I. Abou-Shoer, L. A. Shaala, D. T. A. Youssef, J. M. Badr and A-A. M. Habib, *J. Nat. Prod.*, **2008**, *71*, 1464.
- ² E. Fattorusso, L. Minale, G. Sodano, K. Moody, and R. H. Thomson, *Chem. Commun.*, **1970**, 752.
- ³ K. Moody, R. H. Thomson, E. Fattorusso, L. Minale and G. Sodano, *J. Chem. Soc., Perkin Trans. 1*, **1972**, 18.
- ⁴ J. A. McMillan, I. C. Paul, Y. M. Goo and K. L. Rinehart Jr., *Tetrahedron Lett.*, **1981**, 22, 39.
- ⁵ L. Minale, *Pure Appl. Chem.*, **1976**, *48*, 7.
- ⁶ J. Kobayashi, K. Honma, T. Sasaki and M. Tsuda, *Chem. Pharm. Bull.*, **1995**, *43*, 403.
- ⁷ A. Benharref, M. Païs and C. Debitus, *J. Nat. Prod.*, **1996**, *59*, 177.
- ⁸ L. Rahbæk and C. Christophersen, *The Alkaloids*, **2001**, *57*, 185.
- ⁹ N. Takada, R. Watanabe, K. Suenaga, K. Yamada, K. Ueda, M. Kita and D. Uemura, *Tetrahedron Lett.*, **2001**, *42*, 5265.
- ¹⁰ I. Hayakawa, T. Teruya and H. Kigoshi, *Tetrahedron Lett.*, **2006**, *47*, 155.
- ¹¹ M. Kita, Y. Tsunematsu, I. Hayakawa and H. Kigoshi, *Tetrahedron Lett.*, **2008**, *49*, 5383.
- ¹² A. L. Acosta and A. D. Rodríguez, *J. Nat. Prod.*, **1992**, *55*, 1007.
- ¹³ Y. Gopichand and F. J. Schmitz, *Tetrahedron Lett.*, **1979**, *20*, 3921.
- ¹⁴ J. N. Tabudravu and M. Jaspars, *J. Nat. Prod.*, **2002**, *65*, 1798.
- ¹⁵ F. Hentschel and T. Lindel, *Synthesis*, **2010**, 181.
- ¹⁶ A. Aiello, E. Fattorusso, M. Menna and M. Pansini, *Biochem. Syst. Ecol.*, **1995**, *23*, 377.
- ¹⁷ G. Zhu, F. Yang, R. Balachandran, P. Höök, R. B. Vallee, D. P. Curran and B. W. Day, *J. Med. Chem.*, **2006**, *49*, 2063.
- ¹⁸ M. Murakata, M. Tamura and O. Hoshino, *J. Org. Chem.*, **1997**, *62*, 4428.
- ¹⁹ T. Ogamino, R. Obata and S. Nishiyama, *Tetrahedron Lett.*, **2006**, *47*, 727.
- ²⁰ E. Erlenmeyer, *Justus Liebigs Ann. Chem.*, **1893**, *275*, 1.
- ²¹ B. M. Chanda and R. S. Sulake, *Tetrahedron Lett.*, **2005**, *46*, 6461; P. Busca, F. Paradisi, E. Moynihan, A. R. Maguire and P. C. Engel, *Org. Biomol. Chem.*, **2004**, *2*, 2684.

- 22 N. Kotoku, H. Tsujita, A. Hiramatsu, C. Mori, N. Koizumi and M. Kobayashi, *Tetrahedron*, **2005**, 61, 7211.
- 23 S. Nishiyama and S. Yamamura, *Tetrahedron Lett.*, **1983**, 24, 3351
- 24 T. Ogamino, Y. Ishikawa and S. Nishiyama, *Heterocycles*, **2003**, 61, 73.
- 25 T. R. Boehlow, J. J. Harburn and C. D. Spilling, *J. Org. Chem.*, **2001**, 66, 3111.
- 26 M. Murakata, K. Yamada and O. Hoshino, *Tetrahedron*, **1996**, 52, 14713.
- 27 J. J. Harburn, N. P. Rath and C. D. Spilling, *J. Org. Chem.*, **2005**, 70, 6398.
- 28 W. J. Gensler, F. A. Johnson and D. B. Sloan, *J. Am. Chem. Soc.*, **1960**, 82, 6074.
- 29 S. Nishiyama and S. Yamamura, *Bull. Chem. Soc. Jap.*, **1985**, 58, 3453.
- 30 G. Bartoli, M. Bosco, A. Carlone, M. Locatelli, E. Marcantoni, P. Melciorre, P. Palazzo and L. Sambri, *Eur. J. Org. Chem.*, **2006**, 4429.
- 31 P. Ciminiello, V. Costantino, E. Fattorusso, S. Magno, A. Mangoni and M. Pansini, *J. Nat. Prod.*, **1994**, 57, 705.
- 32 E. A. Santalova, V. A. Denisenko and V. A. Stonik, *Nat. Prod. Commun.*, **2010**, 5, 377; M. S. Buchanan, A. R. Carroll, D. Wessling, M. Jobling, V. M. Avery, R. A. Davis, Y. Feng, J. N. A. Hooper and R. J. Quinn, *J. Nat. Prod.*, **2009**, 72, 973; P. Ciminiello, C. Dell'Aversano, E. Fattorusso, S. Magno and M. Pansini, *J. Nat. Prod.*, **2000**, 63, 263; R. Mierzwa, A. King, M. A. Conover, S. Tozzi, M. S. Puar, M. Patel and S. J. Coval, *J. Nat. Prod.*, **1994**, 57, 175; M. Gunasekera and S. P. Gunasekera, *J. Nat. Prod.*, **1989**, 52, 753; G. Cimino, S. De Rosa, S. De Stefano, R. Self and G. Sodano, *Tetrahedron Lett.*, **1983**, 24, 3029.
- 33 A. Ozanne-Beaudenon, T. Buffeteau, D. Cavagnat and A. Chenede, *Angew. Chem. Int. Ed.*, **2009**, 48, 4605; S. M. Altermann, R. D. Richardson, T. K. Page, R. K. Schmidt, E. Holland, U. Mohammed, S. M. Paradine, A. N. French, C. Richter, A. M. Bahar, B. Witulski and T. Wirth, *Eur. J. Org. Chem.*, **2008**, 5315.
- 34 T. Dohi, A. Maruyama, N. Takenaga, K. Senami, Y. Minamitsuji, H. Fujioka, S. B. Caemmerer and Y. Kita, *Angew. Chem. Int. Ed.*, **2008**, 47, 3787.
- 35 M. Uyanik, T. Yasui and K. Ishihara, *Angew. Chem. Int. Ed.*, **2010**, 49, 2175; M. Uyanik, T. Yasui and K. Ishihara, *Tetrahedron*, **2010**, 66, 5841.

-
- ³⁶ R. Córdoba, N. Salvador Tormo, A. F. Medarde and Plumet, J. *Bioorg. Med. Chem.*, **2007**, *15*, 5300.

CHAPTER 4

Towards the Total Syntheses of the Ceratamines

Compound Numbering

In this chapter, the atoms of the ceratamines are numbered according to the system outlined by Andersen and co-workers (Figure 37).¹

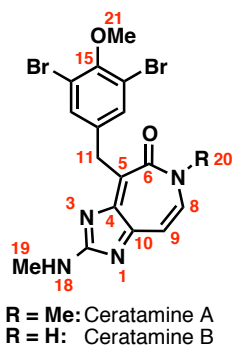


Figure 37 Atom labeling of ceratamine A and B.

4.1 Introduction

Currently, total synthesis represents the only feasible method to obtain sufficient quantities of the ceratamines (Figure 38) for further biological evaluation because, due to their low abundance from the natural source, re-harvesting the reef organism would inevitably have a negative ecological impact on the environment. Embarking on a total synthesis also provides the opportunity to develop new synthetic methods towards the construction of these unique molecules.

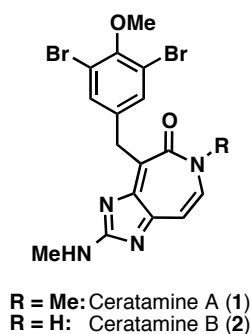


Figure 38 Structure of Ceratamine A (**1**) and B (**2**).

The unprecedented structures of **1** and **2** along with their novel biological activity have garnered interest within the scientific community. During the course of this project the Coleman group disclosed the total syntheses of ceratamines A and B, and the Andersen group described the preparation of several ceratamine analogues. This research is reviewed in Sections 4.1.2 and 4.1.3.

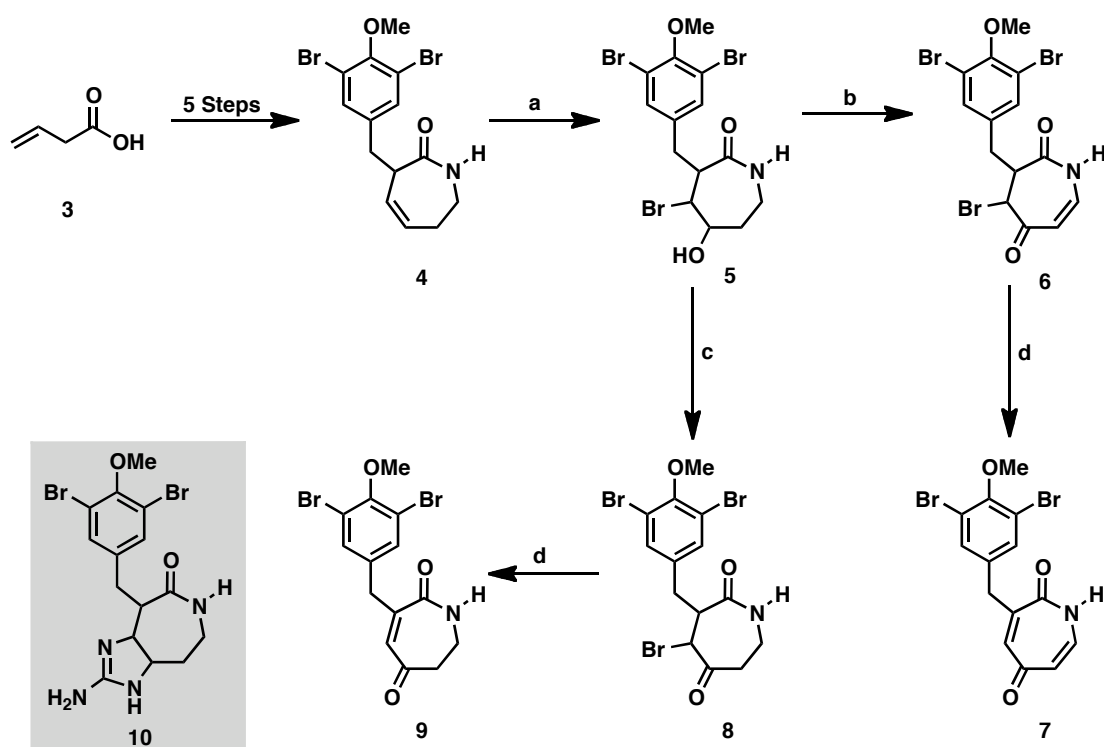
4.1.2 Andersen Group Approaches to the Ceratamines

Andersen and co-workers have investigated synthetic strategies towards the ceratamines ever since they were identified as a potential lead structure for the development of a novel class of microtubule-stabilising agents. Ultimately, these synthetic investigations, while not providing access to the natural products, have produced synthetic analogues that have proved valuable in gaining insight into the ceratamine A pharmacophore. The details of this SAR study will be discussed in Section 4.1.4.

4.1.2.1 First-Generation Approach

The first-generation approach proposed by Andersen and co-workers was to construct the heterocyclic core of the ceratamines by appending the aminoimidazole moiety onto a functionalised azepine ring.² If successful, it was envisaged that oxidation of the intermediate **10** (Scheme 46) would be favoured as the fully dehydrogenated core present in the natural products is thought to have an aromatic character.

Initially, five steps were required to convert commercially available butenoic acid (**3**) to caprolactam **4** (Scheme 46). Treatment of **4** with NBS followed by opening of the bromonium ion with water gave bromohydrin **5** in 98% yield. At this stage, oxidation of **5** to the corresponding α -bromoketone was performed with either DMP or IBX to furnish bromoenamide **6** and the fully saturated **8**, respectively. Disappointingly, all attempts to condense guanidine derivatives with **6** and **8** only gave the eliminated products **7** and **9**, respectively, albeit in good yield. Eventually, it was possible to access **10** *via* an alternative route (not shown), however, difficulties associated with its purification and instability led to this strategy being abandoned.



Scheme 46 First-generation strategy by Andersen and co-workers.

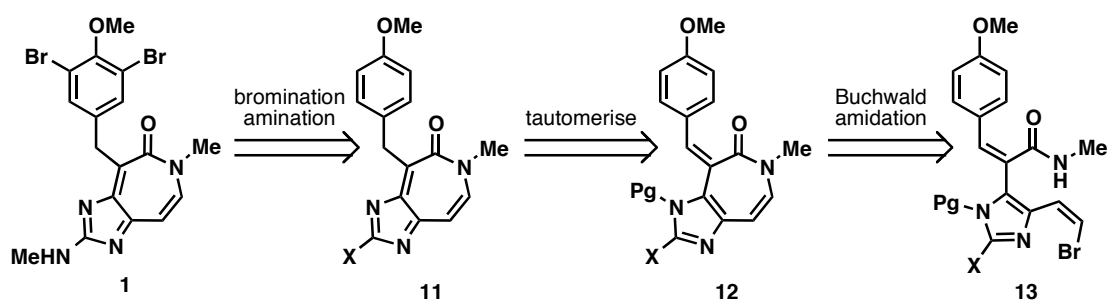
Reagents and conditions: (a) NBS, acetone/H₂O (3:1), rt, 72 h, 98%; (b) DMP, CH₂Cl₂, rt, 24 h, 98%; (c) IBX, DMSO, rt, 5 h, 84%; (d) guanidine HCl or acetylguanidine, DMF, rt, 48 h, 7, 71%; 9, 87%.

4.1.2.2 Second-Generation Approach

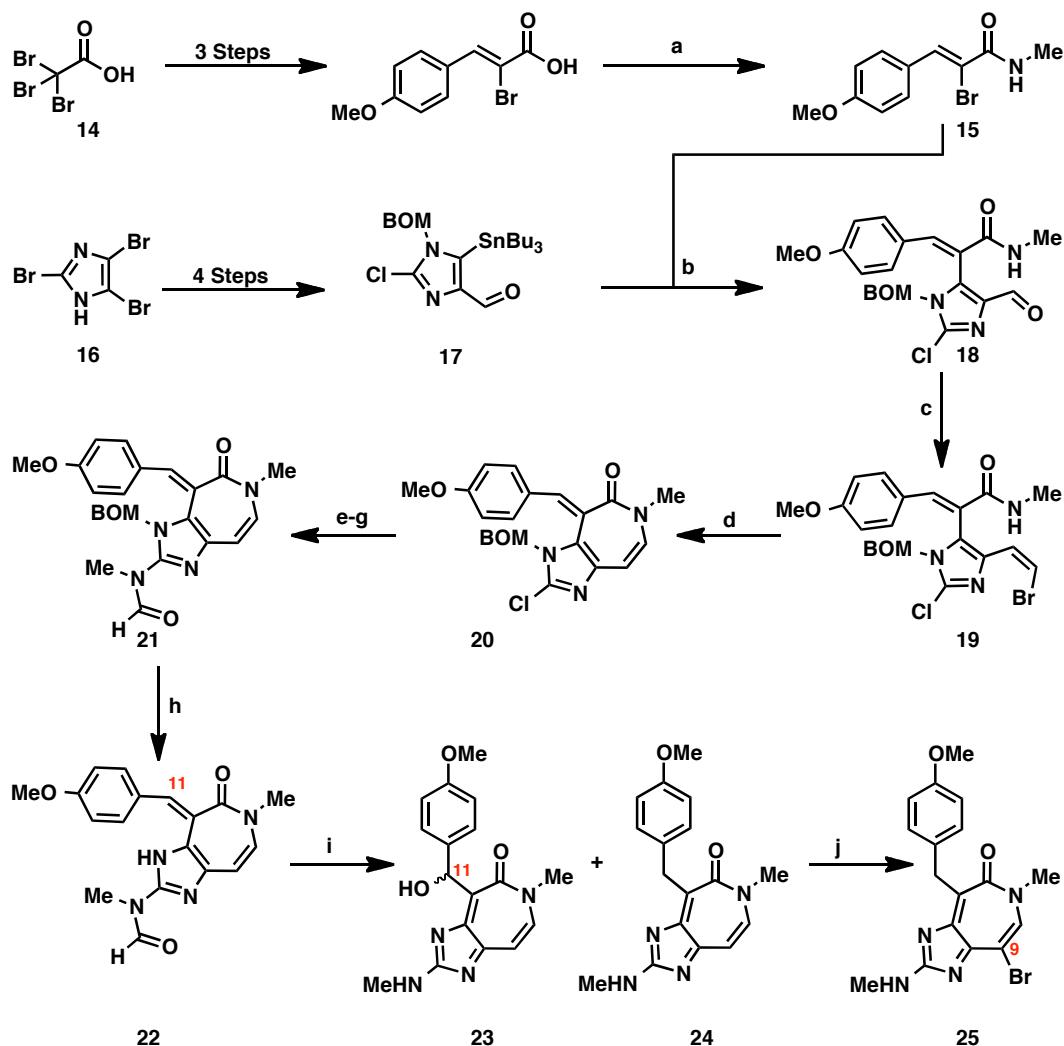
In light of the problems surrounding the feasibility of grafting the aminoimidazole ring to a preformed azepine, the second-generation approach aimed to construct the azepine ring onto a pre-existing imidazole. It was envisaged that this could be achieved by the intramolecular Buchwald vinyl amidation of a suitably functionalised precursor (**13**) (Scheme 47). With similar foresight to the first approach, it was expected that upon removal of the protecting group in **12**, tautomerisation would occur to give the more thermodynamically stable product, **11**. Late stage installation of the amino substituent and bromine functionality (given the difficulty in working with aminoimidazoles* and the tolerance of C-Br bonds to the planned transition metal chemistry) would give ceratamine A (**1**).†

* Compounds possessing 2-aminoimidazoles are notoriously problematic to carry through multiple synthetic manipulations due to their intractability, poor solubility, and reactivity.

† It is worth mentioning that this route was designed to give access to ceratamine A, the more active member of the family.



Scheme 47 Second-generation retrosynthesis by Andersen and co-workers.



Scheme 48 Second-generation strategy by Andersen and co-workers.

Reagents and conditions: (a) i) DIC, HOBT, DMAP, CH₂Cl₂, 0 °C to rt, 1 h; ii) MeNH₂, THF, 10 min, 95%; (b) Pd(PPh₃)₄, CuI, THF, rt, 20 h, 73%; (c) (bromomethyl)triphosponium bromide, KO^tBu, −78 °C, then **18**, 30 min, 80%; (d) CuI, Cs₂CO₃, DMEDA, THF, 70 °C, 20 h, 85%; (e) Ph₃SiNH₂, Pd₂(dba)₃, XPhos, LiHMDS, PhMe, 100 °C, 1 h; (f) acetic formic anhydride, DMAP, THF, rt, 24 h, 54%; (g) MeI, K₂CO₃, DMF, rt, 24 h, 48% over 3 steps; (h) AlCl₃, CH₂Cl₂, rt, 30 min; (i) HCl_(g), 1,4-dioxane/H₂O (1:1), 0 °C, 3 min, **25**, 25% over 2 steps; (j) Br₂, AcOH, rt, 1 h, 43%.

The stannane **17** and cinnamidyl bromide **15** required for synthesis of aldehyde **18** were readily accessible from commercially available tribromoacetic acid (**14**) and 2,4,5-tribromoimidazole (**16**), respectively (Scheme 48). Stille coupling of these partners at room temperature furnished **18** in good yield and this could then be converted to the desired *Z*-vinyl bromide amidation precursor **19** by a Stork–Zhao olefination. The pivotal copper(I)-catalysed intramolecular coupling between the *Z*-vinyl bromide and *N*-methyl amide functionalities in **19** proceeded in excellent yield to furnish the 2-chloroimidazo[4,5-*d*]azepine **20**.

A three-step procedure installed the *N*-methylformamide which was required to mask the problematic 2-aminoimidazole functionality. The chloride **20** was converted to the corresponding amine by heating with triphenylsilylamine and LiHMDS in the presence of Pd₂(dba)₃ and Buchwald's XPhos ligand. Formylation of the amine with acetic formic anhydride followed by *N*-methylation of the secondary formamide gave **21** in a 48% yield over the 3 steps. Next, removal of the BOM group with AlCl₃ was presumed to have occurred cleanly (by TLC and HRMS) to give **22** although the structure could not be explicitly confirmed by ¹H NMR due to its rotameric nature.

The penultimate step of removing the *N*-formyl group proved problematic. Prior mechanistic studies had indicated that once unmasked, the molecule could be oxidised at C-11 by atmospheric oxygen because of the electron-donating ability of the 2-amino substituent. After extensive experimentation, it was found that sparging dry HCl gas through a solution of **22** in 1,4-dioxane/water (1:1) gave the desired desbromoceratamine A (**24**) in 25% yield with the formation of only minimal amounts of the C-11 oxygenated product **23**. Attempts to convert **23** to **24** *via* hydrogenolysis and Barton deoxygenation procedures resulted in decomposition.

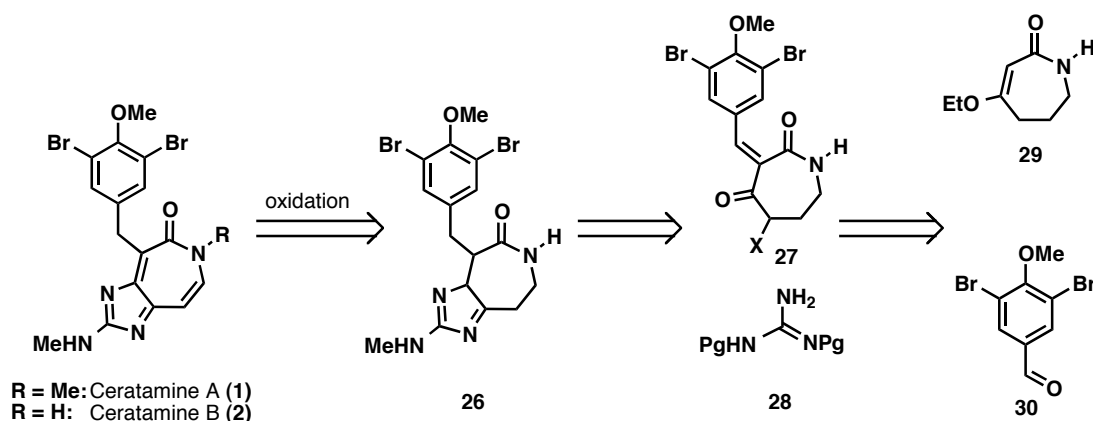
The final stage *bis*-bromination of **24** required to give ceratamine A (**1**) could not be achieved; two equivalents of NBS or Br₂/AcOH gave the 9-monobrominated compound **25** and the use of excess amounts of bromine led to complex mixtures. This highlights the fallible nature of a late-stage bromination strategy on a highly electron rich system and is an important consideration when attempting to synthesise such compounds.

Despite these approaches failing to deliver the targeted natural product the value of total synthesis is evident as it has been possible to access molecules with

modifications that are inaccessible by traditional medicinal chemistry approaches. More recently, a variation on the second-generation route has been used for the synthesis of ceratamine analogues (see Section 4.1.4).³

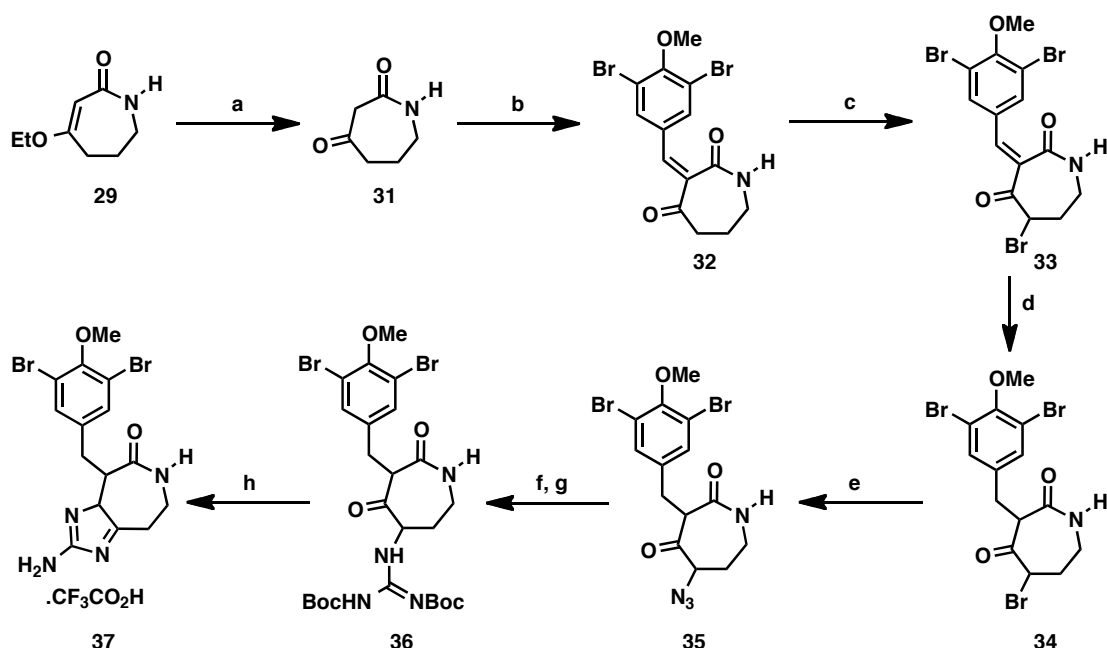
4.1.3 Coleman Group Total Synthesis

To date, the only successful total synthesis of the ceratamines was reported by Coleman and co-workers in 2009. To allow for a convergent synthesis and in a remarkably similar approach to the first-generation strategy of Andersen and co-workers, they planned to construct the imidazo[4,5-*d*]azepine ring system in **26** by a condensation reaction between an activated azepane-2,4-dione (**27**) and a nitrogen-based nucleophile such as the protected guanidine derivative **28** (Scheme 49). However, the success of this strategy hinged on the ability to perform an unprecedented double dehydrogenation to access the oxidation state required for the ceratamines.



Scheme 49 Coleman's retrosynthetic analysis of the ceratamines.

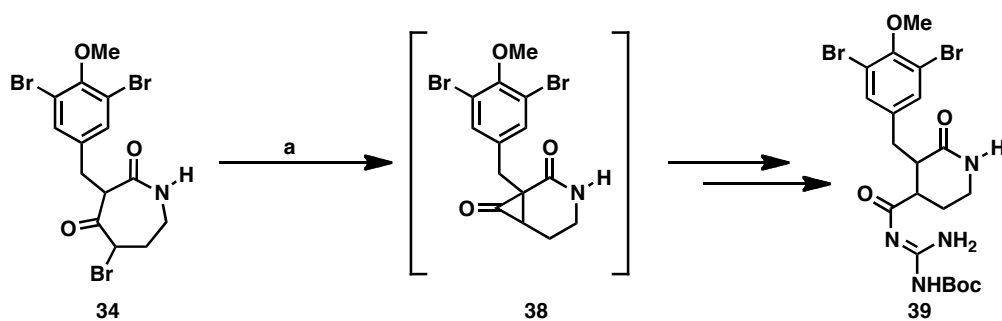
The synthesis commenced from known lactam **29**⁴ which could be readily hydrolysed under acidic conditions to hydroazepinedione **31** (Scheme 50). A subsequent Knoevenagel condensation with 3,5-dibromo-4-methoxybenzaldehyde (**30**) gave adduct **32** which was then brominated to furnish the α -bromoketone **33**. At this stage, attempts were made to append the imidazole ring by direct displacement of the bromide with *N*-Boc-guanidine but ultimately this proved unsuccessful as a competing Michael addition to C-11 took precedence over the desired substitution.

Scheme 50 Coleman's synthesis of **37**.

Reagents and conditions: (a) HCl (10% aq), acetone, rt, 12 h, quant; (b) **30**, AcOH, piperidine, CH₂Cl₂, 3 Å MS, rt, 4 h, quant; (c) NBS, Amberlyst-15, EtOAc, 48 h, 67%; (d) Hantzsch ester, EtOH/C₆H₆ (1:1), rt, 24 h, 88%; (e) NaN₃, DMSO, rt, 1 h, quant; (f) H₂, 5% Pd on BaSO₄, conc. HCl, MeOH, rt, 2 h; (g) HgCl₂, Et₃N, *bis*-Boc-*S*-methylisothiurea, 0 °C, 1 h, 74% over 2 steps; (h) TFA, CH₂Cl₂, rt, 1 h, quant.

In order to prevent this competing conjugate addition, α -bromoketone **33** was reduced to **34** using Hantzsch ester (diethyl-1,4-dihydro-2,6-dimethyl-3,5-pyridine carboxylate). Unexpectedly, reaction of this substrate (**34**) with *N*-Boc-guanidine did not lead to the desired imidazole annulation product but instead furnished guanidine amide **39** in 88% yield (Scheme 51). It is believed this occurred *via* a unprecedented Favorskii-type rearrangement whereby the protected guanidine promotes formation of an enolate which then cyclises to give the putative cyclopropanone **38**. Finally, nucleophilic addition of the guanidine breaks open the cyclopropanone to give **39**.

Coleman and co-workers were able to bypass this issue by converting bromide **34** to the corresponding azide **35** (Scheme 50). Following hydrogenolysis of the azide, condensation of the resulting primary amine with *bis*-Boc-protected *S*-methylisothiurea gave the desired annulation precursor **36**. Construction of the imidazo[4,5-*d*]azepine ring system was achieved by treatment with TFA which gave the trifluoroacetate salt **37** in quantitative yield.

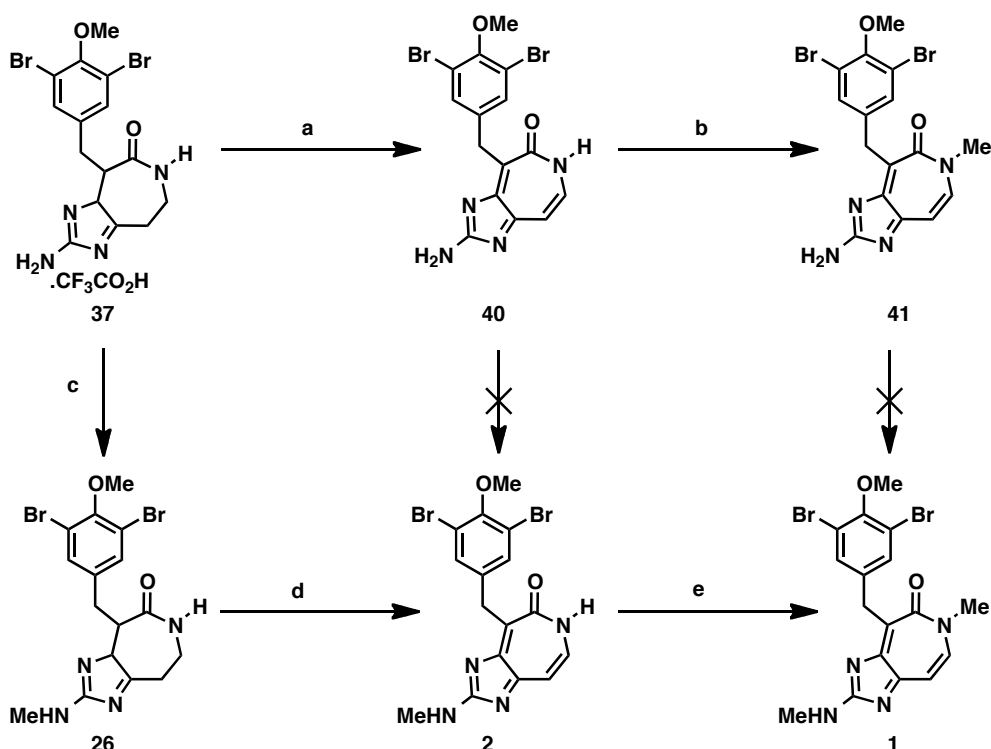


Scheme 51 Unprecedented Favorskii-type rearrangement.

Reagents and conditions: (a) *N*-Boc-guanidine, MeCN, 70 °C, 24 h, 88%.

With the heterocyclic framework now in place the major challenge that remained was how to effect the double dehydrogenation needed to obtain the fully oxidised ring system present in the ceratamine core. Ultimately, this was achieved by the treatment of **37** with IBX and pyridine in DMSO to give des-methyl ceratamine B (**40**) in excellent yield (Scheme 52). This could then be converted to des-methyl ceratamine A (**41**) by methylation of the lactam nitrogen. Unfortunately, installation of the *C*-19 methyl group by reductive alkylation failed due to the sensitive nature of the oxidised ring system to the reducing conditions. However, reversing the order of the transformations easily solved this problem. Treatment of **37** with triethylorthoformate followed by NaBH₄ reduction of the resulting ethyl formimidate afforded **26** which, upon oxidation with IBX, furnished ceratamine B (**2**) in 67% over the two steps. Finally, methylation of the lactam nitrogen provided ceratamine A (**1**).

In summary, this route represents the first and only total synthesis of both members of the ceratamine family. Starting from lactam **29**, the synthesis of **2** and **1** was achieved in 10 and 11 steps in an overall yield of 28% and 12%, respectively, thus belying the concise and efficient nature of this strategy.



Scheme 52 Synthesis of ceratamine A (**1**) and B (**2**).

Reagents and conditions: (a) IBX, DMSO, py, 35 °C, 1 h, 86%; (b) NaHMDS, DMF/THF (1:1), 0 °C, then MeI, −78 °C to −10 °C, 50%; (c) HC(OEt)₃, 80 °C, 5 h, then NaBH₄, 0 °C to 40 °C, 1 h; (d) IBX, DMSO, py, 35 °C, 1 h, 81%; (e) NaHMDS, DMF/THF (1:1), 0 °C, then MeI, −78 °C to −10 °C, 44%.

4.1.4 Ceratamine A Structure-Activity Relationship

Synthetic analogues of ceratamine A (**1**) were screened against MCF-7mp53 cells[‡] to evaluate their ability to arrest cells in a TG-3[§] cell-based assay.³ In this assay, the activity of ceratamine A (IC₅₀ ≈ 10.6 μM; 54% cells arrested in mitosis at optimal concentration)^{**} was used as the benchmark. Synthetic analogues **42** to **45** (Figure 39) were inactive, indicating that a fully planarised dehydrogenated core and a 2-*N*-methylamino substituent are required for activity. The desbromo analogues **46** and **47** that possess *C*-11 oxygenation were also completely inactive. Compound **48** which differed from the natural product by loss of the *C*-14/16 bromides and the 2-*N*-methylamino group showed no activity. Desbromoceratamine A (**24**) was the only member in the series that caused significant mitotic arrest (20%) albeit at a high

[‡] A breast cancer cell line expressing a p53 mutation which can inactivate endogenous p53 (a tumour suppressor gene) in a dominant-negative fashion.

[§] A monoclonal antibody that has an affinity for mitotically phosphorylated nucleolin and can therefore be used to identify mitotic cells (*Cancer Res.*, **2000**, *60*, 5052).

^{**} The optimal concentration of 25 μg/mL is independent of the IC₅₀ value and was used by Andersen and co-workers to compare efficacies of the tested compounds.

concentration (160 μM), indicating that the bromine atoms were necessary to impart the full biological activity.

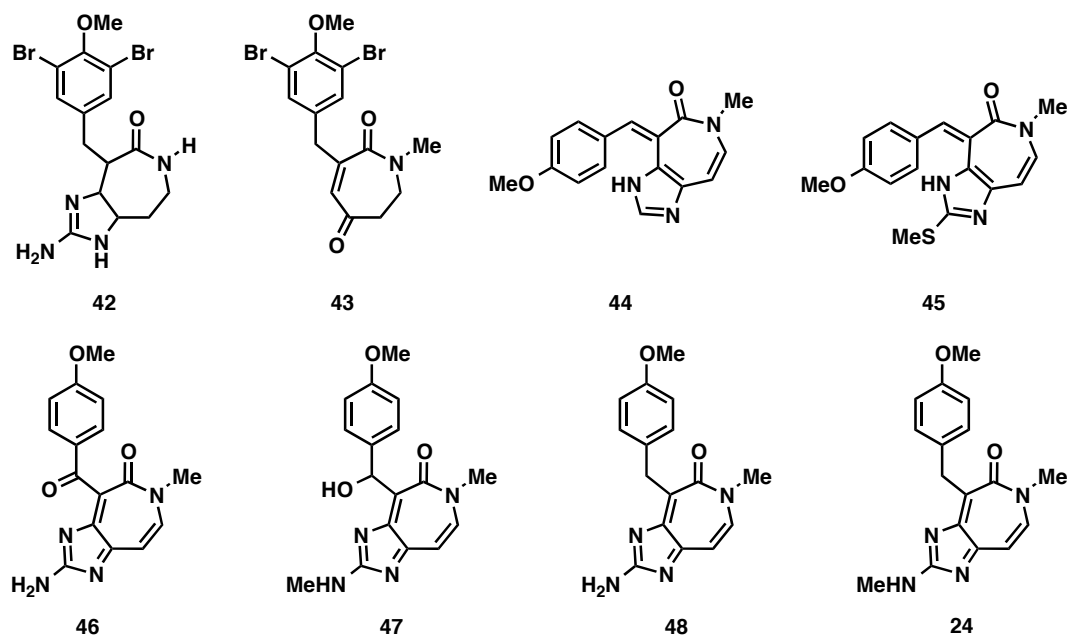


Figure 39 Structures of ceratamine A analogues.

To explore the role of bromine further, Andersen and co-workers sought initially to substitute the bromines in **1** for a moiety possessing similar steric bulk—hypothesising that the bromines were exploiting pockets of space in the binding site. As a methyl group aptly fitted this criteria (Van der Waals radius of 1.80 Å *cf.* 1.86 Å for bromine) a small library of compounds containing a 3,5-dimethyl-4-methoxy aryl motif (Figure 40) was synthesised. Indeed, the dimethyl analogue **49** ($\text{IC}_{50} \approx 10.3 \mu\text{M}$; 67% cells arrested in mitosis at optimal concentration) had comparable activity to the natural product. The analogues **51** (lacking the 2-*N*-methyl substitution), **52** (*C*-11 hydroxylated) and **53** (acylated at *N*-2) were all inactive, giving further evidence that *N*-2 methylation is required and *C*-11 functionalisation is not tolerated. However, the dimethyl analogue **50** exhibited the greatest antimitotic activity ($\text{IC}_{50} \approx 8.5 \mu\text{M}$; 82% cells arrested in mitosis at optimal concentration) of all the ceratamine compounds. More importantly, **50** was easier to synthesise than **49** and consequently has been selected as a candidate for *in vivo* mouse models; however, the results of this study are yet to be disclosed.

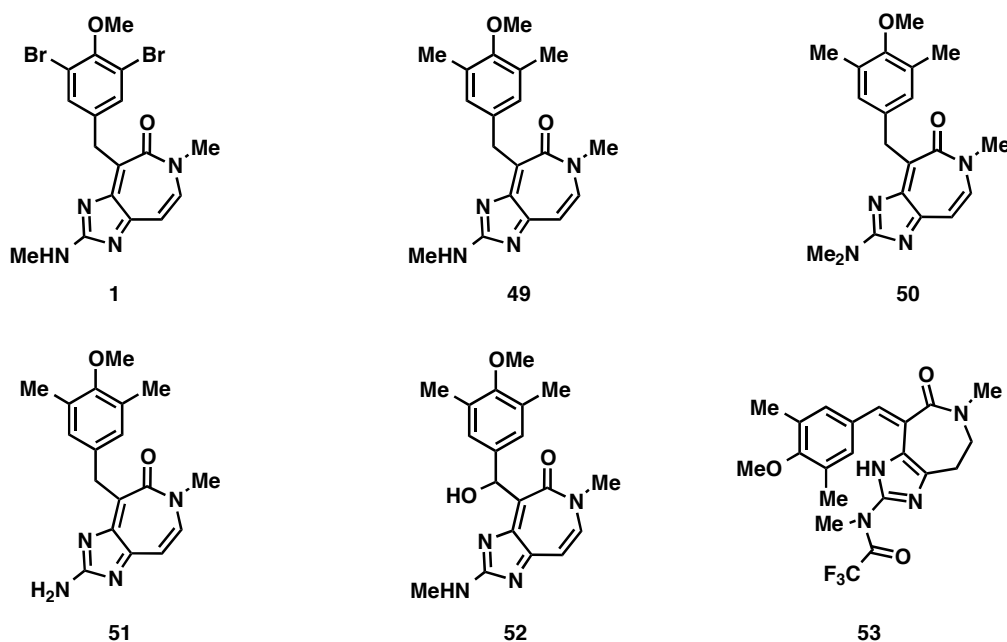


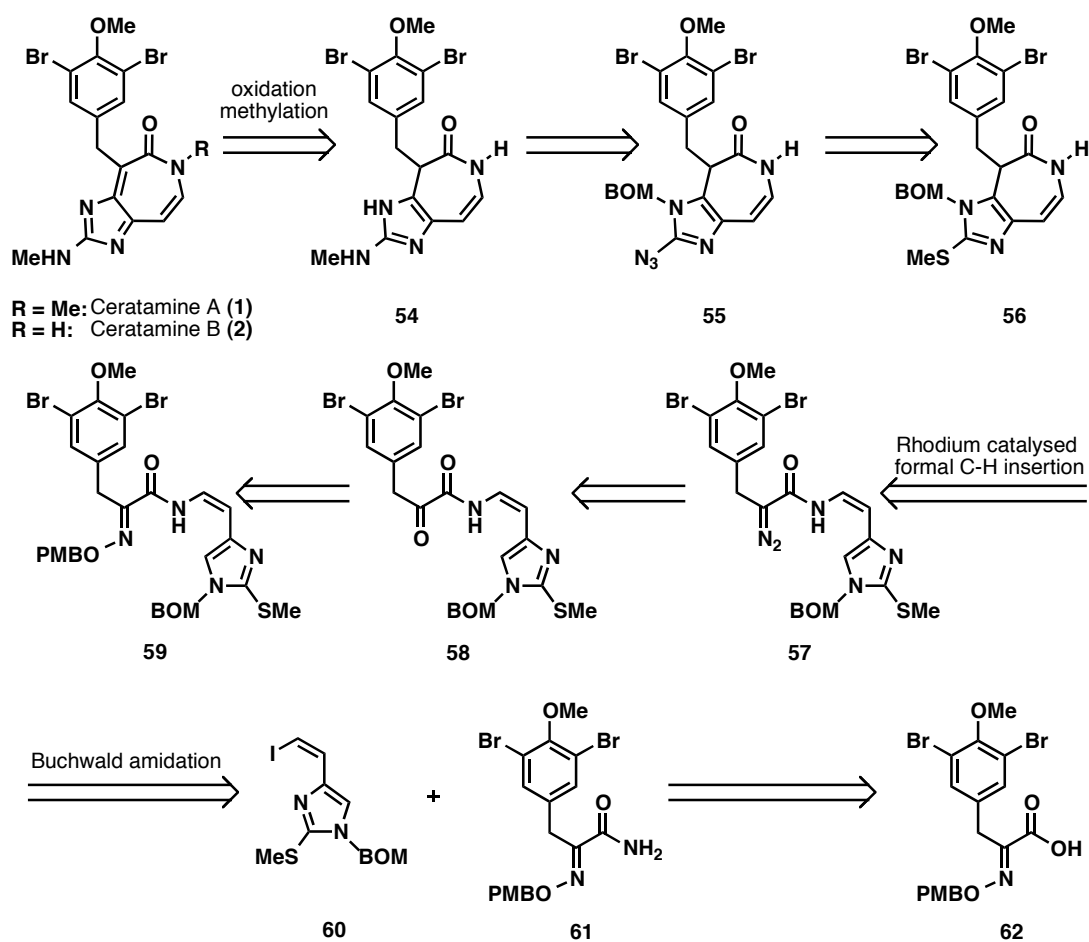
Figure 40 Dimethylated analogues of the ceratamines.

4.1.5 Ley Group Strategy

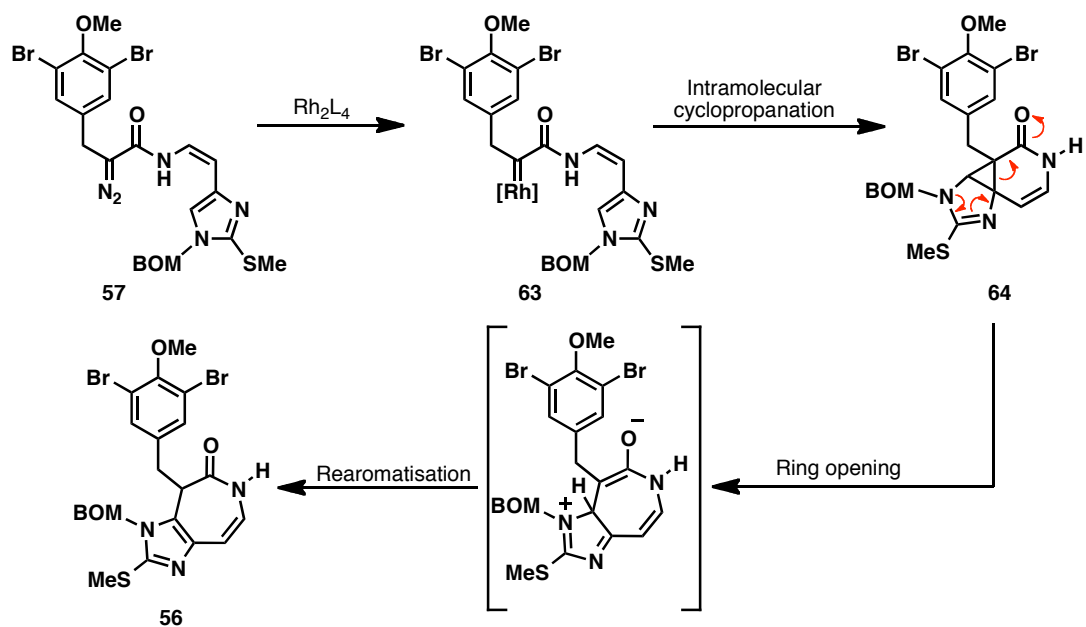
As highlighted in the previous sections, it was envisaged that the most challenging aspect of the ceratamine synthesis would be the construction of the heterocyclic core. Taking inspiration from the proposed biosynthesis of the ceratamines (Section 1.3.4) the Ley group strategy hinged on an ambitious intramolecular cyclisation between C-4 and C-5 to form the core heterocycle. Importantly, it was planned that the cyclisation precursor (**57**) would also contain the fully elaborated 3,5-dibromo-4-methoxyaryl appendage which would therefore negate the need for late stage installation of the bromine substituents.

We planned to synthesise the cyclisation precursor **57** from the same α -oximino acid (**62**) that was used for the synthesis of (5)-bromoverongamine, ianthelline, and JBIR-44 in Chapter 2 (Scheme 53). A proposed Buchwald amidation⁵ between the known vinyl iodide **60**⁶ and primary amide **61** would furnish the *Z*-enamide **59**.^{††} Then, unmasking of the α -keto amide **58** and subsequent treatment with tosylhydrazine and base should furnish the α -diazo carbonyl cyclisation precursor **57**.

^{††} It should be noted that since this route was designed prior to the disclosure of the IBX-mediated double dehydrogenation (Scheme 52), we planned to install the C-8/C-9 unsaturation prior to cyclisation despite the fact that increasing the rigidity of the molecule may hinder the proposed cyclisation.



Scheme 53 Ley group retrosynthetic analysis of the ceratamines.



Scheme 54 Proposed mechanism for the key step.

With the stage set for the key step, it was anticipated that following generation of an electrophilic Rh(II) carbenoid species (**63**), a Buchner-type cyclopropanation^{††} would occur between the imidazole olefin and the electrophilic centre of the carbenoid α -carbon atom (Scheme 54).⁷ It was then envisaged that ring-opening of the cyclopropane (**62**) and subsequent rearomatisation would give the desired product **56**. This ring-opening would be favoured due to the electron donating imidazole and the electron accepting carbonyl functionality in the vicinal positions of the cyclopropane. Of relevance to this, a recent theoretical study of ring-enlargement reactions of donor-acceptor cyclopropanes revealed that the transition state energy for this process is dramatically lowered with more electron-donating and withdrawing vicinal substituents.⁸

Commencing the final steps, conversion of the methyl thioether **56** to azide **55**, which following reduction, methylation and removal of the BOM protecting-group would give **54**. Lastly, oxidation of the ring system would furnish ceratamine B (**2**) that in turn could be converted to ceratamine A (**1**) by methylation of the amide nitrogen.

4.2 Results and Discussion

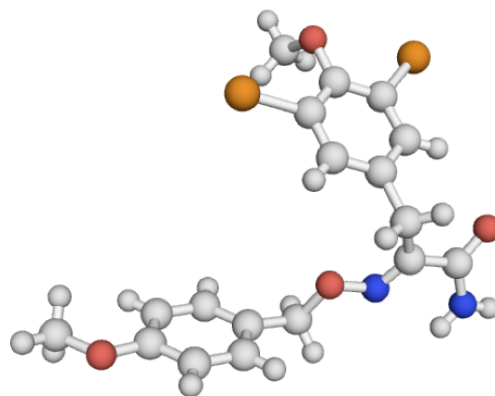
A number of conditions were screened in an effort to find a convenient and high yielding method to convert the α -oximino acid **62** to the primary amide coupling partner **61** (Table 10). It is known that benzoic and aliphatic acids can be converted to the corresponding amides by heating them in the presence of urea and imidazole under microwave irradiation.⁹ Although this procedure worked on a simplified substrate, subjecting **62** to the same conditions resulted in decomposition (entry 1). A more conventional approach using DCC/HOBt as the coupling reagents and ammonium hydroxide as the ammonia source gave a complex mixture (entry 2).

It was possible to isolate the desired product when CDI was used as the coupling reagent; however, the imidazole side product was difficult to remove (entry 3). Instead, the acid was activated with ethyl chloroformate and the acyl carbonate reacted cleanly with the ammonia source to give **61** in 80% yield (entry 4). Furthermore, the structure of the primary amide was confirmed by X-ray crystallography.

^{††} Mechanistically, this cyclopropanation could either proceed *via* a direct insertion or stepwise process.

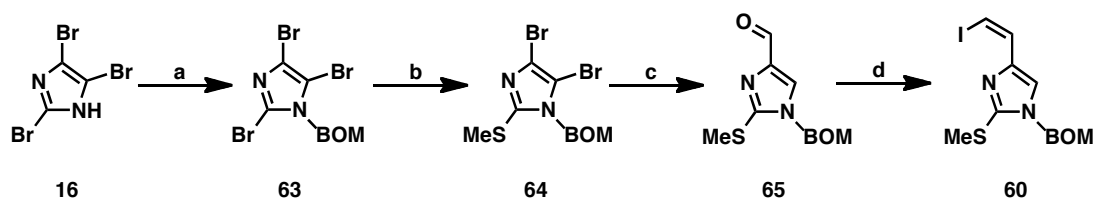
Table 10 Conditions for primary amide formation.

| Entry | Reagents | Solvent | Conditions | Yield |
|-------|--|--------------------------|----------------------------|-------------|
| 1 | Urea/Imidazole | Neat | 200 °C (μ W) 5 min | Decomp. |
| 2 | DCC, HOBT, NH_4OH | CH_2Cl_2 | rt | Complex mix |
| 3 | CDI, NH_4OH | THF | 0 °C to rt | 78% |
| 4 | Ethyl chloroformate, Et_3N , NH_4OH | THF | 0 °C to rt | 80% |

**Figure 41** X-ray crystal structure of primary amide **61**.

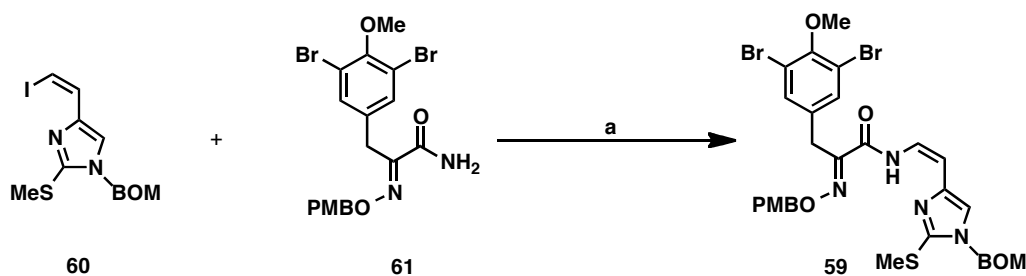
The vinyl iodide coupling partner (**60**) was synthesised from 2,4,5-tribromoimidazole (**16**) following a known literature procedure (Scheme 55).⁶ Regioselective transmetallation of the benzyloxymethyl-protected imidazole **63** and quenching the resulting carbanion with dimethyl disulfide gave sulfide **64**. Next, in a one-pot procedure, **64** was firstly lithiated and silylated with trimethylsilyl chloride,^{§§} and then lithiated and formylated with DMF. Subsequent removal of the silyl protecting group afforded aldehyde **65**. Lastly, a Stork–Zhao olefination of the aldehyde **65** with (iodomethyl)triphenylphosphonium iodide¹⁰ gave the *Z*-vinyl iodide **60** in 56% yield. It was also possible to isolate the corresponding alkyne (not shown) in 19% yield from the reaction mixture.

^{§§} This was necessary to achieve the regiospecific formylation at C-10.

Scheme 55 Synthesis of vinyl iodide **60**.

Reagents and conditions: (a) BOM-Cl, K_2CO_3 , DMF, rt, 24 h, 69%; (b) *n*-BuLi, THF, $-78\text{ }^\circ\text{C}$, 10 min then MeSSMe, $-78\text{ }^\circ\text{C}$, 15 min then rt; (c) *n*-BuLi, THF, $-78\text{ }^\circ\text{C}$, 10 min then TMSCl, 20 min then *n*-BuLi, 10 min then DMF, $-78\text{ }^\circ\text{C}$, 1 h then rt, K_2CO_3 , 3 h, 74% over 2 steps; (d) (iodomethyl)triphenylphosphonium iodide, KOtBu, rt, 5 min then $-78\text{ }^\circ\text{C}$, **65**, 30 min, 56%.

The vinyl iodide and amide coupling partners were united with conditions developed by Buchwald and co-workers.⁵ The *Z*-enamide was obtained in excellent yield by heating **60** and **61** to $70\text{ }^\circ\text{C}$ in a sealed tube in the presence of 10 mol% copper(I) iodide and 20% *N,N'*-dimethylethylenediamine.

Scheme 56 Buchwald coupling of **60** and **61**.

Reagents and conditions: (a) Cs_2CO_3 , CuI (10 mol%), DMEDA (20 mol%), THF, $70\text{ }^\circ\text{C}$, 4 h, 82%.

The crystal structure of **59** not only confirmed the *Z*-geometry of the enamide but also revealed that (in the solid state), the imidazole nitrogen was hydrogen bonding to the amide hydrogen (Figure 42). As a result, this bonding locks the molecule in such a way that it distances the *C*-4/*C*-10 olefin in the imidazole ring from *C*-5. This has obvious implications for the intramolecular cyclisation since the proposed cyclopropanation requires these positions to be in proximity to one another. It may well be the case that this bonding interaction is not relevant when dealing with the solution phase chemistry of this molecule. Nevertheless, this should not be disregarded for the cyclisation reaction and an appropriate choice of solvent may be required to minimise this bonding interaction.

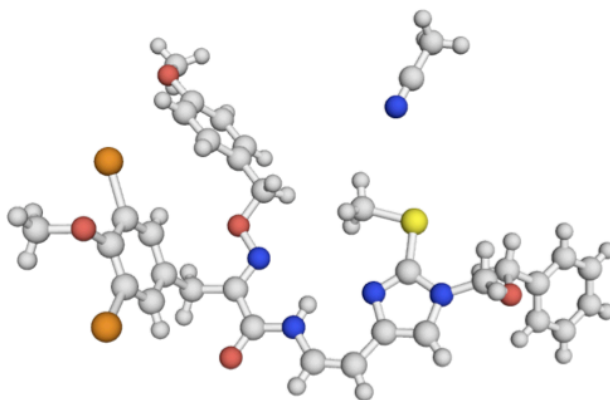
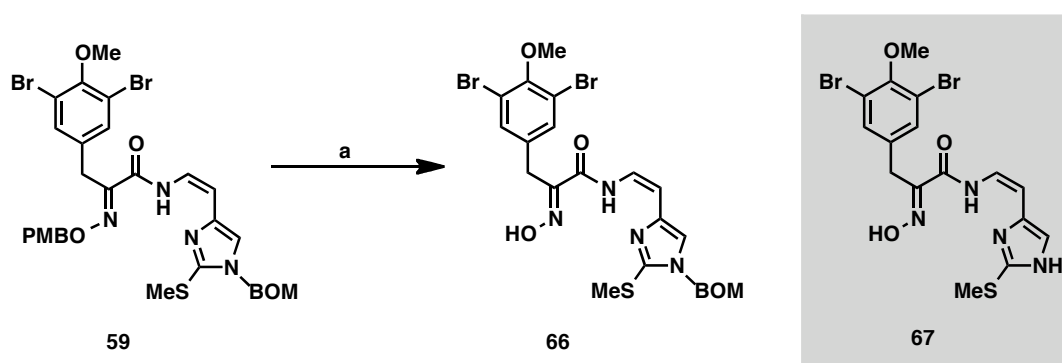


Figure 42 X-ray crystal structure of Z-enamide **59** co-crystallised with acetonitrile.

It was anticipated that the removal of the PMB group with the previously mentioned Lewis acidic conditions (Chapter 2) would be problematic given the acid sensitive nature of the BOM group. Therefore, oxidative cleavage of the PMB ether with DDQ was attempted but unfortunately no conversion occurred. As expected, treatment of **59** with aluminium trichloride and anisole for an extended reaction time (3 hours) led to a complex mixture of products and gave oxime **66** in 20% yield with **67** being the only other identifiable product. However, only minimal formation of **67** was observed when the substrate was exposed to the conditions for 1 minute and the desired product **66** was obtained in a moderate yield of 59% (Scheme 57).

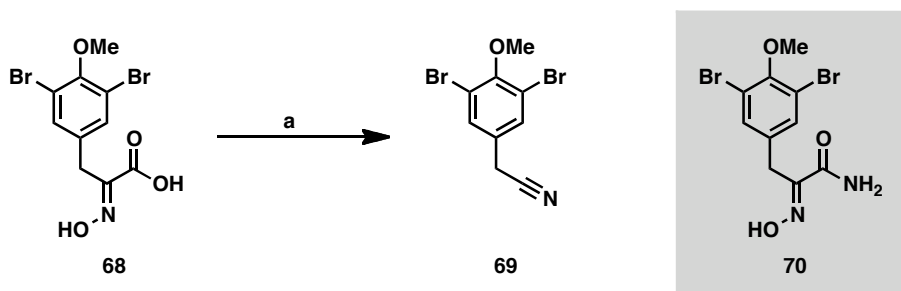


Scheme 57 PMB deprotection of Z-enamide **59**.

Reagents and conditions: (a) AlCl_3 , anisole, CH_2Cl_2 , rt, 1 min, 59%.

Despite being able to obtain small quantities of **66** via this method, the problems associated with this PMB deprotection led us to reconsider the synthetic strategy and explore other possibilities. Initially, this included investigating whether protection of the oxime was actually necessary.

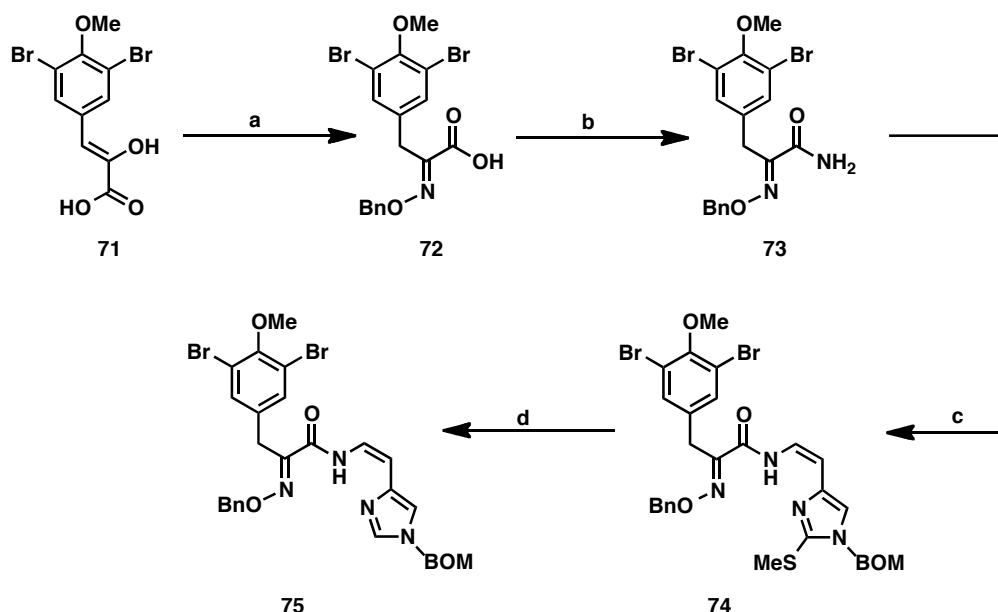
It was envisaged that the primary amide with the free oxime (**70**) could be accessed from the α -oximino acid **68** whose synthesis has previously been reported in Chapter 2. Unfortunately, subjecting this substrate to the amidation conditions described in Table 10 (entry 4) gave the nitrile **69**. On closer inspection it was found that **69** was formed following treatment of **68** with ethyl chloroformate and triethylamine. Interestingly, **69** is a naturally occurring metabolite and has been isolated from *Psammaphysilla purpurea*.¹¹



Scheme 58 Attempted synthesis of **70**.

Reagents and conditions: (a) ethyl chloroformate, Et₃N, THF, 0 °C, 1 h.

Therefore, as protection of the free oxime was clearly necessary, a suitable protecting group that could be selectively cleaved in the presence of the BOM group was required. Making use of the research into the subereamollines (Chapter 3), it was decided that protecting the oxime as a benzyl ether would be a viable option since it could be cleaved smoothly by hydrogenolysis over palladium black. Starting with the phenylpyruvic acid derivative (**71**) described in Chapter 2, condensation with *O*-benzylhydroxylamine gave the α -oximino acid **72** (Scheme 59). This was converted to the corresponding primary amide **73**, which could then coupled to the vinyl iodide **60** to form the *Z*-enamide **74** in 64% yield over the two steps. In this case, subjecting **74** to the hydrogenolysis conditions did not lead to cleavage of the benzyl ether. Instead, it was possible to isolate the imidazole **75**, which resulted from hydrogenolysis of the carbon–sulfur bond. This was not wholly unexpected, as it is known that palladium black can desulfurise hydrocarbons.¹² It was perhaps surprising that no debenzylation or reduction of the *C*-8/*C*-9 olefin was observed however, poisoning of the palladium catalyst may account for this. It is worth bearing in mind that this procedure could be used in the latter stages of the ceratamine synthesis to affect the desulfurisation of **56** (Scheme 53).



Scheme 59 Attempted synthesis of **66** from **74**.

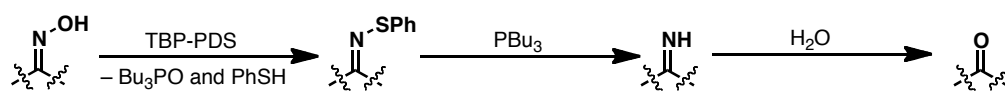
Reagents and conditions: (a) *O*-benzylhydroxylamine, NaOAc, EtOH, rt, 1 h, 98%; (b) ethyl chloroformate, Et₃N, THF, 0 °C, 45 min then NH₄OH, 30 min then rt, 1 h, 78%; (c) **60**, Cs₂CO₃, CuI (10 mol%), DMEDA (20 mol%), THF, 70 °C, 9 h, 82%; (d) Pd-black, H₂, 1,4-dioxane/AcOH (1:1), rt, 4 h, 16%.

We felt there was no value at this stage in pursuing an alternative oxime protecting group, as we were yet to attempt the cleavage of the oxime **66** to the corresponding carbonyl; any further research into a suitable protecting group would be futile if there was an inability to unmask the carbonyl functionality.

A variety of methods for the deoximation of aldoximes and ketoximes to their carbonyl derivatives have been reported in the literature and include: acid-catalysed (*e.g.* Mg(HSO₄)₂,¹³ and HCl/TiCl₃),¹⁴ reductive (*e.g.* Raney Ni/B(OH)₃/H₂),¹⁵ oxidative (*e.g.* N₂O₄,¹⁶ HIO₄,¹⁷ Mn(OAc)₃,¹⁸ and *t*-BuOOH),¹⁹ and photosensitised oxidative cleavage (*e.g.* hv/O₂/Pt(II) complex).²⁰ Since the stability of oximes is relatively high (when compared to hydroxylamines and imines), these methods are usually harsh and require forcing conditions that are often not compatible with highly functionalised substrates. When considering oxime **66**, we were concerned about the susceptibility of the *C*-8/*C*-9 olefin and thioether to oxidation and the lability of the BOM group towards acidic conditions. Therefore, a mild method to effect this transformation was desirable.

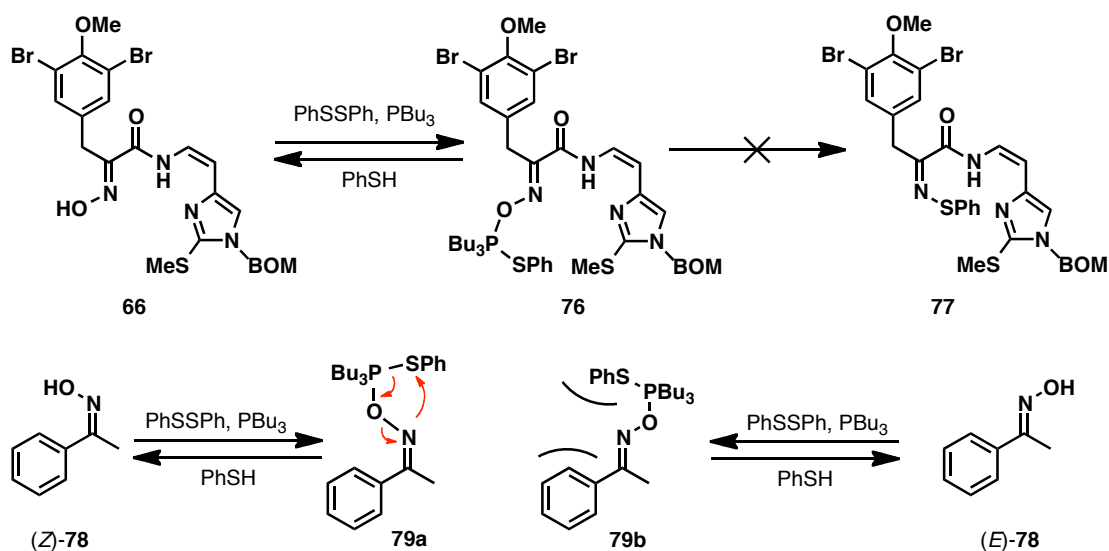
Zard and co-workers reported the use of a tributylphosphine–diphenyl disulfide (TBP-PDS) reagent system for the reduction of oximes to imines, which upon work-up

produced the corresponding ketones.²¹ Research by Lukin and co-workers provided further insight into this reaction mechanism.²² In the first step, TBP-PDS converts the oxime to a phenylthioimine with the loss of tributylphosphine oxide and thiophenol (Scheme 60). Tributylphosphine then reduces the thioimine, *via* attack of the sulfur atom, to give the imine that is subsequently hydrolysed upon work-up.



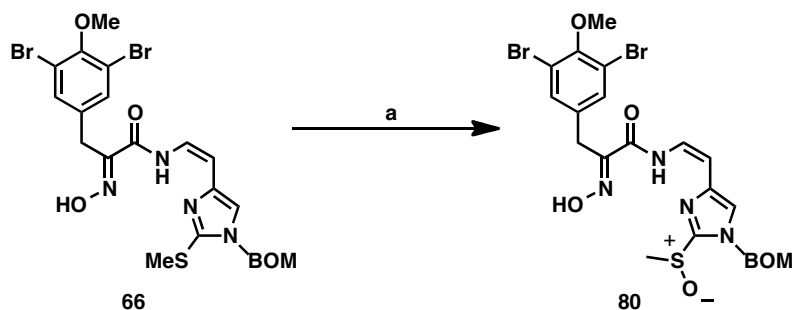
Scheme 60 Reaction pathway for oxime cleavage with TBP-PDS.

Disappointingly, using the reported conditions, treatment of oxime **66** with TBP-PDS gave no conversion. It appeared that **66** was unreactive towards this reagent system since using an excess of reagent or heating the mixture also proved unsuccessful. To account for this observation, we postulate that it was not possible for the phenylthioimine **77** to form due to unfavourable steric interactions. This is based on the work of Vilarrasa and co-workers who observed that, while acetophenone oxime (*Z*)-**78** was readily converted to the corresponding phenylthioimine, (*E*)-**78** gave only a trace amount of the product (Scheme 61).²³ They reasoned that the difference in steric hindrance around the nitrogen atom lone pair could account for this reactivity. For the intermediate **79a**, the molecule can adopt the necessary reactive conformation whereas, in the case of **79b** this is not possible because of an unfavourable steric clash between the SPh group and the phenyl ring. In our system, as illustrated in the crystal structure in Figure 42, these steric effects are even more pronounced and it is therefore unlikely that, if formed, **76** could collapse to the phenylthioimine **75**.



Scheme 61 The effects of steric hindrance in the formation of phenylthioimines.

The deoxygenation of **66** was also unsuccessful using a mild oxidative method developed by Akamanchi and co-workers.²⁴ The reaction of **66** with Dess–Martin periodinane in wet dichloromethane was monitored by HRMS which showed that, although no deoxygenation had occurred, **66** had been oxidized to the sulfoxide **80** (Scheme 62).

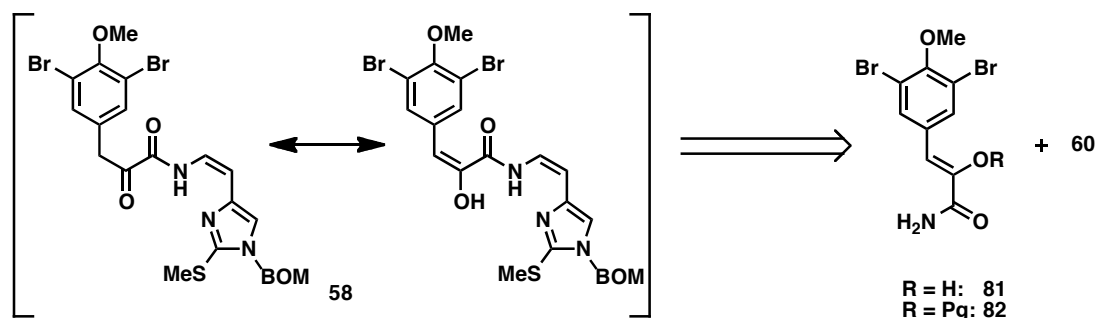


Scheme 62 Reaction of **66** with Dess–Martin periodinane.

Reagents and conditions: (a) Dess–Martin periodinane, CH_2Cl_2 (wet), rt, 30 min.

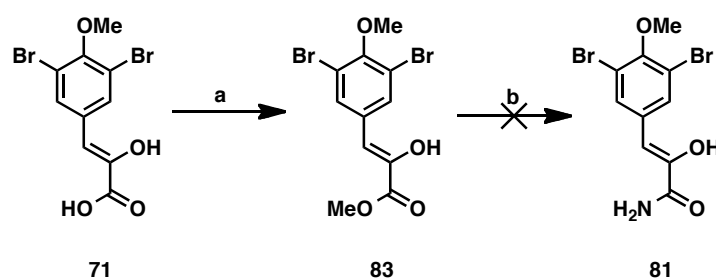
Despite the fact that only a couple of methods had been attempted, it was clear that the complexity of oxime **66** was not conducive to performing an efficient and high yielding deoxygenation. In an effort to overcome this stumbling block the retrosynthetic strategy towards the ketone **58** was revised so as to remove the need for the oxime group altogether (Scheme 63). Instead of masking the carbonyl group, the aim of this new approach was to couple either an unprotected (**81**) or protected (**82**) α -keto primary amide with vinyl iodide **60**. For the former, this would produce **58** directly whereas the coupled product from the latter would require an additional step to

selectively deprotect the enol hydroxyl. It is important to note that **58** would probably exist as its enol tautomer, akin to the phenylpyruvic acids from which it is derived.



Scheme 63 Revised retrosynthetic strategy towards **58**.

Commencing with the synthesis, it was anticipated that obtaining amide (**81**) directly from the acid **71** (using the optimised conditions in Table 10) would be difficult as the polarity of the product would make chromatographic purification challenging. Instead, **71** was methylated with trimethylsilyldiazomethane to give methyl ester **83** with the hope that the primary amide could be accessed by ammonolysis of the ester functionality (Scheme 64). Upon stirring with methanolic ammonia (7 *N*) for 2 hours there was full conversion of **83** to a single product. This was presumed to be amide **81**, however, concentration of the reaction mixture led to significant decomposition.^{***} This phenomenon has also been observed with phenylpyruvic acid derivatives.²⁵



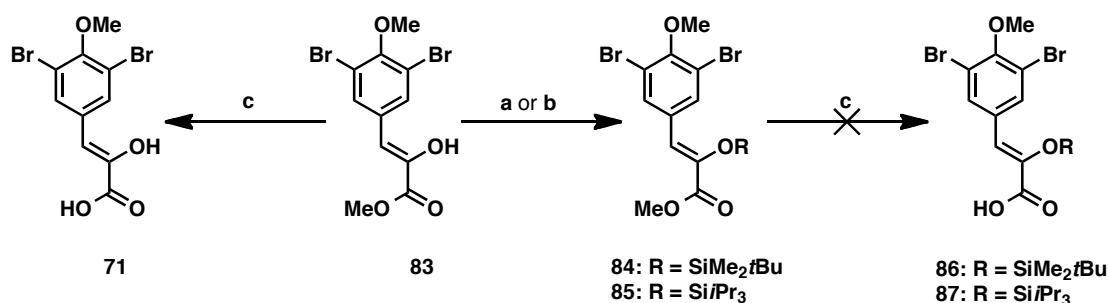
Scheme 64 Attempted synthesis of **81**.

Reagents and conditions: (a) TMSCHN₂, PhMe/MeOH (3:1), 0 °C to rt, 3 h, 83%.

This finding meant that protection of the enol hydroxyl was the only viable option. Further to this, the enol hydroxyl of methyl ester **83**^{†††} was protected using either TBS chloride²⁶ or TIPS triflate to give the silyl enol ethers **84** and **85**, respectively (Scheme 65). We had previously discovered that the methyl ester **83** could be saponified with

^{***} This decomposition was evident with both TLC and ¹H NMR analysis.

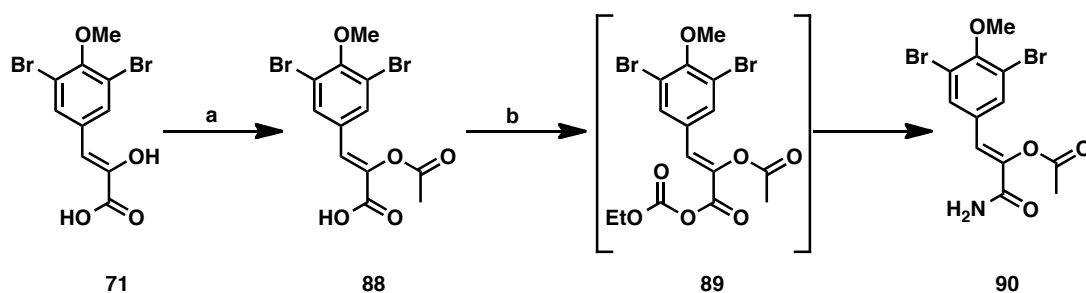
^{†††} The methyl ester was used as it was not possible to protect the free acid.



Reagents and conditions: (a) TBSCl, DMAP, Et₃N, CH₂Cl₂, rt, 30 min, 98%; (b) TIPSOTf, Et₃N, CH₂Cl₂, rt, 30 min, 97%; (c) LiOH·H₂O, MeOH/H₂O (3:1), rt, 1 h, **71**, quant.

This result prompted us to explore other protecting group strategies. Protecting **71** as the enol acetate was the most appealing as the acetate would be easy to install and could be removed under relatively mild conditions. Initially, **71** was treated with sodium acetate in neat acetic anhydride until a white precipitate had formed after which water was added.²⁷ However, the compound isolated after work-up turned out to be the *bis*-acetylated product (not shown) and not the desired mono-acetylated product **88**. We reasoned that the precipitate was the sodium carboxylate salt of **88** and that solubilising it (with water) in the presence of acetic anhydride resulted in the acetylation of the carboxylate moiety. Accordingly, the precipitate^{†††} was isolated from the reaction mixture and subsequently acidified to furnish **88** in 72% yield (Scheme 66). The structure was confirmed by crystallographic analysis (Figure 43).

232



Scheme 66 Synthesis of primary amide **90**.

Reagents and conditions: (a) Ac_2O , NaOAc , 2 h, rt, 72%; ethyl chloroformate, Et_3N , THF, 0°C , 45 min then HMDS, 30 min, 54%.

When attempting to convert acid **88** to primary amide **90** using our optimised conditions, a complex mixture of products was obtained. Further analysis revealed that formation of the carbonate **89** proceeded smoothly in quantitative yield but that this decomposed upon treatment with a solution of ammonium hydroxide. Since the enol acetate was not stable to these conditions, a milder source of ammonia was required. Hexamethyldisilazane has been used to convert acid chlorides²⁸ and both DCC²⁹ and TBTU³⁰ activated acids to primary amides. Pleasingly, addition of a 10 fold excess of HMDS to the activated acid **89** gave the desired primary amide **90** in 54% yield (Scheme 66).^{§§§} To our knowledge this represents the first example of the use of HMDS in a chloroformate-mediated amidation process.

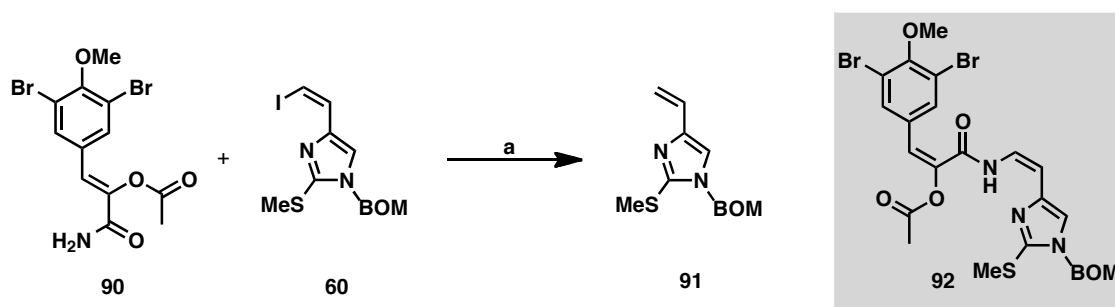


Figure 43 X-ray crystal structure of enol acetate **88**.

The copper-catalysed Buchwald amidation between amide **90** and vinyl iodide **60** was attempted using the conditions described in Scheme 56. TLC and LCMS analysis

^{§§§} This method could also be used to convert the PMB α -oximino acid **62** to the primary amide **61** in 69% yield.

showed that the primary amide had been fully consumed although the starting vinyl iodide (**60**) was still present, along with its protodehalogenated product **91**; the desired product (**92**) could not be detected (Scheme 67). A series of control reactions were performed and these revealed that although **90** was stable at the reaction temperature, it decomposed when treated with caesium carbonate. The reaction was repeated under strictly anhydrous conditions, as it is known that the hydrolysis of enol acetates can be achieved with potassium carbonate in aqueous methanol,³¹ but to no avail.



Scheme 67 Attempted synthesis of **92**.

Reagents and conditions: (a) Cs_2CO_3 , CuI (10 mol%), DMEDA (20 mol%), THF, 70 °C, 4 h.

This outcome was disappointing especially since, in the development of this amidation reaction, Buchwald and co-workers had been able to couple vinyl iodides possessing ester functionalities to primary amides in moderate yields and without significant decomposition.⁵

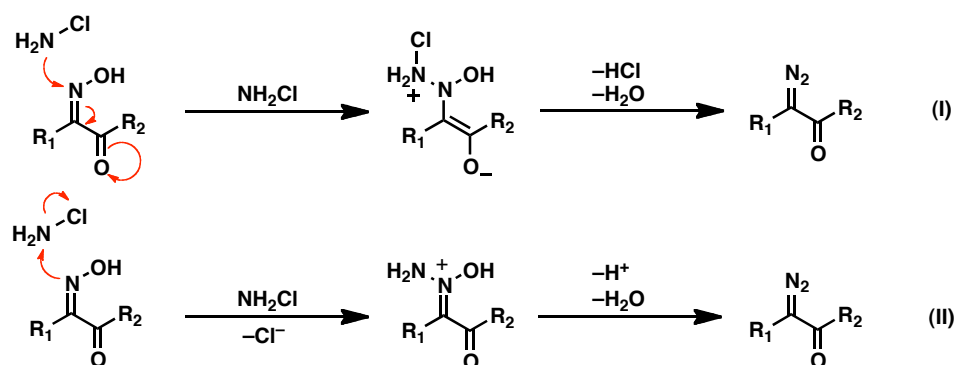
4.3 Conclusion and Future Work

At the time of writing, no further progress has been made towards the synthesis of the ceratamines. To summarise, the major problem that we have encountered in our route towards the ceratamines has been the inability to access compound **58**. So far, attempts to either unmask the carbonyl functionality from the oxime or to protect the ketone as its silyl enol ether/enol acetate have been unsuccessful.

With regards to future synthetic studies, as it was possible to couple the amides **61** and **73** to the vinyl iodide **60**, it appears that masking the carbonyl as an oxime remains the most promising strategy. As previously mentioned, since the deoxygenation of ketoximes is heavily preceded in the literature, a rigorous screen of conditions (compatible with substrate **66**) should uncover an optimal method to perform this

transformation. However, unmasking the carbonyl may not be necessary as it is known that oximes can be converted directly to the corresponding diazo compound by treatment with chloramines (Förster reaction).³² This would also remove the step that would otherwise be necessary to transform the ketone **58** to the diazo compound **57**.

Interestingly, the Förster reaction is much underused in spite of its capabilities and the current interest in C-H activation within the chemistry community. Originally it was believed that this reaction was limited to the transformation of α -oximino ketones to α -diazo ketones based on the proposed mechanistic pathway whereby there is nucleophilic attack onto the oxime nitrogen (in a Michael fashion) by chloramine (Scheme 68 (I)). Meinwald and co-workers put forward an alternate mechanism in which the first step involves nucleophilic displacement at the chloramine nitrogen (Scheme 68 (II)).³³ This was supported by experimental evidence, as it was possible to convert oximes lacking an α -carbonyl moiety (*e.g.* fluorenone and benzophenone oxime) to their diazo derivatives.



Scheme 68 Proposed mechanisms for the Förster reaction.

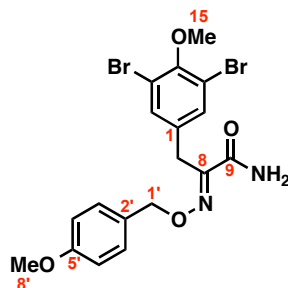
In conclusion, it is hoped that in the near future an appropriate route to the diazo compound **57** will be uncovered which will subsequently allow us to investigate the chemistry of the key intramolecular-cyclisation step.

4.4 Chemistry: Experimental

General Experimental Details

Refer to Section 2.1.6 for general experimental details.

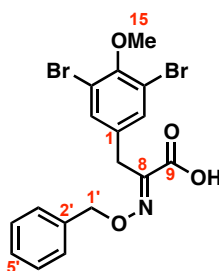
(*E*)-3-(3,5-Dibromo-4-methoxyphenyl)-2-(((4-ethoxybenzyl)oxy)imino)propanamide (61)



To a stirred solution of acid **62** (207 mg, 0.425 mmol) and Et₃N (89.0 μ L, 0.639 mmol) in THF (8 mL) at 0 °C was added ethyl chloroformate (45.0 μ L, 0.471 mmol). After 45 min, ammonium hydroxide (35 %, 200 μ L) was added and the reaction mixture was stirred for a further 30 min at 0 °C. The reaction mixture was allowed to warm to room temperature and, after 1 h, EtOAc (25 mL) and H₂O (25 mL) were added and the organic layer separated. The aqueous layer was extracted with EtOAc (2 x 25 mL) and the combined organic extracts were dried and concentrated *in vacuo*. The residue was purified by flash column chromatography (20-40% EtOAc/Petrol) to furnish **61** (165 mg, 0.339 mmol, 80%) as a white solid.

R_f 0.77 (5% MeOH/CH₂Cl₂); ν_{\max} (thin film)/cm⁻¹ 3424m, 3221w, 2938w, 1684s, 1611s, 1515s, 1251s; δ_H (400 MHz, CDCl₃) 7.40 (2H, s, H-2/6), 7.25 (2H, d J 8.6 Hz, H-3'/7'), 6.91 (2H, d, J 8.6 Hz, H-4'/6'), 6.59 (1H, br s, NH), 5.34 (1H, br s, NH), 5.15 (2H, s, H-1'), 3.84 (3H, s, H-15), 3.82 (3H, s, H-8'), 3.80 (2H, s, H-7); δ_C (100 MHz, CDCl₃) 164.1 (C-9), 159.8 (C-5'), 152.6 (C-4), 150.5 (C-8), 134.7 (C-1), 133.4 (C-2/6), 130.1 (C-3'/7'), 128.2 (C-2'), 117.7 (C-3/5), 114.1 (C-4'/6'), 77.5 (C-1'), 60.5 (C-15), 55.3 (C-8'), 28.3 (C-7); m/z (ESI+) found 506.9509, [M+Na]⁺ C₁₈H₁₈Br₂N₂O₄Na (⁷⁹Br) requires 506.9531; m.p. 100-102 °C.

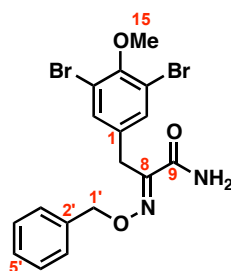
Crystals of **61** were obtained by slow evaporation from MeOH. The structure was confirmed by X-ray crystallographic analysis and given the unique identifier sl0854.

(E)-2-((Benzyloxy)imino)-3-(3,5-dibromo-4-methoxyphenyl)propanoic acid (70)

To a stirred solution of **71** (132 mg, 0.375 mmol) and *O*-benzylhydroxylamine (96%, 45.5 μ L, 0.375 mmol) in EtOH (3.8 mL) was added sodium acetate (92.3 mg, 1.13 mmol). After 1 h, H₂O (20 mL) was added, then the mixture was acidified (pH 0) by the addition of 3 *N* HCl and extracted with EtOAc (3 \times 20 mL). The combined organic extracts were dried and evaporated to dryness *in vacuo* to furnish **70** (168 mg, 0.368 mmol, 98%) as a white solid.

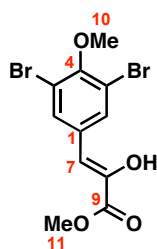
R_f 0.41 (10% MeOH/CH₂Cl₂); ν_{\max} (thin film)/cm⁻¹ 3200-2800br, 1706s, 1471s, 1257s; δ_H (400 MHz, CDCl₃) 10.10 (1H, br s, OH), 7.42-7.37 (5H, m, H-3' to 7'), 7.40 (2H, s, H-2/6), 5.33 (2H, s, H-1'), 3.85 (3H, s, H-15), 3.82 (2H, s, H-7); δ_C (100 MHz, CDCl₃) 164.8 (C-9), 152.9 (C-4), 148.9 (C-8), 135.4 (C-2'), 133.7 (C-1), 133.3 (C-2/6), 128.73 (C-4'/6'), 128.69 (C-5'), 128.5 (C-3'/7'), 117.9 (C-3/5), 78.7 (C-1'), 60.5 (C-15), 29.3 (C-7); m/z (ESI+) found 499.9095, [M-H+2Na]⁺ C₁₇H₁₄Br₂NO₄Na₂ (⁷⁹Br) requires 499.9079.

Consistent with literature data.³⁴

(E)-2-((Benzyloxy)imino)-3-(3,5-dibromo-4-methoxyphenyl)propanamide (73)

To a stirred solution of acid **72** (168 mg, 0.368 mmol) and Et₃N (77.0 μ L, 0.552 mmol) in THF (5 mL) at 0 °C was added ethyl chloroformate (38 μ L, 0.404 mmol). After 45 min, ammonium hydroxide (35%, 200 μ L) was added and the reaction was stirred for a further 30 min at 0 °C. The reaction was allowed to warm to room temperature and, after 1 h, EtOAc (25 mL) and H₂O (25 mL) were added and the organic layer separated. The aqueous layer was extracted with EtOAc (2 x 25 mL) and the combined organic extracts were dried and concentrated *in vacuo*. The residue was purified by flash column chromatography (20-60% EtOAc/Petrol) to furnish **73** (132 mg, 0.289 mmol, 79%) as a white solid.

R_f 0.17 (20% EtOAc/Petrol); ν_{\max} (thin film)/cm⁻¹ 3464s, 3144br, 1698s, 1472s, 1257s; δ_H (400 MHz, CDCl₃) 7.43 (2H, s, H-2/6), 7.40-7.30 (5H, m, H-3' to 7'), 6.60 (1H, br s, NH), 5.76 (1H, br s, NH), 5.23 (2H, s, H-1'), 3.84 (3H, s, H-15), 3.83 (2H, s, H-7); δ_C (100 MHz, CDCl₃) 164.2 (C-9), 152.6 (C-4), 150.7 (C-8), 136.2 (C-2'), 134.6 (C-1), 133.4 (C-2/6), 128.6 (C-4'/6'), 128.4 (C-5'), 128.2 (C-3'/7'), 117.7 (C-3/5), 77.7 (C-1'), 60.5 (C-15), 28.3 (C-7); m/z (ESI+) found 454.9619, [M+H]⁺ C₁₇H₁₇Br₂N₂O₃ (⁷⁹Br) requires 454.9609.

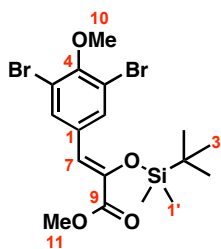
(Z)-Methyl 3-(3,5-dibromo-4-methoxyphenyl)-2-hydroxyacrylate (83)

To a stirred solution of **71** (500 mg, 1.42 mmol) in toluene/MeOH (3:1, 16 mL) at 0 °C was added trimethylsilyl diazomethane (2.0 M in hexane, 1.07 mL, 2.13 mmol) dropwise. The mixture was stirred for 3 h at room temperature and quenched by the addition of 3 *N* HCl (300 μ L). The solvent was removed *in vacuo* and the residue partitioned between H₂O (30 mL) and EtOAc (30 mL). The aqueous phase was extracted with EtOAc (30 mL \times 2) and the combined organic layers were dried and concentrated *in vacuo*. The residue was purified by flash column chromatography (2.5–20% EtOAc/Petrol) to furnish **83** (433 mg, 1.18 mmol, 83%) as a white solid.

R_f 0.27 (10% EtOAc/Petrol); ν_{\max} (thin film)/cm⁻¹ 3416s, 1687s, 1531m, 1431s, 1242s; δ_H (400 MHz, CDCl₃) 7.91 (2H, s, H-2/6), 6.52 (1H, d, *J* 1.6 Hz, OH), 6.34 (1H, d, *J* 1.5 Hz, H-7), 3.92 (3H, s, H-10), 3.90 (3H, s, H-11); δ_C (100 MHz, CDCl₃) 166.0 (C-9), 153.4 (C-4), 140.0 (C-8), 133.7 (C-2/6), 132.8 (C-1), 118.0 (C-3/5), 107.7 (C-7), 60.7 (C-10), 53.5 (C-11).

It was not possible to obtain HRMS data for this compound.

(Z)-Methyl 2-((*tert*-butyldimethylsilyl)oxy)-3-(3,5-dibromo-4-methoxyphenyl)acrylate (84**)**

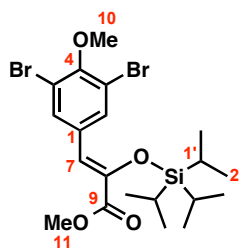


To a stirred solution of methyl ester **83** (84.8 mg, 0.232 mmol), DMAP (5.70 mg, 46.7 μ mol) and Et₃N (32.5 μ L, 0.233 mmol) in CH₂Cl₂ (3 mL) was added a solution of TBSCl (38.5 mg, 0.255 mmol) in CH₂Cl₂ (300 μ L) dropwise. After 30 min the solvent was removed *in vacuo* and the residue partitioned between H₂O (10 mL) and Et₂O (10 mL). The organic layer was separated, dried, and evaporated to dryness *in vacuo* to furnish **84** (109 mg, 0.227 mmol, 98%) as a colourless oil.

R_f 0.67 (10% EtOAc/Petrol); ν_{\max} (thin film)/cm⁻¹ 2951m, 2930m, 2858w, 1724s, 1630s, 1243s; δ_H (400 MHz, CDCl₃) 7.86 (2H, s, H-2/6), 6.34 (1H, d, J 1.5 Hz, H-7), 3.88 (3H, s, H-10), 3.81 (3H, s, H-11), 0.97 (9H, s, H-3'), 0.18 (6H, s, H-1'); δ_C (100 MHz, CDCl₃) 165.2 (C-9), 153.4 (C-4), 141.5 (C-8), 133.4 (C-2/6), 132.8 (C-1), 117.7 (C-3/5), 115.1 (C-7), 60.7 (C-10), 52.3 (C-11), 25.8 (C-3'), 18.6 (C-2'), -3.87 (C-1').

It was not possible to obtain HRMS data for this compound.

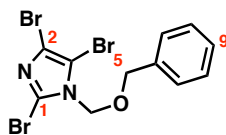
(Z)-Methyl 3-(3,5-dibromo-4-methoxyphenyl)-2-(((triisopropylsilyl)oxy)acrylate
(85)



To a stirred solution of methyl ester **83** (43.6 mg, 0.119 mmol), and Et₃N (16.6 μ L, 0.119 mmol) in CH₂Cl₂ (1.5 mL) was added a solution of TIPSOTf (35.2 μ L, 0.131 mmol) dropwise. After 30 min the solvent was removed *in vacuo* and the residue partitioned between H₂O (10 mL) and Et₂O (10 mL). The organic layer was separated, dried, and evaporated to dryness *in vacuo* to furnish **85** (60.0 mg, 0.115 mmol, 97%) as a colourless oil.

R_f 0.66 (10% EtOAc/Petrol); ν_{\max} (thin film)/cm⁻¹ 2944 s, 2866 s, 1726 s, 1629 m, 1470 s, 1244 s; δ_H (400 MHz, CDCl₃) 7.89 (2H, s, H-2/6), 6.57 (1H, d, J 1.5 Hz, H-7), 3.88 (3H, s, H-10), 3.81 (3H, s, H-11), 1.34 (3H, quint, J 7.5 Hz, H-1') 1.09 (18H, d, J 7.5 Hz, H-2'); δ_C (100 MHz, CDCl₃) 165.3 (C-9), 153.3 (C-4), 141.9 (C-8), 133.2 (C-2/6), 133.1 (C-1), 117.8 (C-3/5), 113.8 (C-7), 60.7 (C-10), 52.3 (C-11), 17.9 (C-2'), 13.9 (C-1').

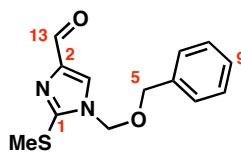
It was not possible to obtain HRMS data for this compound.

1-((Benzyloxy)methyl)-2,4,5-tribromo-1H-imidazole (63)

To a vigorously stirred suspension of 2,4,5-tribromoimidazole (**16**) (23.0 g, 75.5 mmol) and anhydrous K_2CO_3 (94.9 g, 687 mmol) in DMF (200 mL) at room temperature was added benzyloxymethyl chloride (12.5 mL, 90.1 mmol). After 24 h, H_2O (1 L) was added and the solution was extracted with EtOAc (3×600 mL). The combined organic extracts were washed with H_2O (1 L), dried, and evaporated to dryness *in vacuo* to give an oil which slowly crystallised to furnish **63** (22.1 g, 52.1 mmol, 69%) as colourless crystals.

δ_H (400 MHz, $CDCl_3$) 7.33 (5H, m, H-7 to 11), 5.42 (2H, s, H-4), 4.60 (2H, s, H-5); δ_C (100 MHz, $CDCl_3$) 136.1 (C-6), 128.6 (C-8/10), 128.4 (C-9), 127.7 (C-7/11), 119.2 (C-3), 117.9 (C-1), 105.8 (C-2), 75.7 (C-5), 71.2 (C-4); m/z (ESI+) found 422.8343, $[M+H]^+$ $C_{11}H_{10}Br_3N_2O$ (^{79}Br) requires 422.8343.

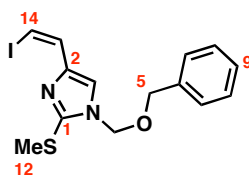
Consistent with literature data³⁵

1-((Benzyloxy)methyl)-2-(methylthio)-1*H*-imidazole-4-carbaldehyde (**65**)

To a solution of **63** (6.84 g, 16.1 mmol) in THF (100 mL) at $-78\text{ }^{\circ}\text{C}$ was added *n*-BuLi (6.71 mL of 2.4 M solution in hexanes, 16.1 mmol). After 10 min, dimethyldisulfide (1.45 mL, 16.1 mmol) was added dropwise and the reaction was stirred for a further 15 min at $-78\text{ }^{\circ}\text{C}$ before warming to room temperature. The mixture was concentrated *in vacuo* and the residue was partitioned between EtOAc (250 mL) and H_2O (250 mL). The organic layer was separated and the aqueous layer was extracted with EtOAc ($3 \times 250\text{ mL}$). The combined organic extracts were washed with brine (500 mL), dried and evaporated to dryness *in vacuo* to give an orange oil (5.95 g) which was used without further purification. To a solution of the oil (5.95 g) in THF (90 mL) at $-78\text{ }^{\circ}\text{C}$ was added *n*-BuLi (6.33 mL of 2.4 M solution in hexanes, 15.2 mmol). After 10 min, trimethylsilyl chloride (1.93 mL, 15.2 mmol) was added dropwise and the mixture stirred for a further 20 min after which, *n*-BuLi (6.33 mL of 2.4 M solution in hexanes, 15.2 mmol) was added dropwise. After 10 min, DMF (3.52 mL, 45.5 mmol) was added dropwise and the mixture was stirred at $-78\text{ }^{\circ}\text{C}$ for 1 h. After warming to room temperature, H_2O (50 mL) was added and the mixture was extracted with CH_2Cl_2 ($3 \times 50\text{ mL}$). The organic extracts were combined and MeOH (20 mL) and anhydrous K_2CO_3 (4.19 g, 30.3 mmol) were added. After stirring for 3 h, H_2O (100 mL) was added and the mixture was extracted with CH_2Cl_2 ($3 \times 50\text{ mL}$). The combined organic extracts were dried, and concentrated *in vacuo*. The residue was purified by flash column chromatography (30% EtOAc/hexane) to furnish **65** (3.12 g, 11.9 mmol, 74%) as a yellow oil.

δ_{H} (400 MHz, CDCl_3) 9.76 (1H, s, H-13), 7.67 (1H, s, H-3), 7.30 (5H, m, H-7 to 11), 5.29 (2H, s, H-4), 4.49 (2H, s, H-5), 2.66 (3H, s, H-12); δ_{C} (100 MHz, CDCl_3) 184.8 (C-13), 147.0 (C-1), 142.3 (C-6), 135.8 (C-8/10), 128.7 (C-9), 128.5 (C-7/11), 128.0 (C-3), 127.3 (C-2), 75.1 (C-4), 71.0 (C-5), 15.6 (C-12).

Consistent with literature data.⁶

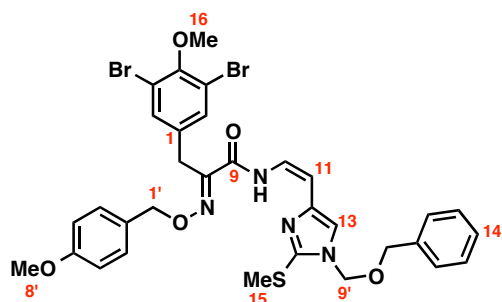
(Z)-1-((Benzyloxy)methyl)-4-(2-iodovinyl)-2-(methylthio)-1H-imidazole (60)

To a suspension of (iodomethyl)triphenylphosphonium iodide¹⁰ (3.10 g, 5.85 mmol) in THF (25 mL) was added KO^tBu (656 mg, 5.85 mmol). After 5 min the mixture was cooled to -78°C and a solution of aldehyde **65** (766 mg, 2.92 mmol) in THF (6 mL) was added dropwise. After 30 min, H₂O (50 mL) was added and the mixture extracted with CH₂Cl₂ (3 \times 40 mL). The combined organic extracts were washed with brine (200 mL), dried, and concentrated *in vacuo*. The residue was purified by flash column chromatography (10-30 % EtOAc/hexane) to furnish **60** (633 mg, 1.63 mmol, 56%) as a yellow oil.

R_f 0.23 (20% EtOAc/hexane); ν_{max} (thin film)/cm⁻¹ 2929w, 1732w, 1615w, 1445m, 1073s; δ_{H} (400 MHz, CDCl₃) 8.02 (1H, s, H-3), 7.44 (1H, d, J 8.7 Hz, H-13), 7.35 (5H, m, H-7 to 11), 6.41 (1H, d, J 8.7 Hz, H-14), 5.34 (2H, s, H-4), 4.53 (2H, s, H-5), 2.63 (3H, s, H-12); δ_{C} (100 MHz, CDCl₃) 143.6 (C-1), 139.5 (C-2), 136.1 (C-6), 132.7 (C-3), 128.5 (C-8/10), 128.1 (C-9), 127.9 (C-7/11), 120.0 (C-14), 76.1 (C-13), 74.6 (C-4), 70.3 (C-5), 16.2 (C-12); m/z (ESI+) found 387.0027, $[\text{M}+\text{H}]^+$ C₁₄H₁₆IN₂OS requires 387.0028.

Consistent with literature data.⁶

(E)-N-((Z)-2-(1-((Benzyloxy)methyl)-2-(methylthio)-1*H*-imidazol-4-yl)vinyl)-3-(3,5-dibromo-4-methoxyphenyl)-2-(((4-methoxybenzyl)oxy)imino)propanamide (59)

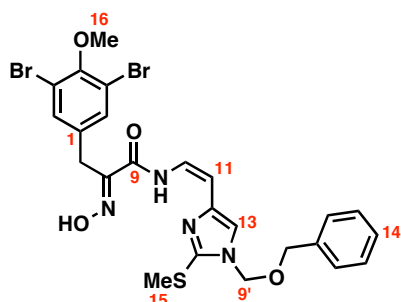


To a stirred mixture of primary amide **61** (277 mg, 0.570 mmol), Cs₂CO₃ (336 mg, 1.03 mmol) and copper(I) iodide (9.85 mg, 51.7 μmol) and THF (1.5 mL) in a sealed microwave vial at room temperature was added vinyl iodide **60** (200 mg, 0.517 mmol) in THF (1 mL). Then, *N,N'*-dimethylethanediamine (11.2 μL, 0.104 mmol) was added and the mixture heated to 70 °C for 4 h. Upon cooling the mixture was filtered through celite and washed with EtOAc (50 mL) and concentrated *in vacuo*. The residue was purified by flash column chromatography (10-30% EtOAc/Hexanes) to furnish **59** (314 mg, 0.422 mmol, 82%) as a yellow oil.

R_f 0.24 (20% EtOAc/Hexanes); ν_{\max} (thin film)/cm⁻¹ 3287w, 2928w, 1658s, 1557s, 1241s; δ_{H} (400 MHz, CDCl₃) 11.72 (1H, d, *J* 10.8 Hz, NH), 7.42 (2H, s, H-2/6), 7.38-7.29 (7H, m, H-3'/7', H-11'/16', H-12'/15' and H-14'), 7.01 (1H, dd, *J* 10.8, 9.2 Hz, H-10), 6.97 (1H, s, H-13), 6.91 (2H, d, *J* 8.6 Hz, H-4'/6') 5.57 (1H, d, *J* 9.2 Hz, H-11), 5.32 (2H, s, H-9'), 5.27 (2H, s, H-1'), 4.48 (2H, s, H-10'), 3.90 (2H, s, H-7), 3.83 (3H, s, H-16), 3.82 (3H, s, H-8'), 2.70 (3H, s, H-15); δ_{C} (100 MHz, CDCl₃) 159.8 (C-9), 159.7 (C-5'), 152.5 (C-4), 151.5 (C-8), 143.6 (C-14), 140.2 (C-12), 136.2 (C-11'), 134.9 (C-1), 133.4 (C-2/6), 130.0 (C-3'/7'), 128.5 (C-13'/15'), 128.1 (C-14'), 127.9 (C-2'), 127.7 (C-12'/16'), 121.0 (C-10), 118.4 (C-13), 117.6 (C-3/5), 114.0 (C-4'/6'), 101.0 (C-11), 77.5 (C-1'), 74.5 (C-9'), 70.3 (C-10'), 60.4 (C-16), 55.2 (C-8'), 28.9 (C-7), 16.8 (C-15); *m/z* (ESI⁺) found 743.0553, [M+H]⁺ C₃₂H₃₃Br₂N₄O₅S (⁷⁹Br) requires 743.0538.

Crystals of **59** were obtained from a solution of MeCN/H₂O (1:1). The structure was confirmed by X-ray crystallographic analysis and given the unique identifier sl0909.

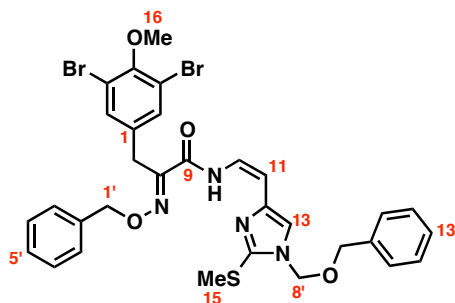
(E)-N-((Z)-2-(1-((Benzyloxy)methyl)-2-(methylthio)-1H-imidazol-4-yl)vinyl)-3-(3,5-dibromo-4-methoxyphenyl)-2-(hydroxyimino)propanamide (66)



To a stirred solution of enamide **59** (22.8 mg, 30.6 μmol) and anisole (33.3 μL , 0.306 mmol) in CH_2Cl_2 (2 mL) at room temperature was added aluminium trichloride (40.8 mg, 0.306 mmol). After 1 min, a saturated aqueous solution of NaHCO_3 (3 mL) was added followed by a saturated aqueous solution of Rochelle's salt (3 mL) and stirred for 10 min. The aqueous phase was extracted with CH_2Cl_2 (3×15 mL) and the combined organic layers were dried, and concentrated *in vacuo*. The residue was purified by flash column chromatography (10-40% $\text{CH}_2\text{Cl}_2/\text{MeOH}$) to furnish **66** (11.2 mg, 17.9 μmol , 59%) as a yellow solid.

R_f 0.19 (20% EtOAc/Petrol); ν_{max} (thin film)/ cm^{-1} s, 3247 br, 2927 w, 1642 s, 1610 m, 1558 s, 1420 s, 1241 s; δ_{H} (400 MHz, CDCl_3) 11.99 (1H, br d, J 9.9 Hz, NH), 7.52 (2H, s, H-2/6), 7.47 (1H, s, OH), 7.37-7.29 (5H, m, H-4'/8', H-5'/7' and H-6'), 6.98 (1H, dd, J 10.7, 9.0 Hz, H-10), 6.92 (1H, s, H-13), 5.56 (1H, d, J 9.0 Hz, H-11), 5.26 (2H, s, H-1'), 4.47 (2H, s, H-2'), 3.96 (2H, s, H-7), 3.84 (3H, s, H-16), 2.76 (3H, s, H-15); δ_{C} (100 MHz, CDCl_3) 159.7 (C-9), 153.2 (C-8), 152.7 (C-4), 144.2 (C-14), 140.1 (C-12), 136.2 (C-3'), 134.7 (C-1), 133.5 (C-2/6), 128.6 (C-5'/7'), 128.2 (C-6'), 127.9 (C-4'/8'), 121.0 (C-10), 118.2 (C-13), 117.8 (C-3/5), 101.2 (C-11), 74.4 (C-1'), 70.4 (C-2'), 60.6 (C-16), 28.1 (C-7), 15.6 (C-15); m/z (ESI+) found 622.9960, $[\text{M}+\text{H}]^+$ $\text{C}_{24}\text{H}_{25}\text{Br}_2\text{N}_4\text{O}_4\text{S}$ (^{79}Br) requires 622.9963.

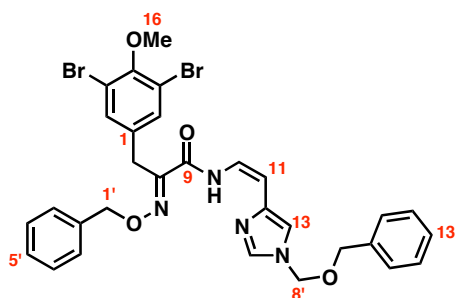
(E)-2-((Benzyloxy)imino)-N-((Z)-2-(1-((benzyloxy)methyl)-2-(methylthio)-1H-imidazol-4-yl)vinyl)-3-(3,5-dibromo-4-methoxyphenyl)propanamide (74)



To a stirred mixture of primary amide **73** (81.1 mg, 0.178 mmol), Cs₂CO₃ (106 mg, 0.324 mmol), copper(I) iodide (7.29 mg, 38.3 μmol) and THF (1.0 mL) in a sealed microwave vial at room temperature was added vinyl iodide **60** (62.4 mg, 0.162 mmol) in THF (1 mL). Then, *N,N'*-dimethylethanediamine (8.26 μL, 76.7 μmol) was added and the mixture heated to 70 °C for 9 h. Upon cooling the mixture was filtered through celite and washed with EtOAc (50 mL) and concentrated *in vacuo*. The residue was purified by flash column chromatography (10-30% EtOAc/Hexanes) to furnish **74** (96.0 mg, 0.134 mmol, 83%) as a yellow oil.

R_f 0.31 (20% EtOAc/Petrol); ν_{\max} (thin film)/cm⁻¹ 3276w, 2928w, 1656s, 1556s, 1471s, 1421s, 1241s; δ_{H} (400 MHz, CDCl₃) 11.74 (1H, d, *J* 10.8 Hz, NH), 7.47 (2H, s, H-2/6), 7.42-7.30 (10H, m, H-3' to H-7' and H-11' to 15'), 7.03 (1H, apparent t, *J* 10.0 Hz, H-10), 6.96 (1H, s, H-13), 5.58 (1H, d, *J* 9.2 Hz, H-11), 5.37 (2H, s, H-8'), 5.32 (2H, s, H-1'), 4.48 (2H, s, H-9'), 3.92 (2H, s, H-7), 3.84 (3H, s, H-16), 2.66 (3H, s, H-15); δ_{C} (100 MHz, CDCl₃) 159.8 (C-9), 152.6 (C-4), 151.7 (C-8), 143.6 (C-14), 140.2 (C-12), 136.2 (C-10'), 136.0 (C-2'), 134.8 (C-1), 133.5 (C-2/6), 128.7 (C-4'/6'), 128.5 (C-12'/14'), 128.4 (C-5'), 128.20 (C-3'/7'), 128.15 (C-13'), 127.8 (C-11'/15'), 121.1 (C-10), 118.4 (C-13), 117.7 (C-3/5), 101.1 (C-11), 77.8 (C-1'), 74.5 (C-8'), 70.4 (C-9'), 60.5 (C-16), 29.0 (C-7), 16.8 (C-15); *m/z* (ESI+) found 713.0459, [M+H]⁺ C₃₁H₃₁Br₂N₄O₄S (⁷⁹Br) requires 713.0433.

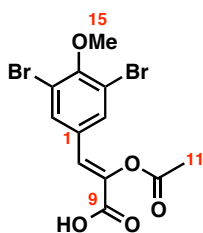
(E)-2-((Benzyloxy)imino)-N-((Z)-2-(1-((benzyloxy)methyl)-1*H*-imidazol-4-yl)vinyl)-3-(3,5-dibromo-4-methoxyphenyl)propanamide (75)



A mixture of **74** (76.0 mg, 0.106 mmol) and palladium black (66 mg, 0.620 mmol) in dioxane/AcOH (1:1, 3 mL) was stirred under an H₂ atmosphere for 4 h. The mixture was filtered through a pad of celite and the solvent removed *in vacuo*. The residue was taken up in EtOAc (20 mL), washed with water (20 mL), dried and concentrated *in vacuo*. The residue was purified by flash column chromatography (10-30% EtOAc/Petrol) to furnish **75** (11.4 mg, 17.1 μmol, 16%) as a white solid.

R_f 0.20 (20% EtOAc/Petrol); ν_{\max} (thin film)/cm⁻¹ 3251w, 2924w, 2853w, 1654s, 1556s, 1468s, 1240s; δ_H (400 MHz, CDCl₃) 12.1 (1H, d, J 10.8 Hz, NH), 7.55 (1H, br s, H-14), 7.48-7.46 (2H, m, Ph-H), 7.45 (2H, s, H-2/6), 7.40-7.28 (8H, m, Ph-H), 7.00 (1H, dd, J 10.8, 9.2 Hz, H-10), 6.96 (1H, d, J 1.3 Hz, H-13), 5.61 (1H, d, J 9.1 Hz, H-11), 5.35 (2H, s, H-8'), 5.31 (2H, s, H-1'), 4.44 (2H, s, H-9'), 3.89 (2H, s, H-7), 3.83 (3H, s, H-16); δ_C (100 MHz, CDCl₃) 159.9 (C-9), 152.6 (C-4), 151.0 (C-8), 141.0 (C-12), 136.6 (C-14), 136.55 (C-2'), 135.9 (C-10'), 134.8 (C-1), 133.4 (C-2/6), 128.7 (C-4'/6'), 128.6 (C-12'/14'), 128.4 (C-3'/7'), 128.38 (C-5'), 128.0 (C-11'/15'), 121.4 (C-10), 117.7 (C-3/5), 116.0 (C-13), 101.0 (C-11), 77.9 (C-1'), 75.1 (C-8'), 70.1 (C-9'), 60.5 (C-16), 28.7 (C-7); m/z (ESI⁺) found 667.0587, [M+H]⁺ C₃₀H₂₉Br₂N₄O₄ (⁷⁹Br) requires 667.0556.

The ¹³C chemical shift for C-13' is hidden.

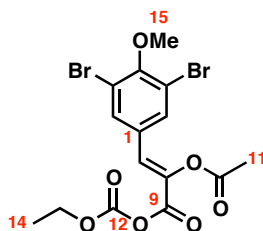
(Z)-2-Acetoxy-3-(3,5-dibromo-4-methoxyphenyl)acrylic acid (88)

A mixture of acetic anhydride (10 mL, 106 mmol), **71** (1.00 g, 2.84 mmol) and sodium acetate (349 mg, 4.25 mmol) was stirred for 2 h. The resultant white precipitate was isolated by filtration, washed with Et₂O (3 × 20 mL) and dissolved in H₂O (100 mL). The aqueous solution was acidified to pH 0 by the dropwise addition of 3 *N* HCl followed by the addition of Et₂O (100 mL). The organic layer was separated and the aqueous phase extracted with Et₂O (2 × 100 mL). The combined organic layers were dried and evaporated to dryness *in vacuo* to furnish **88** (806 mg, 2.04 mmol, 72%) as a white solid.

R_f 0.53 (20% MeOH/CH₂Cl₂); *v*_{max} (thin film)/cm⁻¹ 2827br, 1773s, 1685s, 1649m, 1471s, 1181s; *δ*_H (400 MHz, CD₃OD) 7.80 (2H, s, H-2/6), 7.19 (1H, s, H-7), 3.87 (3H, s, H-15), 2.30 (3H, s, H-11); *δ*_C (100 MHz, CD₃OD) 169.7 (C-10), 164.8 (C-9), 156.2 (C-4), 140.2 (C-8), 135.1 (C-2/6), 132.4 (C-1), 124.5 (C-7), 119.3 (C-3/5), 61.2 (C-15), 20.5 (C-11); *m/z* (ESI⁺) found 392.8980, [M+H]⁺ C₁₂H₁₁Br₂O₅ (⁷⁹Br) requires 392.8973; m.p. 168-170 °C.

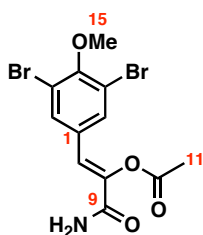
Crystals of **88** were obtained by slow evaporation from Et₂O. The structure was confirmed by X-ray crystallographic analysis and given the unique identifier sl1035.

(Z)-2-Acetoxy-3-(3,5-dibromo-4-methoxyphenyl)acrylic (ethyl carbonic) anhydride (89)



To a stirred solution of acid **88** (100 mg, 0.254 mmol) and Et₃N (53.1 μ L, 0.381 mmol) in THF (5 mL) at 0 °C was added ethyl chloroformate (25.5 μ L, 0.267 mmol). After 1 h, EtOAc (25 mL) and H₂O (25 mL) were added, the organic layer separated, and the aqueous layer extracted with EtOAc (2 x 25 mL). The combined organic extracts were dried and evaporated to dryness *in vacuo* to furnish **89** (112 mg, 0.240 mmol, 95%) as a colourless oil.

R_f 0.45 (20% Et₂O/PE 40-60); ν_{\max} (thin film)/cm⁻¹ 2984 w, 2933 w, 1808 s, 1775 s, 1745 s, 1472 m, 1155 s; δ_H (400 MHz CDCl₃) 7.77 (2H, s, H-2/6), 7.24 (1H, s, H-7), 4.38 (2H, q, J 7.2 Hz, H-13), 3.91 (3H, s, H-15), 2.36 (3H, s, H-11), 1.39 (3H, t, J 7.2 Hz, H-14); δ_C (100 MHz, CDCl₃) 167.7 (C-10), 156.5 (C-9), 155.8 (C-4), 148.0 (C-12), 136.0 (C-8), 134.4 (C-2/6), 129.8 (C-1), 127.3 (C-7), 118.6 (C-3/5), 66.2 (C-13), 60.8 (C-15), 20.4 (C-11), 13.9 (C-14).

(Z)-3-Amino-1-(3,5-dibromo-4-methoxyphenyl)-3-oxoprop-1-en-2-yl acetate (90)

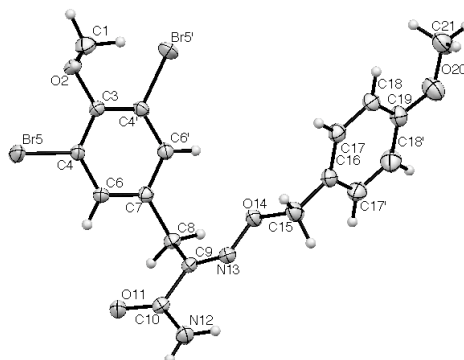
To a stirred solution of acid **88** (105 mg, 0.266 mmol) and Et₃N (55.6 μ L, 0.399 mmol) in THF (5 mL) at 0 °C was added ethyl chloroformate (26.8 μ L, 0.280 mmol). After 45 min, HMDS (555 μ L, 2.66 mmol) was added and the reaction mixture was stirred for a further 30 min at 0 °C. The reaction mixture was allowed to warm to room temperature and after 1 h, EtOAc (25 mL) and H₂O (25 mL) were added, the organic layer separated and the aqueous layer was extracted with EtOAc (2 x 25 mL). The combined organic extracts were dried, and concentrated *in vacuo*. The residue was purified by flash column chromatography (30-70% EtOAc/Petrol) to furnish **90** (56.6 mg, 0.144 mmol, 54%) as a white solid.

R_f 0.22 (40% Et₂O/PE 40-60); ν_{\max} (thin film)/cm⁻¹ 3424m, 3163br, 1753s, 1692s, 1644m, 1615m, 1185s; δ_H (400 MHz, d_6 -DMSO) 7.83 (2H, s, H-2/6), 7.82 (1H, br s, NH), 7.51 (1H, br s, NH), 7.11 (1H, s, H-7), 3.82 (3H, s, H-15), 2.29 (3H, s, H-11); δ_C (100 MHz, d_6 -DMSO) 168.2 (C-10), 163.0 (C-9), 153.6 (C-4), 141.8 (C-8), 133.2 (C-2/6), 131.6 (C-1), 118.9 (C-7), 117.8 (C-3/5), 60.5 (C-15), 20.8 (C-11); m.p. 140-142 °C

4.5 Appendix

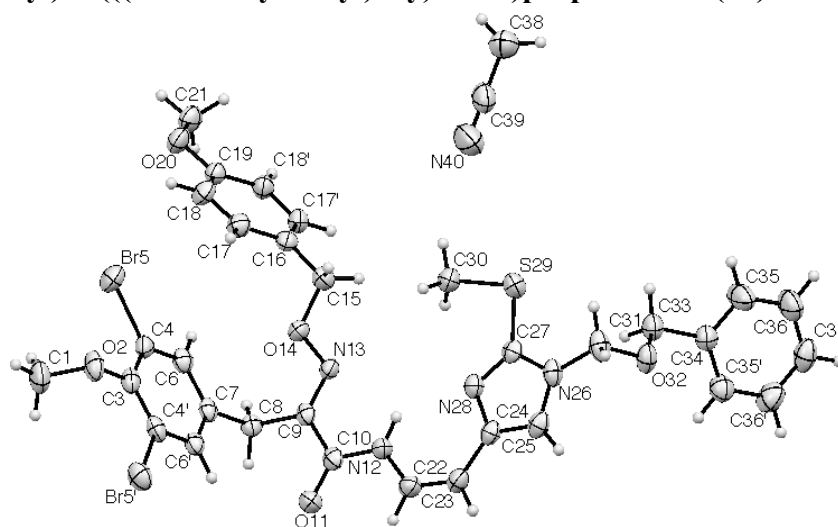
4.5.1 Crystal Structure Data

(*E*)-3-(3,5-Dibromo-4-methoxyphenyl)-2- (((4-methoxybenzyl)oxy)imino)propanamide (61)



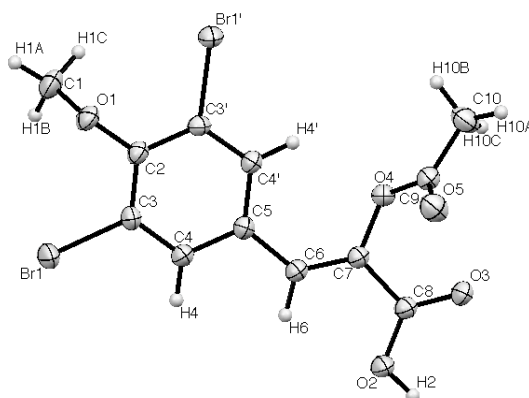
Crystal data and structure refinement for sl0854

| | |
|-----------------------------------|--|
| Identification code | sl0854 |
| Empirical formula | C ₁₈ H ₁₈ Br ₂ N ₂ O ₄ |
| Formula weight | 486.16 |
| Temperature | 180(2) K |
| Wavelength | 0.71073 Å |
| Crystal system | Triclinic |
| Space group | P-1 |
| Unit cell dimensions | a = 8.8998(1) Å α = 68.743° b = 10.1559(2) Å β = 80.052(1)° c = 11.2089(2) Å γ = 86.219(1)° |
| Volume | 929.99(3) Å ³ |
| Z | 2 |
| Density (calculated) | 1.736 Mg/m ³ |
| Absorption coefficient | 4.384 mm ⁻¹ |
| F(000) | 484 |
| Crystal size | 0.35 × 0.32 × 0.28 mm ³ |
| Theta range for data collection | 3.52 to 32.05° |
| Index ranges | -13 ≤ h ≤ 13, -15 ≤ k ≤ 15, -16 ≤ l ≤ 16 |
| Reflections collected | 18490 |
| Independent reflections | 6462 [R(int) = 0.0605] |
| Completeness to theta = 32.05° | 99.4% |
| Absorption correction | Semi-empirical from equivalents |
| Max. and min. transmission | 0.301 and 0.180 |
| Refinement method | Full-matrix least-squares on F ² |
| Data / restraints / parameters | 6462 / 0 / 237 |
| Goodness-of-fit on F ² | 1.036 |
| Final R indices [I > 2sigma (I)] | R1 = 0.0383, wR2 = 0.0962 |
| R indices (all data) | R1 = 0.0487, wR2 = 0.1028 |
| Largest diff. peak and hole | 0.716 and -1.227 e. Å ⁻³ |

(*E*)-*N*-((*Z*)-2-(1-((Benzyloxy)methyl)-1*H*-imidazol-4-yl)vinyl)-3-(3,5-dibromo-4-methoxyphenyl)-2-(((4-methoxybenzyl)oxy)imino)propanamide (59)

Crystal data and structure refinement for sl0909

| | |
|-----------------------------------|--|
| Identification code | sl0909 |
| Empirical formula | C ₃₄ H ₃₅ Br ₂ N ₅ O ₅ S |
| Formula weight | 785.55 |
| Temperature | 180(2) K |
| Wavelength | 0.71073 Å |
| Crystal system | Monoclinic |
| Space group | P2(1)/c |
| Unit cell dimensions | a = 32.4143(4) Å α = 90° b = 4.3270(1) Å β = 114.087(1)° c = 26.7941(6) Å γ = 90° |
| Volume | 3430.82(12) Å ³ |
| Z | 4 |
| Density (calculated) | 1.521 Mg/m ³ |
| Absorption coefficient | 2.472 mm ⁻¹ |
| F(000) | 1600 |
| Crystal size | 0.46 × 0.05 × 0.04 mm ³ |
| Theta range for data collection | 3.67 to 27.49° |
| Index ranges | -28 ≤ h ≤ 41, -5 ≤ k ≤ 5, -34 ≤ l ≤ 34 |
| Reflections collected | 23528 |
| Independent reflections | 7569 [R(int) = 0.0784] |
| Completeness to theta = 27.49° | 95.7% |
| Absorption correction | Semi-empirical from equivalents |
| Max. and min. transmission | 0.906 and 0.556 |
| Refinement method | Full-matrix least-squares on F ² |
| Data / restraints / parameters | 7569 / 0 / 428 |
| Goodness-of-fit on F ² | 1.100 |
| Final R indices [I > 2σ(I)] | R1 = 0.0586, wR2 = 0.1091 |
| R indices (all data) | R1 = 0.1005, wR2 = 0.1254 |
| Largest diff. peak and hole | 0.892 and -0.431 e. Å ⁻³ |

(Z)-2-Acetoxy-3-(3,5-dibromo-4-methoxyphenyl)acrylic acid (88)

Crystal data and structure refinement for sl1035

| | |
|-----------------------------------|--|
| Identification code | sl1035 |
| Empirical formula | C ₁₂ H ₁₀ Br ₂ O ₅ |
| Formula weight | 394.02 |
| Temperature | 181(2) K |
| Wavelength | 0.71073 Å |
| Crystal system | Triclinic |
| Space group | P-1 |
| Unit cell dimensions | a = 8.1680(2) Å α = 103.985(1)° b = 8.6811(2) Å β = 109.084(1)° c = 10.6434(3) Å γ = 96.000(2)° |
| Volume | 678.07(3) Å ³ |
| Z | 2 |
| Density (calculated) | 1.930 Mg/m ³ |
| Absorption coefficient | 5.990 mm ⁻¹ |
| F(000) | 384 |
| Crystal size | 0.23 × 0.23 × 0.12 mm ³ |
| Theta range for data collection | 3.64 to 32.02° |
| Index ranges | -12 ≤ h ≤ 11, -12 ≤ k ≤ 12, -11 ≤ l ≤ 15 |
| Reflections collected | 9902 |
| Independent reflections | 4587 [R(int) = 0.0425] |
| Completeness to theta = 32.02° | 97.4% |
| Absorption correction | Semi-empirical from equivalents |
| Max. and min. transmission | 0.490 and 0.326 |
| Refinement method | Full-matrix least-squares on F ² |
| Data / restraints / parameters | 4587 / 0 / 177 |
| Goodness-of-fit on F ² | 1.036 |
| Final R indices [I > 2σ(I)] | R1 = 0.0337, wR2 = 0.0879 |
| R indices (all data) | R1 = 0.0455, wR2 = 0.0940 |
| Largest diff. peak and hole | 0.740 and -1.026 e. Å ⁻³ |

4.6 References

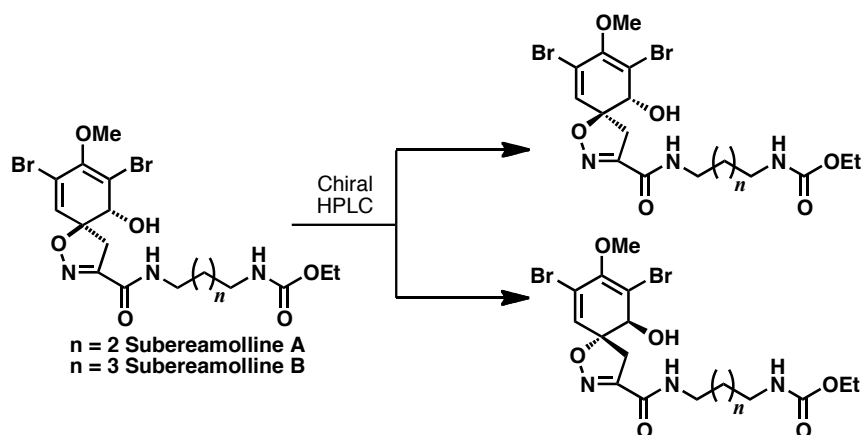
- ¹ E. Manzo, R. van Soest, L. Matainaho, M. Roberge and R. J. Andersen, *Org. Lett.*, **2003**, *5*, 4591.
- ² M. Nodwell, A. Pereira, J. L. Riffell, C. Zimmerman, B. O. Patrick, M. Roberge and R. J. Andersen, *J. Org. Chem.*, **2009**, *74*, 995
- ³ M. Nodwell, C. Zimmerman, M. Roberge and R. J. Andersen, *J. Med. Chem.*, **2010**, *53*, 7843.
- ⁴ C. G. Collison, J. Chen and R. Walvoord, *Synthesis*, **2006**, 2319.
- ⁵ L. Jiang, G. E. Job, A. Klapars and S. L. Buchwald, *Org. Lett.*, **2003**, *5*, 3667.
- ⁶ M. L. Meketa and S. M. Weinreb, *Tetrahedron*, **2007**, *63*, 9112; M. L. Meketa and S. M. Weinreb, *Org. Lett.*, **2007**, *9*, 853.
- ⁷ Strategic Applications of Named Reactions in Organic Synthesis, Eds. L. Kürti and B. Czakó, **2005**, Elsevier Academic Press, pp 68; S. Levin, R. R. Nani and S. E. Reisman, *J. Am. Chem. Soc.*, **2011**, *133*, 774.
- ⁸ T. F. Schneider and D. B. Werz, *Org. Lett.*, **2011**, *13*, 1848.
- ⁹ A. Khalafi-Nezhad, B. Mokhtari and M. N. S. Rad, *Tetrahedron Lett.*, **2003**, *44*, 7325.
- ¹⁰ D. Seyferth, J. K. Heeren, G. Singh, S. O. Grim and W. B. Hughes, *J. Organomet. Chem.*, **1966**, *5*, 267.
- ¹¹ Y. Venkateswarlu and R. Chavakula, *J. Nat. Prod.*, **1995**, *58*, 1087.
- ¹² C. M. Sandison, R. Alexander and R. I. Kagi, *Org. Geochem.*, **2003**, *34*, 1373.
- ¹³ F. Shirini, M. A. Zolfigol, B. Mallakpour, A. R. Hajipour and I. M. Baltork, *Tetrahedron Lett.*, **2002**, *43*, 1555.
- ¹⁴ S. Y. Lee, B. S. Lee, C-W. Lee and D. Y. Oh, *J. Org. Chem.*, **2000**, *65*, 256.
- ¹⁵ D. P. Curran, J. F. Brill and D. M. Rakiewicz, *J. Org. Chem.*, **1984**, *49*, 1654.
- ¹⁶ S. B. Shim, K. Kim and Y. H. Kim, *Tetrahedron Lett.*, **1987**, *28*, 645.
- ¹⁷ Z. Li, R-B. Ding, Y-L. Xing and S-Y. Shi, *Synth. Commun.*, **2005**, *35*, 2515.
- ¹⁸ A. S. Demir, C. Tanyeli and E. Altinel, *Tetrahedron Lett.*, **1997**, *38*, 7267.
- ¹⁹ N. B. Barhate, A. S. Gajare, R. D. Wakaharker and A. Sudalai, *Tetrahedron Lett.*, **1997**, *38*, 653.
- ²⁰ Y. Yang, D. Zhang, L-Z. Wu, L-P. Zhang and C-H. Tung, *J. Org. Chem.*, **2004**, *69*, 4788.

- ²¹ D. H. R. Barton, W. B. Motherwell, E. S. Simon and S. Z. Zard, *J. Chem. Soc., Perkin Trans. 1*, **1986**, 2243.
- ²² K. A. Lukin and B. A. Narayanan, *Tetrahedron*, **2002**, 58, 215.
- ²³ J. Esteban, A. M. Costa, F. Urpí and J. Vilarrasa, *Tetrahedron Lett.*, **2004**, 45, 5563.
- ²⁴ S. S. Chaudhari and K. G. Akamanchi, *Tetrahedron Lett.*, **1998**, 39, 3209.
- ²⁵ P. Busca, F. Paradisi, E. Moynihan, A. R. Maguire and P. C. Engel, *Org. Biomol. Chem.*, **2004**, 2, 2684.
- ²⁶ V. Dalla and J. P. Catteau, *Tetrahedron*, **1999**, 55, 6497.
- ²⁷ C. Dong, Y. Wang, Y. Z. Zhu, *Bioorg. Med. Chem.*, **2009**, 17, 3499.
- ²⁸ M-K. Leung and J. M. J. Fréchet, *J. Chem. Soc., Perkin. Trans. 2*, **1993**, 2329.
- ²⁹ A. P. Kozikowski, W. Tückmantel, I. J. Reynolds and J. T. Wroblewski, *J. Med. Chem.*, **1990**, 33, 1561.
- ³⁰ C. Napolitano, M. Borriello, F. Cardullo, D. Donati, A. Paio and S. Manfredini, *Tetrahedron*, **2010**, 66, 5492.
- ³¹ J. E. Nordlander, M. J. Payne, M. A. Balk, J. L. Gress, F. D. Harris, J. S. Lane, R. F. Lewe, S. E. Marshall, D. Nagy and D. J. Rachlin, *J. Org. Chem.*, **1984**, 49, 133.
- ³² M. O. Förster, *J. Chem. Soc.*, **1915**, 107, 260.
- ³³ J. Meinwald and P. G. Gassman, *J. Am. Chem. Soc.*, **1959**, 81, 4751.
- ³⁴ N. Ullah, S. A. Haladu and B. A. Mosa, *Tetrahedron Lett.*, **2011**, 52, 212.
- ³⁵ R. W. Schumacher and B. S. Davidson, *Tetrahedron*, **1999**, 55, 935.

5 Publications

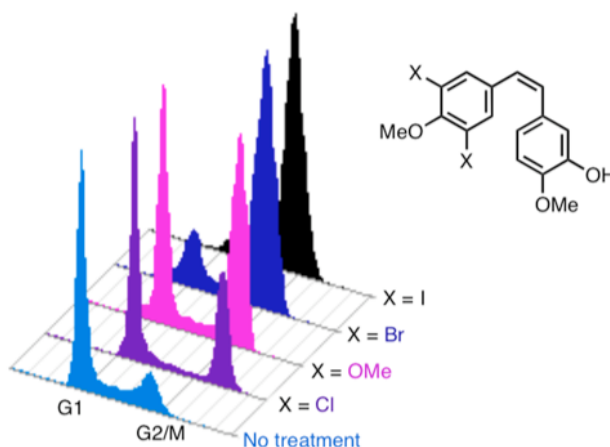
Total synthesis of Subereamollines A and B; J. W. Shearman, R. M. Myers, J. D. Brenton and S. V. Ley, *Org. Biomol. Chem.*, **2011**, *9*, 62-65.

The first total syntheses of (+)- and (-)-subereamollines A and B are reported. The enantiomeric forms of the natural products were obtained by preparative chiral HPLC separation of the corresponding racemates.



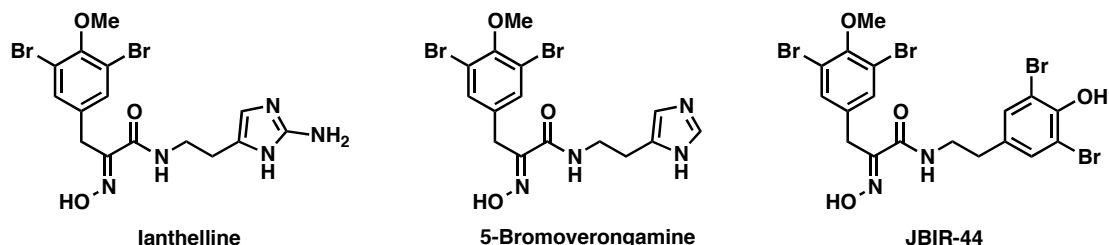
Antivascular and Anticancer Activity of Dihalogenated A-ring Analogues of Combretastatin A-4; T. M. Beale, R. M. Myers, J. W. Shearman, D. S. Charnock-Jones, J. D. Brenton, F. V. Gergeley and S. V. Ley, *Med. Chem. Commun.*, **2010**, *1*, 202-208.

The generally accepted view is that the 3,4,5-trimethoxy-substituted aromatic A-ring of combretastatin A-4 (CA-4) and its analogues should be conserved in order to maintain biological activity through enforcing an active molecular conformation. Contrary to this, we have found that substituting the larger meta-methoxy groups of CA-4 with smaller halogen atoms results in compounds that are equipotent or more potent than CA-4 itself in vitro.



Total Syntheses of the Bromotyrosine-Derived Natural Products Ianthelline, 5-Bromoverongamine and JBIR-44; J. W. Shearman, R. M. Myers, T. M. Beale, J. D. Brenton and S. V. Ley, *Tetrahedron Lett.*, **2010**, *51*, 4812-4814.

The total syntheses of the bromotyrosine-derived natural products ianthelline, 5-bromoverongamine and JBIR-44 are described and their cytotoxic activity in a cervical cancer (HeLa) cell line and human umbilical vein endothelial cells (HUVECs) are reported.



Cancer, Chemistry and the Cell: Molecules that Interact with the Neurotensin Receptors; R. M. Myers, J. W. Shearman, M. O. Kitching, A. Ramos-Montoya, D. E. Neal and S. V. Ley, *ACS Chem. Biol.*, **2009**, *4*, 503-525.

The literature covering neurotensin (NT) and its signalling pathways, receptors, and biological profile is complicated by the fact that the discovery of three NT receptor subtypes has come to light only in recent years. Moreover, a lot of this literature explores NT in the context of the central nervous system and behavioral studies. However, there is now good evidence that the up-regulation of NT is intimately involved in cancer development and progression. This Review aims to summarize the isolation, cloning, localization, and binding properties of the accepted receptor subtypes (NTR1, NTR2, and NTR3) and the molecules known to bind at these receptors. The growing role these targets are playing in cancer research is also discussed. We hope this Review will provide a useful overview and a one-stop resource for new researchers engaged in this field at the chemistry-biology interface.

